

FLOODING IN KWAZULU-NATAL: MODELLING, HISTORY AND FUTURE ASPECTS

by

Zacheus Adriaan Botes

November 2014

Submitted in fulfilment of the academic
requirements for the degree of
Doctor of Philosophy in the
Discipline of Geological Sciences
School of Agricultural, Earth and Environmental Sciences
College of Agriculture, Engineering and Science
University of KwaZulu-Natal
Durban, Republic of South Africa

Preface

The experimental work described in this thesis was carried out in the School of Geological Sciences, University of KwaZulu-Natal, Westville, from July 2010 to November 2014, under the supervision of Dr. Andrew Green and Dr. Alan Smith.

These studies represent original work by the author and have not otherwise been submitted in any form for any degree or diploma to any tertiary institution. Where use has been made of the work of others it is duly acknowledged in the text.

As the candidate's supervisor I have approved this thesis for submission and examination.

Signed: _____ Name: _____ Date: _____

As the candidate's co-supervisor I have approved this thesis for submission and examination.

Signed: _____ Name: _____ Date: _____

Declaration 1 – Plagiarism

I, Zacheus Adriaan Botes declare that:

1. The research reported in this thesis, except where otherwise indicated, is my original research.
2. This thesis has not been submitted for any degree or examination at any other university.
3. This thesis does not contain other persons' data, graphs or other information, unless specifically acknowledged as being sourced from other persons.
4. This thesis does not contain any other persons writing, unless specifically acknowledged as being sourced from other researchers. Where other written sources have been quoted then:
 - a. Their words have been re-written but the general information attributed to them has been referenced
 - b. Where their exact words have been used, then their writing has been placed in italics and inside quotation marks, and referenced.
5. This thesis does not contain text, graphics or tables copied from the Internet, unless specifically acknowledged, and the source being detailed in the thesis and in the References section.

Signed.....

Declaration 2

Details of contributions to publications that form part and/or include research presented in this thesis.

Acknowledgements

The idea for this research project was conceived during discussions with the KwaZulu-Natal Department of Human Settlements around issues of providing housing to people who were located in flood risk areas, where no floodline data exists. I would like to thank Mr. Peter Woolf for his perspectives on this matter.

I would like to thank Prof. Ron Uken, my initial supervisor, for his guidance. I wish him well in his future endeavours.

Dr. Alan Smith, my co-supervisor, provided support and guidance on this project. He was as a sounding board for ideas, a mentor and a guide, especially when the research took me in directions never originally anticipated. Thank you.

I would like to thank Dr. Andrew Green my supervisor for his support and guidance. Thank you for keeping me on track and being the guide or the taskmaster when it was needed. Your guidance was invaluable.

I would like to thank Mr. James Morris from SRK Consulting (Durban) for the many discussions on flood modelling.

To Mr. Calvin Mehl, my nephew. Thank you for your help and many hours of assistance with data processing. It helped immeasurably.

To my wife Catherine. Thank you for the support and encouragement. Could not have done it without you.

Abstract

The current state of flood modelling relies on statistical techniques revolving around either river or rainfall data that are used to produce an estimated flood return period (e.g. 1:100 year). These tend to ignore 1) the geological record as an archive of flood events; 2) the spatial distribution of flood producing weather systems; and 3) climatic cycles which may ultimately control episodes of flooding. This thesis developed a Flood Zone Model (FZM) model from existing Geographic Information Systems (GIS) datasets and GIS software models at a quaternary catchment (4th order basin) level. Model discharge estimates were derived from modified Regional Maximum Flood (Q_{RMF}) equations where it was found that flood elevations produced from Q_{RMF} estimated discharges could be directly related to the geological record of flood. This was achieved using Manning-derived calibration factors (CFs) based on reach slope. Comparison of the modelled flood elevation surfaces against the field data and available 1:100 year return period elevations showed R^2 coefficients of 0.999 for all calibration factors. In one of the quaternary catchments investigated, geological evidence and discussion with local communities identified flood elevations attributed to flash flooding. On this basis, the Flood Zone Model was adapted to estimate peak discharges using the Rational Formula where it was found that the calibration factors were valid for flash flood modelling and that the flood elevations that resulted from flash flooding far exceeded the 1:100 year return period. To evaluate the spatial distribution of flood producing storms, daily rainfall data from KwaZulu-Natal (1890 - 2000) were gridded to produce regional storm event footprints. Storm events typically last between three to four days with the highest associated risk period from January to May. Flooding appears to be mostly influenced by migrating easterly waves. Compilation of all the storm event footprints defined five risk zones with a sixth zone at risk from tropical storms and cyclones. Comparisons between the annual regional storm event count and several climatic cycles show a significant correlation between the Pacific Decadal Oscillation (PDO) and regional storm event as a result of increased easterly wave activity. Assuming no change to the Pacific Decadal Oscillation cycle, increased periods of intense flooding will occur in the future.

Table of Contents

Preface	i
Acknowledgements	iii
Abstract	iv
Acronyms	ix
CHAPTER 1 - INTRODUCTION	1
1. Introduction	1
1.1. Research Aims	4
1.2. Thesis structure	5
CHAPTER 2- LITERATURE REVIEW	7
2. Literature Review	7
2.1. Prediction in ungauged basins (Catchments)	9
2.2. International flood delineation methods	11
2.2.1. Rational Method – Small catchments	12
2.2.2. Stream flow techniques	12
2.2.3. Regional flood frequency analysis (FFA)	13
2.2.4. Flood envelopes	13
2.3. Floodline determination in the Republic of South Africa	14
2.4. Flash flood determination	16
2.5. Flood marks	19
CHAPTER 3 - STUDY AREA	20
3. The context of the study area	20
3.1. Land Cover	21
3.2. Topography	21
3.3. Soil depth and drainage capacity	22

3.4.	Hydrology	23
3.5.	Rainfall and climatic systems	24
3.5.1.	Monthly prevalence of weather systems	26
3.5.2.	Small to medium scale weather systems	27
3.5.3.	Tropical cyclones and tropical storms	27
3.5.4.	Thunderstorms	28
3.6.	Flood history of the Republic of South Africa	29
3.7.	Extreme flood events	30
CHAPTER 4 - METHODOLOGY		33
4.	Introduction	33
4.1.	General modelling philosophy	33
4.2.	GPS Mapping	34
4.3.	Homestead surveys	34
4.4.	Modelling units	34
4.5.	Flood methodology	36
4.5.1.	Flash flood hydrology	38
4.5.2.	Calibration	40
CHAPTER 5 - FIELD OBSERVATIONS		41
5.	Field observations	41
5.1.	Flood markers	41
5.2.	Flood deposits	44
5.3.	Quaternary catchment areas	50
5.3.1.	T40G Quaternary Catchment	51
5.3.2.	U20H Quaternary Catchment	54
5.3.3.	T52D Quaternary Catchment	59
5.3.4.	V12G Quaternary Catchment	62

5.3.5.	W23A Quaternary Catchment	66
5.3.6.	U20M Quaternary Catchment	71
5.4.	Discussion	73
CHAPTER 6 - FLOOD MODELLING		76
6.	Regional Maximum Flood Peak (RMF)	76
6.1.	Regional Maximum Flood Problem	80
6.1.1.	Modified Regional Maximum Flood	81
6.1.2.	Sub-catchments discharge determination	93
6.2.	Calibration	93
6.2.1.	Q_{MRMF} discharges equal field evidence	94
6.2.2.	Calibration factors (CF)	94
6.3.	Results	95
6.3.1.	Q_{MRMF} Results	96
6.3.2.	Q_{M100} Results	105
6.3.3.	Blind test	109
6.4.	Discussion	115
CHAPTER 7 - FLASH FLOOD MODELLING		119
7.	Introduction	119
7.1.	U20H quaternary catchment	120
7.2.	Results	120
7.3.	Discussion	127
CHAPTER 8 - STORM SYSTEMS		129
8.	Introduction	129
8.1.	Methodology	130
8.2.	Results	132

8.2.1.	Regional storm event footprints	134
8.2.2.	Regional storm event characteristics	135
8.2.3.	Regional storm event distribution in time	138
8.2.4.	Regional storm system event spatial distribution	140
8.2.5.	Local storm events (LSEs)	142
8.2.6.	Local storm event distribution in time	142
8.2.7.	Local storm system event spatial distribution	144
8.3.	Discussion	145
CHAPTER 9 – CLIMATIC INFLUENCES ON FLOODING IN KWAZULU-NATAL		158
9.	Introduction	158
9.1.	Results	159
9.1.1.	Mean annual precipitation and Wet/Dry Cycles	161
9.1.2.	Solar and lunar influences	166
9.1.3.	Global temperatures	168
9.1.4.	Indian Ocean Dipole	171
9.1.5.	Atlantic Multi-decadal Oscillation	173
9.1.6.	Pacific Decadal Oscillation	174
9.1.7.	Inter-decadal Pacific Oscillation	176
9.1.8.	Southern Oscillation Index	178
9.1.9.	El Niño Southern Oscillation	180
9.1.10.	Antarctic Oscillation	182
9.2.	Discussion	184
CHAPTER 10 - CONCLUSIONS		192
REFERENCES		195

APPENDIX I – LIST OF HISTORICAL FLOODS	213
APPENDIX II – FLOOD ZONE MODELLING	219
APPENDIX III – COMMUNITY SURVEYS	254
APPENDIX IV – REGIONAL STORM EVENT DATA	255
APPENDIX V – LOCAL STORM EVENT DATA	283
APPENDIX VI – CLIMATE DATA SOURCES	309

Acronyms

A_e - Effective catchment area as the drainage area upstream of the point for which RMF is to be determined. This may comprises one or more catchment (basins). For the MRMF A_e is used as defined by Kovács (1988).

AAO - Antarctic Oscillation

AGIS - Agricultural Geographic Information System

AMO - Atlantic Multi-decadal Oscillation

PUB – Prediction in ungauged basins

CF - Calibration factor

DEM – Digital elevation model

ENSO - El Niño Southern Oscillation

ESE – extreme storm event

FFA - Flood frequency analysis

FFM - Flash flood model

FFM_{200} – Flash flood model's estimated 200 year return period discharge

FFWRS - flood forecast, warning and response system

FZM – Flood zone model

GIS - Geographic information system

GPS – Global positioning system

IOD - Indian Ocean Dipole

IPO - Inter-decadal Pacific Oscillation

K - Regional coefficient expressed as relative flood peak magnitude which is $10(1-\tan^{\alpha})$ where α is the slope of the envelope line as defined by Francou-Rodier (1967). In effect a coefficient indicating variation in rainfall, geology, land form, vegetation cover, in flood production.

K_e – Regional coefficient expressed homogeneous hydrographic regions (envelopes) as defined by Kovács (1988).

KZN - KwaZulu-Natal

LNC – Lunar nodal cycle

LSE – Local storm event

MAP – Mean annual precipitation

PDO - Pacific Decadal Oscillation

Q – Discharge

Q_{200} , Q_{100} and Q_{50} – estimated return period discharges derived from the regional maximum flood peak

Q_{M100} – 1:100 year estimated discharge derived from the modified regional maximum flood peak

Q_{MRMF} – Modified regional maximum flood peak discharge

Q_{RMF} – Regional maximum flood peak discharge

RF – Rational Formula

RF_{20} , RF_{50} , RF_{100} , RF_{200} – 20, 50, 100 and 200 year estimated design rainfall

RMF – Regional maximum flood

RSA – Republic of South Africa

RSE – Regional storm event

SAWS – South African Weather Services

SG - Surveyor General

SOI - Southern Oscillation Index

SST – Sea surface temperature

T_c - Time of concentration

ZAR - Republic of South Africa Rands

CHAPTER 1 - INTRODUCTION

1. Introduction

Floods are natural hazards that have a significant impact on human settlements and infrastructure. They account for two thirds of natural disaster-related deaths at an average of 84 people per annum in the Republic of South Africa (RSA) (Kahn 2003). Worldwide flood related deaths account for 17.1% of natural disaster-related deaths, the third largest after wind storms (36.8%) and earthquakes (33.5%) (Kahn 2003).

Extreme flood events are extraordinary in magnitude for a particular river catchment and can have severe economic and infrastructural consequences (Lundquist 2002). These events are the most destructive due to their large footprint, but even relatively small flood events can impact on homesteads, particularly in rural and informal settlements. Population growth and migration from rural areas to urban centres is leading to a greater demand for land with the resulting expansion and densification of peri-urban and informal settlements. Often these unplanned settlements are located along river courses due to the flatter land and availability of water. Human activities such as environmental degradation, poor agricultural practises (Tilman et al. 2002) and hard surface expansion due to urbanisation (Ganoulis 2003) result in increased run-off, thus exacerbating flood discharge magnitudes and further complicating the hazards posed by flooding.

According to the Intergovernmental Panel on Climate Change (IPCC 2014), extreme events such as floods will become more common because of global warming. Knoesen et al. (2009), predicted the mean annual precipitation (MAP) for large portions of the Republic of South Africa to increase by 10 to 30%. Furthermore, precipitation in the eastern part of the Republic of South Africa could double in the medium term (2046 - 2065) due to global warming (Knoesen et al. 2009), with floods and flood-related deaths increasing as a consequence.

Countries with emerging economies, such as the Republic of South Africa, face severe resource constraints, thus limiting the supply of basic services, hazard assessment and planning, particularly in rural areas. The Republic of South Africa, and in particular the province of KwaZulu-Natal (KZN), is prone to regular flooding (Kovács et al. 1985; Van Bladeren & Burger 1989; SAWS 1991; van Bladeren 1992). In KwaZulu-Natal, the assessment of flood risk remains a low priority compared to other development pressures, despite the encroachment of informal settlements and peri-urban sprawl into flood-prone areas. Authorities therefore have a responsibility to manage human and infrastructural safety; delineating flood zones offers a first step in preventative planning and management of such a risk.

Operational risk management for proactive planning of disaster relief, early warning systems and humanitarian aid all rely on the ability to assess flood risk and the mapping thereof. The lack of this mapping information has far reaching consequences in managing the risk associated with flooding. Integrated risk management strategies (Du Plessis 2002; Benjamin 2008) cannot be effectively implemented at the local or district municipal scale without probable inundation risk assessment as it forms the basis for determining the vulnerability of settlements to flooding.

The characteristics of a catchment and its response to accumulated precipitation are often reflected as a line marked out by the elevation of the flood (floodline) which offers a basic zonation of statistical threat posed by flood waters for that particular system. Such a delineation of KwaZulu-Natal's river catchments is limited; only 1% of the province's rivers having undergone floodline determination. In addition the province faces three main problems:-

- Currently planners and disaster management organisations are faced with limited floodline information. These presently exist for major urban centres and some site specific structures. Presently, floodlines have been produced for only 1 800 km (1%) of the approximate 199 000 km of river lengths in KwaZulu-Natal. Taking into account settled areas outside the major urban centres, another 47 500 km of river lengths require floodline determination. In effect, a further 60% of the rivers in the province require floodlines to guide spatial planning and to reduce flood-related deaths and the socio-economic impact of flood damage.

- There is no detailed record of historical flood events. Where flood events are documented, they concentrate on extreme events only and may neglect smaller, yet equally as damaging on occasions.
- There is no information about the distribution and recurrence of flood event footprints that can delineate areas of flood risk and relate these to the weather/climatic cycles that produce them.

Design flood estimations (return period floodlines produced to meet certain engineering design standards) are routinely produced for specific developments, (e.g. bridges and housing developments), but in reality there are a number of other spatial planning situations that require flood hazard demarcation for all rivers. In the Republic of South Africa, the Revised National Water Act 36 of 1998 (NWA 1998) requires a 1:100 year design floodline estimate for new developments, with the result that structures built prior to 1998 may not comply with this. The same act does not discuss the issue of existing and often extensive traditional and informal settlements which are subject to the same risk. Delineating flood hazard areas over agricultural land is also a necessity. The Water Act (NWA 1998) also requires the protection of the riparian habitat, an area subject to flooding. Floodlines would thus be a benefit in the effective management of these ecosystems. Similarly, disaster management planning cannot be effectively implemented unless flood hazard areas are mapped, potential compromised communication routes are identified and safety zones marked out.

Such an approach, termed design flood modelling, requires detailed information on factors such as climatological variables (*e.g.* historical peak flows and design rainfall information), catchment geomorphology (*e.g.* area, shape, hydraulic length and average slope), catchment variables (*e.g.* land cover, surface roughness and soil characteristics) and channel geomorphology (*e.g.* main watercourse length, average slope, surface roughness and drainage density) (Mark and Marek, 2011). Collecting these data and doing detailed topographic surveys (0.5 m interval contours) makes the process a resource intensive one. Taking into account the length of rivers that require floodline determination, an alternative modelling approach would be welcomed.

In the eThekweni Metropolitan Municipality (Durban, KwaZulu-Natal) homestead data (ESKOM 2010) showed that at least 6 500 homesteads were located within the 1:100 year floodline. Future flooding of the same magnitude as the last major floods in 1987 (60 - 100 years return period: Kovács 1988; van Bladeren 1992) would likely affect 30 000 – 40 000 people within this zone. Despite the local eThekweni Municipality having determined such floodlines for their jurisdictional area, there is virtually no floodline data for the rest of KwaZulu-Natal. Therefore the risk to the other 50 municipalities cannot be yet be quantified and remains a major risk.

Even where floodlines are laid out, the unpredictability of floods and their drivers are not always clearly understood. KwaZulu-Natal has 160 years of flood history (van Bladeren 1992) showing that floods have occurred in various parts of the province on different dates and with varying magnitudes of discharge. These floods were the result of meteorological systems driven at a higher level by climatic factors. The implications of this are that floods will have specific distributions in both time and space and their footprints may vary in response to changing climatic regimes. Flooding can thus be unpredictable in where, and the manner in which, it may strike, the consequences of which can be disastrous. For example, in the Republic of South Africa, the January 2011 floods damaged at least 13 000 houses with a death toll of 91 and 321 injured. Preliminary infrastructural damages were estimated to be over ZAR one billion (OCHA 2011) and agricultural infrastructure and crop losses were similarly estimated to be in excess of ZAR one billion (Kendall 2011).

1.1. Research Aims

In light of the above concerns, the aims of this thesis are to:-

- Develop a Geographic Information System (GIS) model based on existing datasets such as 1: 50 000 scale river, water bodies, wetlands, 5 m contour and road network data to produce regional flood routing models to estimate flood elevations.
- Develop a means to calibrate estimated flood elevation surfaces to the elevations of flood deposits measured in the field.

- Aims to provide flood information as a guide without design flood data and to serve as a means to determine target areas for design flood studies.
- Examine the model in the context of flash floods.
- Examine the historical rainfall data to identify previously unrecorded flood events.
- Use the results of the historical analyses to determine areas of greatest flood hazard.
- Use the results of the historical analysis to investigate changes to the storm footprints over time and the overarching climatological factors that may control flood events.

The research undertaken in this thesis is attempting three new approaches to understand floods and their casual climatic drivers:

- Model flood elevations using geological data created by floods as the primary means to calibrate discharge.
- Use historical rainfall data to identify flood related storms and to identify their spatial distribution where flooding is most likely to occur to produce a hazard map.
- Use the storm data characteristics to identify correlations in global climatic cycles to predict future extreme flood events.

1.2. Thesis structure

Chapter 1 introduces the theme of the research, briefly discussing the socio-economic impact of flooding and the constraints on developing countries to provide hazard maps. This chapter also lists the research aims.

Chapter 2 reviews the literature particularly with reference to prediction in ungauaged basins and international and national flood delineation methods (regional and flash flooding).

Chapter 3 discusses the study area and contextualises factors that will influence run-off such as land cover, topography and hydrology. Weather systems that impact on the study area are also reviewed. The documented flood history of the study area is discussed with particular reference to extreme flood events.

Chapter 4 describes methodology and general philosophy of the model to be developed and what data was gathered for the modelling process. Model units and modelled data calibration to field data is discussed.

Chapter 5 discusses the issues of flood markers and flood deposits. Field observation for the five representative areas is also described. The results and observations of the field data is discussed.

Chapter 6 gives a detailed review the Regional Maximum Flood (RMF) peak method and how it is applied in the R.S.A. The need and process of modifying RMF (MRMF) from a method to determine peak discharges at a given point, to a method where peak discharge can be determined for a basin (catchment) area. The results and methodology is discussed.

Chapter 7 reviews flash flooding and presents the modelling results of a basin (catchment) where evidence of flash flooding was observed. The adaption of the MRMF and results of modelling flash flooding is discussed.

Chapter 8 describes the methods used to identify and analyse storms that most likely produced some level of flooding. The results of the analyses for both regional and local storms is presented and discussed. The development of a flood hazard map for the study area is also presented.

Chapter 9 reviews global climatic cycles that have some impact on the study area. The graphed results of mean discharge and annual occurrence of regional storms are compared to various climatic cycles. The correlation between flood producing storms and certain climatic cycles is discussed.

Chapter 10 contains a number of concluding remarks based on the discussions from previous chapters.

CHAPTER 2- LITERATURE REVIEW

2.Literature Review

Storm system duration and rainfall depths produce a continuum of flood-types from localised, short-duration, high-intensity events to long, low to medium-intensity events that cover large geographic areas. Merz & Blöschl (2003) have proposed categorising floods according to distinct processes based on catchment saturation state, dynamics and precipitation. Long-rain floods (*regional floods*) are characterised by rainfall over large areas occurring for several days. This leads to catchment saturation and high flow river conditions. Short-rain floods form from short duration, high intensity precipitation which can saturate a catchment leading to excess run-off and thus producing high flow conditions. *Flash floods*, as defined by Merz & Blöschl (2003), are short, high intensity precipitation events that result in flooding even under relatively dry catchment conditions, where precipitation exceeds infiltration resulting in a rapid catchment response. These events are usually local and effect only small catchments. In this thesis, short-rain floods are grouped with flash floods for discussion purposes as they result from similar meteorological events and are mainly distinguished by the catchment response and antecedent conditions (as discussed in Chapter 7).

Although both long-rain and flash floods are caused by the inability of drainage systems to effectively remove excess run-off from a catchment, the main difference is the timeframe involved in concentrating excess run-off. In KwaZulu-Natal, regional floods last two to five days (Kovács 1988) whereas flash floods occur over periods of hours. Generally, when flooding occurs within 6 hours of a storm event, it is considered a flash flood (Kobiyama & Goerl 2007). In KwaZulu-Natal the highest recorded one day rainfall during a long-rain flood was 548 mm at St Lucia in 1984 during Tropical Storm Domoina (Kovács 1988), whereas a thunderstorm event can produce rainfall depths in excess of 100 mm in an hour (highest recorded 211 mm/h at Ulundi, Republic of South Africa, 2004) (Fashuyi et al. 2006).

A number of factors can affect the highest water elevation or flood peak under flood conditions (Bell 1999; Alexander 2002b). These are climatological factors such as high rainfall regions (Alexander 2002b; Makwananzi and Pegram 2004); climate states such as El Niño and La Niña (Neiff et al. 2000; Franks 2007); weather systems such as thunderstorms (Preston-Whyte & Tyson 1997; Dyson 2009); orographic control on storm systems (Medina 2005; Nel 2008; Prat & Barros 2010); and the location in climatic belts subject to tropical cyclones (Jury & Pathack 1991; Malherbe et al. 2012) and hurricanes (Elsner & Jagger 2008). The direction of travel of a storm system across a catchment can also significantly affect the amount of precipitation that can accumulate (Alexander 2002b). Storms that move downstream in a catchment result in more accumulated precipitation, than storms crossing a catchment perpendicular to the main drainage direction.

Conditions such as antecedent soil moisture conditions also control the amount of run-off (Alexander 2002b; Michele & Salvadori 2002; Norbiato et al. 2008; Javelle et al. 2010). Precipitation absorption by soils can reduce run-off, unless limited infiltration occurs (e.g. Lee et al. 1991; Kirchner 1993). This is known to occur in thin soils or clay-rich substrates (Beven 2004). Evapotranspiration (the loss of water from a catchment due to plant transpiration and evaporation) can reduce antecedent soil moisture conditions (Arnold et al. 1998; SANRAL 2013) thereby reducing run-off. Calculating evapotranspiration can be a complex task (Hughes 2004) and a number of models have been developed for this purpose (See e.g. Arnold et al. 1998) including the use of remote sensing (Mulder et al. 2011). Evapotranspiration is usually calculated as a factor when determining antecedent soil conditions in flood delineation methods and not as a separate factor (SANRAL 2013). Catchment size will also determine the area that can collect precipitation. As the flood peak moves downstream, contributions from other catchments will increase the flood peak. However, the opposite can also occur, attenuating the flood peak and reducing its size downstream (Alexander 2002b). Long, thin catchments will attenuate the flood peak, while short, rounder catchments will increase the flood peak but have a shorter duration (Bell 1999; Alexander 2002b). Catchment shape itself is controlled by factors such as the mean annual rainfall, topography and underlying geology, all of which result in different drainage patterns and drainage density (Bell 1999; Bridge 2003). Lastly, land cover and topography can influence run-off (Mark and Marek 2011). Due to the coverage of paved surfaces resulting in decreased soil absorption, urban areas tend to have higher of run-off when compared to wooded areas (medium run-off) and grasslands (low run-off) (Mark and Marek 2011). Topographically, areas of high relief and steep slopes limit the time available for run-off

to be absorbed by the soil when compared to the shallower slopes on rolling hills or flat land (Mark and Marek 2011).

River and valley morphology may also affect flood peaks. When water moves downhill under the force of gravity steeper slopes will produce greater velocities (Bridge 2003). A slower velocity results in the reduced ability of a catchment to discharge water, causing it to back up and increase flood levels. When drainage lines meander, water flow loses energy and reduces flow. This results in the reduction of river capacity and a similar impoundment of water (James & King 2010). Channel and valley shape typically affect the flood peak elevation where broad channels tend to have little vertical rise compared to horizontal expansion, whereas narrow V-shaped channel will have more vertical rise with little horizontal expansion. Lastly, the length and slope of a drainage line controls the time a unit of water takes to move from the furthest part of a basin to the outflow point, also known as the time of concentration (T_c) (Gericke & Du Plessis 2011). Short time of concentrations result in a rapid rise of the flood peak with flash flooding being the extreme case (Bridge 2003; Gericke & Du Plessis 2011). Ultimately, longer drainage lines will result in a slower flood wave rise and a more rounded flood peak that will last longer.

2.1. Prediction in ungauged basins (Catchments)

It is unlikely that any river or river network will contain river gauges and rainfall stations with records that exceed a hundred unbroken years. As a result, most flood modelling/prediction is done in catchments without any measured historical data. Improving the prediction ability in these ungauged basins is seen as one of biggest challenges for the hydrological community (Norbiato 2008), the International Association of Hydrological Sciences (IAHS) thus embarked on a 10 year initiative to improve Prediction in Ungauged Basins (PUB) (Sivapalan et al. 2003). According to (Sivapalan et al. 2003) the basis of PUB is firstly that the past can be assumed to be a guide to the future and secondly, that data and model results from any given basin can be extrapolated to other basins.

The PUB initiative was based on six themes or target areas of research (Sivapalan et al. 2003). Themes ranged from re-analysing and re-interpreting existing data to producing new models and processes. There was also greater emphasis on climate – soil – land cover interactions. Of particular relevance to this research were the promotion of new data collection techniques such as remote sensing and the expansion in the range of observations beyond those of the normal hydrological monitoring network.

Prediction in ungauged basin flood modelling largely relies on statistical manipulation of rainfall and/or gauge data extrapolated from other catchments. The other commonality between currently used regional flood modelling techniques is that flood risk results are return period based. None of these predictive techniques attempt to determine the maximum risk of flooding. On a similar basis, flood models do not take into account the evidence provided in the geological record concerning historical and geological-term flooding. Sediments that are deposited by floods represent a combination of hydrological, geological and climatic process that record the flood history (Koltermann & Gorelick 1992). Where recorded lengths of historical data are insufficient, statistical methods are not appropriate and sediments deposited during extreme flood events can be used to effectively extend these records (Kochel & Baker 1982).

The characteristics of a catchment and its response to accumulated precipitation are reflected as a line marked out by the elevation of the flood. These lines, termed floodlines, can represent two different functions. The first is the annual exceedance probability (SCC 2013) or return period for a flood with a given discharge size (de Moel et al. 2009). This return period is usually reported as a probability over time (1 chance in 100 years) or a 1% chance of a flood of a certain magnitude discharge occurring every year. Their second function is to display the return period of discharge elevation on a map as a line below which no development may take place. Currently any new development in the Republic of South Africa may not be located within the 1:100 year flood line (Boshof et al. 2005). Any structures crossing rivers, such as roads and pipelines must comply with the Republic of South Africa 1:100 year floodline specifications.

2.2. International flood delineation methods

Internationally, design flood determination methods are often subdivided by the source data used. These are namely rainfall data or data derived from stream flow measurements (Smithers & Schulze 2003; Chetty & Smithers 2005; Smithers 2012). Models derived from rainfall data take into account the spread of rainfall as received from several meteorological stations over several catchments, each of which may have marked differences in slope, soil characteristics and vegetation cover. The continued use of design event models Smithers (2012) is that they provide a single process by lumping together complex parameters, whereby the average of each variable that may affect surface run-off is fed into a model in order to derive the average catchment discharge. This is performed in conjunction with an analysis of the catchment elevation, which has been known to affect rainfall distribution by orographic or topographic control.

Several techniques are available to link rainfall to run-off. Continuous simulation modelling converts historical rainfall data to run-off (Cameron et al. 1999; Blazkova & Beven 2004; Chetty & Smithers 2005; Viviroli et al. 2009; Smithers 2012; SANRAL 2013), by incorporating catchment variables such as topography (basin size, shape, slope, stream pattern, soils and vegetation cover), antecedent soil moisture conditions, developmental influences (land use, surface storage capacity) and climatological factors (rainfall, storm temporal and spatial distribution and climate). This process produces long timeframe hydrographs which can be statistically analysed for peaks in discharge and the probability of their recurrence. A similar technique, the unit hydrograph model, can be used. This assumes an uniform averaged depth of precipitation across a catchment for a selected storm event (UCAR 2010b). The ensuing run-off models are used to determine where excess precipitation has occurred over the time of the storm event thus promoting flooding (UCAR 2010b). The excess precipitation is calculated as an average depth for the catchment and adjusted to a selected unit depth for a particular stream (UCAR 2010b). The unit depth discharge is plotted against duration (the time for one unit of precipitation depth to occur) in order to determine the peak discharge and its duration (UCAR 2010b). This method is widely used particularly in the United Kingdom (Sutcliffe 1978), the United States of America (Ford et al. 2008) and the Republic of South Africa (HRU1/72 1972; SANRAL 2013). Both of the aforementioned techniques are only applicable to large catchments greater than 15 km².

2.2.1. Rational Method – Small catchments

For smaller catchments the Rational Method (using the Rational Formula) is widely used (Weingartner et al. 2003; Faber 2006; Viglione et al. 2010). This is based on storm intensity, storm duration and the time taken for run-off from the furthest extent of the catchment to reach the catchment outflow point (Smithers 2012). This technique is further elaborated on in Chapters 4 and 7 regarding flash flood modelling in small catchments.

2.2.2. Stream flow techniques

Techniques based on stream flow observations use the measured peak discharges from river gauge data; thus producing a frequency analysis of floods based on peak discharge (Mwakalila 2003; Perez-Pena et al. 2009; Ahmad et al. 2011; Smithers 2012). The results are fitted to a probability curve in order to estimate the return period discharges, such as 1:100, 1:50, 1:20 year return periods etc.

Successful stream flow modelling requires an extensive network of gauging systems in the streams comprising a catchment. For any gauge point, the issue of selecting a suitable probability curve can vary with season, storm type and flood duration. This has been questioned by Schulze (1989). This technique also tends to be constrained by record lengths and completeness of the record (Smithers & Schulze 2003). Missing gauge data of stream flow, or records of less than 100 years in length, may not have recorded a maximum peak discharge event (Smithers 2012). As such, this type of analysis can only be performed where a river is gauged and cannot be applied to ungauged catchments (Kjeldsen et al. 2001). Ideally every catchment should have a gauging station with at least a 100 years of recordings (Smithers 2012). However, this is rare in the global context, let alone the Republic of South African one. In the context of this study, the area examined spans 275 catchments, only 130 of which are gauged. Additionally, gauge station records vary significantly as many stations have records of less than 100 years in length.

2.2.3. Regional flood frequency analysis (FFA)

Where catchments are not suitably gauged but stream flow is still considered paramount to modelling, a flood frequency analysis (FFA) of the regional flooding is undertaken. This takes into account several regions (with limited gauge data) that are identified as having similar flood responses and similar physical characteristics such as rainfall, elevation, soil, vegetation cover. (Smithers 2012). Limited gauge data from several sites, as opposed to a single site, are used to estimate the frequency distribution of flooding (Smithers 2012). Many researchers have applied different statistical models to determine the flood probability and frequency distribution, such as L moments (Ahmad et al. 2011), Log-Pearson III (Griffis & Stedinger 2007) and Bayesian distribution (Gaume et al. 2010). The index-flood method, a modified version of the flood frequency analysis (Hosking & Wallis 1997), uses annual maximum flood discharges from various sites to determine a mean *annual* flood probability for homogeneous regions (Kjeldsen et al. 2001; Kjeldsen et al. 2002). An estimated flood discharge return period can then be determined for both gauged and ungauged sites (Kjeldsen et al. 2001; Kjeldsen et al. 2002). It is on this basis that the regional flood frequency analysis is considered the *preferred* method for design flood estimation (Smithers 2012).

2.2.4. Flood envelopes

A final technique that is based on stream flow data is the flood envelope method (Francou & Rodier 1967; Kovács 1988; Biondić et al. 2007; Castellarin et al. 2007). Like the flood frequency analysis, a series of regionally similar zones (otherwise termed homogenous hydrological regions) are used to extrapolate the maximum discharge for all gauge stations that fall within these zones. This is an empirical technique whereby the global averages for catchment size and discharge (based on homogeneous hydrological regions) have been used to create a series of standard curves or envelopes (Francou & Rodier 1967). It is then possible to extrapolate the maximum discharge based on the measure of the independent variable which is the upstream catchment area. This is termed the Regional Maximum Flood discharge (RMF). Kovács (1988) has further refined this technique by applying a statistical probability function used for skewed data distributions known as the Log-Pearson III to define the flood return period discharges based on the Regional Maximum Flood discharge (RMF) values derived using the flood envelopes.

2.3. Floodline determination in the Republic of South Africa

There is no standard design flood estimation technique accepted for the Republic of South Africa (Smithers 2012); the techniques mentioned in the previous sections are often widely applied. Figure 2.1 summarises the various design flood estimation techniques in use in the Republic of South Africa. The most widely used of these is a modified version of the unit hydrograph technique, the HRU1/72 approach. Like the international examples, this uses *design rainfall* (rainfall data used for the interpolation of flood design parameters) to generate synthetic unit hydrographs from which discharges are estimated. Smithers & Schulze (2003) have produced an updated method, available as a computer programme, from which design rainfall can be extracted for any catchment in the Republic of South Africa. Additional modelling can therefore be made using these data.

In the Republic of South Africa, design flood determination has also been subdivided according to three main approaches; namely deterministic, statistical and empirical (Table 2.1). For a comprehensive review of these techniques, the reader is referred to the works of several authors (Zawada et al. 1996; Hughes 2004; Pegram & Parak 2004; van Bladeren et al. 2007; Benjamin 2008; Prinos 2008; Smithers 2011; Smithers 2012; SANRAL 2013).

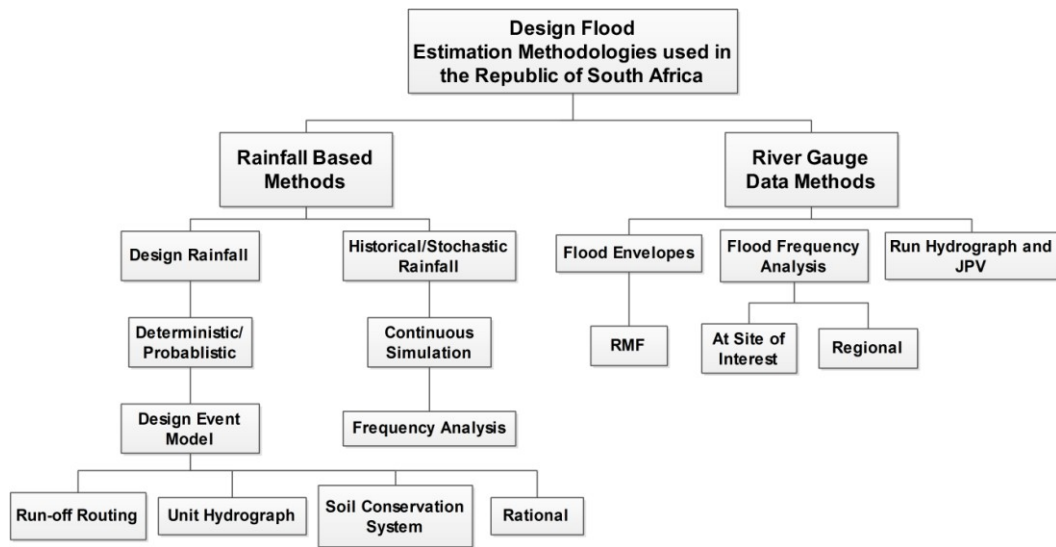


Figure 2.1. Chart of design flood determination types (After Smithers & Schulze 2003).

Deterministic methods use rainfall input and catchment characteristics to determine run-off discharges (e.g. Pegram & Parak, 2004) such as the Rational Method and the Unit Hydrograph. Empirical methods use measured flood discharges related to catchment area to estimate the regional maximum flood peak (RMF) envelopes for a specific geographic area (e.g. Kovács 1988). The advantages and disadvantages of each technique are listed in Table 2.2.

Table 2.1 Summary of design flood determination methods used in the Republic of South Africa. (After Smithers 2012; SANRAL 2013)

Data source	Type	Method	Input data	Recommended maximum area (km²)	Return period range (years)
Run-off	Statistical	Statistical Frequency distribution analysis	Historical flood peak records	No limitation (larger areas)	2 - 200 (depending on record length)
Rainfall	Deterministic	Rational Methods	Catchment area, water course length, average slope, catchment characteristics, design rainfall intensity	Usually < 15, depends on method of calculating rainfall intensity	2 - 200, PMF (probable maximum flood)
Rainfall	Deterministic	SCS-SA method	Design rainfall depth, catchment area, Curve Number (soils, land cover), catchment lag	< 30	2 - 100
Run-off	Deterministic	Unit Hydrograph method	Design rainfall, catchment area, watercourse length, length to catchment centroid (centre), mean annual rainfall, veld type and synthetic regional unit hydrographs	15 - 50000	2 - 100, PMF (probable maximum flood)
Run-off	Deterministic	Standard Design Flood (SDF) method	Catchment area, watercourse length, slope and SDF basin number	No limitation	2 - 200
Run-off	Empirical	Empirical methods	Catchment area, watercourse length, distance to catchment centroid, mean annual rainfall	No limitation (larger areas)	10 - 100, RMF (regional maximum flood peak)

2.4. Flash flood determination

A significant component of flash flood research is the aim to develop an early warning system (Grunfest and Ripps 2000; Dyson & Heerden 2002; Du Plessis 2002; Gupta et al. 2002; Anquetin et al. 2004) or 'Nowcasting System' (Makwananzi & Pegram 2004; Pegram et al. 2007). The objective of this is to provide a warning of up to at least 24 hours prior to the event (Mcenery et al. 2005; Blöschl et al. 2008). Du Plessis (2002) recommended an integrated flood

forecast, warning and response system (FFWRS), an element of which is accurate flood hazard mapping. Hydrological models in combination with hydraulic flood routing modelling can produce flash flood inundation maps which are an important component of flash flood forecasting and warning systems (UCAR 2010a). As valuable as early warning systems are, KwaZulu-Natal and the Republic of South Africa have no mapped inundation data available that demarcate flash flood risk areas to guide development in the same way as 1:100 year design flood estimates.

Table 2.2 Advantages and disadvantages of deterministic, statistical and empirical flood modelling techniques

Method	Advantage	Disadvantage
Deterministic	Integrates many variables that impact on run-off. A holistic approach (Kovács 1988). Easy to apply and use (Pegram & Parak, 2004).	Many of the variables are unknown and often difficult to quantify (Kovács 1988). Usually valid for smaller catchments < 15km ² .
Statistical	If gauge data are available over a long period and are complete it can provide a best flood probability estimate (van Bladeren et.al 2007). Data can be easily obtained (van Bladeren et.al 2007).	Problematic if there are gaps in the data or extreme flood events are not recorded (Zawada et.al 1996). Can be applied to any catchment size (Alexander 2002a).
Empirical	Based on a large flood peak database for Southern Africa (Kovacs, 1988; Zawada et.al 1996).	Boundaries of homogenous zones may be vague (Kovács 1988). Not reliable for catchments < 100km ² (Kovács 1988).

Flash flooding, as a distinctly different mechanism for flood generation, poses several different challenges in the modelling of its recurrence interval and also its maximum regional extent. Flash floods are typically produced by thunderstorms and as such can be described as common localised events which can have an impact on people and property in small geographic areas (Foody et al. 2004; Carpenter & Georgakakos 2006; Ntelekos et al. 2006; Kobiyama & Goerl 2007; Kim & Choi 2011). To illustrate this point, flash floods account for 96% of the flood-related infrastructural damage, deaths and injuries worldwide (2003 - 2005) (HRC 2012). World

death tolls from flash flooding alone are in the order of 5 000 people per year (HRC 2012) and thus pose a significant threat to humans.

The different meteorological processes and timeframes involved in long-rain floods and flash floods imply that peak discharge estimates cannot necessarily be applied to all flood types. Neither rainfall data nor gauge data are of the temporal resolution that can adequately portray a flash flood episode (Creutin et al. 2003). It is clear that the data available (either rainfall or stream gauge) are not capable of calculating the flow hydrographs at a level of detail sufficient to analyse the hydrology of these events. However, weather radar networks have increased the ability to monitor rainfall distribution at much shorter temporal scales (Borga et al. 2008) and can thus be incorporated into flash flood hydrological models.

Flash flood hydrological models are divided into three types based on the level of detail used to define the catchment parameters. Lumped models, such as the continuous simulation and unit hydrographs techniques, reduce the spatial variables to a single value assuming uniform catchment conditions (Paudel 2010). Alternatively, models can be *distributed* where more than one spatial variable is incorporated, particularly when catchment conditions can subtly vary (Johnson & Miller 1997; Reed et al. 2007; Blöschl et al. 2008; Vischel et al. 2008). It is argued that distributed (as opposed to lumped) hydrological models provide better results over larger catchments with greater heterogeneous hydrological characteristics (Kajami et al. 2004; Carpenter & Georgakakos 2006; Paudel 2010). Advances in remote sensing which can provide more detailed observations of the soil characteristics (Mulder et al. 2011), land cover, weather radar (Borga et al. 2008) and satellite storm tracking systems (Grunfest and Ripps 2000; Blöschl et al. 2008) can provide more refined temporal and spatial data. This has sufficient resolution to make distributed models a better choice for flash flood forecasting (UCAR 2010a).

Where only coarser resolution data are available, or when catchments are divided into smaller units and the sub-catchments are assumed to have uniform parameters, a semi-distributed model can be used (Kajami et al. 2004; Paudel 2010). Irrespective of which modelling approach is used, certain parameters such as rainfall intensity, run-off coefficient, the time of water concentration, soil conditions and land cover need to be measured or inferred. The run-off coefficient itself is a subjective estimate (Pegram & Parak 2004) of the factors contributing to

water (rainfall) retention in a catchment that reduce the water volume that will reach a drainage line and contribute to channel flow. The main factors to consider are soil properties, land cover and catchment characteristics (Alexander 2002b; Smithers & Schulze 2003; Parak & Pegram 2006; Ntelekos et al. 2006; WSUD 2012).

2.5. Flood marks

When flooding occurs, irrespective of flood elevation, it will leave some form of evidence on the landscape known as flood marks. Use of flood marks to determine flood elevations have mainly been used in the case of flash flooding (Anquetin et al. 2004; Naulet et al. 2005; Lumbroso et al. 2008; Balasch et al. 2011). Depending on what forms the flood mark is (See Chapter 5 for detailed descriptions of flood marks), their continued existence on the landscape varies so that flood marks can only be mapped where they are still extant (Balasch et al. 2010). Flood marks have also been used to map out flood levels directly after a flood event as part of a post-flood survey (Gaume & Borga 2008). There has been no literature found that uses the highest elevation flood marks to improve regional flood modelling except for Büchele et al. (2006) who attempted to incorporate flood marks into their design flood return period estimates. They (Büchele et al. 2006) also made a very important observation that the observed flood marks in their study area exceeded the estimated 1:100 year design flood protection structures.

Data on paleofloods (old flood events unrecorded by humans (Baker 2008)) have been used in attempts to extend flood records, particularly extreme events (e.g. Zawada 1997; Castellarin et al. 2005; England Jr. et al. 2007). The interpretation of paleoflood data should perhaps be tempered with caution because they may have occurred during periods of different climates, perhaps where there were phases with higher flood frequency and increased erosion than historical/modern times (Baker 2008).

CHAPTER 3 – STUDY AREA

3. The Context of the Study Area

KwaZulu-Natal (KZN) is located in the eastern part of the Republic of South Africa (RSA) (Fig. 3.1) and is the third smallest province with a surface area of 93 350 km². It has the third largest population in the country at 10.5 million, comprising about 21% of the overall population (StatsSA 2009). KwaZulu-Natal comprises one metropolitan municipality (eThekweni – Durban) and 10 District Municipalities, which in turn are made up of 54 Local Municipalities (Fig. 3.1).

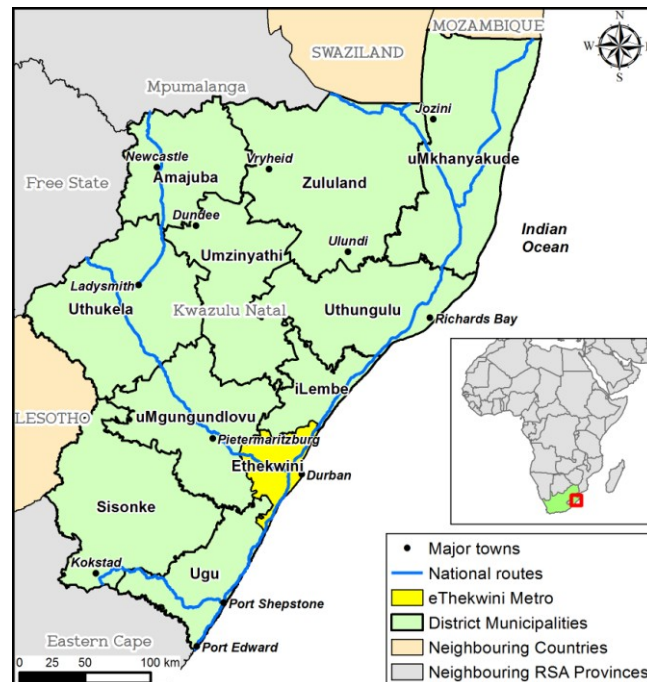


Figure 3.1. Locality map of KwaZulu-Natal showing political and municipal boundaries, major towns and the national road network (Data MDB 2011).

3.1. Land Cover

In general the land cover/land use of the province comprises 5 main elements (Fig. 3.2A). Commercial agriculture (grasslands and cultivation) (39.4%) and urban and traditional settlements (37%) comprise 76.4% of the total land cover of KwaZulu-Natal. As this land is generally not in its natural state, it has reduced precipitation retention and is subjected to the risk of increased runoff.

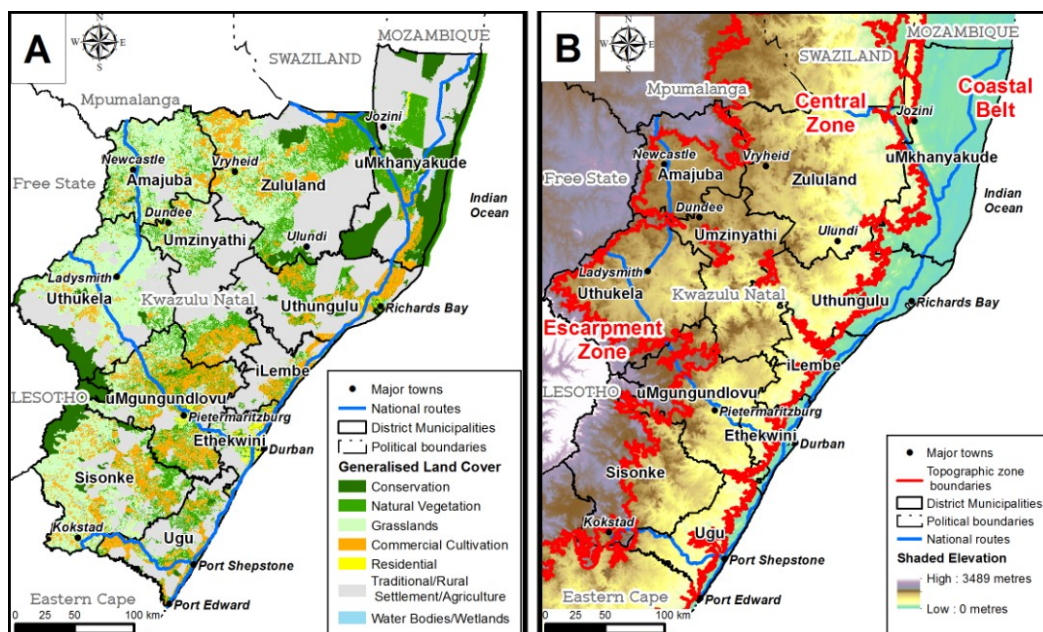


Figure 3.2. (A) Generalised Land cover map of KwaZulu-Natal. (B) Digital elevation model of KwaZulu-Natal showing the three major topographic zones (Data A - EKZNW (2011). B - ASTER (2010)).

3.2. Topography

Topographically, the study area can be divided into three zones (Fig. 3.2B):-

- The coastal belt is a narrow zone, broadening from south to north. It typically ranges from sea level to an elevation of 200 m.

- The central zone is parallel to the coastal zone. In the eastern portion it consists of rolling hills while in the west it is made up of large flat areas interrupted by residual hills. This zone ranges in elevation from approximately 200 m to 1 400 m.
- The escarpment zone is situated in the western part of the study area. It is typified by deeply incised valleys. The elevations range from approximately 1 400 m to 3 500 m.

3.3. Soil depth and drainage capacity

Soil development in the study area is typically thin with the bulk of the area having soil depths of < 100 mm (Fig. 3.3A). Scattered areas have deeper soil development, but these are in the minority. The deepest soil development occurs along the northern coastal belt.

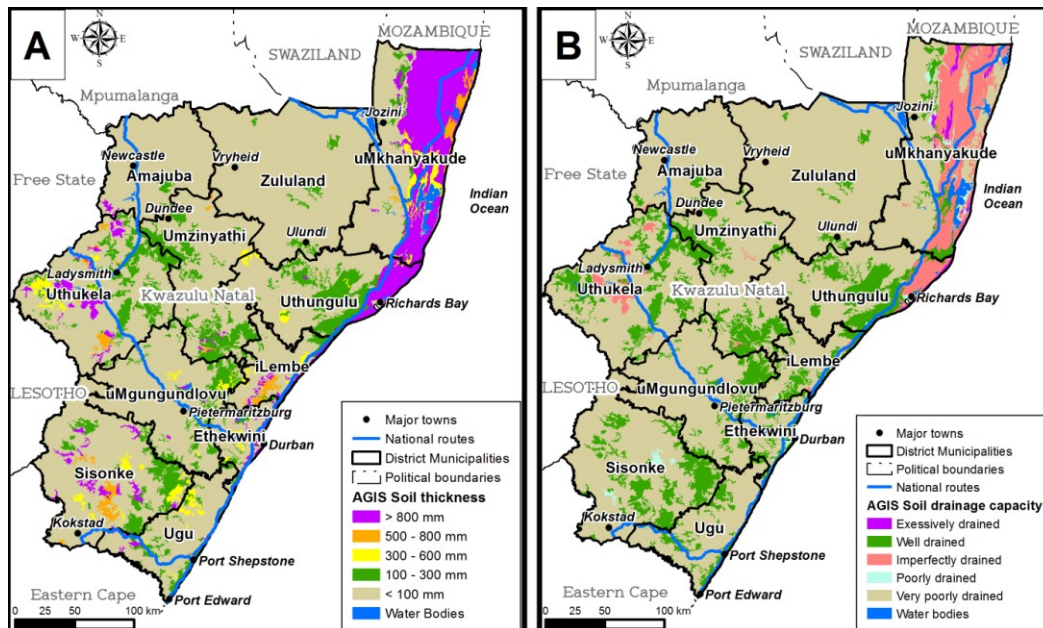


Figure 3.3. (A) Soil thickness for KwaZulu-Natal. (B) Drainage capacity for KwaZulu-Natal (After AGIS, Schoeman et al. 2002)

The Agricultural Geographic Information System (AGIS) data (Schoeman et al. 2002) also show that most of the study area soils are very poorly drained with a similar distribution to that of the soil depths (Fig. 3.3B). The thin soil development and very poor drainage capacity implies that soils will take up a relatively small percentage of precipitation before they are saturated. Most of the precipitation will thus be converted to run-off.

3.4. Hydrology

The rivers in the study area generally flow from west to east (Fig. 3.4A). Drainage follows a dendritic pattern with smaller streams feeding progressively larger rivers. Drainage length is 198 550 km, with main drainage lines totalling a length of 12 320 km. Drainage density (total length of rivers divided by the total area drained) is 2.12 km/km². This drainage density value is associated with vegetated humid areas where the values of up to 10 km/km² can occur (Bridge 2003).

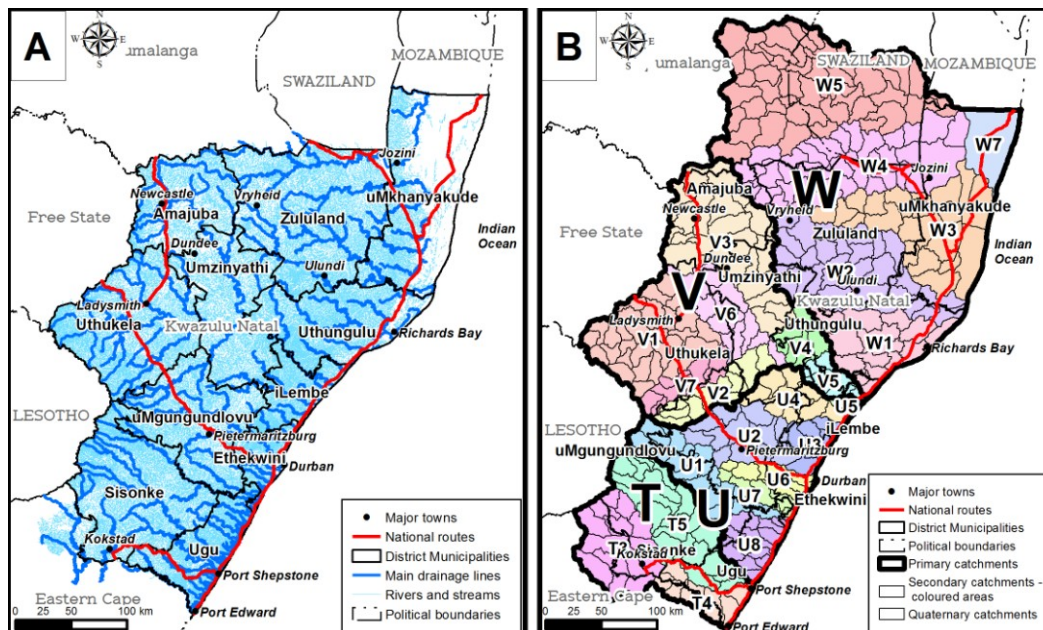


Figure 3.4 (A) Drainage lines of KwaZulu-Natal. (B) Primary catchments of the study area. Coloured areas represent the secondary catchments (Data A - DWA (2008) Data B - (MDB 2011)).

In the Republic of South Africa, drainage basins and sub-basins are named according to a hierarchical order. These are referred to as primary, secondary, tertiary and quaternary catchments. Primary catchments define the overall drainage basins of major rivers and are labelled alphabetically (A, B, C,...). Secondary catchments are labelled numerically (A1, A2, A3,...). Tertiary catchments are also labelled numerically (A10, A11, A12,...). Quaternary catchments are labelled alphabetically (A1A, A10B, A10C, ...) (Fig. 3.4B).

The study area of this thesis comprises a portion of the T, U, V and a portion of the W primary catchments. The Mtamvuma, Mgeni, Tugela and Pongola Rivers drain these primary catchments respectively. Modelling in this study is aimed at the level of the quaternary catchment, of which the study area consists of 275 of these.

The combination of thin (75.3% of study area) poorly drained soils (76.5% of study area) and land cover conditions (76.4% of the study area) that do not promote runoff retention are a large contributor to the amount of excess runoff generated under storm conditions. With the longest distance from the start of the primary catchments to the ocean being only 270 km (a gradient of 13 m/km), drainage distances are relatively short. The result is that catchments in the study area have limited ability to attenuated flood waters (as discussed in Chapter 2).

3.5. Rainfall and climatic systems

The various planetary and mesoscale atmospheric circulation systems interact in such a way that repeatable weather systems are created. Eleven such weather systems that affect Southern Africa have been identified (Tyson, 1986), of these seven can produce significant quantities of rainfall that can result in flooding. These are Easterly Waves and Tropical/Subtropical Lows, Westerly Waves and Cut-off Lows, Thunderstorms and Tropical Cyclones/depressions. All these systems produce summer rainfall (November to February), however the Cut-off Lows most often associated with flooding (Preston-Whyte & Tyson 1997) predominate from September to May. It must be noted that any one of these systems can overlap on the same day,

making it difficult to distinguish between the system predominantly responsible for the rainfall (Tyson 1986). These weather systems are summarised in Table 3.1.

Table 3.1. Weather systems of Southern Africa (After Tyson 1986). The light grey shading indicates weather systems which may produce flooding. Dark grey shading represents cut-off lows most associated with flooding (Preston-Whyte & Tyson 1997)

Circulation Direction	Weather System	Description	Rainfall	Region	Period
Easterlies	Waves	Travelling cyclonic waves	Heavy rains	Eastern portion of Southern Africa	December to January
	Tropical Lows	Associated with the Inter-Tropic Convergence Zone	Heavy rains that may last a few days	Eastern and central portion and Southern Africa	December to January
	Subtropical Lows	Associated with strong anticyclonic circulation over the continent	Can produce heavy rainfall	Various parts of Southern Africa	September to March
Westerlies	Waves	Travelling anticyclonic waves	Can produce heavy rainfall	Southern Coastal area	October to April but concentrated October to November and January to March
	Cut-off Lows	Intense closed circulation unstable depression	Heavy rainfall associated with flooding		March to May and September to November. Lower frequency December to February
	Ridging Anticyclones	Advection of moist air from the Indian Ocean over the land	Widespread general rainfall	Eastern parts of Southern Africa	October to February
	Southerly Meridional Flow	Circulation pattern over the southern ocean with a strong pressure gradient from west to east	Light rains	Coastal belt	September to November
	West Coast Troughs	Low pressure system off the western coast of Southern Africa	Widespread general rainfall	Western and Central Southern Africa	December to March
	Cold Fronts	Movement of cold air from the south in winter producing cold weather	Dry conditions preceding the front with possible serve weather behind the front	Southern Africa	April to August
Thunderstorms	Thunderstorms	Associated with many weather systems that will allow of local convection systems	Intense localised rain	Southern Africa	November to January
Tropical Cyclones	Tropical Cyclones/Depressions	Develop in the Indian Ocean and recurve south. May follow Mozambique Channel	Intense concentrated rain along storm path	Eastern and South-eastern coastal region	December to March

3.5.1. Monthly prevalence of weather systems

Tyson (1986) compiled a series of weather system frequency observations first made by Vowinckel (1956) and Taljaard (1982). These data are reproduced graphically in Figure 3.5.

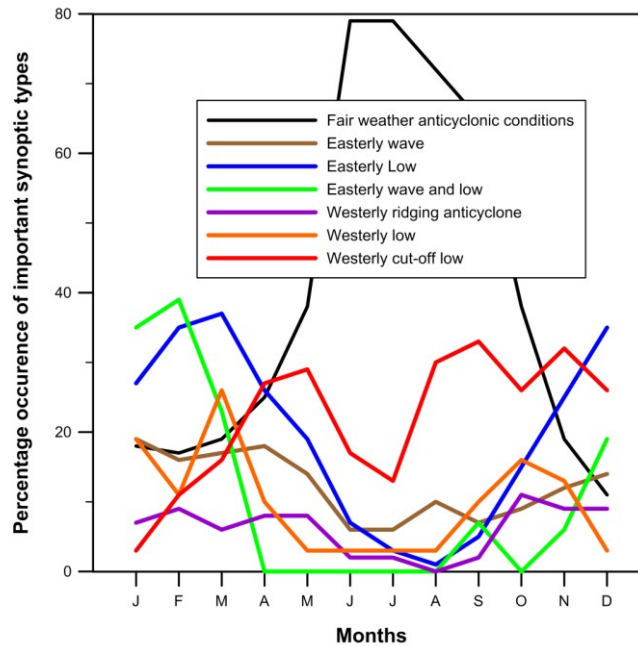


Figure 3.5. Graph of synoptic weather system frequencies over the eastern part of the Republic of South Africa (After Tyson 1986).

These data show that the Easterly air flow predominates in the period from October to April mainly in the form of Easterly lows and Easterly waves and lows. Westerly air flow weather systems are less prevalent compared to the Easterly air flow. The Westerly weather systems tend to have higher frequencies from September to November and February to April. Westerly cut-off lows predominate from March to November.

3.5.2. Small to medium scale weather systems

Small to medium scale weather systems can also have a significant impact by producing rainfall that results in flooding. Tropical cyclones and tropical depressions have produced extensive flooding along the eastern portion of Southern Africa. Localised thunderstorm activity can similarly produce copious amounts of rain in a short space of time, often leading to flash floods.

3.5.3. Tropical cyclones and tropical storms

Tropical cyclones form in the Indian Ocean and follow a westerly path which curves south and can affect the Republic of South Africa when they cross over Madagascar or move south down the Mozambique Channel (Fig. 3.6) (Preston-Whyte & Tyson 1997). These develop as weak low pressure cells that develop into well-defined high intensity low pressure cyclonic systems. Tropical cyclones develop in summer and autumn and can last between two and eight days (Preston-Whyte & Tyson 1997). The high wind speeds and copious rainfall associated with these systems make them very destructive (Preston-Whyte & Tyson 1997). When tropical cyclones encounter a land mass they slow down and degrade from cyclones to tropical depressions. Tropical storms have lower wind speeds but still produce significant volumes of rain.

According to Jury & Pathack (1991), on average 11 tropical cyclones/tropical storms develop during a South West Indian Ocean (SWIO) cyclone season. Only a limited number make landfall where they deflect north or south or continue west (Malherbe et al 2012). The bulk of the tropical cyclones/tropical storms that make landfall do so along central Mozambique and move inland into the Republic of South African Lowveld region. Malherbe et al (2012) documented 43 tropical cyclones/tropical storms that made landfall between 1948 and 2007. In the same period only three tropical cyclones/tropical storms made landfall that affected the KwaZulu-Natal study area (Claude, 1966; Eugenie, 1972 and Domoina, 1984) (Kovács et al. 1985; Preston-Whyte & Tyson 1997; JTWC 2014).

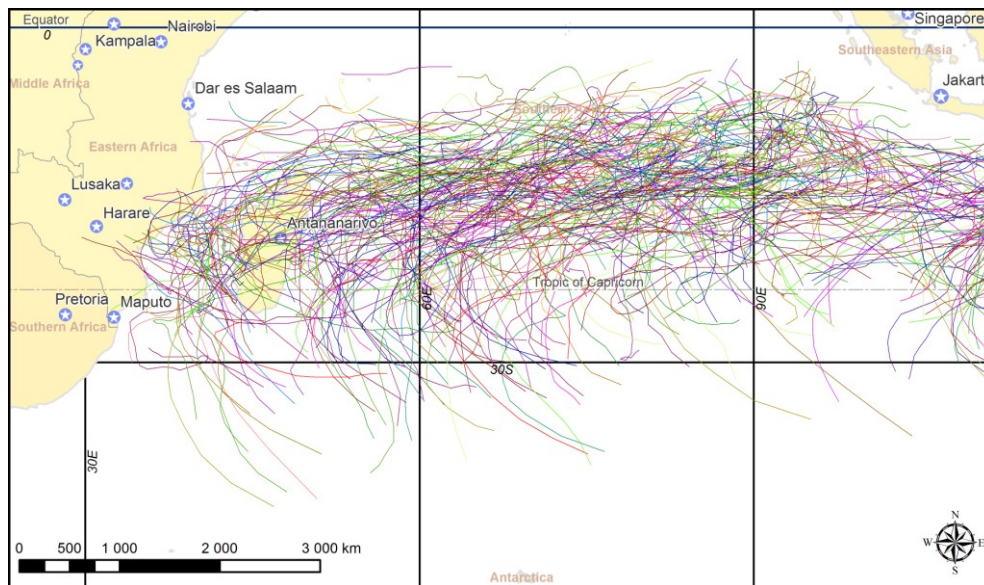


Figure 3.6. Tropical cyclone tracks in the SWIO (1982 – 2013). Coloured lines represent different annual tracks. Data from the Joint Typhoon Warning Centre (JTWC 2014).

3.5.4. Thunderstorms

Thunderstorms can range from single cells to multi-cells (Preston-Whyte & Tyson 1997). These may take the form of line storms, scattered cells or isolated single cells (Preston-Whyte & Tyson 1997). These storms are formed by vertical uplift of air resulting from localised surface heating. Multi-cell storms are the result of surface heating and mesoscale air mass circulation (Preston-Whyte & Tyson 1997).

Single cell storms usually cover a small geographic area (5 – 10 km) and last less than an hour (Preston-Whyte & Tyson 1997). Apart from localised surface heating, daytime upslope winds also produce horizontal convergence and vertical uplift (orographically driven). As the warm air rises it expands and starts to cool and water vapour condenses (Preston-Whyte & Tyson 1997). Precipitation particles grow while being supported by the updraft. When the updraft cannot support the weight of the particles and precipitation occurs. The falling particles force a downdraft to develop creating cooling and unstable conditions and increasing wind speeds

(Preston-Whyte & Tyson 1997). Rainfall can exceed 100 mm/hour during the storm (Preston-Whyte & Tyson 1997).

Multi-cell thunderstorms can be 30 - 50 km in extent and develop as single cell storms merge or develop as a grouping of cells within a storm (Preston-Whyte & Tyson 1997). The multi-cell storm systems can last many hours and can similarly produce rainfall in excess of 100 mm/hour (Preston-Whyte & Tyson 1997). Thunderstorms (either single or multi-celled) can result in flash flooding and thus have a large potential impact over a small geographic area (Foody et al. 2004; Carpenter & Georgakakos 2006; Ntelekos et al. 2006; Kobiyama & Goerl 2007; Kim & Choi 2011).

3.6. Flood history of the Republic of South Africa

Complete records reflecting flood history of the Republic of South Africa can indicate in which season floods are most likely to occur, which catchments are most likely to be affected and what peak discharges can be expected. Mapped storm rainfall isohyets can be invaluable in the determination of the flood producing storm footprints and can also help to define the spatial distributions and geographic repeatability of these storm systems. There are two sources of historical flood events in KwaZulu-Natal. The South Africa Weather Services (SAWS 1991) documents extraordinary weather events including floods and heavy rain events, but often the details on the spatial extent and duration of the event are unavailable. Van Bladeren (1992) documented extreme flood events from 1848 to 1989 based on the magnitude of gauge discharge data. Available rain gauge data, discharges, affected rivers and flood return periods were also documented. Van Bladeren (1992) used the sixth largest discharges per river to define his extreme flood events. These sources have not always recorded small to medium flood events and consequently there is no comprehensive flood history documented for KwaZulu-Natal. A compilation of the South Africa Weather Services (SAWS 1991), van Bladeren (1992) data and internet sources lists a total of 123 flood events from 1848 to 2000 (Appendix I). In comparing the historical flood data (SAWS 1991, internet sources) for the Republic of South Africa from 1652 to 2010, this shows that KwaZulu-Natal and the Western Cape are the provinces with the highest incidences of flooding (Table 3.2).

Table 3.2. Comparison of recorded floods per province (SAWS 1991, Internet and newspaper sources)

Province	Recorded events
KwaZulu-Natal	125
Western Cape	121
Gauteng	61
Eastern Cape	50
Mpumalanga	26
Northern Cape	26
Free State	22
Limpopo	11
Multi Region	11
North West	9
TOTAL	462

3.7. Extreme flood events

Van Bladeren (1992) identified 34 flood events when using gauging station records. He classified 19 of these flood events as extreme floods (Table 3.3). In comparing the peak discharges for the extreme events (Fig. 3.7), it is clear that these range from approximately 1 000 m³/s to 12 000 m³/s. Overall, there are 10 extreme events that exceed 4 000 m³/s.

**Table 3.3. List of extreme flood events in KwaZulu-Natal (KZN) (1891 – 1989)
(After van Bladeren 1992). Grey shading indicates extreme flood with discharges
> 4000 m³/s**

Year	Month	Start Date	End Date	Days	Geographic Area
1891	March	15 March 1891	16 March 1891	2	Durban, Richards Bay
1893	January	3 January 1893	3 January 1893	1	Durban
1905	May	30 May 1905	01 June 1905	3	South Coast, Durban to Richards Bay
1908	April	17 April 1908	19 April 1908	3	South Coast, Durban to Richards Bay
1913	March	03 March 1913	08 March 1913	5	Scattered across Southern KZN
1917	October	25 October 1917	29 October 1917	5	Southern KZN
1918	February	13 February 1918	17 February 1918	5	KZN
1925	March	07 March 1925	20 March 1925	14	South to North KZN
1932	February	19 February 1932	22 February 1932	4	KZN
1940	May	04 May 1940	06 May 1940	3	South Coast, Central KZN
1959	May	16 May 1959	18 May 1959	3	Southern KZN
1963	July	02 July 1963	05 July 1963	4	Northern KZN
1974	February	04 February 1974	08 February 1974	5	Scattered Locations, KZN
1977	February	05 February 1977	07 February 1977	3	Coastal Belt
1978	April	19 April 1978	23 April 1978	5	South Coast
1984	January	28 January 1984	01 February 1984	5	Northern KZN
1985	February	07 February 1985	10 February 1985	4	KZN
1987	September	25 September 1987	30 September 1987	6	KZN
1989	November	28 November 1989	01 December 1989	4	KZN

KwaZulu-Natal has the largest number of recorded flood events in the Republic of South Africa (Table 3.2) in seeming contradiction to Van Bladeren's (1992) number of flood events. This discrepancy appears to be a common problem in the Republic of South African flood records. The South Africa Weather Services (SAWS, 1990) compilation is based on reports from various sources with no attempt at estimating the discharge magnitude. Nor is there clarity on whether these floods were regional or of a flashy nature. The nature of Van Bladeren's (1992) research aimed at identifying extreme flood events and hence made little attempt to identify lesser magnitude flood events. These leave a gap in the current knowledge regarding KwaZulu-Natal's flood history, and thus one of the main aims of this thesis is to address this.

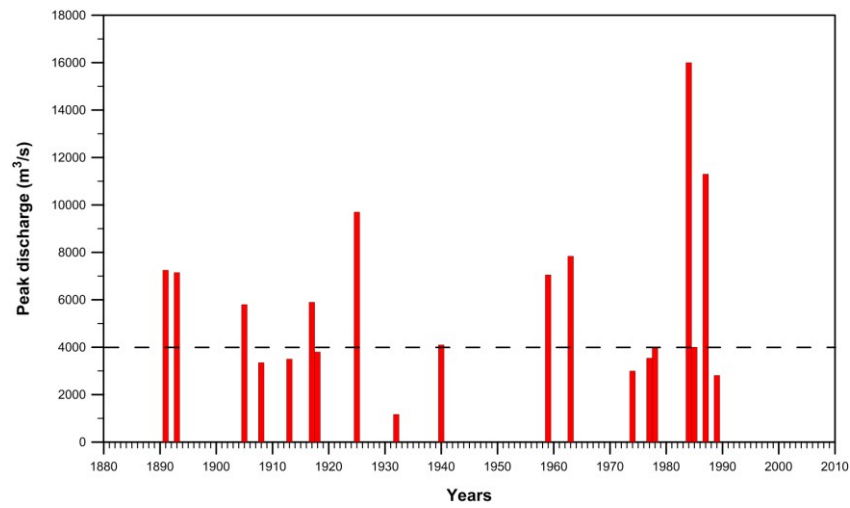


Figure 3.7. Peak discharges for extreme flood events (After Van Bladeren 1992).
The dashed black line marks the 4 000 m³/s discharge line.

CHAPTER 4 - METHODOLOGY

4. Introduction

As discussed in the introduction, design flood modelling requires numerous and detailed data, the collection of which is time consuming, costly and often not possible to achieve to a degree that would satisfy typical model constraints. Coupled with the length of rivers in KwaZulu-Natal (KZN) that still require floodline determination, an alternative modelling approach is investigated in this thesis that can produce acceptable results with the benefit of requiring less detailed information.

4.1. General modelling philosophy

The modelling technique developed here is based on two main premises, firstly that the geological record in the form of the highest elevation flood deposits equates to the largest discharge recorded. Measurement of flood deposit elevation can then be used as a means to calibrate the model. Secondly, that a large component of the modelling can be based on existing GIS software and GIS datasets already available in the public domain. The detailed modelling steps are set out in Appendix II.

4.2. GPS Mapping

Field mapping of flood deposits were mapped using a sub-metre differential GPS system. The data were captured directly into GIS using ArcPad® GPS software and located on a series of digital elevation models (DEM) in order to assess the spatial distribution of flood deposits.

4.3. Homestead surveys

Homestead surveys were carried out along river courses to identify homesteads that had been affected by flooding in the past. The term homestead used here refers to an extended family unit of clustered structures. Homestead survey information was obtained from an independent socio-economic homestead survey (January 2010) undertaken in the study area by a provincial government department. Three flood related questions were accommodated in the questionnaire. Homesteads were asked:-

- 1. If they have been flooded before?
- 2. How long ago this occurred (> 1, >5, > 10 years)?
- 3. Could they point out the flood water level?

The results are presented in Appendix III.

4.4. Modelling units

The smallest delineated catchments at a national level are the quaternary catchments. Quaternary catchments were chosen as a modelling unit because they form discrete spatial areas that allows for reasonable computer processing times at high levels of detail. Five representative quaternary catchments (T40G, U20H, T52D, V12G, and W23A) were used to develop the model (Fig. 4.1). They were selected on the basis of either having some updated design floodline estimates, they had well preserved physical flood evidence, or there were areas where

settlements had clearly been affected by periodic flooding and historical accounts were available (such as in the homestead surveys; Appendix III). Descriptions of these quaternary catchments can be found in Table 4.1. An additional 11 quaternary catchments (T40A, T40B, T40C, T52C, U10M, U20M, U30D, W12E, W12F, W12H and W12J) have been modelled where design flood estimates (1:100 year return periods) were available (Fig 4.1).

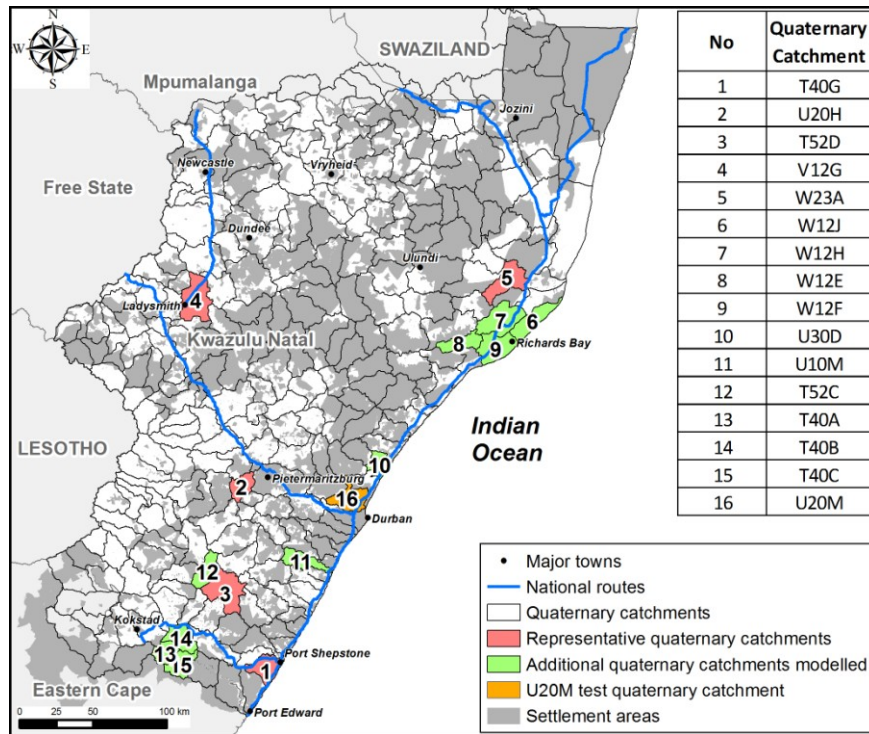


Figure 4.1. Map of KwaZulu-Natal showing representative and additional quaternary catchments in relation to settled areas. The U20M quaternary catchment (No.16) shows the location of the blind test area (See Chapter 6, Section 6.3.3.

Table 4.1. Description of the five representative quaternary catchments used for the model development.

Municipal area/s	The Msunduzi and Richmond	Emnambithi/Ladysmith	Umzimkhulu; Umzumbe and Ubuhlebezwe	Hibiscus Coast and Ezingoleni	Mbonambi; Hlabisa and Mtubatuba
Quaternary catchment	U20H	V12G	T52D	T40G	W23A
Quaternary catchment area	220 km ²	509 km ²	530 km ²	300 km ²	413 km ²
Upstream catchment area	No upstream catchments	1 643 km ²	3 640 km ²	No upstream catchments	8 840 km ²
RMF estimated discharge	1 931 m ³ /s	4 639 m ³ /s	7 926 m ³ /s	2 855 m ³ /s	16 792 m ³ /s
Homestead estimate	17 000 homesteads	13 100 homesteads (Excluding formal area of Ladysmith)	9 300 homesteads	11 500 homesteads (Excluding formal area of Port Shepstone)	8 800 homesteads
Estimated homesteads within flood zone	653	500	400	600	500
Land use	Formal urbanisation and industry. Large portion is dense low cost development and informal and traditional settlement.	Predominantly commercial agriculture with a mix of urban and rural settlement.	Mainly a mixture of traditional settlement and agriculture.	The area has a mix of formal urban settlement and low cost housing development, agriculture and traditional settlement.	Predominantly traditional settlement with minor urban settlement and agriculture
Selection criteria	Area has a history of flooding. The Edendale area is under pressure for further development and settlement densification with associated encroachment into flood risk areas. This site is selected to test the model in a dense urban/peri-urban environment.	There is a long flood history. This site is selected to test the model against engineering flood line data and to measure its performance in broad, low relief valleys. Also tests within an informal densification area.	There are recent flood line calculations available to test against. This site is selected to test the model in predominantly hilly terrain.	There are some recent engineering flood line calculations available to test against. This is also a coastal catchment. This area is selected to test the model on a developed coastal catchment and the inland settlement densification in progress.	The site is selected to test the model along a major drainage line, contrasting traditional settlement areas situated on undulating hills and settlement development around Kwamsane. The area has an extensive flooding history.

4.5. Flood methodology

This thesis focuses on developing its own model for flooding, hereafter termed the Flood Zone Model (FZM) (as described in Botes et al. 2010; Botes et al. 2011). This has been developed as a planning and disaster management modelling tool to estimate regional maximum and 1:100

year return period flood elevations. The Flood Zone Model aims to provide flood information as a guide for areas without design flood data and to serve as a means to determine target areas for detailed design flood studies. This is a rapid and cost effective approach to delineate flood zones at quaternary catchment level using limited resources. The hydraulic component of the Flood Zone Model utilizes existing GIS data (1:50 000 Surveyor General (SG) 5 m and 20 m contour data) to construct 10 m digital elevation models for a quaternary catchment. Digital elevation models are reprocessed using ArcHYDRO Tools[®] (Maidment 2002) to level out areas for water bodies, enforce drainage paths and eliminate sinks (holes in the digital elevation model surface where water can flow into but not out of) to produce a final hydrological drainage surface. The hydrological digital elevation model is used as a base to determine water flow direction and accumulation to delineate 2 km² sub-catchments and river reaches (river segment between tributaries). Cross-sections placed at approximately 50 m intervals or less, depending on slope and topographic features, are used to extract valley profiles from the hydrological digital elevation models.

The hydrological component of the Flood Zone Model is derived from the Regional Maximum Flood peak (RMF) as discussed in depth in Chapter 6. Kovács (1988) applied this method to southern Africa where he defined eight hydrologically homogeneous zones. By calculating the upstream catchment area of the position to be determined, and applying the appropriate Kovács formulae, the maximum flood peak discharge can be estimated. Kovács (1988) also produced theoretical probabilistic distributions allowing the estimation of design 1:100 year return periods. In the Flood Zone Model, sub-catchment cross-section profiles and reach data are extracted from the GIS and imported into HEC-RAS[®], a hydraulic river analysis flood routing software package where it is combined with the estimated sub-catchment peak discharges to produce flood elevation model simulations.

As the Regional Maximum Flood peak is derived from the measured maximum peak discharges from long-rain flood events, the equivalent field evidence in the form of flood deposits, erosion marks and debris line can be mapped and correlated to this. A series of calibration factors (CF) have been developed based on reach slope that are used to adjust the modelled flood elevations to the mapped flood deposits and existing 1:100 year design flood estimates. The calibration factors (CF) are based on an averaged reach Manning roughness coefficient. By increasing or decreasing the calibration factor value, it has the effect of increasing/decreasing energy losses

from interaction of the water with the channel substrate, affecting the travel time and elevation of the water moving through the drainage system.

4.5.1. Flash flood hydrology

HEC-RAS[®] is capable of processing multiple simulations concurrently. As the flood routing parameters for the sub-catchments of a quaternary catchment are already established for the Flood Zone Model, peak discharges estimated from a model better suited for small catchments can be used to model *flash* flood inundation zones. In estimating peak discharges and extracting soil, topographic and land cover data from existing GIS datasets, and lumped at sub-catchment level, a semi-distributed flash flood modelling (Flash Flood Model - FFM) approach can be applied.

To determine the peak discharges, the Rational Formula (RF) (Alexander 2002; Pegram & Parak 2004) (*Eq1*) was selected because it is widely applied in the Republic of South Africa (Alexander 2002; Pegram & Parak 2004; Parak & Pegram 2006) for calculating discharges in small catchments. Additionally, the input parameters could be derived from existing GIS datasets in keeping with the Flood Zone Model methodology approach:

$$Q = icA/3.6 \quad \dots\dots\dots [Eq1]$$

Where:

$$Q = \text{discharge (m}^3/\text{s)}$$

$$i = \text{rainfall intensity (mm/h)}$$

$$c = \text{Run-off coefficient dimensionless value between 0-1}$$

$$A = \text{Area of catchment (km}^2\text{)}$$

Design rainfall depths for 20, 50, 100 and 200 years (probabilistically based estimate of rainfall depths and duration) (Smithers & Schulze 2003) for the area were extracted from Hydrorisk (Smithers & Schulze 2003). This calculates design rainfall return periods using a Regional

Linear Moment Algorithm and Scale Invariant approach (RLM&SI) (Smithers & Schulze 2003; Gericke & Du Plessis 2011).

Since rainfall intensity (i) is a function of time of concentration and recurrence interval, intensity – duration – frequency (IDF) tables are used to establish intensities (Parak & Pegram 2006). Parak and Pegram (2006) fitted power law curves to 29 catchments and computed parameters for calculating intensity (Eq2):

$$i = ad^c \quad \dots\dots\dots [Eq2]$$

Where:

i = rainfall intensity (mm/h)

a = return period rainfall depth (mm)

d = time of concentration (hours)

c = power law parameters

Time of concentration (T_c) values was calculated using the Bransby-Williams formula (WSUD 2012) (Eq3):

$$T_c = 91 L/A^{0.1} S^{0.2} \quad \dots\dots\dots [Eq3]$$

Where:

T_c = Time of concentration (minutes)

L = main reach length (km)

A = Area (km²)

S = reach slope (m/km)

The run-off coefficient (c) is a subjective estimate of the factors such as soil conditions and land cover, contributing to water (rainfall) retention in a catchment thereby reducing the water volume that will reach a drainage line and contribute to channel flow (Pegram & Parak 2004). Published values (Anquetin et al. 2010; Mark and Marek 2011) relate to larger catchments and

may not apply to small sub-catchments. Considering the rainfall intensities involved, Hortonian flow (Stomph et al. 2002; Beven 2004; Lee et al. 1991) may also be a factor in that there is insufficient time for absorption and most of the precipitation converts to run-off. The method set out by Mark and Marek (2011), which sums estimations of relief, soil infiltration, vegetation cover and surface conditions with a weighted factor for return periods, was used to determine a run-off coefficient. Slope data were derived from the hydrological DEM and the average slope per sub-catchment was determined and categorized (Mark & Marek 2011). Soil permeability and depth for the sub-catchments were extracted from the AGIS (Schoeman et al. 2002) soil data and averaged for each sub-catchment. Land cover data were taken from the Ezemvelo KZN Wildlife land cover dataset and the predominant land cover type was extracted for each sub-catchment.

Variables were calculated for each sub-catchment and substituted into the relevant formulas. The peak discharges estimated using the rational formula for the 20, 50, 100 and 200 years design rainfall (RF_{20} , RF_{50} , RF_{100} , RF_{200}) was processed in HEC-RAS[®] to produce flash flood elevation surfaces.

4.5.2. Calibration

Calibrations of the Flash Flood Model results are based on field observations which consisted of mapped flood deposits with a differential GPS to establish the highest flood elevations, together with first hand reports documented in the homestead surveys. Calibration of the Flash Flood Model results had to be approached differently to that of the Flood Zone Model. In the Flood Zone Model the maximum flood elevation surfaces could be directly related and calibrated to well-established peak discharges using the Regional Maximum Flood. In the Flash Flood Model, the maximum flood elevation surfaces (inundation levels) were established from field observations and homestead surveys (control data), but the rainfall depths that resulted in the peak discharges to achieve these inundation levels were unknown. The flash flood elevation surfaces from HEC-RAS[®] were overlain on the control data and the one that was the closest match to the control data was selected. Initial results were based on the Flood Zone Model calibration factors. An iterative process was applied using a series of calibration factors until the selected flash flood elevation surface produced a best fit to the control data.

CHAPTER 5 – FIELD OBSERVATIONS

5. Field observations

Evidence of flood elevations can be determined from features such as debris lines, river terraces, watermarks on structures, denuded vegetation lines and sedimentary flood deposits. Soil material transported to drainage lines by means of overland flow, combined with fluvial sediments released by scouring of river banks and channels are taken up by the water as either bedload or suspended load. Included in the suspended load are vegetation and anthropogenic materials collected by flood waters. Under flood conditions, water at the edges of the floodplain experience elevated friction with the underlying ground surface. This results in the deposition of the finer clay and silt fractions of the suspended load and wash load, marking out the peak discharge elevation for a particular flood event. Associated with this line are the vegetation debris lines. A key component of the work described here is the establishment of the relationship between field evidence of flooding and the Regional Maximum Flood (RMF) peak discharge.

5.1. Flood markers

Flood markers on structures in rivers such as bridges, weirs and pump stations can provide good evidence of flood elevations. A drawback of relying on this evidence is that the structures may be younger than the highest flood and hence will not record this event. Figure 5.1 shows an example of flood marks on a pump station in the Mkomazi River. A number of flood elevations can be seen on the pump station wall but they are difficult to equate to a specific flood event.



Figure 5.1. Photograph of flood marks on a pump station in the Mkomazi River. The dashed black lines indicate various flood elevations recorded on the pump station.

Debris washed out at the edge of a flood, or trapped in trees and structures, provides good evidence of flood elevations (Fig 5.2). However, the preservation potential of this debris is likely low. These lines are useful to determine the elevation of a recent flood known flood event but may not necessarily record the highest flood event. Likewise, the scouring action of flood water will often denude vegetation along river banks (Fig 5.3). Denuded vegetation lines thus provide a limited usefulness as markers of flood elevation because the water elevation and flood deposits can and often do occur above the removed vegetation.



Figure 5.2. (Top) Accumulated debris along the Zotshe River. The dashed yellow line indicates a flood elevation from 2012. Floods in 2009 covered the roof of the house. (Bottom). A flood damaged house along a tributary of the Mzinto River in 2012. The yellow dashed line represents the flood elevation.

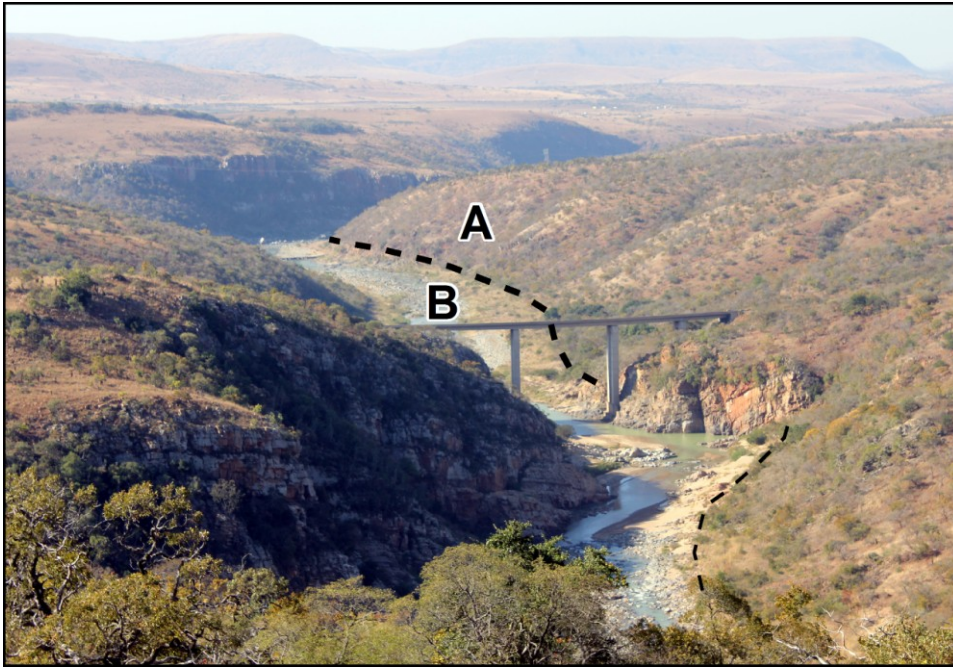


Figure 5.3. Photograph showing scoured vegetation along the White Mfolozi River channel. The area marked A, above the dashed black line consists of undisturbed natural bushy vegetation. The area (B) below the dashed black line consists of remnant short grasses where larger vegetation has been removed. The elevation of the dashed black line is approximately 633 m AMSL and the riverbed is approximately 627 m AMSL. This indicates a flood elevation of at least 6 m.

5.2. Flood deposits

A more accurate reflection of flood elevation are the silt and clay deposits related to the upper portion of the suspended load and wash load that are deposited at the margins of the flood. Structurally they consist of a thin wedge of sediment thickening in the direction of the river channel. Typically they onlap or cross cut older soils and can be distinguished from the residual colluvial and hillwash soils by their darker colouring and unstructured appearance. In certain cases they can exhibit limited bedding structures.

The fluvial deposits that result from the deposition of the sedimentary loads carried by a river can range in size from boulders (metres in size) to clay particles. These deposits typically comprise grits, sands, silts and clays. Figure 5.4 shows examples of fluvial sedimentary deposits resulting from bed load and suspended load transportation and deposition.

Alluvial deposits such as those in Figure 5.4 are continuously subjected to erosion and re-deposition. Alluvium is mainly associated with periods of channel activity and it is very difficult to relate these deposits to discharges. This is because they are mainly comprised of bedload material which does not represent sediments from the total water column. The water column carrying the suspended load and wash load may also be significantly deeper than that within which the bed load deposits are constrained.

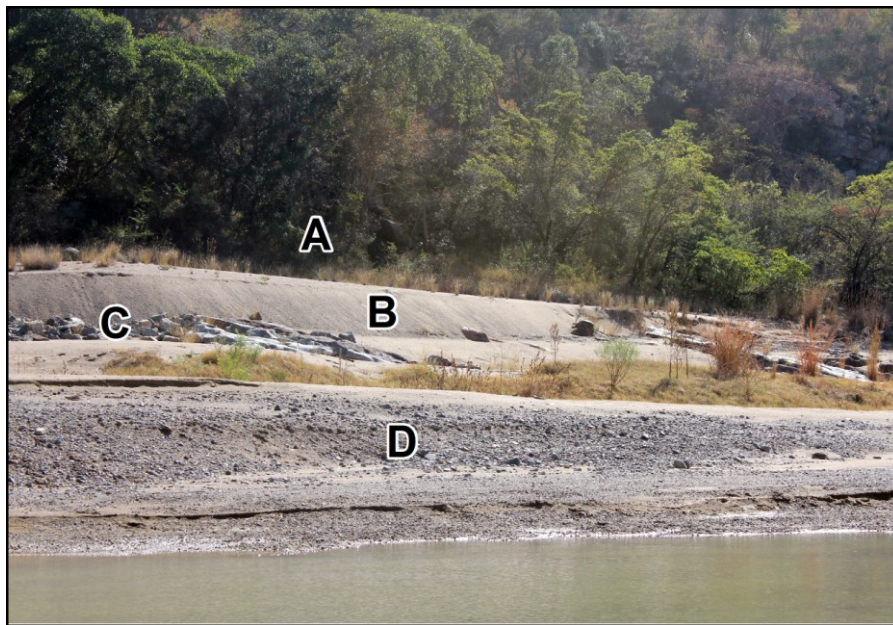


Figure 5.4. Photograph of fluvial deposits. A – Suspended load flood clays. B – Point bar sandy deposit produced under high flow conditions. C – Basal gravel. D- Mixture of sand and gravel.

Flood deposits typically show a fining upward sequence (Fig. 5.5) with a gravel base fining to silts and clays. Although the example shown in Figure 5.5 resulted from relatively smaller floods, it

demonstrates the principles that apply to extreme flood events. Anthropogenic material such as tins, plastic, fabric and bottles trapped in the flood deposits can be used to estimate the relative ages of these flood deposits. In Figure 5.5 the upper flood unit contains machine woven fabric suggesting that the deposit is at least as old as the Industrial Revolution.

Large floodplains can accumulate a number of successive alluvial flood events marked out by root bases, indicating long periods of aerial exposure (Fig. 5.6). It is very difficult to relate any one of these deposits to a specific flood event, but they do have value in recording the minimum number of events that the area was exposed to.

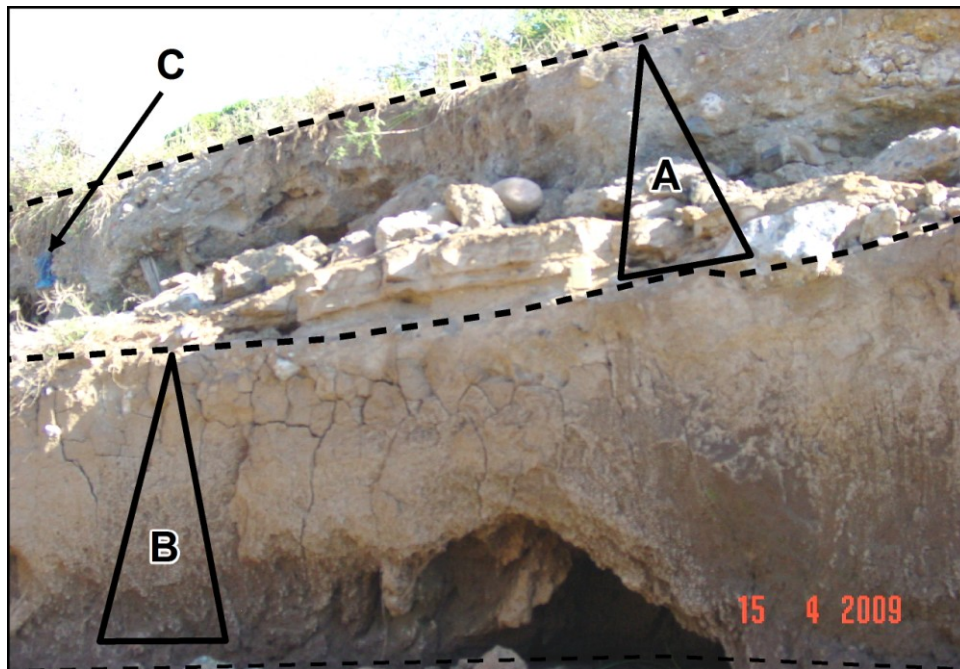


Figure 5.5. Fining upward sequences in a succession of flood deposits along the Mkhomazi River. Triangles A and B denote flood units. C – Fabric within the flood deposit.

Suspended and wash load deposits provide a more accurate measure of flood elevations as demonstrated in Figure 5.7. Here the recent flood elevation is recorded as thin clay and silt deposits at the margins of the flood waters.

Figure 5.8 shows a wedge of flood deposits along the Thukela River. The massive nature of this deposit distinguishes it from the underlying residual soils.



Figure 5.6. Photograph of successive alluvial deposits in the Klip River. The dashed black lines indicate root bases separating the flood events. At least 7 events have occurred in the past.

Another example of a flood deposit is shown in Figure 5.9, where the characteristic wedge of poorly sorted clay and silt remnant flood deposits are located in close proximity to the scoured vegetation line shown in Figure 5.3.



Figure 5.7. Clay and silts deposits indicating the extent and elevation of a flood in 2012 along a tributary of the Mzinto River. Yellow dashed line marked the edge of the flood deposits.

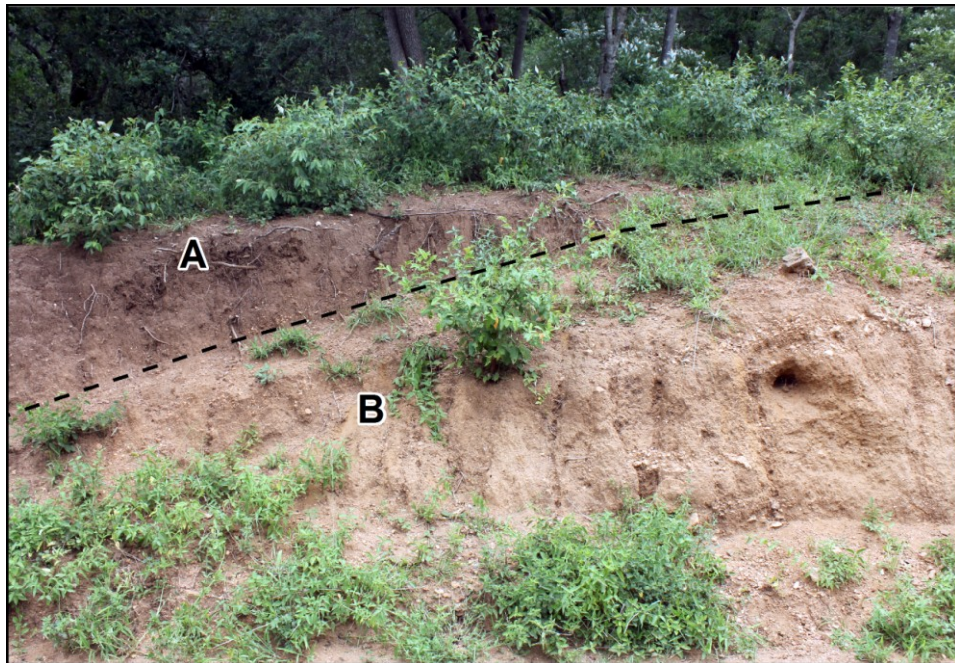


Figure 5.8. Photograph of flood clay wedge overlying residual soils along the Tugela River. Black dashed line represents the base of the flood deposit.

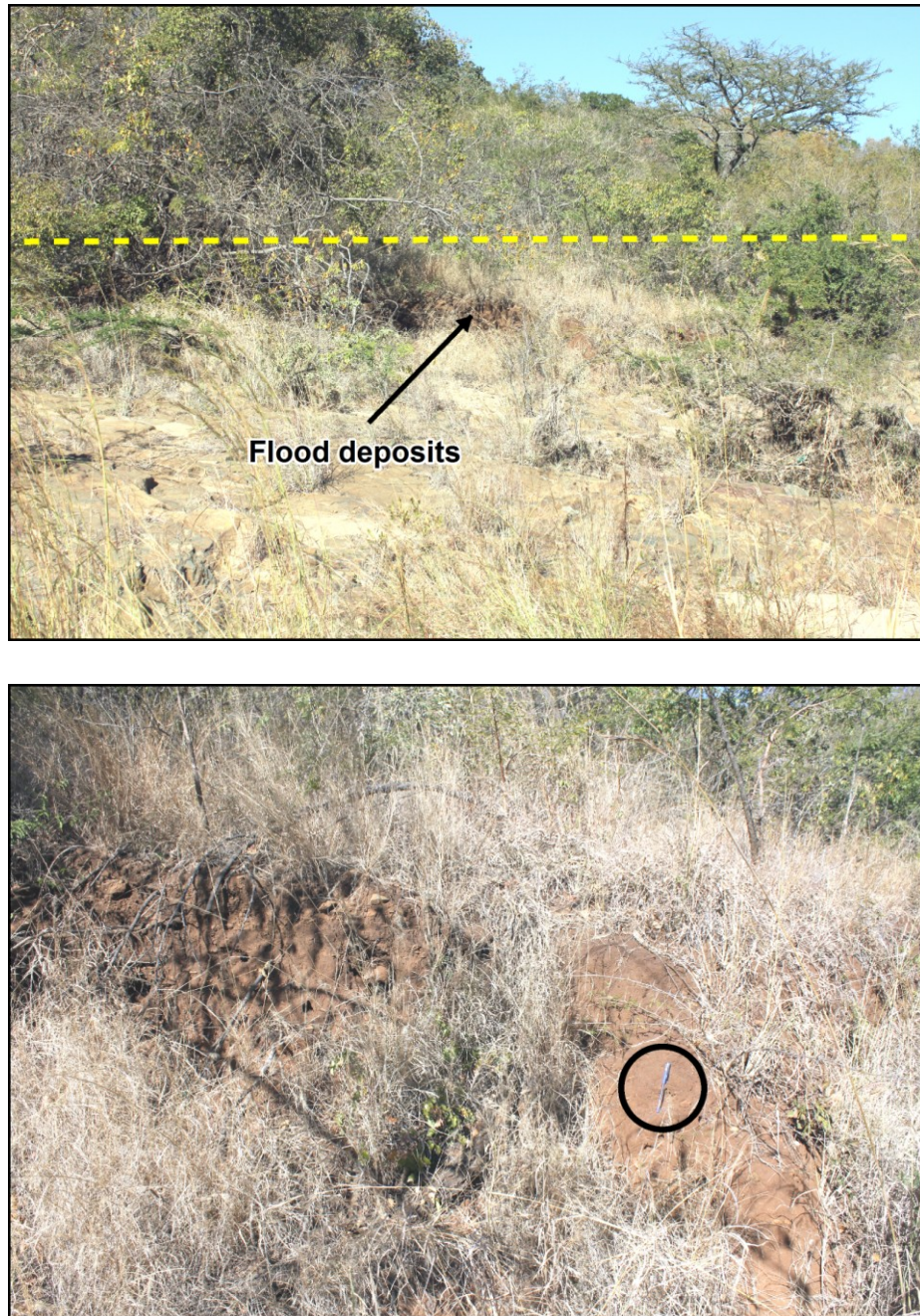


Figure 5.9. (Top) Photograph showing historical example of flood deposits along the bank of the Mfolozi River. The yellow dashed line indicates the edge of the flood deposits. (Bottom) Detailed photograph showing the clay-rich flood deposits. Note pen for scale in black circle.

The continuing process of erosion and deposition, interspersed with flood events, creates a complex sedimentary profile. The relationship between various ages of flood deposits and the sample position

targeted to measure the highest flood elevation are schematically demonstrated in Figure 5.10. It is clear that it is very difficult to assign fluvial deposits to any specific event. The only reliable marker is that of the maximum flood elevation deposits.

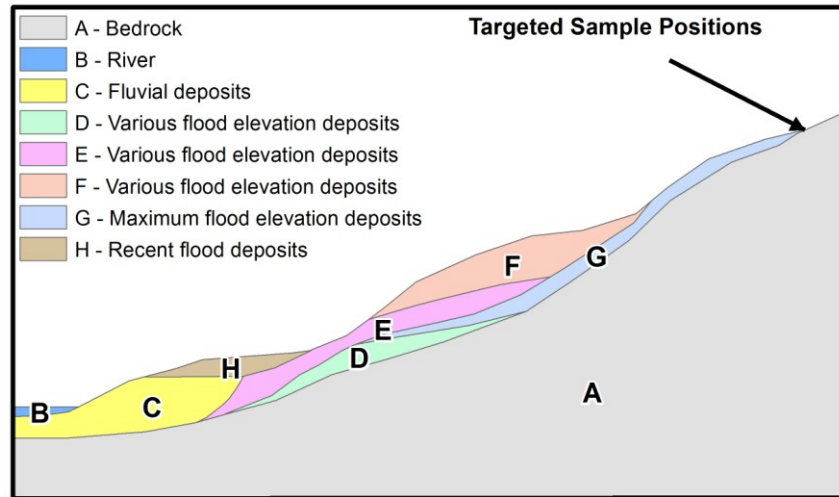


Figure 5.10. Schematic diagram showing the relationship between various ages of flood deposits in cross-section view.

Provided that field evidence is gathered from the active floodplain, the assumption can be made that the flood clays furthest from the river centreline represent the maximum flood elevation recorded in the current climatic cycle. The aim of the fieldwork was thus to identify flood deposits that represent the maximum flood elevation in the quaternary catchments.

5.3. Quaternary catchment areas

The five representative quaternary catchments (T40G, T52D, U20H, V12G, W23A) (Fig. 4.1) were investigated to map and record flood deposits.

5.3.1. T40G Quaternary Catchment

The locations of the field observation points are shown in Figure 5.11 and described in Table 5.1. Figures 5.12 and 5.13 show examples from some field observation points.

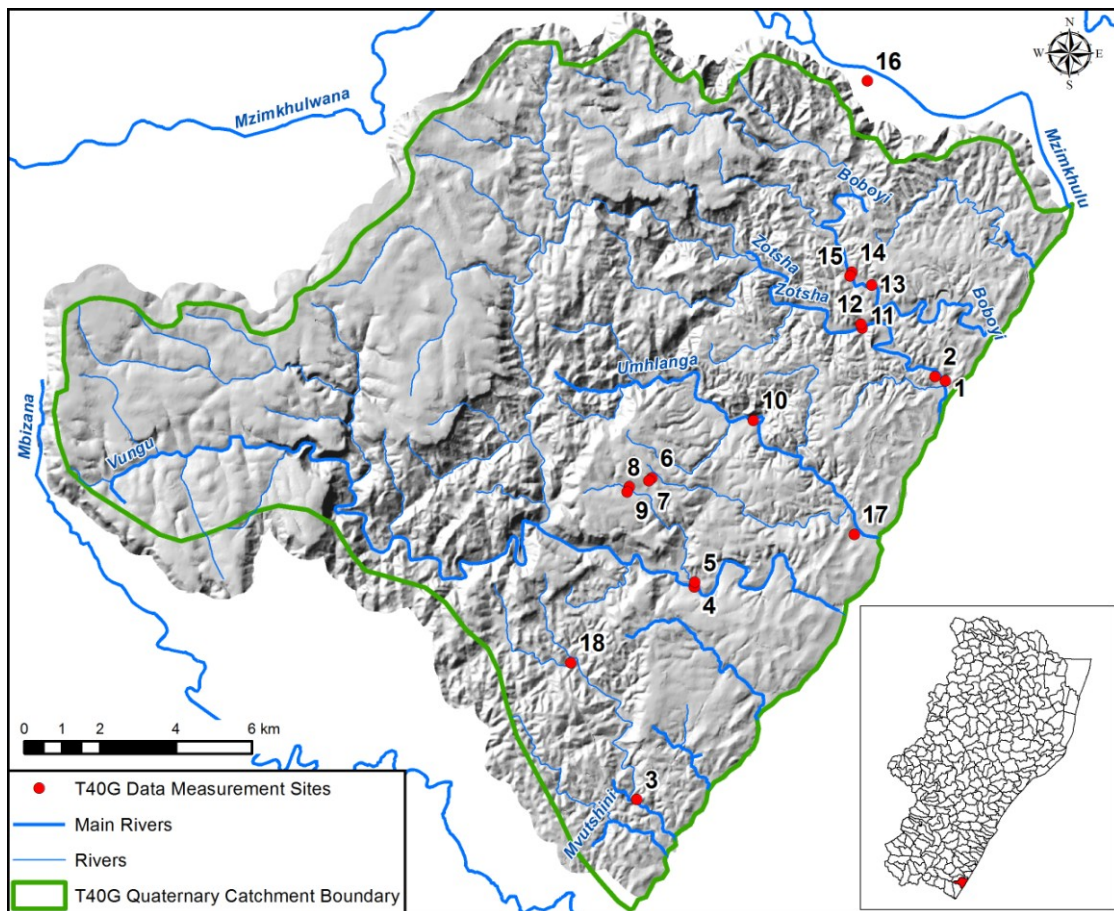


Figure 5.11. Hillshaded DEM Map of T40G showing field measurement sites of elevated flood deposits and main rivers.

The main rivers in the T40G quaternary catchment drain into the Indian Ocean. The coastal floodplains are broad and flat, bounded by hills (Fig. 5.12). River and flood deposits indicate that under flood conditions, water will fill the width of the floodplain. Increased discharges will result in water levels rising up against the sides of the hills resulting in a more vertical than lateral than expansion of the floodwaters. Other soil types do not always underlie flood deposits. Figure 5.13 shows an example of flood deposits directly overlying bedrock.

Table 5.1. Description of the sample sites in quaternary catchment T40G.

Site No	Catchment	South	East	Site description
1	T40G	30° 46' 54.57" S	30° 25' 26.99" E	Flood deposits on the left bank of the Zotshe River near the mouth
2	T40G	30° 46' 50.64" S	30° 25' 16.91" E	Flood deposits on the right bank of the Zotshe River near the mouth
3	T40G	30° 52' 51.13" S	30° 20' 18.77" E	Flood deposits on the right bank of the Bilankholo River
4	T40G	30° 49' 49.59" S	30° 21' 17.33" E	Flood deposits on the right bank of a tributary of the Vungu River
5	T40G	30° 49' 45.59" S	30° 21' 17.63" E	Flood deposits on the left bank of a tributary of the Vungu River
6	T40G	30° 48' 16.15" S	30° 20' 35.56" E	Flood deposits on the left bank of unnamed river in Gamalake Township
7	T40G	30° 48' 18.61" S	30° 20' 32.61" E	Flood deposits on the right bank of unnamed river in Gamalake Township
8	T40G	30° 48' 23.66" S	30° 20' 13.19" E	Flood deposits on the left bank of unnamed river in Gamalake Township
9	T40G	30° 48' 27.98" S	30° 20' 11.32" E	Flood deposits on the right bank of unnamed river in Gamalake Township
10	T40G	30° 47' 27.27" S	30° 22' 16.67" E	Flood deposits on the right bank of the uMhlanga River
11	T40G	30° 46' 08.98" S	30° 24' 04.92" E	Flood deposits on the left bank of a tributary of the Zotshe River
12	T40G	30° 46' 05.37" S	30° 24' 03.59" E	Flood deposits on the right bank of a tributary of the Zotshe River
13	T40G	30° 45' 32.18" S	30° 24' 14.53" E	Flood deposits on the left bank of the Bobhoyi River
14	T40G	30° 45' 21.13" S	30° 23' 54.97" E	Flood deposits on the left bank of the Bobhoyi River
15	T40G	30° 45' 24.26" S	30° 23' 53.25" E	Flood deposits on the right bank of the Bobhoyi River
16	T40G	30° 42' 37.51" S	30° 24' 11.44" E	Flood deposits on the right bank of the Mzimkhulu River (Outside pilot area)
17	T40G	30° 49' 05.26" S	30° 23' 56.08" E	Flood deposits on the right bank of the uMhlanga River floodplain
18	T40G	30° 50' 53.84" S	30° 19' 14.28" E	Flood deposits on the right bank of the Bilankholo River



Figure 5.12. View of the Zotshe River floodplain at Site 2 (Fig. 5.11). The yellow dashed line marks the maximum flood elevation as defined by flood deposits.



Figure 5.13. Flood deposits at Site 3 (Fig. 5.11). Yellow dashed line represents the base of the flood deposits.

5.3.2. U20H Quaternary Catchment

The locations of the field observation points are shown in Figure 5.14 and described in Table 5.2. Figures 5.15 to 5.17 show examples from some field observation points.

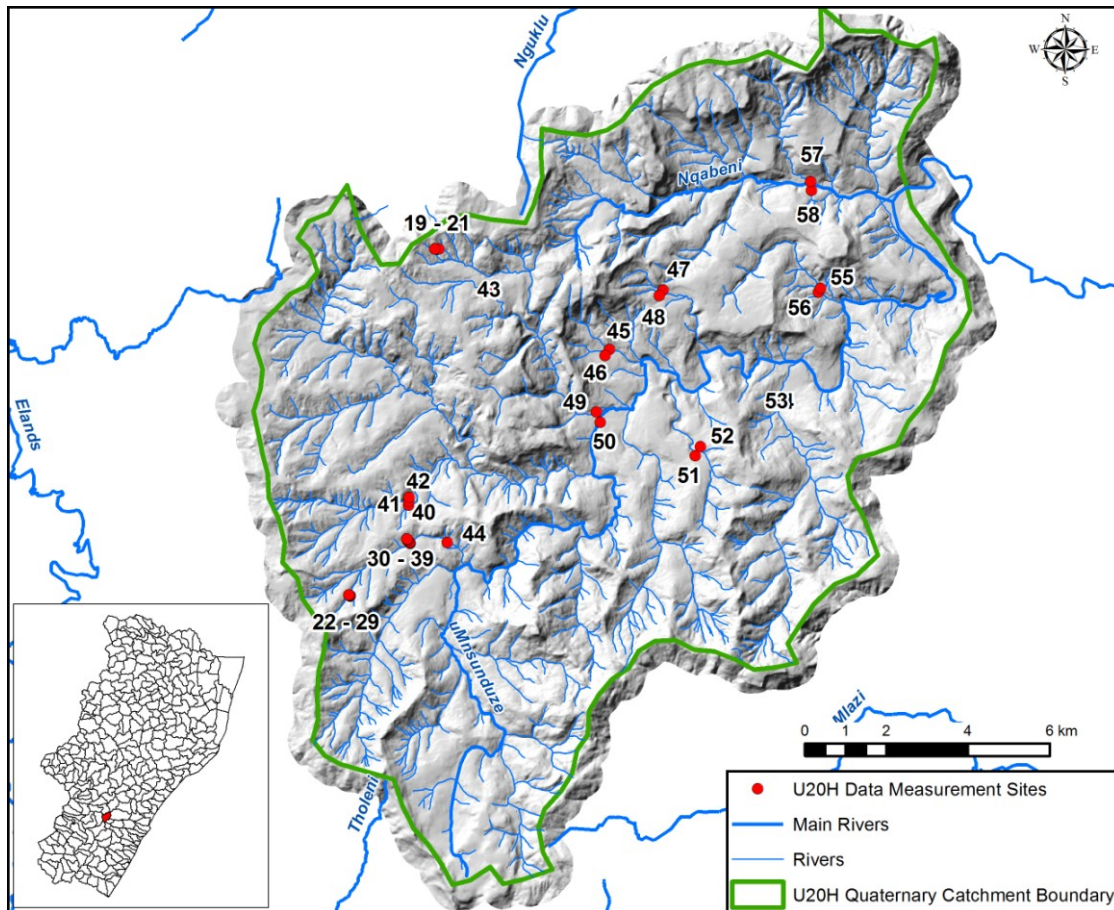


Figure 5.14. Hillshaded DEM Map of U20H showing field measurement sites of elevated flood deposits and major rivers.

In the U20H quaternary catchment, terrace development along the mid to upper reaches of streams is common. Terraces one and two (Fig. 5.15) appear to result from normal to above normal seasonal discharges as vegetation tends to be much shorter and sparser than that further away from the river course. Terrace three and four consist of relatively modern flood deposits (Fig. 5.15) and in the other representative areas terrace three appears to be closely related to the Regional Maximum Flood elevations. The development of terrace four is unusual and has probably been formed by flash flooding (See Chapter 7). Topographically the lower reaches of the Msunduze River in quaternary

catchment U20H consist of very broad low relief valleys. This has resulted in wide floodplains with their extents demarcated by flood deposits (Fig 5.16). Flood deposits can overlies other fluvial deposits such as river sand and gravels (Fig. 5.17), in this case they formed as a settling drape over the underlying deposits during the falling river energy levels (Bridge 2003).

Table 5.2. Description of the sample sites in quaternary catchment U20H.

Site No	Catchment	South	East	Site description
19	U20H	29° 38' 10.87" S	30° 07' 42.03" E	Flood deposits on the left bank at terrace 3 of a tributary of the Nkobongwana River
20	U20H	29° 38' 10.38" S	30° 07' 43.90" E	Flood deposits on the left bank at terrace 3 of a tributary of the Nkobongwana River
21	U20H	29° 38' 10.55" S	30° 07' 39.72" E	Flood deposits on the left bank at terrace 4 of a tributary of the Nkobongwana River
22	U20H	29° 38' 10.55" S	30° 07' 39.72" E	Flood deposits on the left bank at terrace 2 of a tributary of the Nkobongwana River
23	U20H	29° 42' 46.36" S	30° 06' 20.48" E	Flood deposits on the right bank at terrace 4 of a tributary of the Msunduze River
24	U20H	29° 42' 46.13" S	30° 06' 20.20" E	Flood deposits on the right bank at terrace 3 of a tributary of the Msunduze River
25	U20H	29° 42' 45.67" S	30° 06' 19.70" E	Flood deposits on the right bank at terrace 2 of a tributary of the Msunduze River
26	U20H	29° 42' 45.68" S	30° 06' 19.66" E	Flood deposits on the right bank at terrace 2 of a tributary of the Msunduze River
27	U20H	29° 42' 45.68" S	30° 06' 19.65" E	Flood deposits on the right bank at terrace 2 of a tributary of the Msunduze River
28	U20H	29° 42' 45.66" S	30° 06' 19.63" E	Flood deposits on the right bank at terrace 2 of a tributary of the Msunduze River
29	U20H	29° 42' 45.54" S	30° 06' 19.51" E	Flood deposits on the right bank at terrace 1 of a tributary of the Msunduze River
30	U20H	29° 42' 45.30" S	30° 06' 19.25" E	Centre of a tributary of the Msunduze River
31	U20H	29° 42' 04.68" S	30° 07' 15.42" E	Flood deposits on the right bank at terrace 4 of a tributary of the Msunduze River
32	U20H	29° 42' 04.67" S	30° 07' 15.41" E	Flood deposits on the right bank at terrace 4 of a tributary of the Msunduze River
33	U20H	29° 42' 04.47" S	30° 07' 15.26" E	Flood deposits on the right bank at terrace 3 of a tributary of the Msunduze River
34	U20H	29° 42' 04.36" S	30° 07' 15.13" E	Flood deposits on the right bank at terrace 2 of a tributary of the Msunduze River
35	U20H	29° 42' 04.14" S	30° 07' 14.98" E	Flood deposits on the right bank at terrace 1 of a tributary of the Msunduze River
36	U20H	29° 42' 03.95" S	30° 07' 14.84" E	River bank of the tributary of the Msunduze River
37	U20H	29° 42' 03.90" S	30° 07' 14.75" E	Flood deposits the tributary of the Msunduze River
38	U20H	29° 42' 02.41" S	30° 07' 13.49" E	Flood deposits on the left bank at terrace 3 of a tributary of the Msunduze River
39	U20H	29° 42' 01.69" S	30° 07' 13.05" E	Flood deposits on the left bank at terrace 3 of a tributary of the Msunduze River
40	U20H	29° 42' 01.11" S	30° 07' 12.35" E	Flood deposits on the left bank at terrace 4 of a tributary of the Msunduze River

Table 5.2. cont. Description of the sample sites in quaternary catchment U20H

Site No	Catchment	South	East	Site description
41	U20H	29° 41' 34.22" S	30° 07' 14.18" E	Flood deposits on the right bank of a tributary of the Msunduze River
42	U20H	29° 41' 31.29" S	30° 07' 14.53" E	Confluence of two tributaries
43	U20H	29° 41' 28.00" S	30° 07' 14.86" E	Flood deposits on the left bank of a tributary of the Msunduze River
44	U20H	29° 38' 41.73" S	30° 08' 29.21" E	Flood deposits on the left bank of a tributary of the Nkobongwana River
45	U20H	29° 42' 04.21" S	30° 07' 49.36" E	Flood deposits on the right bank of a tributary of the Msunduze River
46	U20H	29° 39' 30.42" S	30° 10' 19.65" E	Flood deposits on the left bank of a tributary of the Msunduze River
47	U20H	29° 39' 35.22" S	30° 10' 15.56" E	Flood deposits on the right bank of a tributary of the Msunduze River
48	U20H	29° 38' 44.36" S	30° 11' 07.93" E	Flood deposits on the left bank of a tributary of the Msunduze River
49	U20H	29° 38' 48.85" S	30° 11' 04.21" E	Flood deposits on the right bank of a tributary of the Msunduze River
50	U20H	29° 40' 21.19" S	30° 10' 05.96" E	Flood deposits on the left bank of a tributary of the Msunduze River
51	U20H	29° 40' 29.27" S	30° 10' 09.58" E	Flood deposits on the right bank of a tributary of the Msunduze River
52	U20H	29° 40' 56.52" S	30° 11' 35.99" E	Flood deposits on the left bank of a tributary of the Msunduze River
53	U20H	29° 40' 49.47" S	30° 11' 40.84" E	Flood deposits on the right bank of a tributary of the Msunduze River
54	U20H	29° 40' 18.01" S	30° 12' 50.39" E	Flood deposits on the right bank of the KwaGezubuso River
55	U20H	29° 40' 18.04" S	30° 12' 54.82" E	Flood deposits on the left bank of the KwaGezubuso River
56	U20H	29° 38' 47.14" S	30° 13' 29.06" E	Flood deposits on the right bank of the Nembes River
57	U20H	29° 38' 43.93" S	30° 13' 31.29" E	Flood deposits on the left bank of the Nembes River
58	U20H	29° 37' 25.98" S	30° 13' 23.42" E	Flood deposits on the left bank of the Nqabeni River
59	U20H	29° 37' 18.90" S	30° 13' 22.73" E	Flood deposits on the right bank of the Nqabeni River

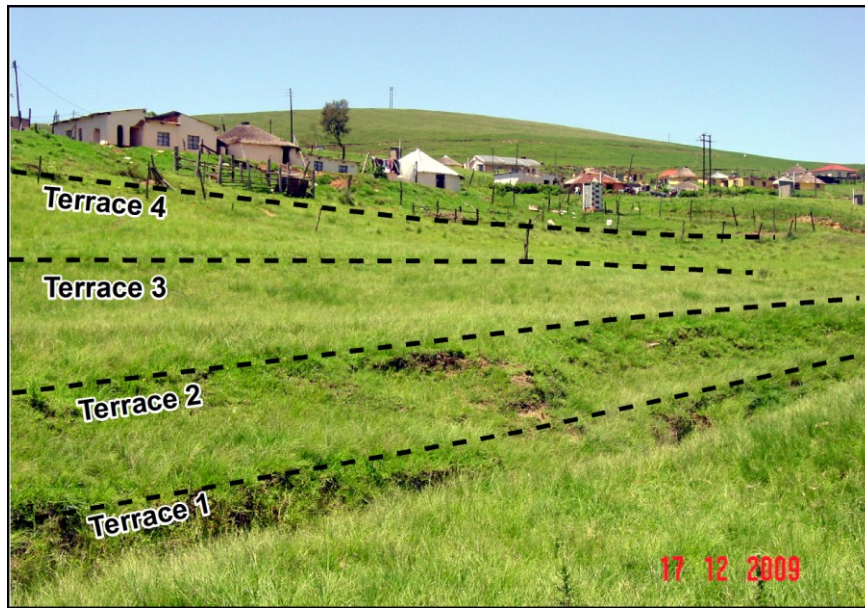


Figure 5.15. Example of terrace development at Site 38 (Fig. 5.14). Dashed black lines demarcate the terraces.



Figure 5.16. Floodplain at Site 40 (Fig. 5.14). The dashed black line defines the edge of the flood deposits.

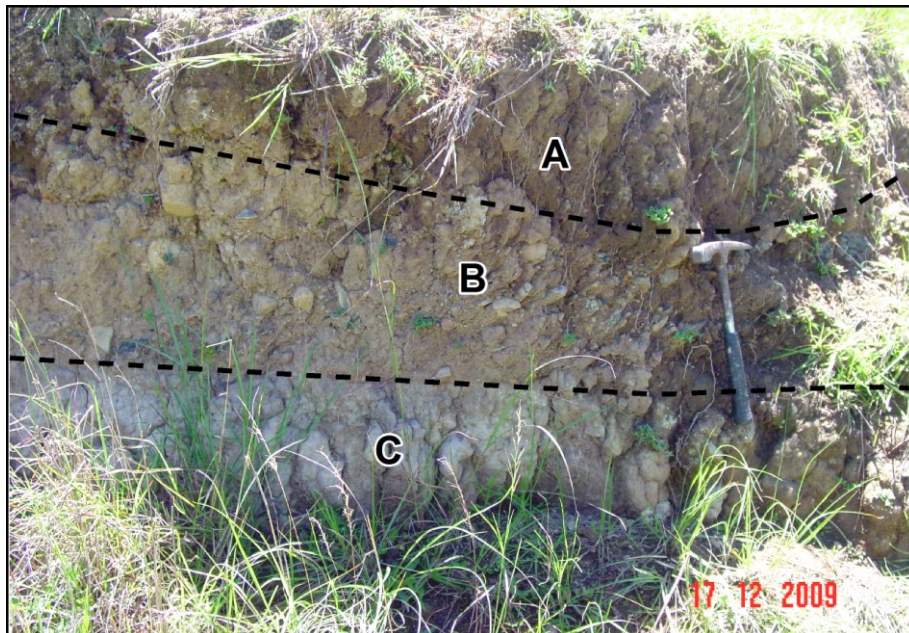


Figure 5.17. Alluvial deposits at Site 54 (Fig. 5.14). A – Flood deposits. B – River gravels and sand. C – Residual sandstone.

5.3.3. T52D Quaternary Catchment

Table 5.3. Description of the sample sites in quaternary catchment T52D.

Site No	Catchment	South	East	Site description
60	T52D	30° 17' 29.70" S	29° 56' 11.19" E	Flood deposits on the left bank of a tributary of the Mzimkhulu River
61	T52D	30° 17' 39.77" S	29° 56' 25.05" E	Flood deposits on the right bank of a tributary of the Mzimkhulu River
62	T52D	30° 17' 45.73" S	29° 56' 41.31" E	Flood deposits on the left bank of a tributary of the Mzimkhulu River
63	T52D	30° 17' 48.75" S	29° 56' 32.12" E	Flood deposits on the left bank of a tributary of the Mzimkhulu River
64	T52D	30° 16' 29.83" S	29° 56' 08.69" E	Flood deposits on the right bank of a tributary of the Mzimkhulu River
65	T52D	30° 16' 25.24" S	29° 56' 00.91" E	Flood deposits on the left bank of a tributary of the Mzimkhulu River
66	T52D	30° 17' 51.19" S	29° 56' 51.10" E	Flood deposits on the right bank of a tributary of the Mzimkhulu River
67	T52D	30° 17' 49.46" S	29° 57' 01.03" E	Flood deposits on the right bank of a tributary of the Mzimkhulu River
68	T52D	30° 18' 07.36" S	29° 56' 35.28" E	Flood deposits on the right bank of a tributary of the Mzimkhulu River
69	T52D	30° 16' 48.17" S	29° 58' 11.91" E	Flood deposits on the right bank of a tributary of the Ncatu River
70	T52D	30° 15' 11.33" S	29° 58' 35.00" E	Flood deposits on the right bank of a tributary of the Mzimkhulu River
71	T52D	30° 15' 29.49" S	29° 56' 47.40" E	Flood deposits on the right bank of the Mzimkhulu River
72	T52D	30° 15' 46.90" S	29° 56' 17.49" E	Flood deposits on the left bank of the Mzimkhulu River
73	T52D	30° 13' 09.96" S	30° 01' 24.09" E	Flood deposits on the left bank of a tributary of the Ncatu River
74	T52D	30° 15' 00.52" S	30° 00' 39.72" E	Flood deposits on the left bank of a tributary of the Ncatu River
75	T52D	30° 15' 18.15" S	29° 56' 44.91" E	Flood deposits on the right bank of the Mzimkhulu River

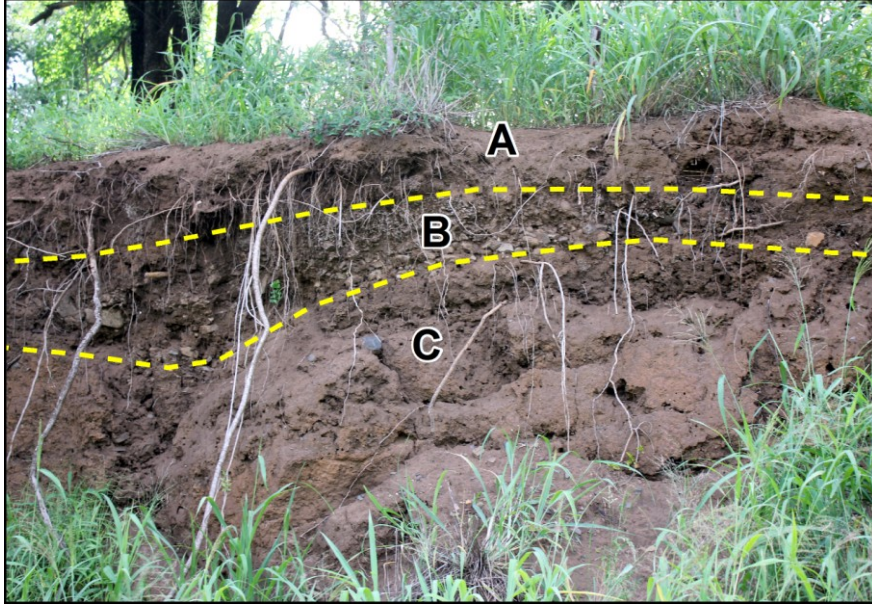


Figure 5.19. Multiple flood deposits at Site 59 (Fig. 5.18). A – Recent flood deposits. B – Associated flood deposit (A) gravel. C – Previous flood deposits.

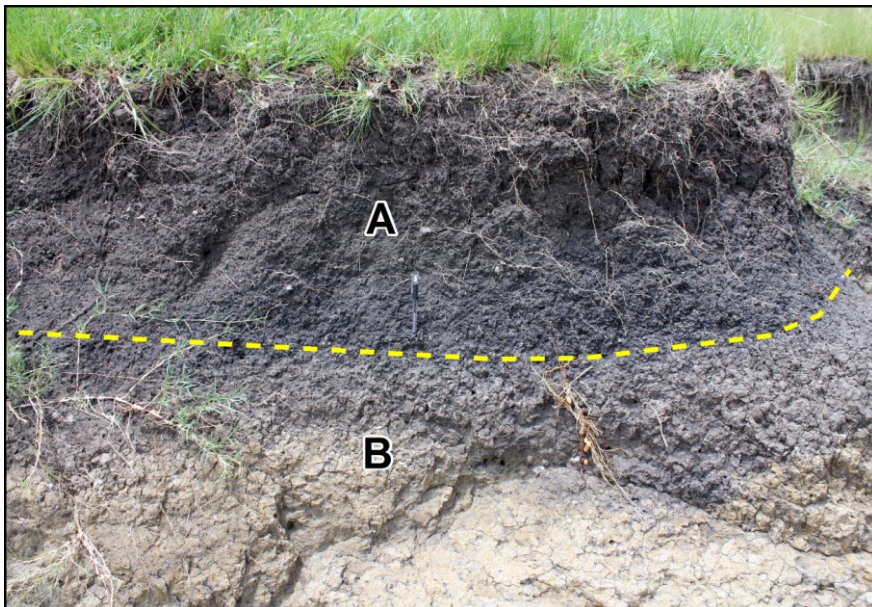


Figure 5.20. Flood deposits at Site 69 (Fig. 5.18). Yellow dashed line marks the base of the flood deposits. A – Flood deposits. B – Residual shale.

5.3.4. V12G Quaternary Catchment

Generally this area comprises flat-lying terrain with low undulating hills. As expected, the drainage valleys are broad, resulting in wide, shallow floodplains. The area along the Klip River forms the major catchment line and destructive flooding can be expected close to the river course with inundation expected along the margins. The locations of the field observation points are shown in Figure 5.21 and described in Table 5.4. Figures 5.22 to 5.24 show examples from some field observation points.

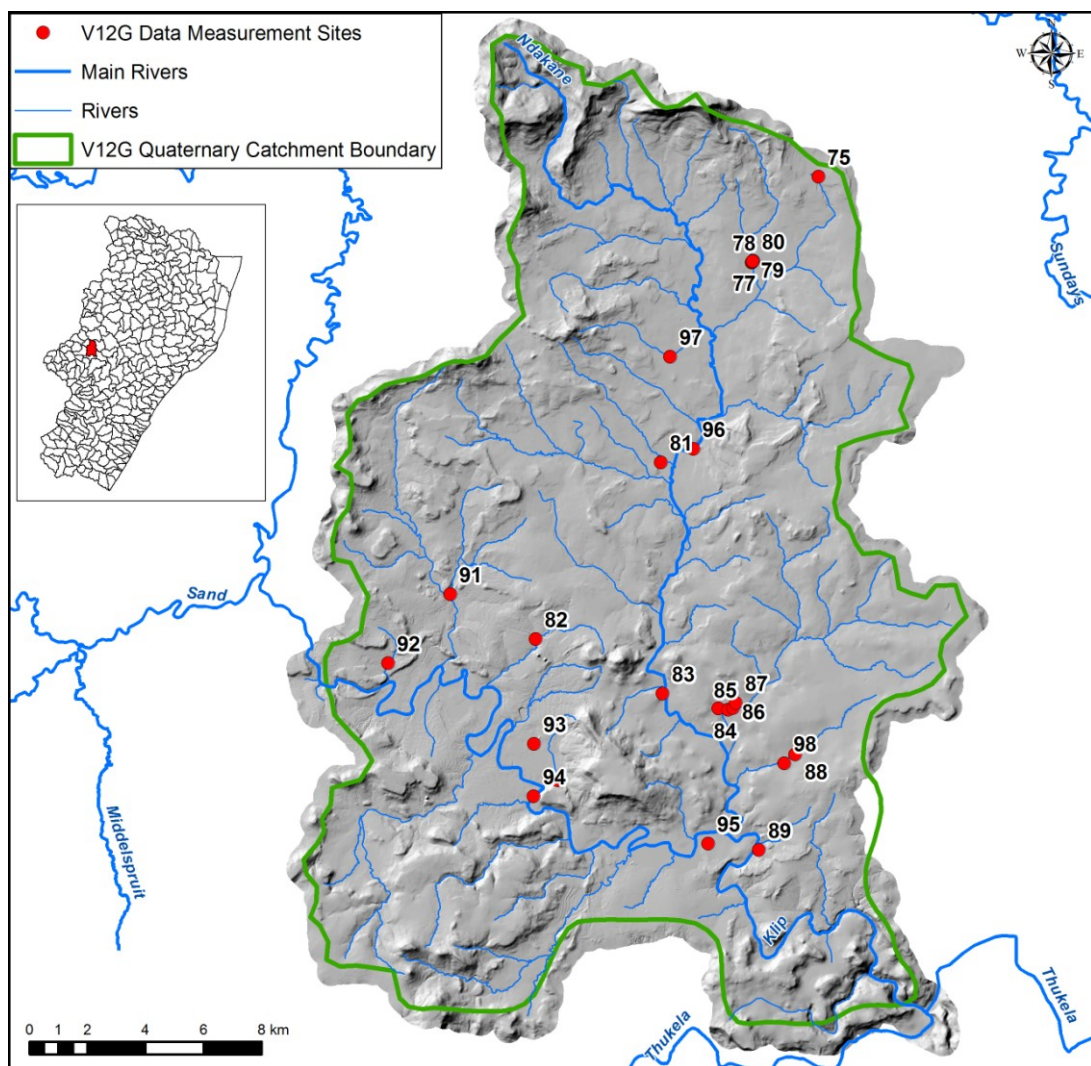


Figure 5.21. Hillshaded DEM Map of V12G showing field measurement sites of elevated flood deposits and major rivers.

Table 5.4. Description of the sample sites in quaternary catchment V12G

Site No	Catchment	South	East	Site description
76	V12G	28° 24' 18.41" S	29° 55' 37.75" E	Flood deposits on the left bank of a tributary of the Modderspruit River
77	V12G	28° 25' 51.86" S	29° 54' 14.29" E	Flood deposits on the left bank of a tributary of the Modderspruit River
78	V12G	28° 25' 51.86" S	29° 54' 14.30" E	Flood deposits on the left bank of a tributary of the Modderspruit River
79	V12G	28° 25' 53.70" S	29° 54' 12.47" E	Flood deposits on the right bank of a tributary of the Modderspruit River
80	V12G	28° 25' 53.15" S	29° 54' 13.00" E	Flood deposits on the right bank at terrace 1 of a tributary of the Modderspruit River
81	V12G	28° 25' 52.33" S	29° 54' 13.81" E	Flood deposits on the left bank at terrace 1 of a tributary of the Modderspruit River
82	V12G	28° 29' 36.38" S	29° 52' 15.18" E	Flood deposits on the right bank of a tributary of the Rietkuil River
83	V12G	28° 32' 52.53" S	29° 49' 34.71" E	Flood deposits on the left bank of the Flag River
84	V12G	28° 33' 54.73" S	29° 52' 14.73" E	Flood deposits on the right bank of a tributary of the Modderspruit River
85	V12G	28° 34' 11.82" S	29° 53' 25.26" E	Flood deposits on the right bank of the Mabumane River
86	V12G	28° 34' 12.31" S	29° 53' 32.42" E	Flood deposits on the right bank of the Mabumane River
87	V12G	28° 34' 11.54" S	29° 53' 43.67" E	Flood deposits on the right bank of the Mabumane River
88	V12G	28° 34' 08.29" S	29° 53' 46.78" E	Flood deposits on the left bank of the Mabumane River
89	V12G	28° 35' 04.66" S	29° 55' 04.21" E	Flood deposits on the left bank of a tributary of the Modderspruit River
90	V12G	28° 36' 50.86" S	29° 54' 15.09" E	Flood deposits on the left bank of the Klip River
91	V12G	28° 35' 30.39" S	29° 50' 00.57" E	Flood deposits on the left bank of the Klip River
92	V12G	28° 32' 01.56" S	29° 47' 46.88" E	Flood deposits on the left bank of a tributary of the Belt's River
93	V12G	28° 33' 17.58" S	29° 46' 27.45" E	Flood deposits on the left bank of a tributary of the Klip River

Table 5.4 cont. Description of the sample sites in quaternary catchment V12G

Site No	Catchment	South	East	Site description
94	V12G	28° 34' 52.72" S	29° 49' 32.96" E	Flood deposits on the left bank of the Klip River
95	V12G	28° 35' 48.40" S	29° 49' 30.19" E	Left bank of the Klip River
96	V12G	28° 36' 43.24" S	29° 53' 10.46" E	Flood deposits on the right bank of the Klip River
97	V12G	28° 29' 21.24" S	29° 52' 56.47" E	Flood deposits on the left bank of the Rietkuil River
98	V12G	28° 27' 38.31" S	29° 52' 28.41" E	Flood deposits on the left bank of a tributary of the Modderspruit River
99	V12G	28° 35' 13.16" S	29° 54' 47.99" E	Flood deposits on the left bank of a tributary of the Modderspruit River

Riverbank erosion can provide a good contextual relationship between the river water level and its flood deposits and underlying bedrock and residual soils (Fig. 5.22). The flood deposits are approximately 2 – 3 m above the river. When floodplains are very broad, as in the case of the V12G quaternary catchment, the edge of the flood deposits can be a significant distance from the river course (Fig. 5.23). Informal settlements are often erected on these types of floodplains with the mistaken belief that the distance from the river is sufficient protection. An example of unsafe development on a floodplain can be seen in Figure 5.24, where a school has been built over flood deposits.

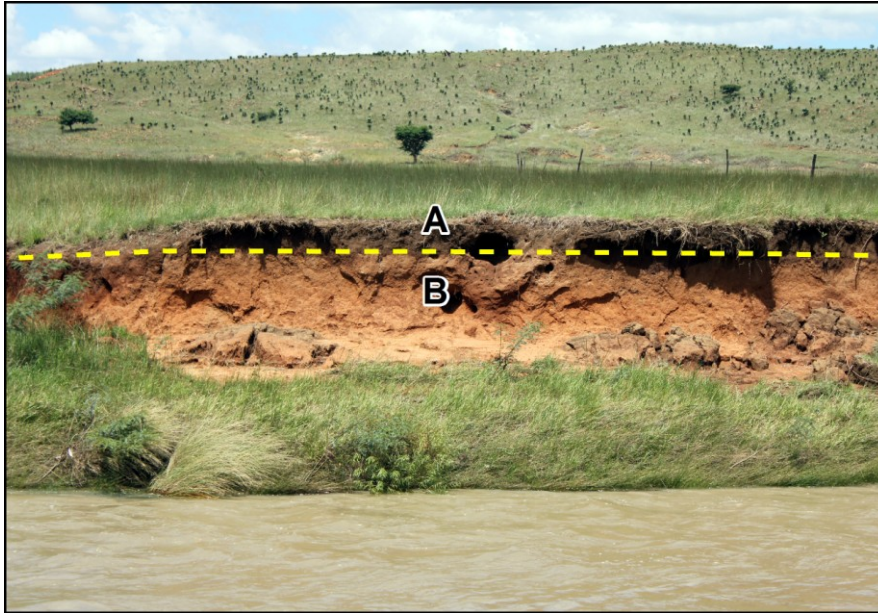


Figure 5.22. Flood deposits at Site 98 (Fig. 5.21). The yellow dashed line separates the flood deposits (A) from the underlying sediment and residual soils (B). The flood deposits are estimated to be 2 – 3 m above the river.



Figure 5.23. Terraces at Site 81 (Fig. 5.21). The black dashed lines show the terraces. Flood deposits are located at terrace 3 at the tree in the distance.



Figure 5.24. The yellow dashed line marks the edge of the flood deposits at Site 89 (Fig. 5.21). The school (Blue building) is partially built on flood deposits. The big boulders in foreground have been deposited by river action.

5.3.5. W23A Quaternary Catchment

Geomorphologically, this catchment is characterized by broad u-shaped valleys that have very shallow gradients. This results in wide, shallow flood plains along the secondary drainage lines that promote inundation with the destructive force limited to the main channel areas. The locations of the field observation points are shown in Figure 5.25 and described in Table 5.5. Figures 5.26 to 5.28 show examples from some field observation points.

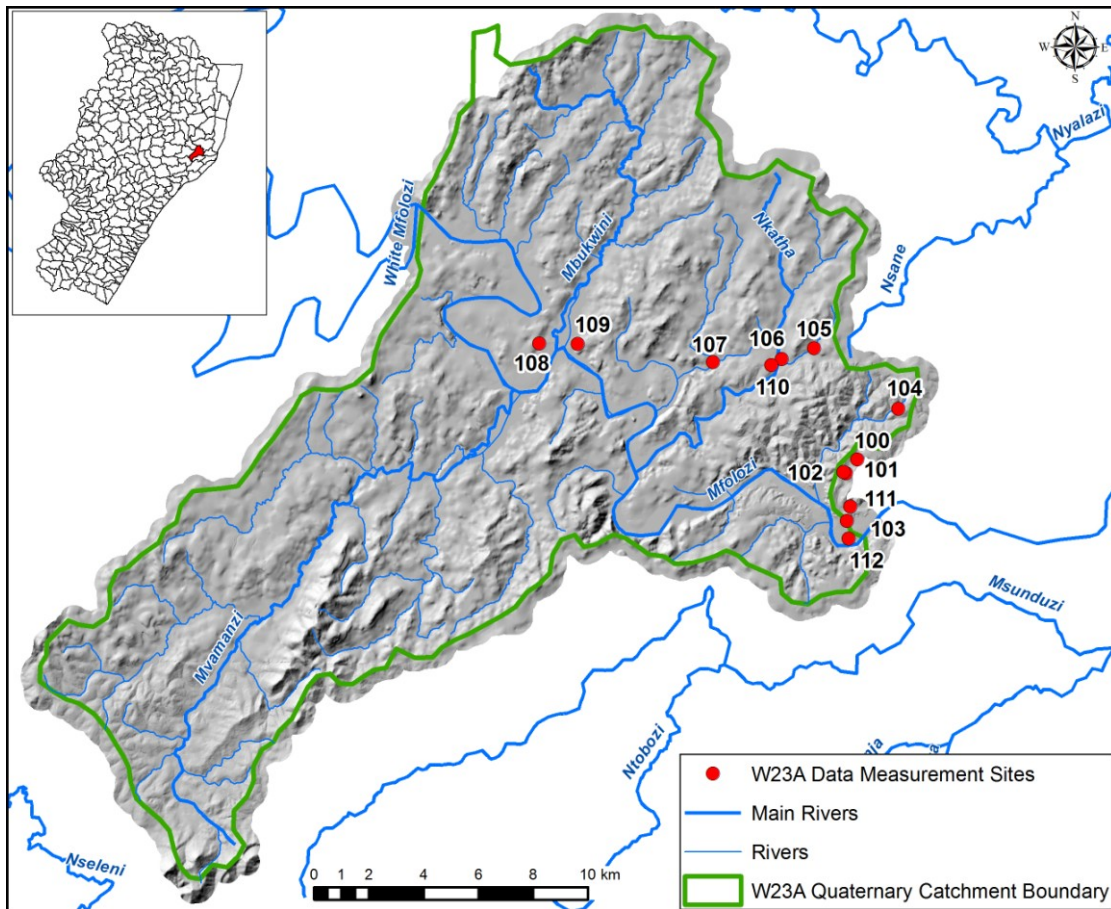


Figure 5.25. Hillshaded DEM Map of W23A showing field measurement sites of elevated flood deposits and major rivers.

The relationship between successive flood deposits can be complex as can be seen in Figure 5.27, where a previous flood deposit has been truncated by a more recent flood deposit. The flood deposits have been laid down as a series of gravel and sandy clay couplets A – B and C – D (Fig. 5.27). The repetition of the A – B couplets indicates that a series of floodwater pulses are the most likely cause (Charlton 2007). The A – B and C – D couplet sediments appear to be very similar sedimentologically and it is very difficult to determine if the C – D couplet formed during the early phase of a flood event and was then eroded at a later stage during the same event, or whether they result from two separate flood events. Flood deposit thicknesses can vary within a quaternary catchment and is probably a function of suspended sediment content and reaches of the river where slack water conditions prevail. In Figure 5.28 an example of a +2 m thick flood deposit is given.

Table 5.5. Description of the sample sites in quaternary catchment W23A.

Site No	Catchment	South	East	Site description
100	W23A	28° 25' 54.03" S	32° 08' 38.58" E	Flood deposits on the left bank of a tributary of the Mvanyamvanya River
101	W23A	28° 26' 10.75" S	32° 08' 23.52" E	Flood deposits on the left bank of the Mvanyamvanya River
102	W23A	28° 26' 09.33" S	32° 08' 20.32" E	Flood deposits on the right bank of the Mvanyamvanya River
103	W23A	28° 27' 06.85" S	32° 08' 25.29" E	Flood deposits on the left bank of the Mfolozi River
104	W23A	28° 24' 53.76" S	32° 09' 32.77" E	Flood deposits on the right bank of a tributary of the Mfolozi River
105	W23A	28° 23' 43.27" S	32° 07' 39.24" E	Flood deposits on the left bank of the Nkatha River
106	W23A	28° 23' 56.02" S	32° 06' 55.86" E	Flood deposits on the left bank of the Nkatha River
107	W23A	28° 23' 40.60" S	32° 01' 3..60" E	Flood deposits on the right bank of the Ntweni River
108	W23A	28° 23' 40.92" S	32° 01' 43.43" E	Flood deposits on the left bank of the Mfolozi River
109	W23A	28° 23' 39.44" S	32° 02' 14.48" E	Flood deposits on the left bank of the Mfolozi River
110	W23A	28° 24' 03.36" S	32° 06' 42.21" E	Flood deposits on the right bank of the Nkatha River
111	W23A	28° 26' 49.89" S	32° 08' 29.85" E	Flood deposits on the left bank of the Mvanyamvanya River
112	W23A	28° 27' 27.61" S	32° 08' 28.01" E	Alluvial and flood deposits on the left bank of the Mfolozi River

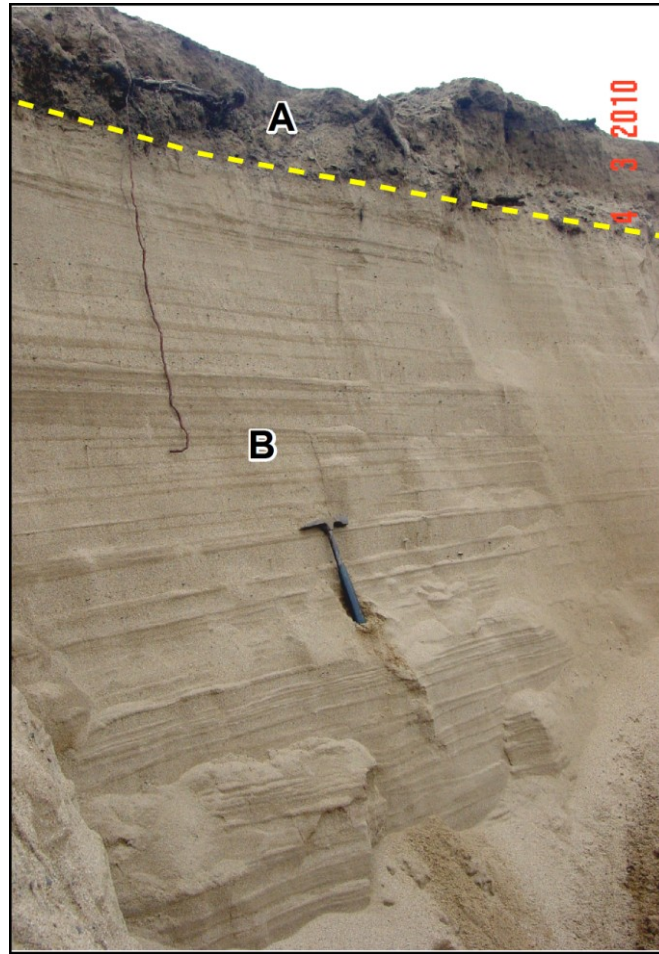


Figure 5.26. Laminar point bar alluvial deposits (B) overlain by flood deposits (A) at a sand mining operation, Site 112 (Fig. 5.25).

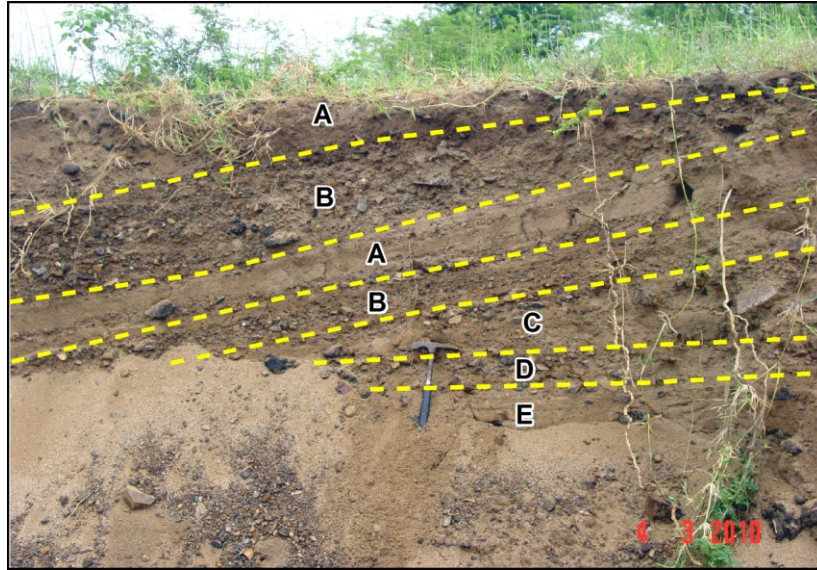


Figure 5.27. A repetitive series of gravels and clay flood deposits at near Site 112 (Fig. 5.25). A and B – flood clays and gravel couplets respectively. C and D – Flood couplet from a previous flood truncated by overlying flood deposits. E – Laminar point bar alluvial sand deposits.



Figure 5.28. Thick flood clay deposits at Site 109 (Fig. 5.25).

5.3.6. U20M Quaternary Catchment

The U20M catchment used as a blind test area (see Chapter 6, Section 6.3.3) is situated in the eThekweni Metro (Durban) and covers the area below Inanda Dam extending to the coast along the Mgeni River (Fig. 5.29). It has an area of 360 km² within primary drainage region U of 4027 km². Four major floods are recorded, *i.e.* 7 200 m³/s (1856), 4 550 m³/s (1868), 5 920 m³/s (1917) and 5 500 m³/s (1987) (van Bladeren, 1992). The U20M has detailed 1:100 year floodlines calculated for 1 km² sub-catchments across a range of slopes and land uses (Morris 2011). Topographically the area is hilly with a relatively narrow coastal plain. The coastal plain and surrounding areas are highly urbanised with development and settlement densities diminishing away from the coast. Figures 5.30 and 5.31 show the photographs taken at the photography site.

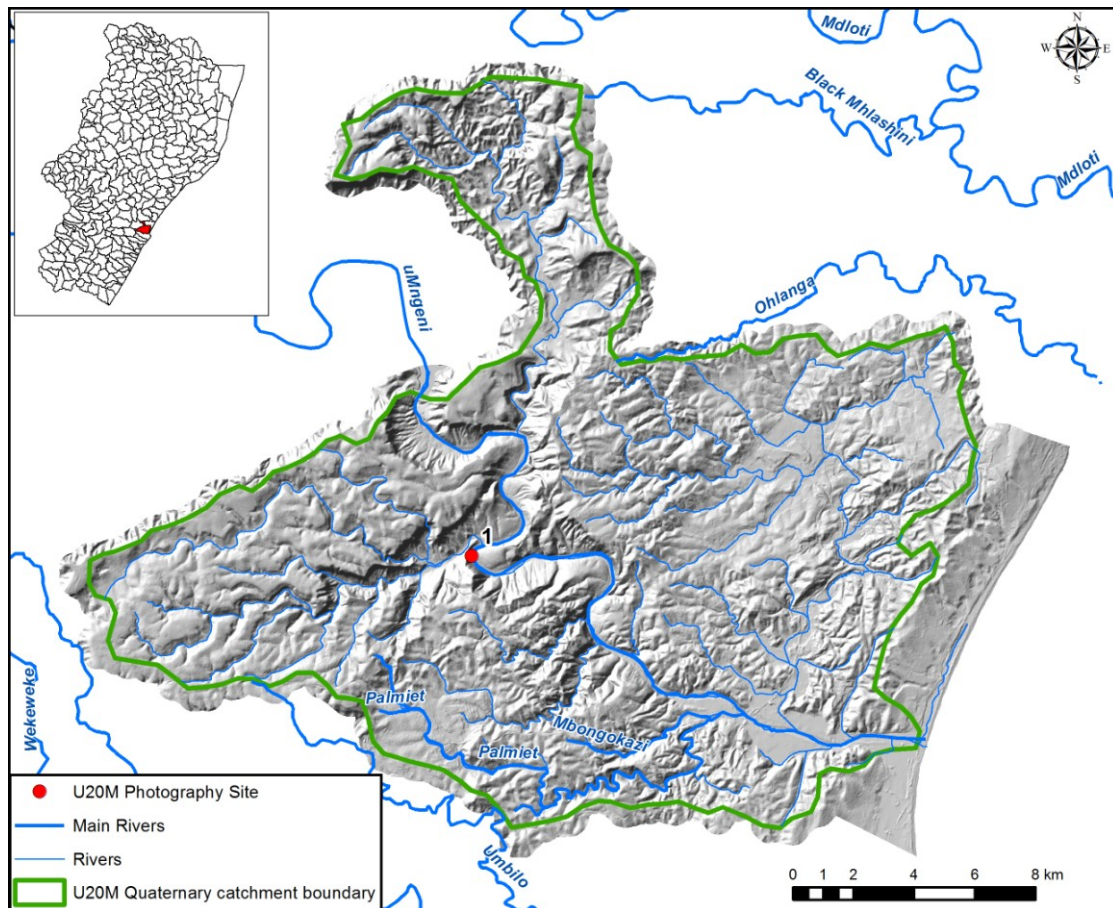


Figure 5.29. Hillshaded DEM Map of U20M showing the data photography site and major rivers.

In some cases flood deposits from different events can easily be identified. This can be seen in Figure 5.30 where the gravel and flood clays are overlain by a later gravel deposit. The root bases in horizon B (Fig. 5.30) indicate that there was at least a minimum timeframe between events that allowed vegetation to establish and cover the older flood deposits. The photograph in Figure 5.31 was taken approximately 20 m downstream of Figure 5.30., and shows a flood couplet of gravels and flood clays overlying alluvial sands. As there is no continuous exposure between the two closely related sites, the gravel horizon B in Figure 5.31 could be an extension of either horizon A or C in Figure 5.30.

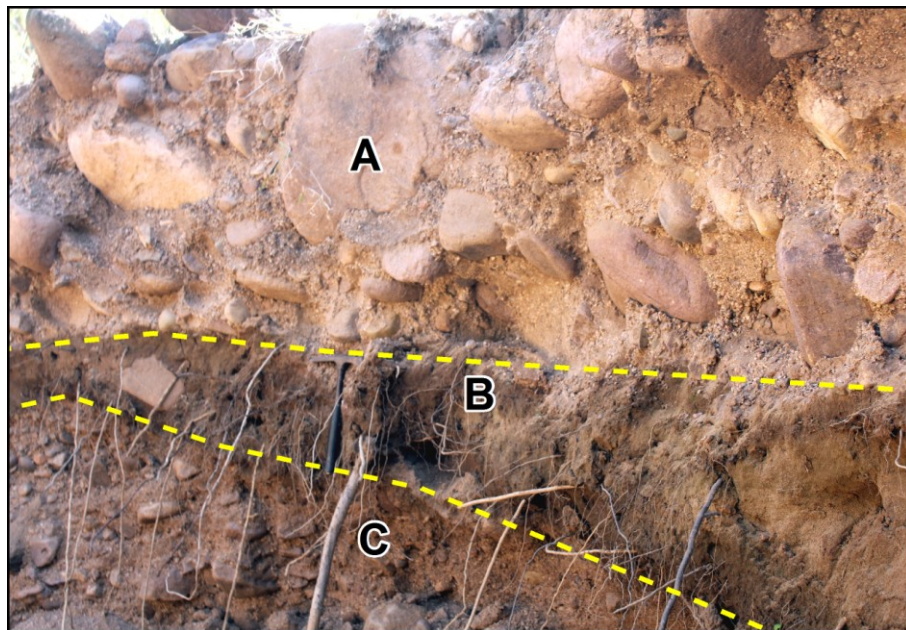


Figure 5.30. Gravel deposits from a more recent flood (A) overlying flood clays (B) and gravels (C) from an older flood. Note root bases in flood clays (B).

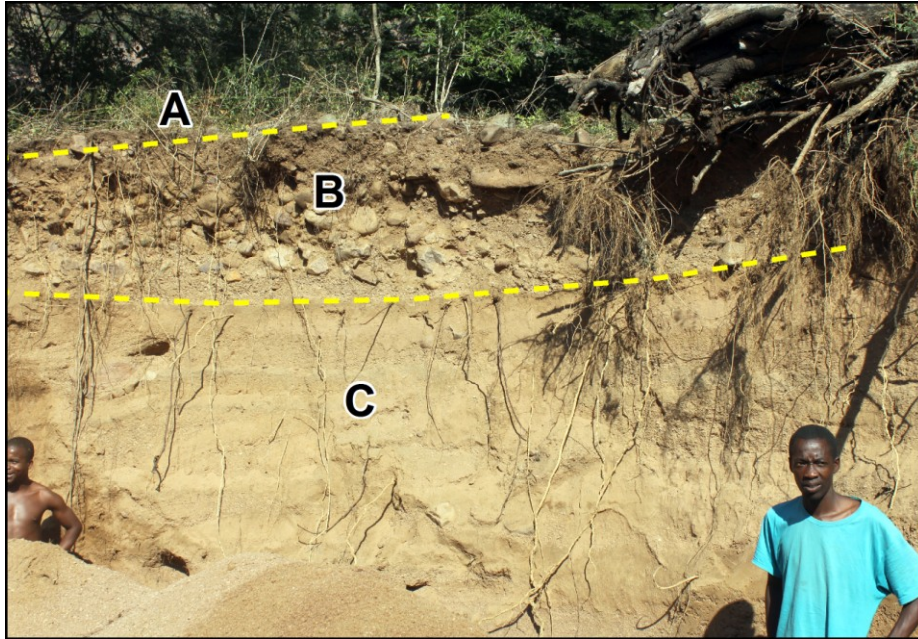


Figure 5.31. Flood clays (A) overlying the associated gravels (B). This couplet overlies older alluvial deposits (C).

5.4. Discussion

Of the various physical evidences of flood elevations, the highest level of flood deposits can be considered the most suitable for determining the highest historical flood elevations. While evidence such as debris lines and vegetation scouring may only reflect the height of the most recent flood, flood deposits can be preserved for a long time. Fieldwork has shown that the well preserved flood deposits can be used to determine the highest flood elevations. In urbanised areas the highest elevation flood deposits are generally not preserved but may still be extant in open space areas and parks. In the five representative areas only the coastal strip of T40G is urbanised. As expected the flood deposit elevations vary across the quaternary catchments reflecting different levels of water accumulation from the lowest stream order tributaries to the highest stream order main river. In general flood deposits are lowest along sub-tributaries and tributaries and reach progressively higher elevations towards the quaternary catchment discharge point.

Although river terraces were not used in this study to determine highest flood elevations, it was generally observed that the highest flood level coincided with the top of the third terrace in cross sectional profile (e.g. Fig. 5.15). Terrace one appeared to be a function of increased seasonal discharge to bank-full conditions and terrace two was the probable result of small to medium scale flooding. Terraces from four upward are generally poorly preserved and most likely represent palaeo-floodplains abandoned during river incision to the modern level (e.g. Charlton 2007).

As quaternary catchment T40G is located on the coastline it does not have a single discharge point like the other four representative quaternary catchments. Instead the accumulated runoff is distributed amongst nine main drainage points. Drainage lines are relatively short, longest being 32.6 km (Vungu River). T40G (Fig 5.11) the highest flood level was measured at point 17 (6.4 m) and upstream at point 10 (4.7 m) on the Umhlanga River. A similar relationship can be seen on the Zotsha River where point 1, near the river mouth, has the highest flood deposit level of 5.8 m and inland at point 12, 4.9 m. The lower flood deposit levels are along tributaries, e.g. point 9 (3.3 m) compared to point 4 (4.3 m) on the Vungu River. There are no historical flood discharge records for this catchment but the highest recorded discharge for the Mzimkhulu River along the northern border of the T40G quaternary catchment was 7050 m³/s in May 1959 (van Bladeren 1992). The flood levels recorded are most likely related to the 1959 flood event.

Quaternary catchment U20H (Fig. 5.14) has no upstream inflowing river. It is the headwater for the Umsunduze River which has a 39.8 km draining length through the U20H quaternary catchment. The highest flood deposit levels along the tributaries of the Umsunduze River range from approximately 10.2 m to 12.6 m (Points 20, 21, 51, 55). There is a second set of distinctive flood levels ranging from 5.4 m to 7.1 m (Points 39, 40, 47, 52) that have not been completely eroded by the 10.2 to 12.6 m event. The highest recorded flood level at the discharge point is a gauge height of 3.85 m and a discharge of 492 m³/s during the 1987 floods (van Bladeren & Burger 1989). The 1987 flood level is too low to account for the flood levels recorded in the field. This quaternary catchment has been subjected to a number of flash floods in the past that may account for the recorded flood deposit levels.

The 68 km length of the Mzimkhulu River drains through the T52D quaternary catchment (Fig 5.18). The highest flood deposit levels along the Mzimkhulu River are approximately 14.2 m (Point 68) and 15.7 m (Point 71). Along the tributaries of the Mzimkhulu River the highest flood deposit levels range

from 2.8 m (Point 62) to 4.1 m (Point 73). The highest recorded discharges were recorded in 1959 at a value of 3795 m³/s (estimated level of 12.16 m) at the gauge station corresponding to the entrance of the quaternary catchment and 7050 m³/s below the T52D quaternary catchment (van Bladeren 1992).

Quaternary catchment V12G is primary drained by the 48.7 km Klip River with the secondary 41.3 km drainage line of the Ndakane River. The highest flood deposits recorded along the Klip River are approximately 11.1 m at point 89 and 10.6 m at point 93. Along the Ndakane River the highest flood level found is 3.3 m (Point 83). The highest flood levels along the tributaries ranged from approximately 0.9 m (Point 76) to 2.3 m (point 84). This quaternary catchment has experienced repeated flooding particularly along the Klip River affecting the town of Ladysmith. Up to 1998 the Klip River has flooded 29 times in 110 years (Bell & Mason 1998) with the most recent in 2012. According to data presented by Bell & Mason (1998) peak estimated discharges for 1886, 1918 and 1923 were between 1600 m³/s and 1750 m³/s. The highest flood levels identified along the Klip River are probably related to one of these events.

The Mfolozi River (39.5 km) forms the main drainage line through quaternary catchment W23A (Fig. 5.25). The highest flood deposits along the Mfolozi River was found at point 102 (21.5 m) near the quaternary catchment discharge point and further upstream at points 107 (19.9 m) and point 108 (18.2 m). Along the tributaries the highest flood deposit levels range from 2.1 m (Points 103 and 106) to 2.4 m (Point 104). According to Kovács et al. (1985) and van Bladeren (1992) peak estimated discharge at the quaternary catchment discharge point was 16 000 m³/s with a gauge level of 12.8 m during Tropical Storm Domoina in 1984. However according to van Heerden & Swart (1986) a storm event in 1925, thought to be a tropical cyclone, produced flooding in excess of that of Tropical Storm Domoina in 1984. The gauge level of 12.8 m is based on an estimated flood level as the river gauges had been damaged or destroyed during Tropical Storm Domoina in 1984 (Kovács et al. 1985). It is apparent that the gauge station was destroyed before the flood level reached its peak elevation of 21.5 m as evidenced by the edge of the flood deposits at point 102.

CHAPTER 6 – FLOOD MODELLING

6. Regional Maximum Flood Peak (RMF)

The Regional Maximum Flood is an empirical approach to estimate the maximum flood peak based on the methodology proposed by Francou and Rodier (1967). These authors plotted the maximum recorded global flood peaks (approximately 1200), representative of most regions of the world against their catchment areas and found that plotting peak discharge against catchment area on log/log axes for hydrologically homogeneous regions produced regional envelope curves (K) that were straight lines for catchments exceeding 100 km². These regional envelope curves (hydrologically homogeneous regional boundaries) had an apparent convergence point where the runoff and area represented the total world mean annual runoff and total world drainage areas respectively. Francou & Rodier (1967) produced an equation (Eq4) to calculate discharge for a given drainage area (catchment) in a given regional envelope in relation to world runoff and discharge.

The Francou-Rodier (1967) equation is expressed as:

$$Q = 10^6 (A/10^8)^{1-0.1K} \dots\dots[Eq4]$$

Where:

$$Q = \text{Flood Peak (m}^3/\text{s)}$$

$$10^6 = \text{Mean annual discharge from all the drained land on earth (m}^3/\text{s)}$$

$$A = \text{Catchment area (km}^2\text{)}$$

$$10^8 = \text{Total drained land surface on earth (km}^2\text{)}$$

K = Regional coefficient expressed as relative flood peak magnitude which is $10(1-\tan^\alpha)$ where $^\alpha$ is the slope of the envelope line (Kovács, 1988).

Francou and Rodier (1967) identified three flood envelope zones based on drainage area *i.e.* flood, storm and transitional zones. In the flood zone where drainage areas $> 100 \text{ km}^2$, the flood peak discharge depends on the spatial and temporal rainfall distribution and catchment characteristics. The storm zone is where the drainage area is $< 1 \text{ km}^2$ and discharge depends only on the maximum 15 minute rainfall intensity ($i \leq 15$ minutes). The transitional zone (drainage area $> 1 \text{ km}^2$ and $< 100 \text{ km}^2$) was introduced (Francou & Rodier 1967) to provide smooth transition between the flood and storm zones. The Francou-Rodier (1967) equation is only applicable to the flood zone; the discharge for a drainage area $< 100 \text{ km}^2$ (storm and transition zones) should be determined by other means designed for small catchments.

Kovács (1988) applied the Francou-Rodier (1967) methodology to Southern Africa where he delineated nine homogeneous hydrographic regions (K envelopes) for Southern Africa based on maximum three day storm rainfall depths, catchment orientation with respect to the dominant storm generating weather systems, topography, soil permeability, main drainage systems and the location of major dams. By plotting the peak discharges (Q), calculated using Equation 4, against catchment size for the individual homogenous hydrographic regions (Fig 6.1) Kovács (1988) determined the regional envelope coefficients (K_e) of 519 flood peaks (354 from South Africa and 165 from neighbouring countries) for events which occurred between 1856 and 1988. Kovács (1988) termed this method the Regional Maximum Flood (RMF) peak. Of the nine Regional Maximum Flood homogeneous hydrographic regions (RMF regions) only the 5, 5.2, 5.4 and 5.6 overlie the study area. The relevant formulae (Eq 5 – Eq 8) (Table 6.1) for determining peak discharge (Q_{RMF}) for the Regional Maximum Flood regions are listed in Table 6.1. The Regional Maximum Flood regions delineated by Kovács (1988) generally form a series of coast parallel zones in the study area (Fig. 6.2).

Table 6.1. Regional Maximum Flood (RMF) regional formulae (After Kovács 1988).

Region (K_e)	Q_{RMF} (m^3/s)	Areal Range (km^2)	Equation
5.0	$Q = 100A_e^{0.50}$	100 - 100 000	Eq 5
5.2	$Q = 145A_e^{0.48}$	100 - 30 000	Eq 6
5.4	$Q = 209A_e^{0.46}$	100 - 20 000	Eq 7
5.6	$Q = 302A_e^{0.44}$	100 - 10 000	Eq 8
A_e = Effective Catchment area (km^2) and Q = RMF peak discharge			

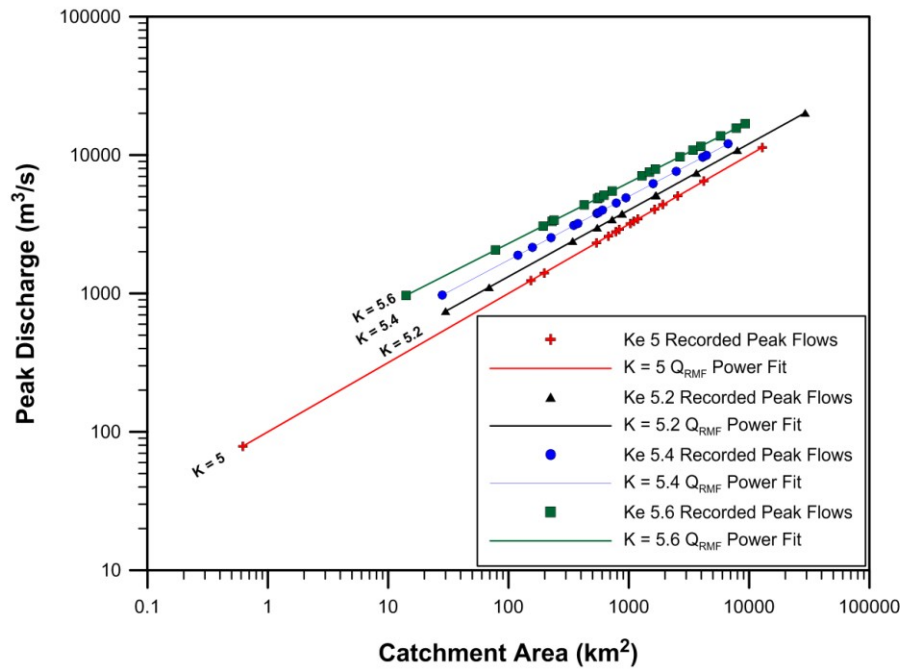


Figure 6.1. Plot of Peak discharges (Q_{RMF}) for Regional Maximum Flood K regions 5, 5.2, 5.4 and 5.6 versus catchment area (km^2) using log/log axes (Data after Kovács 1988).

Kovács (1988) also produced a series of theoretical probabilistic distributions (using the Log Pearson 3 Type method) whereby the 1:50, 1:100 and 1:200 year return period floods could be estimated (Table 6.2).

Table 6.2. Return period factors for the Regional Maximum Flood (RMF) regions (after Kovács 1988). Q_t – return period discharge, Q_{RMF} – Regional Maximum Flood peak discharge.

$Q_t - Q_{RMF}$ factors								
RMF Region	K = 5		K = 5.2		K = 5.4		K = 5.6	
Area (km^2)	100	200	100	200	100	200	100	200
10	0.550	0.661	0.556	0.676	0.556	0.661	0.668	0.803
30	0.521	0.636	0.528	0.650	0.525	0.635	0.645	0.788
100	0.488	0.608	0.494	0.624	0.492	0.607	0.617	0.769
300	0.517	0.633	0.524	0.650	0.523	0.633	0.640	0.784
1000	0.550	0.661	0.556	0.676	0.556	0.661	0.668	0.803
3000	0.582	0.687	0.588	0.701	0.588	0.687	0.695	0.821

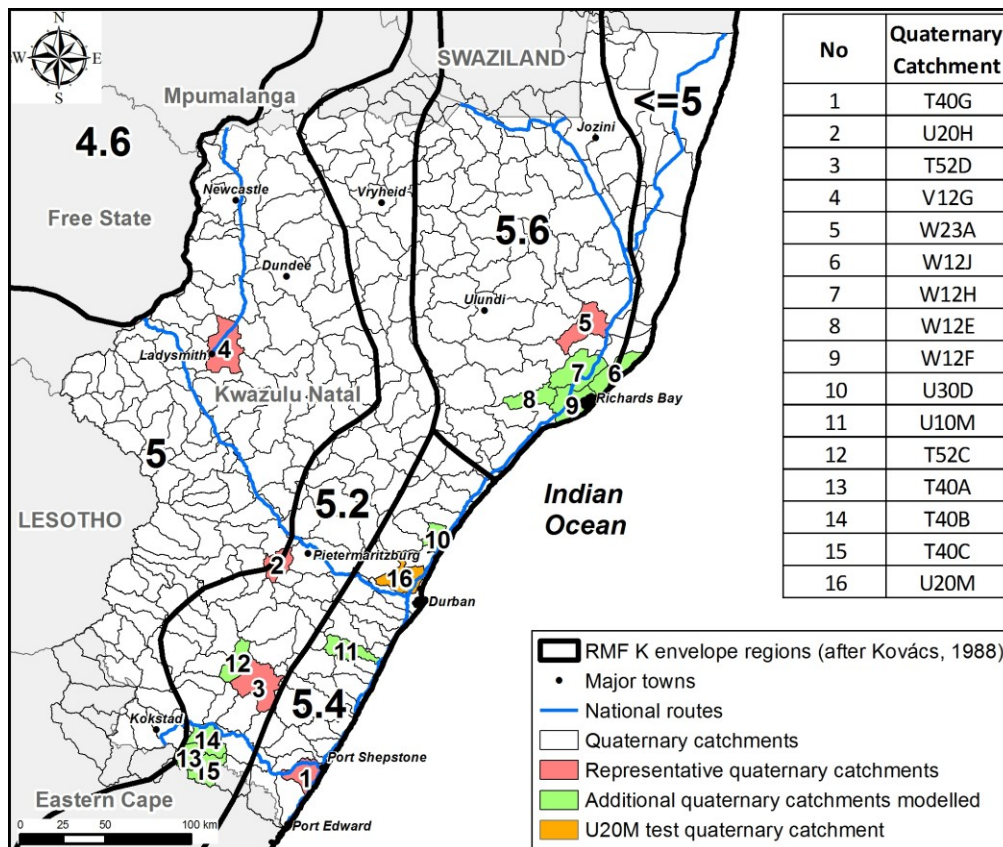


Figure 6.2. Map of Regional Maximum Flood homogenous hydrographic envelopes (After Kovács 1988) in relation to the representative areas and quaternary catchments.

The process for calculating the Regional Maximum Flood peak discharge (Q_{RMF}) for a *specific* site is:

- To determine the geographic position of the site and then the Regional Maximum Flood hydrographic region.
- To determine the total upstream catchment area.
- To apply the relevant formula from Table 6.1.
- Based on the area and Regional Maximum Flood hydrographic region and required return period select the factor from Table 6.2 and multiply it with the results of the formula from Table 6.1.

6.1. Regional Maximum Flood Problem

It was found during this study, that in applying the above approach to determine the Q_{RMF} discharges for individual quaternary catchments (modelling units), the Q_{RMF} flood peak is inflated and that the more quaternary catchments that are added to the process, the larger the inflation of the Q_{RMF} . The Mfolozi catchment is used as an example to demonstrate the problem (Fig. 6.3). The Mfolozi River catchment W2 comprises 25 quaternary catchments, and during the 1984 Tropical Storm Domoina floods, these produced a flood peak of 16 000 m³/s. Q_{RMF} calculations for the total catchment yields a discharge of 16 500 m³/s. If the Q_{RMF} for each quaternary catchment is calculated, the sum of the Q_{RMF} far exceeds the known Q_{RMF} adding up to 490% more discharge into the system than previously expected. Calculating all the upstream catchments as a unit and adding this to the catchment being processed still over calculates the expected discharge (12 %). Calculating the catchment areas to be processed, and the upstream catchments, then subtracting the two gives a significantly lower discharge. This over-inflation is demonstrated in Figures 6.4 and 6.5 where the results for the summed quaternary catchments are compared to the Q_{RMF} . Using a different approach where the total upstream area of a catchment is used, instead of a series of quaternary catchments, and summed with the quaternary catchment being calculated reduces the inflation effect but still does not match the expected Q_{RMF} model values (Fig. 6.3 and 6.4).

This situation arises because the discharge from each catchment does not equally contribute to the flood peak, which is assumed by summing the discharge values for linked quaternary catchments. This situation may occur if a catchment characteristic, mainly the time taken for the flood peak to pass out of a quaternary catchment, matches an adjacent catchment. However, this is probably unlikely, with the result that only a portion of discharge from a catchment will contribute to the flood peak with the balance of the discharge attenuating the flood period. To address this issue a modification to the Regional Maximum Flood peak discharge is required and forms part of the focus of the sections below.

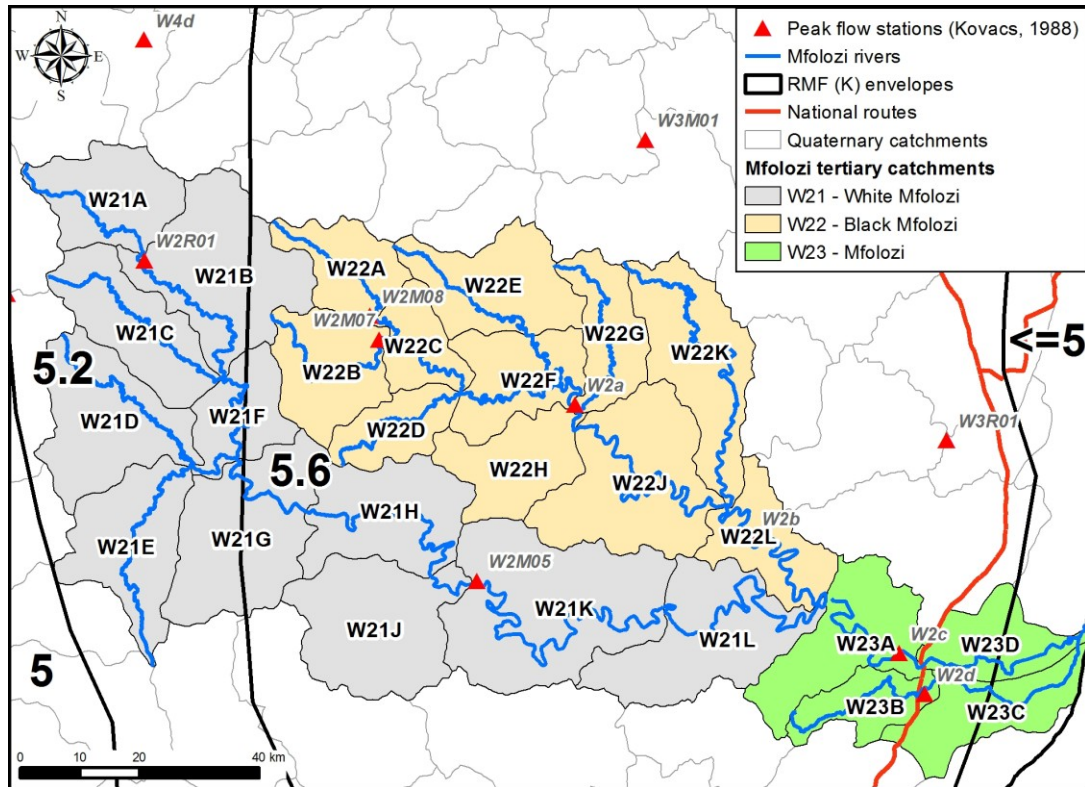


Figure 6.3. Map of the Mfolozi River Catchment showing the quaternary catchments that comprise the White Mfolozi River (W21), Black Mfolozi River (W22) and Mfolozi River (W23). The gauging stations used to define RMF (Kovács, 1988) and hydrographic envelopes (K) are also shown.

6.1.1. Modified Regional Maximum Flood

Calculating the timing of flood peaks can be complex and is beyond the parameters of the Flood Zone Model (FZM) of this thesis which aims at a simplistic methodology. It is clear from the graphs in Figures. 6.4 and 6.5 that the upstream catchment inflow and individual quaternary

catchment Q_{RMF} values need to be systematically reduced so that they are similar to the Q_{RMF} model value for the same catchment area.

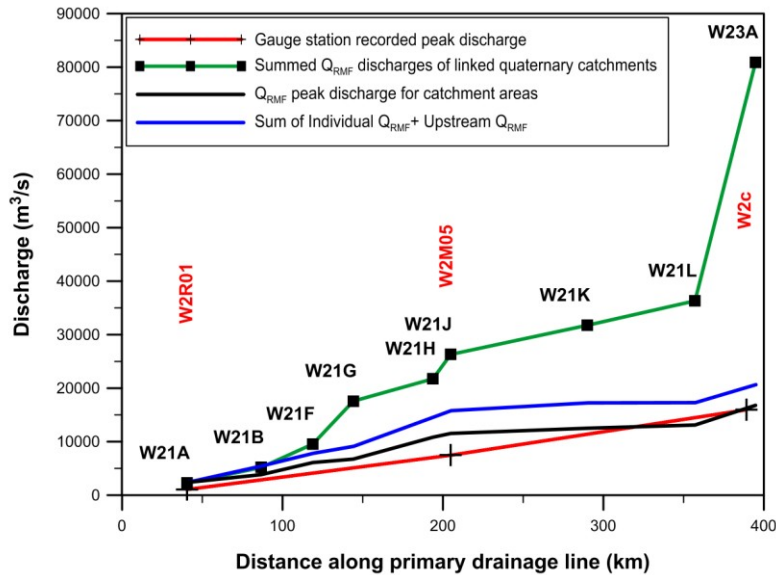


Figure 6.4. Graph of discharge (m^3/s) versus distance (km) along the primary drainage line of the White Mfolozi River showing Q_{RMF} , summed individual quaternary catchments, individual quaternary catchments and total upstream catchment compared to gauge station discharge.

Using a portion of the Black Mfolozi quaternary catchment systems as a specific demonstrative example (Fig. 6.6), to calculate the Q_{RMF} model peak at Point A (Fig. 6.6) the quaternary catchment area of W22A (239 km^2) is used. Similarly the calculation for the Q_{RMF} model peak discharge at Point B and C (Fig. 6.6) will be the area of W22A + W22B + W22C (756 km^2) and W22A + W22B + W22C + W22D + W22E + W22F (1651 km^2) respectively. Calculating the Q_{RMF} model discharge for W22F (Fig. 6.5 - Point C), which is the sum of the upstream quaternary catchments plus the Regional Maximum Flood model peak discharge for W22F, results in a discharge far greater than that calculated from the standard Regional Maximum Flood method. It is clear the same problem arises with the Regional Maximum Flood discharge for the White Mfolozi (W21) as discussed above.

The similar results for the plots of Sum of Individual Q_{RMF} + Upstream Q_{RMF} and Q_{RMF} peak discharge for catchment areas (Figs. 6.4 and 6.5), indicates that a dual reduction factor can be applied to deal with the upstream catchment area and the individual quaternary catchment areas separately. To test this, a spreadsheet was created for all the quaternary catchments in KZN (275). The areas of all the upstream quaternary catchments were calculated for each individual quaternary catchment, summed and then compared to the total of the upstream and individual quaternary catchments as shown in Table 6.3.

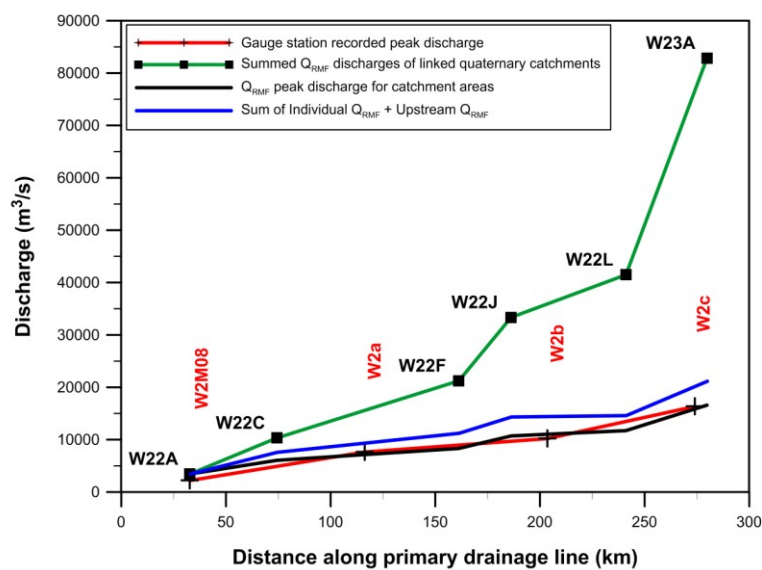


Figure 6.5. Graph of discharge (m^3/s) versus distance (km) along the primary drainage line of the Black Mfolozi River showing Q_{RMF} , summed individual quaternary catchments, individual quaternary catchments and total upstream catchment compared to gauge station discharge.

An individual quaternary catchment reduction factor and a separate upstream catchment reduction factor were applied for each hydrographic region and the areal range, as defined by Kovács (1988) and depicted in Table 6.4, was used. The reduction factors were applied to the catchment areas (as the Regional Maximum Flood method is based on area) and by reducing the area, the Regional Maximum Flood peak discharge is automatically reduced. The reduction factors were gradually reduced and varied by experimentation until the average Q_{RMF} percentage

error for all the quaternary catchments within each hydrographic region and areal range was close to zero (Table 6.4).

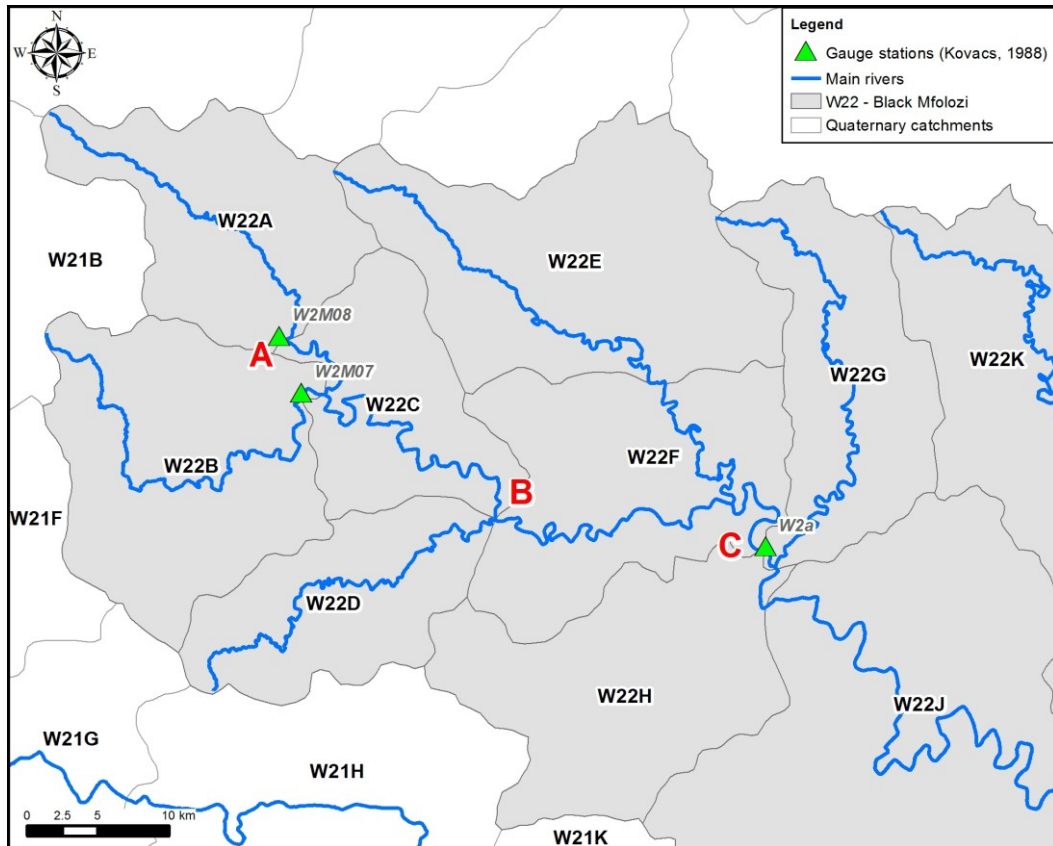


Figure 6.6. Map of a portion of the Black Mfolozi Catchment showing Q_{RMF} peak discharge areas calculated. A – W22A (239 km²), B - W22A + W22B + W22C (756 km²) and C - W22A + W22B + W22C + W22D + W22E + W22F (1651 km²).

Table 6.3. Example of the comparison between the sum of an individual and upstream quaternary catchments with the total for all the quaternary catchments of the same area.

	Individual Quaternary Catchment	Upstream Quaternary Catchments	Sum of Individual and Upstream Quaternary Catchments	Total Quaternary Catchments	% Q_{RMF} Error
Catchment(s)	W22F	W22A - E	W22A - E + W22F	W22A – F	
Area (km ²)	312	1339	1651	1651	
Q_{RMF} (m ³ /s)	3780	7174	10954	7867	39

Table 6.4. Area reduction factors and average percentage error for each hydrographic region and areal range.

Individual Quaternary Catchment Area Reduction Factors $F_{R(I)}$					Upstream Catchment Area Reduction Factors $F_{R(U)}$					Average % Error Between the Sum of the Individual and Upstream Catchment Q_{RMF} and Total Q_{RMF}				
Area/ K_e	5	5.2	5.4	5.6	Area/ K_e	5	5.2	5.4	5.6	Area/ K_e	5	5.2	5.4	5.6
100			1	1	100					100			0	
300	1	1	1	1	300	0.2	0.2	0.2	0.2	300	0	0	0	0
1000	0.9	0.9	0.9	0.9	1000	0.35	0.35	0.3	0.3	1000	-1	1	1.9	0.7
3000	0.8			0.8	3000	0.45	0.45	0.4	0.35	3000	0.8	1.8	2.5	2.7
10000					10000	0.6	0.6	0.55	0.5	10000	0	2.8	1.2	1.3
30000					30000	0.75	0.8			30000	0.5	1.4		

The results of the modified discharges (Q_{MRMF}) were tested against the highest peak gauge station discharge data used by Kovács (1988) to define the Regional Maximum Flood hydrographic region envelopes. Table 6.5 lists the gauge station data and the Q_{MRMF} method results compared to the projected Q_{RMF} peak discharge for each station. The estimated 1:50, 1:100 and 1:200 Year return period estimates are also shown and used to check that the measured peak at each gauge station is comparable to the return period peak.

Table 6.1. List of gauging stations showing highest recorded flood peaks and return periods with a comparison of the modified Regional Maximum Flood (Q_{MRMF}) calculations to the projected Regional Maximum Flood (Q_{RMF}) calculations for each station.

GAUGE STATIONS							QUATERNARY CATCHMENT AREA UPSTREAM OF GAUGE STATION						UPSTREAM QUATERNARY CATCHMENTS AREA (Inflow)					
Gauging Site	River	Area (km ²)	Peak (m ³ /s)	Return Period (Years)	RMF Envelope	Q_{RMF} (m ³ /s)	Q_{MRMF} (m ³ /s)	Q_{M200} (m ³ /s)	Q_{M100} (m ³ /s)	Q_{M50} (m ³ /s)	Effective Area (km ²)	Catchment Area (km ²)	Q_{MRMF} (m ³ /s)	Q_{M200} (m ³ /s)	Q_{M100} (m ³ /s)	Q_{M50} (m ³ /s)	Effective Area (km ²)	Catchment Area (km ²)
T3M04	Mzimhlava	1029	1029	41	5	3205	1832	1160	947	753	335.7	373	1513	1000	832	676	228.9	654
T4M01	Mtamvuna	715	2270	190	5.2	3418	2001	1301	1049	822	237	237	1706	1109	894	701	170.1	486
T4	Mtamvuna	1557	3170	75	5.4	6188	3424	2167	1791	1407	436.5	485	3429	2267	1941	1533	438	1095
T5M04	Mzimkulu	545	651	39	5	2319	1449	917	749	596	210	210	1071	678	554	440	114.8	328
T5M07	Mzimkulu	3586	3800	57	5.2	7425	2096	1362	1098	861	261	261	5607	3930	3297	2702	2027.4	3379
T5M02	Bisi	867	1300	54	5.2	3737	1935	1258	1014	795	221	221	1962	1275	1028	806	227.5	650
T5M06	Mzimkulwana	534	1110	39	5.4	3973	2266	1376	1115	861	178	178	1944	1231	1017	799	127.5	425
T5	Mzimkulu	6630	6520	57	5.4	12000	2799	1772	1464	1151	281.7	313	8916	6384	5554	4663	3495.25	6355
U1M06	Mkomazi	4375	7000	132	5.4	9898	2792	1767	1460	1147	280	280	7293	5011	4289	3515	2258.85	4107
U2R03	Mgeni	1644	2530	60	5.2	5083	2416	1570	1266	993	351	390	2384	1576	1311	1066	568.35	1263
U2M10	Msindusaan	30	255	24	5	742	742	482	389	305	30	30						
U2	Dorpspruit	69	340	41	5.2	1107	1052	711	585	470	62.1	69						
U2M22	Msunduze	877	1440	40	5.2	3750	3103	2098	1725	1387	591.3	657	892	556	441	339	44	220
U2M15	Mgeni	4023	5500	70	5.4	9572	2860	1811	1496	1176	295.2	328	6996	4806	4113	3372	2063.05	3751
U3R01	Mdloti	377	1830	125	5.4	3197	3046	1928	1593	1252	338.4	376						
U3M01	Tongati	318	2100	200	5.4	3081	1778	1079	875	676	105	105	1245	756	613	473	48.4	242
U4M05	Mvoti	2473	5000	170	5.4	7604	3046	1928	1593	1252	338.4	376	4624	3177	2719	2229	838.8	2097
U5a	Zinkwazi	28	400	85	5.4	968	968	613	506	398	28	28						
U5b	Nonoti	157	1160	120	5.4	2139	2139	1354	1119	879	157	157						
U6R01	Mlazi	781	1500	30	5.4	4488	3004	1902	1571	1235	328.5	365	1935	1225	1012	795	126.3	421
U6	Mhaltuzana	119	750	55	5.4	1883	1883	1192	985	774	119	119						
U7M02	Lovu	936	2000	30	5.4	4882	2435	1541	1273	1001	208	208	2503	1654	1416	1119	220.8	736
U8d	Mzumbe	536	1320	30	5.4	3779	2402	1521	1256	987	202	202	1752	1109	916	720	101.7	339
U8c	Mtwalume	565	992	29	5.4	3815	2009	1220	989	764	137	137	1923	1217	1006	790	124.5	415
U8b	Fafa	225	1000	29	5.4	2524	2524	1598	1320	1038	225	225						
U8a	Mpambanyoni	548	1230	29	5.4	3824	2301	1457	1204	946	184	184	1826	1156	955	751	111.3	371
V1M26	Tugela	1894	1400	21	5	4384	1200	730	586	456	144	144	2829	1870	1556	1264	800.1	1778
V1M38	Klip	1644	2200	65	5	4053	1716	1086	887	705	294.3	327	2146	1359	1110	882	460.6	1316
V1M22	Mazomgwana	0.62	7.9	24	5	79	75	47	39	31	0.558	0.62						
V1M10	Little Tugela	782	630	17	5	2796	1600	1013	827	658	256	256	1026	649	530	422	105.2	526
V1M01	Tugela	4176	3400	28	5	6487	1497	947	774	615	224	224	4889	3359	2845	2357	2390.4	3984
V2a	Mooi	1186	1380	54	5	3444	1552	1026	854	694	241	241	1819	1202	1000	813	330.75	945
V2R01	Mnyamvubu	152	377	25	5	1241	1241	755	606	472	154	154						
V2b	Mooi	2482	2000	54	5	5054	2330	1540	1281	1041	542.7	603	2963	2036	1724	1428	877.95	1951
V3M05	Slang	676	400	33	5	2600	2467	1630	1357	1103	608.4	676						
V3R01	Ngagane	830	1270	24	5	2888	2740	1811	1507	1225	750.6	834						

GAUGE STATIONS							QUATERNARY CATCHMENT AREA UPSTREAM OF GAUGE STATION						UPSTREAM QUATERNARY CATCHMENTS AREA (Inflow)					
Gauging Site	River	Area (km²)	Peak (m³/s)	Return Period (Years)	RMF Envelope	Q _{RMF} (m³/s)	Q _{M_{RMF}} (m³/s)	Q _{M₂₀₀} (m³/s)	Q _{M₁₀₀} (m³/s)	Q _{M₅₀} (m³/s)	Effective Area (km²)	Catchment Area (km²)	Q _{M_{RMF}} (m³/s)	Q _{M₂₀₀} (m³/s)	Q _{M₁₀₀} (m³/s)	Q _{M₅₀} (m³/s)	Effective Area (km²)	Catchment Area (km²)
V3M11	Bloed	543	1200	80	5	2982	2835	1916	1576	1267	489.6	544						
V3M01	Buffels	7930	2380	18	5	10790	4073	2695	2212	1772	613.8	682	8144	5725	4870	4070		
V5M02	Tugela	28490	15100	71	5.2	20120	1591	993	786	605	147	147	18033	13669	11902	10207	23117.6	28897
V6M02	Tugela	12862	4610	41	5	11339	1787	1131	924	735	319.5	355	9683	7243	6362	5490	9376.5	12502
V7M12	Little Bushmans	196	1050	58	5	1407	1407	891	727	578	198	198						
V7M12	Bushmans	1100	2030	58	5	3317	697	441	360	287	48.6	54	2170	1434	1193	970	470.7	1046
W1R02	Mlalazi	14	132	10	5.6	965	921	722	589	463	12.6	14						
W1R01	Mhlathuze	1273	3650	40	5.6	7031	5004	4018	3343	2687	590.4	656	3017	2365	1931	1517	186.9	623
W1e	Matigulu	583	3170	90	5.6	4927	4704	3777	3142	2526	513	570						
W1b	Mfule	618	3300	95	5.6	5106	4874	3821	3120	2452	556.2	618						
W1a	Nseleni	547	4250	200	5.6	4839	3100	2431	1984	1559	198.9	221	2269	1779	1452	1141	97.8	326
W1d	Mlalazi	230	930	20	5.6	3305	3305	2591	2115	1662	230	230						
W2R01	White Mfolozi	340	1090	65	5.2	2379	2262	1470	1185	930	306	340						
W2M05	White Mfolozi	3939	7500	75	5.6	11540	4556	3658	3043	2446	477	530	7983	6554	5548	4551	1707	3414
W2M08	Black Mfolozi	238	2180	110	5.6	3361	3361	2635	2151	1691	239	239						
W2M07	Bizamkulu	78	585	23	5.6	2054	2054	1610	1314	1033	78	78						
W2a	Black Mfolozi	1635	7500	200	5.6	7867	3608	2829	2309	1815	280.8	312	4520	3630	3020	2427	468.65	1339
W2b	Black Mfolozi	3393	10000	200	5.6	10801	2350	1843	1504	1182	106	106	7851	6446	5457	4475	1643.5	3287
W2c	Mfolozi	9216	16000	200	5.6	16792	4069	3190	2604	2047	369	410	12134	10168	8785	7365	4420	8840
W2d	Mzinduzi	179	1330	63	5.6	3060	3060	2399	1958	1539	193	193						
W3M01	Mkuze	1467	3320	25	5.6	7486	3718	2915	2380	1870	300.6	334	4213	3383	2814	2262	399.35	1141
W3M02	Mkuze	2647	5500	60	5.6	9683	4772	3832	3188	2563	530.1	589	5462	4386	3648	2933	720.3	2058
W3R01	Hluhluwe	734	3060	63	5.6	5471	4264	3343	2729	2145	410.4	456	1738	1337	1073	824	53.4	267
W4d	Bivane	878	1060	38	5.2	3752	1691	1099	886	695	167	167	2048	1385	1139	916	248.85	711
W4c	Pongolo	1731	2750	75	5.2	5123	2693	1751	1411	1107	440.1	489	2960	2001	1646	1323	535.95	1191
W4b	Mozane	426	3020	125	5.6	4335	4138	3244	2648	2082	383.4	426						
W4M03	Pongolo	5788	9200	80	5.6	13653	3990	3128	2553	2007	352.8	392	9758	8177	7065	5923	2693.5	5387
W4R01	Pongolo	7831	13000	200	5.6	15563	5188	4166	3465	2786	640.8	712	10998	9216	7962	6676	3535	7070

Table 6.5 (Continued). List of gauging stations showing highest recorded flood peaks and return periods with a comparison of the modified Regional Maximum Flood (Q_{MRMF}) calculations to the projected Regional Maximum Flood (Q_{RMF}) calculations for each station.

GAUGE STATIONS							COMBINED AREA OF CATCHMENT UPSTREAM OF GAUGING STATION					ERROR CHECKING		
Gauging Site	River	Area (km ²)	Peak (m ³ /s)	Return Period (Years)	RMF Envelope	Q_{RMF} (m ³ /s)	Q_{MRMF} (m ³ /s)	Q_{M200} (m ³ /s)	Q_{M100} (m ³ /s)	Q_{M50} (m ³ /s)	Catchment Area (km ²)	$Q_{MRMF} + Q_{MRMF}$ Inflow	Difference to Q_{RMF}	% Error
T3M04	Mzimhlava	1029	1029	41	5	3205	3205	2202	1865	1545	1027	3345	140	4.2
T4M01	Mtamvuna	715	2270	190	5.2	3418	3418	2310	1900	1528	723	3707	290	7.8
T4	Mtamvuna	1557	3170	75	5.4	6188	6188	4251	3638	2982	1580	6853	666	9.7
T5M04	Mzimkulu	545	651	39	5	2319	2319	1533	1276	1037	538	2521	201	8.0
T5M07	Mzimkulu	3586	3800	57	5.2	7425	7425	5443	4648	3906	3640	7702	277	3.6
T5M02	Bisi	867	1300	54	5.2	3737	3737	2527	2078	1671	871	3897	160	4.1
T5M06	Mzimkulwana	534	1110	39	5.4	3973	3973	2626	2249	1776	603	4210	238	5.6
T5	Mzimkulu	6630	6520	57	5.4	12000	12000	8592	7476	6276	6668	11715	-285	-2.4
U1M06	Mkomazi	4375	7000	132	5.4	9898	9898	7087	6166	5177	4387	10085	187	1.9
U2R03	Mgeni	1644	2530	60	5.2	5083	5083	3563	2989	2450	1653	4800	-283	-5.9
U2M10	Msindusaan	30	255	24	5	742	742	482	389	305	30	742	0	0.0
U2	Dorpspruit	69	340	41	5.2	1107	1107	748	615	495	69	1052	-55	-5.2
U2M22	Msunduze	877	1440	40	5.2	3750	3750	2535	2085	1676	877	3995	245	6.1
U2M15	Mgeni	4023	5500	70	5.4	9572	9572	6854	5963	5006	4079	9856	284	2.9
U3R01	Mdloti	377	1830	125	5.4	3197	3197	2113	1809	1429	376	3046	-151	-5.0
U3M01	Tongati	318	2100	200	5.4	3081	3081	2037	1744	1377	347	3023	-58	-1.9
U4M05	Mvoti	2473	5000	170	5.4	7604	7604	5224	4471	3665	2473	7670	66	0.9
U5a	Zinkwazi	28	400	85	5.4	968	968	613	506	398	28	968	0	0.0
U5b	Nonoti	157	1160	120	5.4	2139	2139	1354	1119	879	157	2139	0	0.0
U6R01	Mlazi	781	1500	30	5.4	4488	4488	2966	2540	2006	786	4940	452	9.1
U6	Mhaltuzana	119	750	55	5.4	1883	1883	1192	985	774	119	1883	0	0.0
U7M02	Lovu	936	2000	30	5.4	4882	4882	3227	2763	2182	944	4937	55	1.1
U8d	Mzumbe	536	1320	30	5.4	3779	3779	2498	2139	1689	541	4154	375	9.0
U8c	Mtwalume	565	992	29	5.4	3815	3815	2521	2159	1705	552	3932	118	3.0
U8b	Fafa	225	1000	29	5.4	2524	2524	1598	1320	1038	225	2524	0	0.0
U8a	Mpambanyoni	548	1230	29	5.4	3824	3824	2528	2164	1709	555	4127	303	7.3
V1M26	Tugela	1894	1400	21	5	4384	4384	3012	2552	2113	1922	4029	-355	-8.8
V1M38	Klip	1644	2200	65	5	4053	4053	2679	2229	1812	1643	3862	-192	-5.0
V1M22	Mazomgwana	0.62	7.9	24	5	79	79	52	43	35	0.62	75	-4	-5.4
V1M10	Little Tugela	782	630	17	5	2796	2796	1848	1538	1250	782	2626	-171	-6.5
V1M01	Tugela	4176	3400	28	5	6487	6487	4658	4015	3406	4208	6386	-101	-1.6
V2a	Mooi	1186	1380	54	5	3444	3444	2366	2004	1660	1186	3371	-73	-2.2

GAUGE STATIONS							COMBINED AREA OF CATCHMENT UPSTREAM OF GAUGING STATION					ERROR CHECKING		
Gauging Site	River	Area (km ²)	Peak (m ³ /s)	Return Period (Years)	RMF Envelope	Q _{RMF} (m ³ /s)	Q _{MRRMF} (m ³ /s)	Q _{M200} (m ³ /s)	Q _{M100} (m ³ /s)	Q _{M50} (m ³ /s)	Catchment Area (km ²)	Q _{MRRMF} + Q _{MRRMF} Inflow	Difference to Q _{RMF}	% Error
V2R01	Mnyamvubu	152	377	25	5	1241	1241	786	642	510	154	1241	0	0.0
V2b	Mooi	2482	2000	54	5	5054	5054	3472	2941	2436	2554	5293	239	4.5
V3M05	Slang	676	400	33	5	2600	2600	1719	1430	1162	676	2467	-133	-5.4
V3R01	Ngagane	830	1270	24	5	2888	2888	1909	1588	1291	834	2740	-148	-5.4
V3M11	Bloed	543	1200	80	5	2982	2982	2016	1658	1333	544	2835	-147	-5.2
V3M01	Buffels	7930	2380	18	5	10790	10790	7564	6344	5201	7930	12217	1427	11.7
V5M02	Tugela	28490	15100	71	5.2	20120	20120	15251	13279	11388	29044	19624	-497	-2.5
V6M02	Tugela	12862	4610	41	5	11339	11339	8481	7450	6429	12857	11471	132	1.1
V7M12	Little Bushmans	196	1050	58	5	1407	1407	930	774	629	198	1407	0	0.0
V7M12	Bushmans	1100	2030	58	5	3317	3317	2279	1930	1599	1100	2867	-450	-15.7
W1R02	Mlalazi	14	132	10	5.6	965	965	774	644	518	14	921	-44	-4.7
W1R01	Mhlathuze	1273	3650	40	5.6	7031	7031	5773	4887	4008	1279	8021	989	12.3
W1e	Matigulu	583	3170	90	5.6	4927	4927	3956	3291	2646	570	4704	-223	-4.7
W1b	Mfule	618	3300	95	5.6	5106	5106	4100	3411	2742	618	4874	-231	-4.7
W1a	Nseleni	547	4250	200	5.6	4839	4839	3885	3232	2598	547	5369	530	9.9
W1d	Mlalazi	230	930	20	5.6	3305	3305	2591	2115	1662	230	3305	0	0.0
W2R01	White Mfolozi	340	1090	65	5.2	2379	2379	1609	1323	1064	340	2262	-117	-5.2
W2M05	White Mfolozi	3939	7500	75	5.6	11540	11540	9671	8355	7005	3944	12539	999	8.0
W2M08	Black Mfolozi	238	2180	110	5.6	3361	3361	2635	2151	1691	239	3361	0	0.0
W2M07	Bizamkulu	78	585	23	5.6	2054	2054	1649	1372	1103	78	2054	0	0.0
W2a	Black Mfolozi	1635	7500	200	5.6	7867	7867	6459	5468	4484	1651	8129	262	3.2
W2b	Black Mfolozi	3393	10000	200	5.6	10801	10801	9051	7820	6556	3393	10202	-599	-5.9
W2c	Mfolozi	9216	16000	200	5.6	16792	16792	14072	12158	10193	9250	16203	-589	-3.6
W2d	Mzinduzi	179	1330	63	5.6	3060	3060	2399	1958	1539	193	3060	0	0.0
W3M01	Mkuze	1467	3320	25	5.6	7486	7486	6146	5203	4267	1475	7931	445	5.6
W3M02	Mkuze	2647	5500	60	5.6	9683	9683	7950	6730	5519	2647	10234	551	5.4
W3R01	Hluhluwe	734	3060	63	5.6	5471	5471	4393	3654	2938	723	6002	532	8.9
W4d	Bivane	878	1060	38	5.2	3752	3752	2536	2086	1677	878	3740	-12	-0.3
W4c	Pongolo	1731	2750	75	5.2	5123	5123	3591	3012	2469	1680	5654	531	9.4
W4b	Mozane	426	3020	125	5.6	4335	4335	3481	2896	2328	426	4138	-196	-4.7
W4M03	Pongolo	5788	9200	80	5.6	13653	13653	11441	9885	8287	5779	13747	94	0.7
W4R01	Pongolo	7831	13000	200	5.6	15563	15563	13042	11267	9447	7782	16185	622	3.8

The results from Table 6.5 were plotted on log/log axis graphs for peak discharge versus area with a best fit power function similar to the plot of Figure 6.2 used to define the Regional Maximum Flood hydrographic region envelopes. Each Regional Maximum Flood hydrographic region was plotted separately (Figs. 6.7 – 6.10) to compare the Q_{RMF} , Q_{200} , Q_{100} and Q_{50} peaks with that of the equivalent results from the Q_{MRMF} calculations. The correlation coefficients for the various hydrographic regions and return periods for the Regional Maximum Flood and modified Regional Maximum Flood range from 0.0995 to 0.998. The R^2 least squares fit for the original data varies between 0.996 and 1.000 while the modified data yielded R^2 values 0.994 and 0.997.

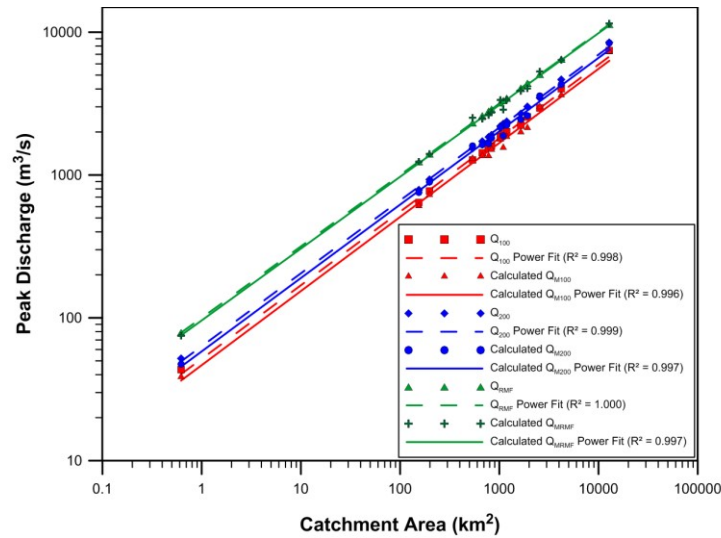


Figure 6.1. Graph of highest recorded flood peaks for hydrographic region 5 comparing Q_{RMF} and the results for the modified Q_{MRMF} and the associated return periods.

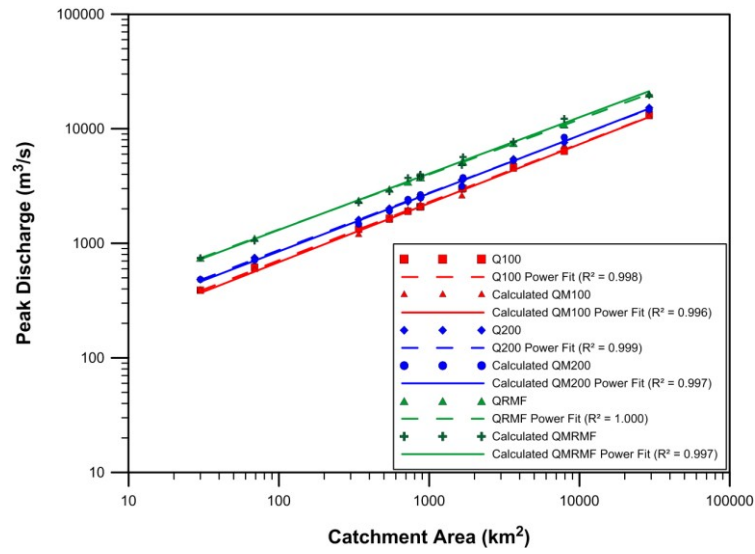


Figure 6.2. Graph of highest recorded flood peaks for hydrographic region 5.2 comparing Q_{RMF} and the results for the modified Q_{MRMF} and the associated return periods.

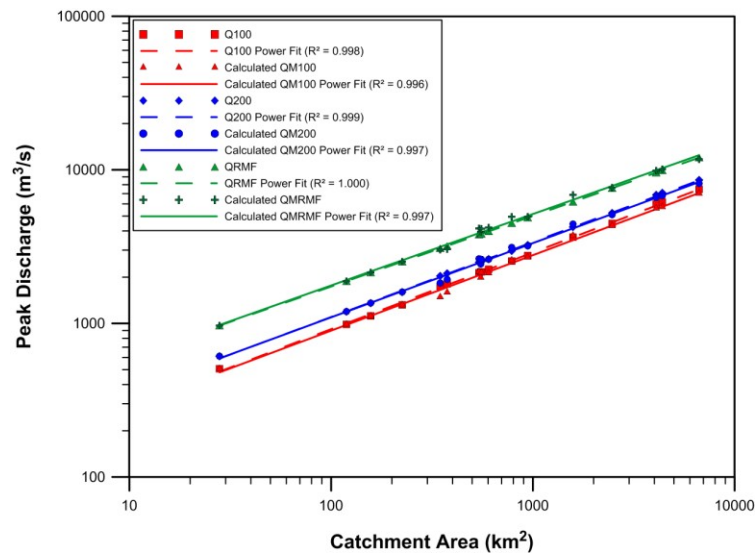


Figure 6.3. Graph of highest recorded flood peaks for hydrographic region 5.4 comparing Q_{RMF} and the results for the modified Q_{MRMF} and the associated return periods.

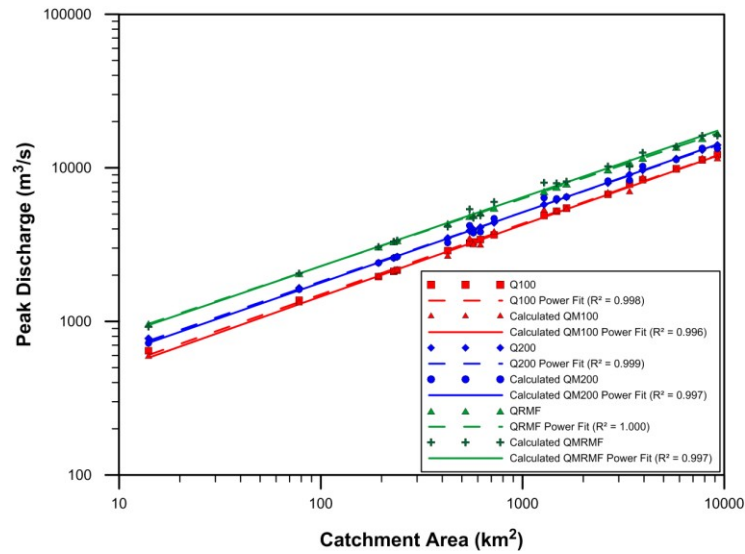


Figure 6.4. Graph of highest recorded flood peaks for hydrographic region 5.6 comparing Q_{RMF} and the results for the modified Q_{MRMF} and the associated return periods.

The Modified Q_{MRMF} Formulae (Table 6.6) are then used to determine the discharge per quaternary catchment. If discharge at a point such as a river crossing needs to be calculated the standard Q_{RMF} formulae (Eq 5 – Eq 8) applies.

Table 6.1. Modified Q_{MRMF} Formulae incorporating the Reduction Factor

Hydrographic Region	Q_{MRMF} (m³/s)	Equation
5.0	$Q_{MRMF} = 100(A_e F_{R(I,U)})^{0.50}$	Eq 9
5.2	$Q_{MRMF} = 145(A_e F_{R(I,U)})^{0.48}$	Eq 10
5.4	$Q_{MRMF} = 209(A_e F_{R(I,U)})^{0.46}$	Eq 11
5.6	$Q_{MRMF} = 302(A_e F_{R(I,U)})^{0.44}$	Eq 12
A_e = Effective Catchment area (km²) Q_{MRMF} = Modified RMF peak discharge $F_{R(I,U)}$ = Individual (I) or Upstream (U) Catchment Reduction Factor		

The modified process used to calculate the Q_{MRMF} discharge for a quaternary catchment being modelled is:

- To determine the geographic position of the quaternary catchment and its relationship to the Regional Maximum Flood hydrographic regions. If it locates across two regions the higher value region is used (Kovács 1988).
- The areas of the upstream quaternary catchments are summed and treated as a single catchment and the Regional Maximum Flood hydrographic region determined as described above.
- To then calculate the Q_{MRMF} for the inflow and the target quaternary catchment separately using the formulae in Table 6.6.
- The return periods for the above are calculated from the factors in Table 6.2.

1.1.1. Sub-catchments discharge determination

To determine the flood elevations in HEC-RAS[®] the discharge for each sub-catchment (river reach) is required. Sub-catchment areas are too small to be used in the Regional Maximum Flood method, but logically the accumulated discharge of a sub-catchment equals the total Q_{MRMF} or Q_{M100} discharge for that quaternary catchment. By distributing the Q_{MRMF} or Q_{M100} discharge using the ratio of sub-catchment areas to quaternary catchment area, the individual sub-catchment discharges are derived.

1.2. Calibration

This model consists of three components; the flow regime geometry of the derived sub-catchments, volume of water in the system that produces peak discharge (Q_{MRMF}) and the roughness effect on travel time of the water moving through the system. The first two components are fixed by virtue of the available data used for the geometry development and the estimated Q_{MRMF} peak discharges. The only variable that can be adjusted to make the model results match the field observations (as depicted in Chapter 5) is the friction variable.

Flood elevations can be modified by raising or lowering the roughness coefficient. Larger roughness coefficient values imply greater interaction between the water and the wetted perimeter, both increasing energy losses and increasing the travel time for water to move through the system, resulting in backwater curves with associated increased water levels. HEC-RAS[®] uses Manning n values as a roughness coefficient, which tends to be user subjective (Bridge, 2003) and can be a large source of error in flood modelling. The Chezy equation or the Darcy-Weisbach are alternative methods used to calculate the roughness coefficient. The latter is preferred as the Manning and Chezy equation's roughness coefficients are dimensional whereas the Darcy-Weisbach is dimensionless (Bridge, 2003). Although this is a drawback of the HEC-RAS[®] software, it is an advantage for the modelling process described here, in that the HEC-RAS[®] Manning value variable can be used as a calibration factor (CF) to adjust the modelled flood elevation surface to match the field observations/1:100 year return period design floodline estimate control data.

1.2.1. Q_{MRMF} discharges equal field evidence

The assumption is made that the highest elevations of flood clay deposits represent the maximum peak discharge recorded. This assumption is supported by field evidence of extant flood clay deposits related to Tropical Storm Domoina in 1984 (Mfolozi River) and the 1987 floods (Mgeni River) (Smith 1992b), two of the largest flood peak discharges recorded in KZN. Flood clay deposits were mapped in the various catchments (Chapter 5) ensuring that measurements were recorded along major and minor drainage lines.

1.2.2. Calibration factors (CF)

As the Flood Zone Model aims to model reaches defined by sub-catchments, various catchment parameters were tested to determine which would be suitable and could be consistently applied across the study area as a means to adjust the friction variable. A series of calibration factors at 0.01 intervals were used to create flood elevation surfaces for comparison to the field observations from the five representative quaternary catchments. The results showed that a single calibration factor did not apply to all reaches. Upper sub-catchment reaches required larger calibration factor values and lower catchment reaches smaller calibration factor values to

match the field observations (e.g. Fig 5.9, Fig. 5.12, Fig. 5.23, Fig. 5.31). Investigating the commonality between reaches and calibration factors, which matched the various modelled results, it was found that these could be grouped based on reach slope. Slope categories could then be applied where a single calibration factor value had relevance. Initially three slope categories were applied (Botes et al. 2011) but this has since been amended to four categories with the collection of additional field data (Table 6.7).

Table 6.2. Characteristics of floodplains and defined slopes categories

Slope category	Calibration factor applied	Floodplain characteristics
< 0.001	0.001	Reaches with very little or no elevation change. Valleys tend to be broad. Rivers tend to meander within the flood plain. Primarily major rivers. Common on coastal flood plains
0.01 – 0.001	0.05	Low relief. Valleys tend to be broad. Rivers tend to meander within the flood plain. Primarily major rivers.
0.01 - 0.025	0.2	Intermediate phase between the low relief drainage and the steep drainage.
> 0.025	0.4	High relief with steep sided valleys incised into the topography. Narrow floodplains.

1.3. Results

To compare the modelled results with the control data (field data/1:100 year design estimate floodlines) the points where the cross-sections cut the model results and the control data were determined. Since the cross-sections may cross flood surfaces more than once, elevation point data were averaged per cross-section for model results and control data respectively to produce an average flood elevation per surface and then assigned to the relevant slope categories. The control data results were plotted against the model results per slope category for comparison. A best fit line through the origin was drawn for the plotted data points and compared to the ideal

1:1 ratio. If the best fit line plots below the 1:1 ratio line then the calibration factor used was too low and if it plots above, then the calibration factor is too high.

1.3.1. Q_{MRMF} Results

As a first test, the plotted results for the field data from the five representative quaternary catchments are compared to the modelled Q_{MRMF} (Fig. 6.11, Table 6.8). The four calibration factor slope categories are plotted on the same axes for comparison. All four slope categories show a high R^2 fit correlation of 0.999 indicating that the selected calibration factors give acceptable results and can be applied across a range of quaternary catchments. The residual errors for the 0.001 and 0.2 calibration factors are larger than that of the 0.4 and 0.05 calibration factors. The greater error for the 0.001 calibration factor is a function of the broad shallow flood plains, consequently these areas are difficult to model (Maidment, 2002) as small differences in elevation can result in larger horizontal errors. Calibration factor 0.2 is applied to an intermediate category between calibration factor 0.4 and 0.05. Field testing the results for this range of slopes showed greater variation than the other categories. These results suggest that calibrated models based on Q_{MRMF} peak discharge can be related to field mapped flood deposits with an acceptable level of confidence (Fig. 6.11).

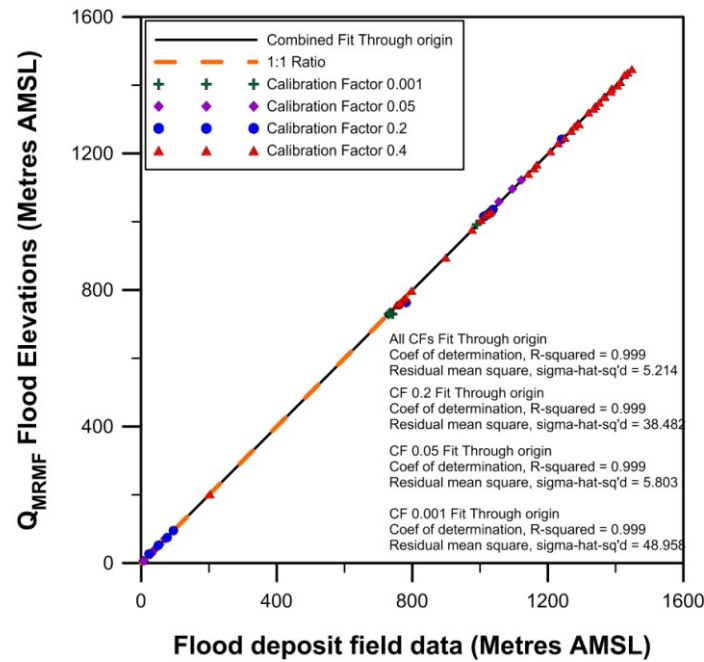


Figure 6.5. Plot of flood deposit field data for the representative quaternary catchments against Q_{MRMF} flood zone elevations with best fit through origin for all slope categories using the calibration factors.

Table 6.3. Statistical results for the representative quaternary catchments comparison between the field data elevations and Q_{MRMF} for the four slope categories

Slope range	Calibration factor	Correlation coefficient	Average difference (metres)	Average percentage error	Field data average elevation (metres)	Q_{MRMF} average elevation (metres)
< 0.001	0.001	0.999	2.148	0.005	799.20	795.89
0.001 - 0.01	0.05	0.999	1.267	3.184	953.00	951.87
0.01 - 0.025	0.2	0.999	0.250	0.019	671.68	670.40
> 0.025	0.4	0.999	0.963	0.002	777.07	776.24

Figures 6.12 to 6.19 present the Q_{RMF} modelled results of the pilot quaternary catchments (T40G, T52D, V12g and W23A), comparing the data measurement site elevations and the modelled Q_{MRMF} surface elevations. The comparison for the quaternary catchment U20H is presented and discussed in Chapter 7 (Figs 7.4 and 7.5).

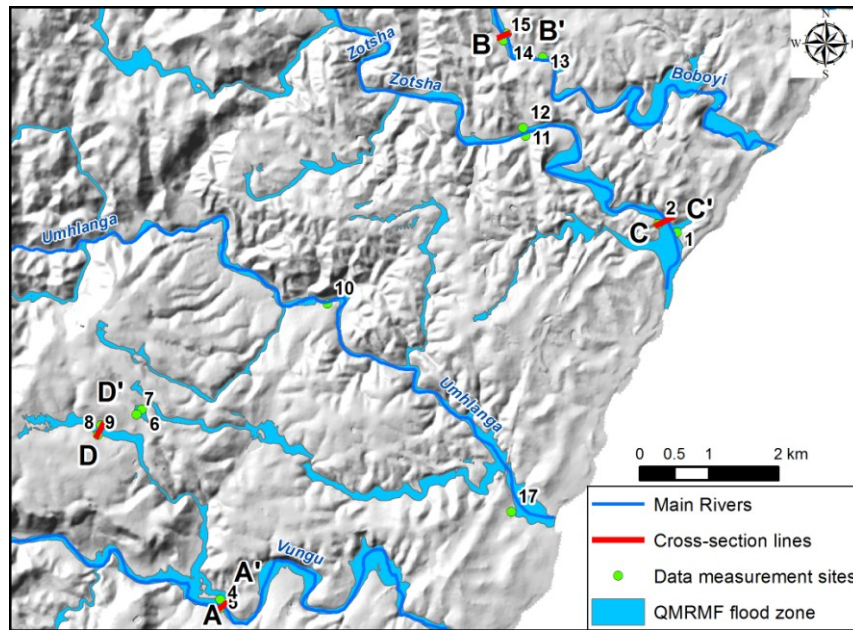


Figure 6.6. Map of a portion of the T40G quaternary catchment showing positions of cross-sections and modelled Q_{MRMF} flood zones.

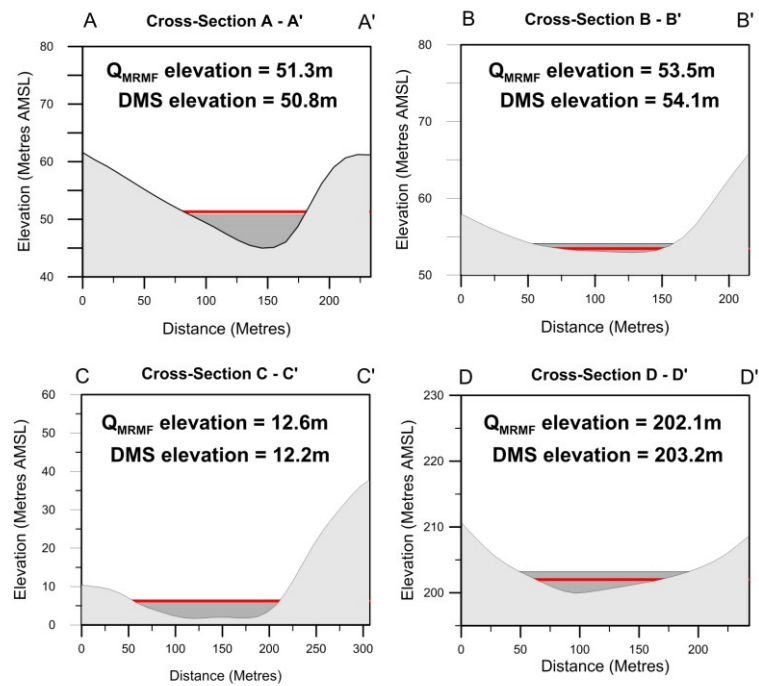


Figure 6.7. Cross-sections of quaternary catchment T40G comparing the modelled elevation surfaces with the data measurement sites. Red line (DMS) – data measurement site elevation. Dark grey – Q_{MRMF} modelled elevation.

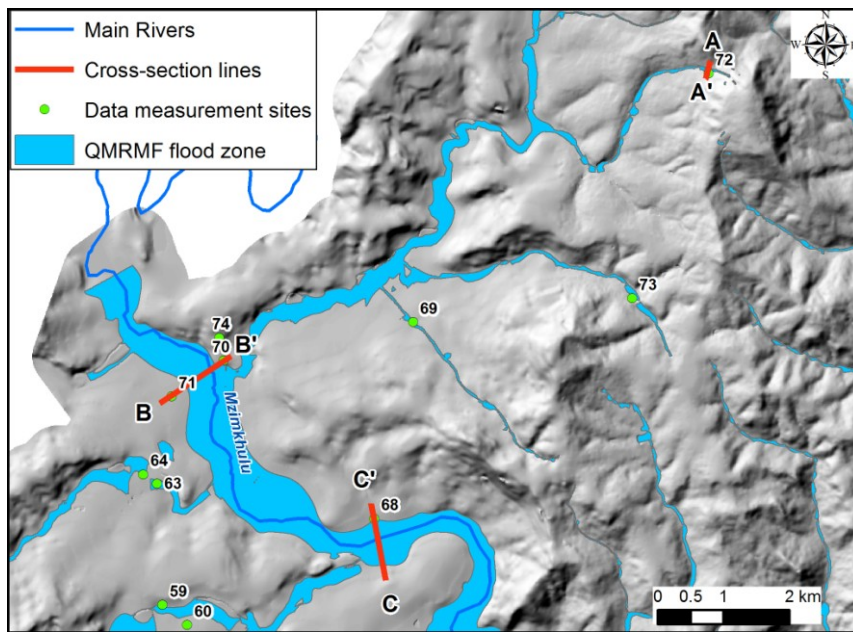


Figure 6.8. Map of a portion of the T52D quaternary catchment showing positions of cross-sections and modelled Q_{MRMF} flood zones.

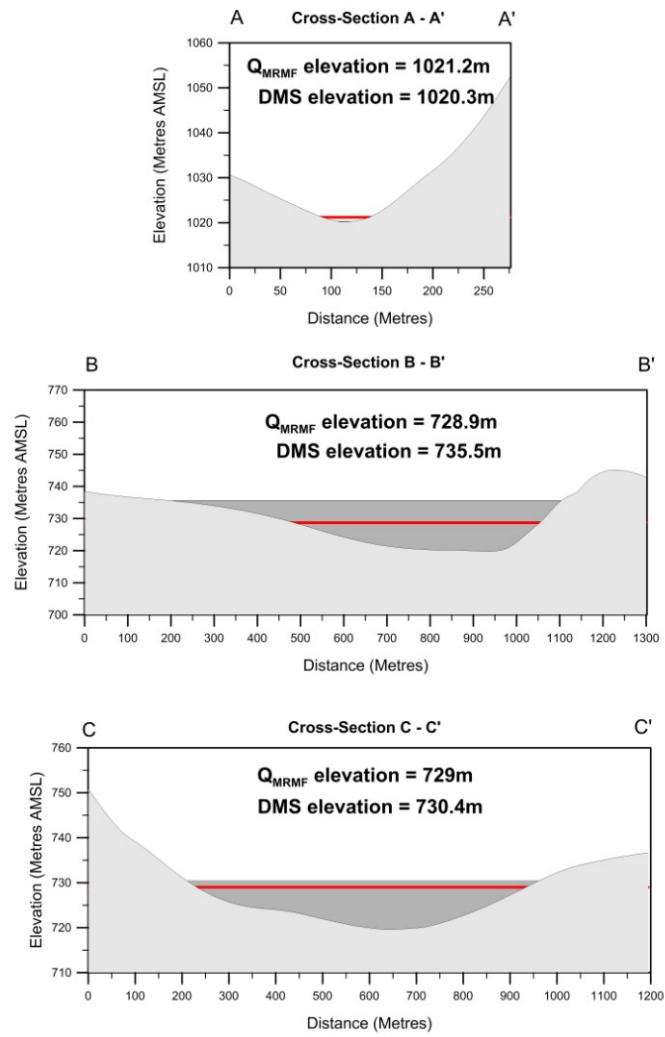


Figure 6.9. Cross-sections of quaternary catchment T52D comparing the modelled elevation surfaces with the data measurement sites. Red line (DMS) – data measurement site elevation. Dark grey – Q_{MRMF} modelled elevation.

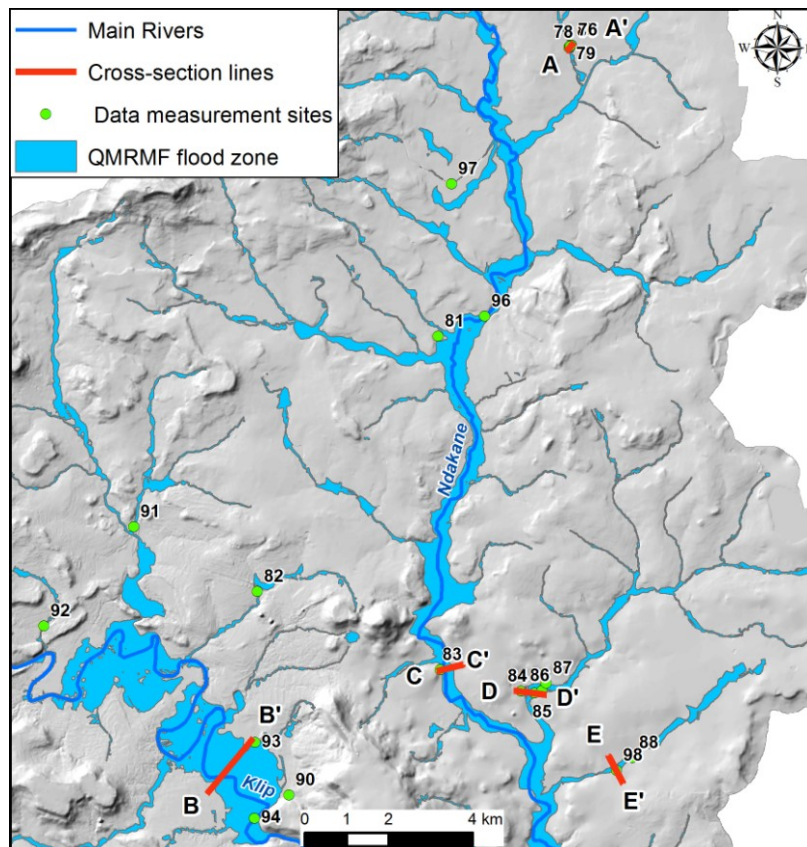


Figure 6.10. Map of a portion of the V12G quaternary catchment showing positions of cross-sections and modelled Q_{MRMF} flood zones.

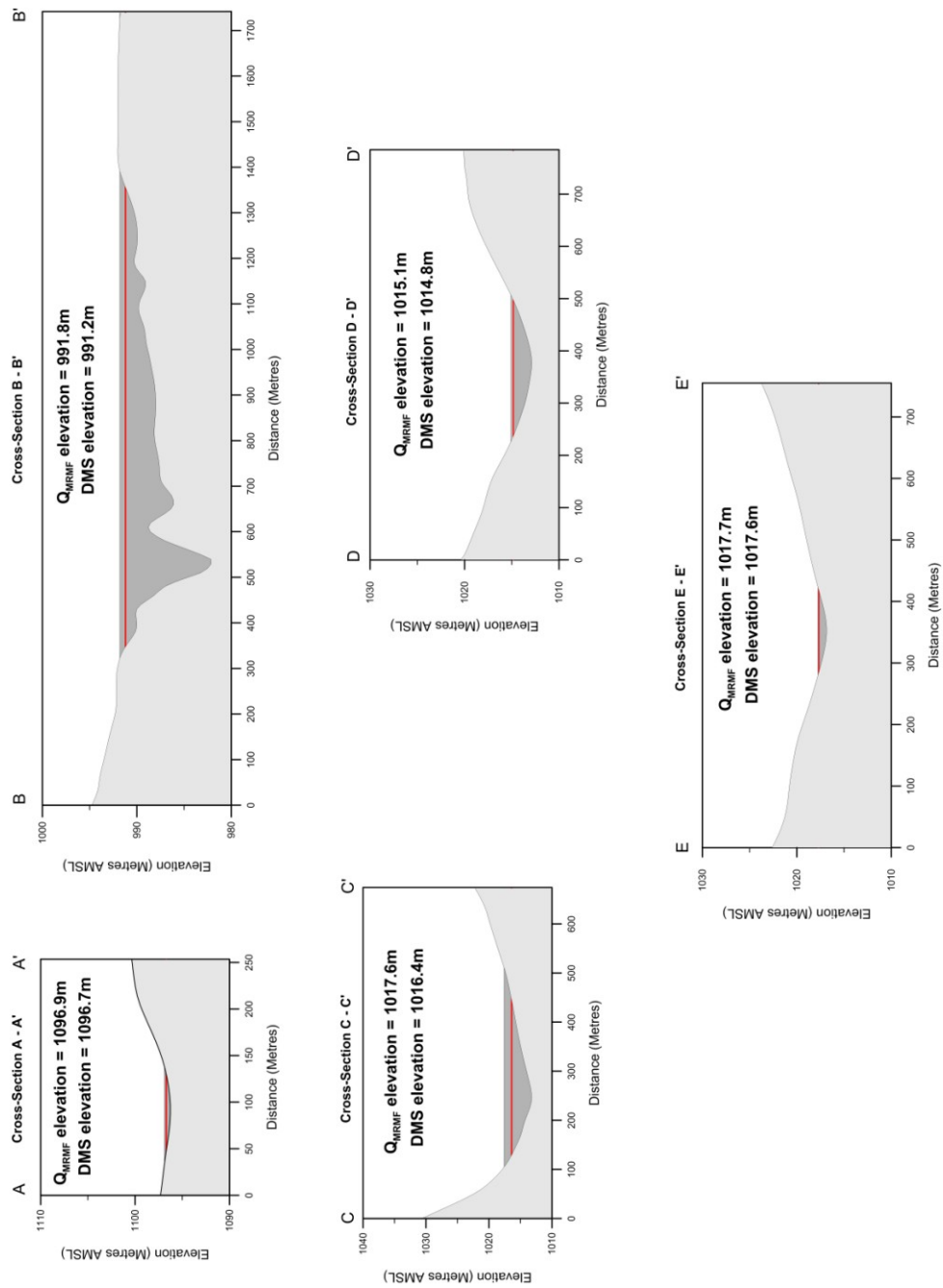


Figure 6.11. Cross-sections of quaternary catchment V12G comparing the modelled elevation surfaces with the data measurement sites. Red line (DMS) – data measurement site elevation. Dark grey – Q_{MRMF} modelled elevation.

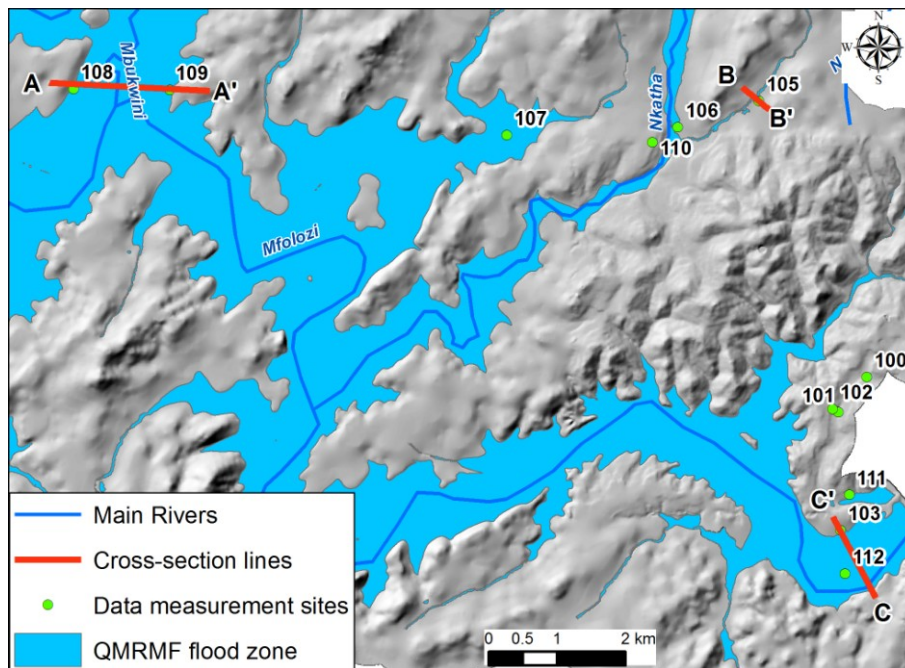


Figure 6.12. Map of a portion of the W23A quaternary catchment showing positions of cross-sections and modelled Q_{RMF} flood zones.

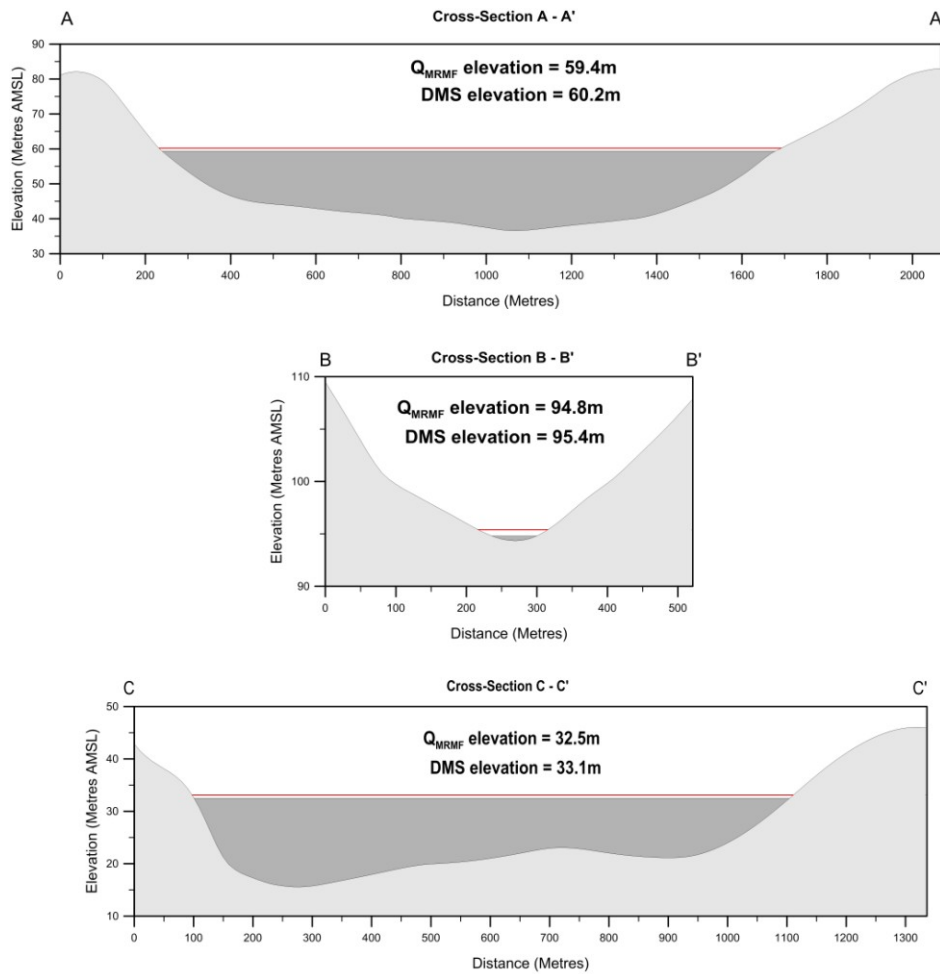


Figure 6.13. Cross-sections of quaternary catchment W23A comparing the modelled elevation surfaces with the data measurement sites. Red line (DMS) – data measurement site elevation. Dark grey – Q_{MRMF} modelled elevation.

The results from the cross-section comparisons (Figures 6.13, 6.15, 6.17, 6.19), show that the data measurement site elevations and model results are generally within 1m of each other. The worst results are those from quaternary catchment T52D where the elevation model was constructed from 20 m contours and consequently had a much lower resolution.

1.3.2. Q_{M100} Results

As a second test of the modelled results, the Q_{MRMF} derived 1:100 year return period estimate discharges (Q_{M100}) were modelled for ten quaternary catchments (Fig. 6.20 a-d, Table 6.9). This comparison produced similar results to that of the Q_{MRMF} /data measurement site comparison in that the R^2 coefficient of best fit was also 0.999 for all calibration factors. Comparisons between 1:100 year design floodlines and the modelled Q_{M100} surfaces for selected quaternary catchments are presented in Figures 6.21 to 6.25.

Table 6.4. Statistical results for the ten quaternary catchment comparisons between the 1:100 year design estimated floodline elevations and Q_{M100} for the four slope categories

Slope range	Calibration factor	Correlation coefficient	Average difference (metres)	Average percentage error	1:100 year average elevation (metres)	Q_{M100} average elevation (metres)
< 0.001	0.001	0.999	1.147	-0.112	236.21	237.15
0.001 - 0.01	0.05	0.999	1.141	0.009	254.11	254.44
0.01 - 0.025	0.2	0.999	1.578	0.013	303.91	304.88
> 0.025	0.4	0.999	0.895	-0.005	538.34	538.13

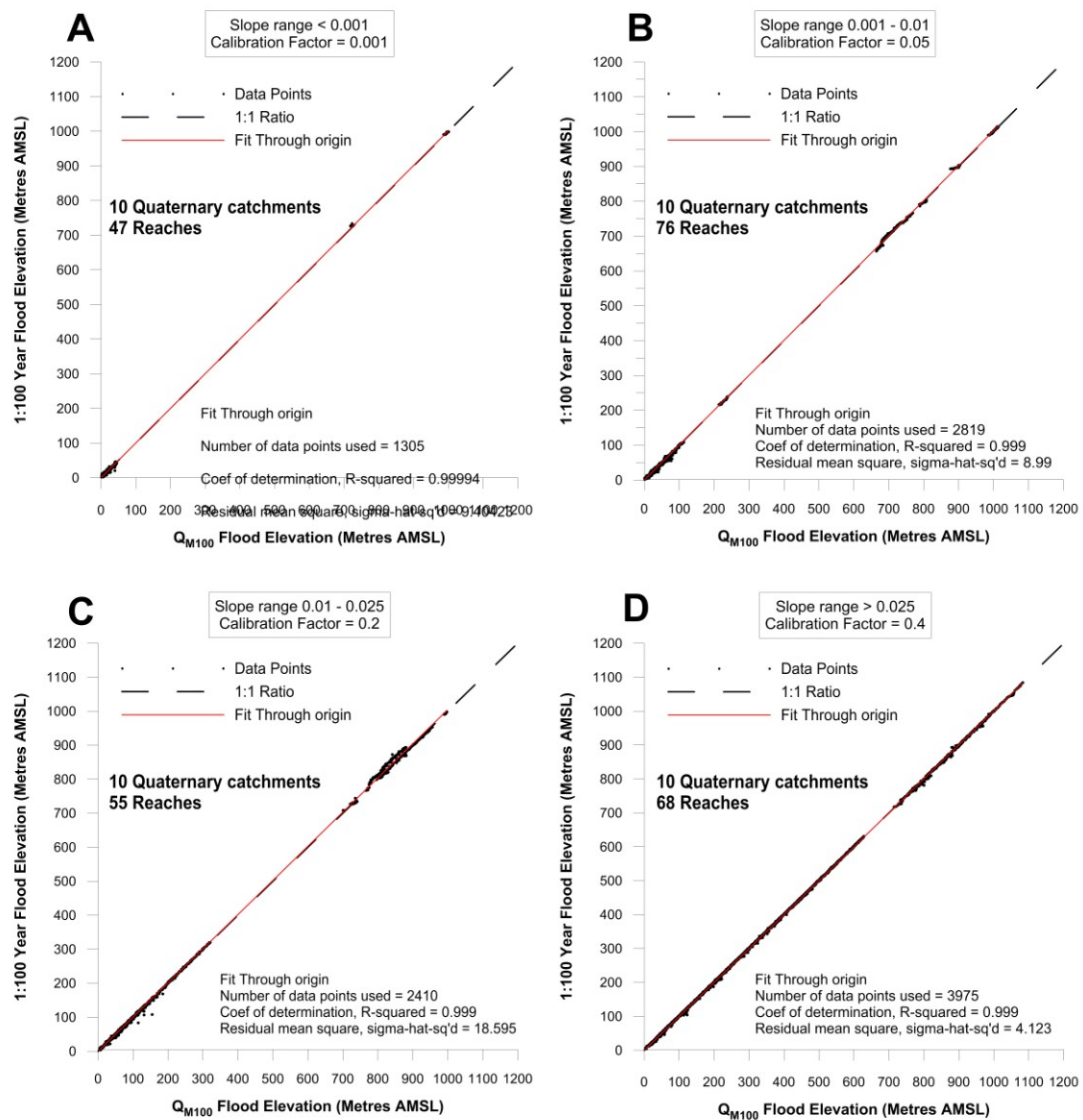


Figure 6.14. A. Plot of the pilot and additional quaternary catchments with design floodline estimates comparing 1:100 year return period design flood estimate elevations against Q_{M100} flood zone elevations with best fit through origin for slope category < 0.001.

B. Plot of the pilot and additional quaternary catchments with design floodline estimates comparing 1:100 year return period design flood estimate elevations against Q_{M100} flood zone elevations with best fit through origin for slope category < 0.05.

C. Plot of the pilot and additional quaternary catchments with design floodline estimates comparing 1:100 year return period design flood estimate elevations against Q_{M100} flood zone elevations with best fit through origin for slope category < 0.2.

D. Plot of the pilot and additional quaternary catchments with design floodline estimates comparing 1:100 year return period design flood estimate elevations against Q_{M100} flood zone elevations with best fit through origin for slope category < 0.4.

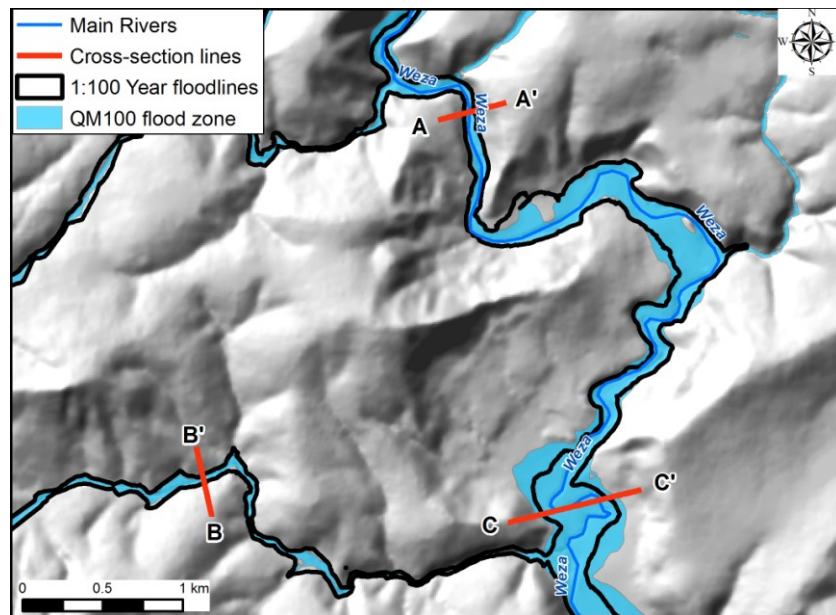


Figure 6.15. Map of the T40B Quaternary catchment showing positions of cross-sections.

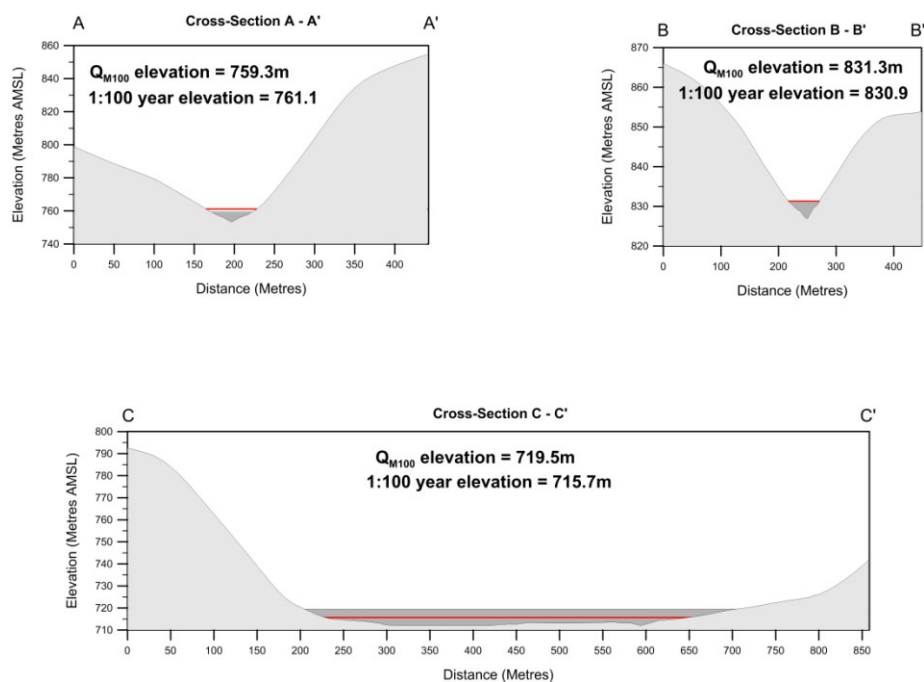


Figure 6.16. Cross-sections of quaternary catchment T40B comparing the modelled elevation surfaces with the data measurement sites. Red line – 1:100 year design floodline. Medium grey – Q_{M100} modelled elevation.

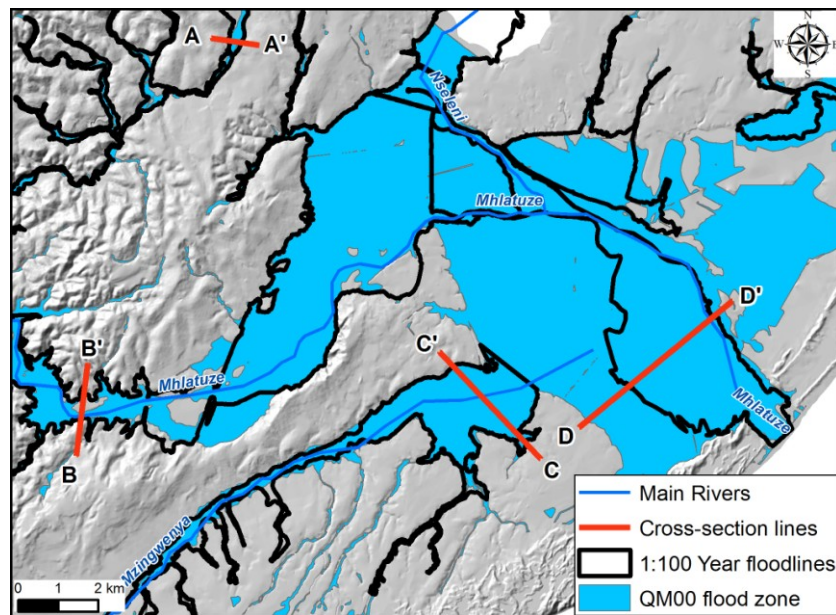


Figure 6.17. Map of a portion of the W12F Quaternary catchment showing positions of cross-sections.

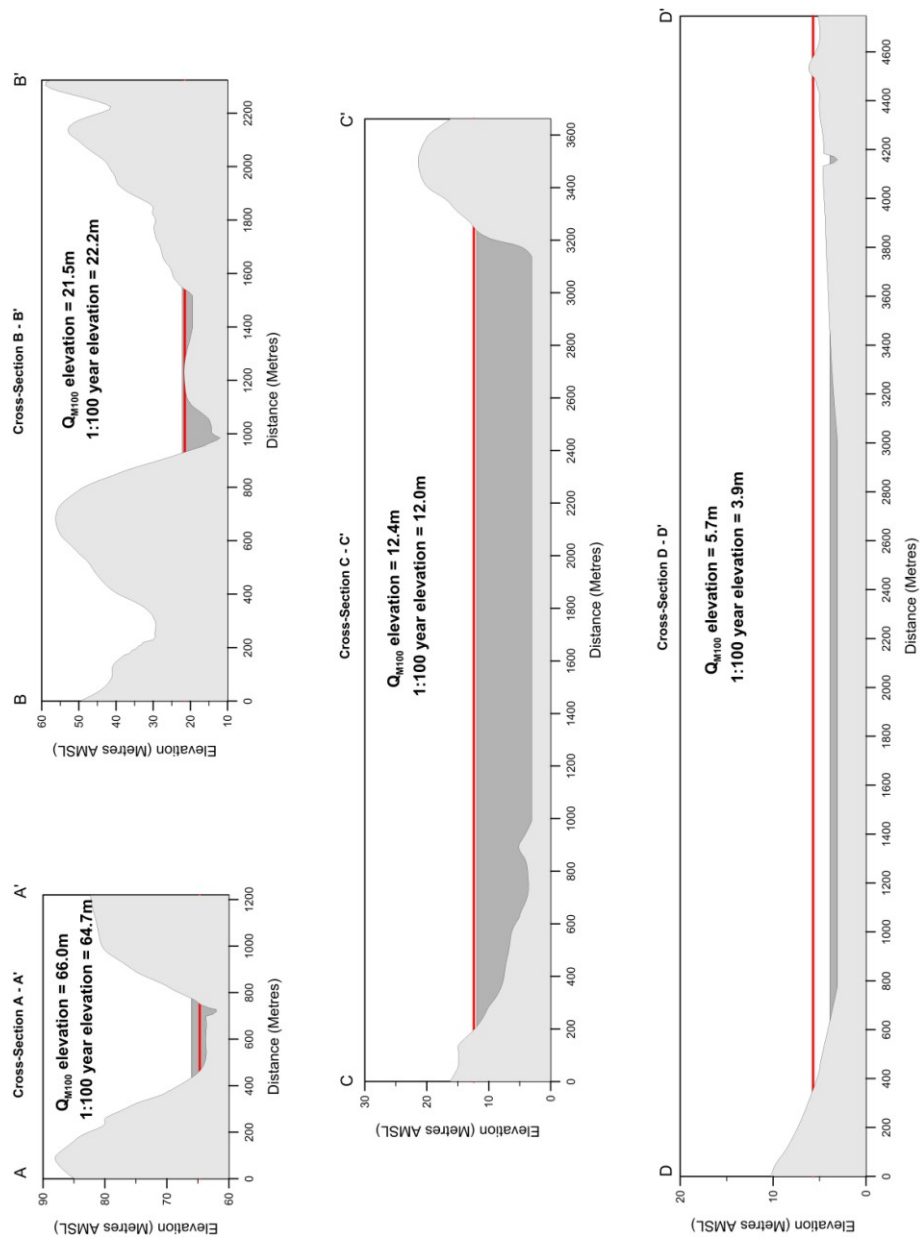


Figure 6.18. Cross-sections of quaternary catchment W12F comparing the modelled elevation surfaces with the data measurement sites. Red line – 1:100 year design floodline. Medium grey – Q_{M100} modelled elevation.

1.3.3. Blind test

A third test was carried out using a quaternary catchment that was not used to define the model parameters or data measurement sites, but had well-defined 1:100 year design floodline

estimates. The U20M quaternary catchment of the Mgeni River was used to test the validity of the modelling approach by comparing the derived Q_{M100} Flood Zone Model results against the 1:100 year design floodline estimate.

All the slope categories show the same high level of R^2 fit coefficient of 0.99 as that of the test model results (Table 6.10). Calibration factor 0.001 (Fig. 6.25A) despite its good fit, shows a large scatter of the plotted data as expected due to the issue of modelling these broad flood plains. An added difficulty with the U20M quaternary catchment is the extensive anthropogenic (man-made) changes, particularly along the lower Mgeni River. This detail is not exhibited by the 5 m contour line data. For calibration factor 0.05 (Fig. 6.25B) the data scatter is greatly reduced. The data scatter around the best fit line for calibration factor 0.2 (Fig. 6.25C) and calibration factor 0.4 (Fig. 6.25D) is very small. This decreasing trend of reduced scatter with increasing slope is attributed to the tendency for steeper slopes being associated with narrower valleys, where the vertical error between the modelled surfaces and the control surface results in a smaller horizontal difference.

Table 6.5. Results for the U20M quaternary catchment comparison between the 1:100 year design estimated floodline elevations and Q_{M100} for the four slope categories.

Slope ratio range	Calibration factor	Correlation coefficient	Average difference	Average percentage error	1:100 year average elevation (metres)	Q_{M100} average elevation (metres)
< 0.001	0.001	0.942	-0.653	-8.817	14.06	14.71
0.001 - 0.01	0.05	0.999	1.267	3.184	55.52	54.25
0.01 - 0.025	0.2	0.999	0.250	0.019	128.35	128.10
> 0.025	0.4	0.999	-0.492	-0.429	260.26	260.75

Figures 6.26 and 6.27 show the spatial comparison between the model results and the 1:100 year design estimate data. The surface elevation comparison is shown in Figures 6.28 and 6.29.

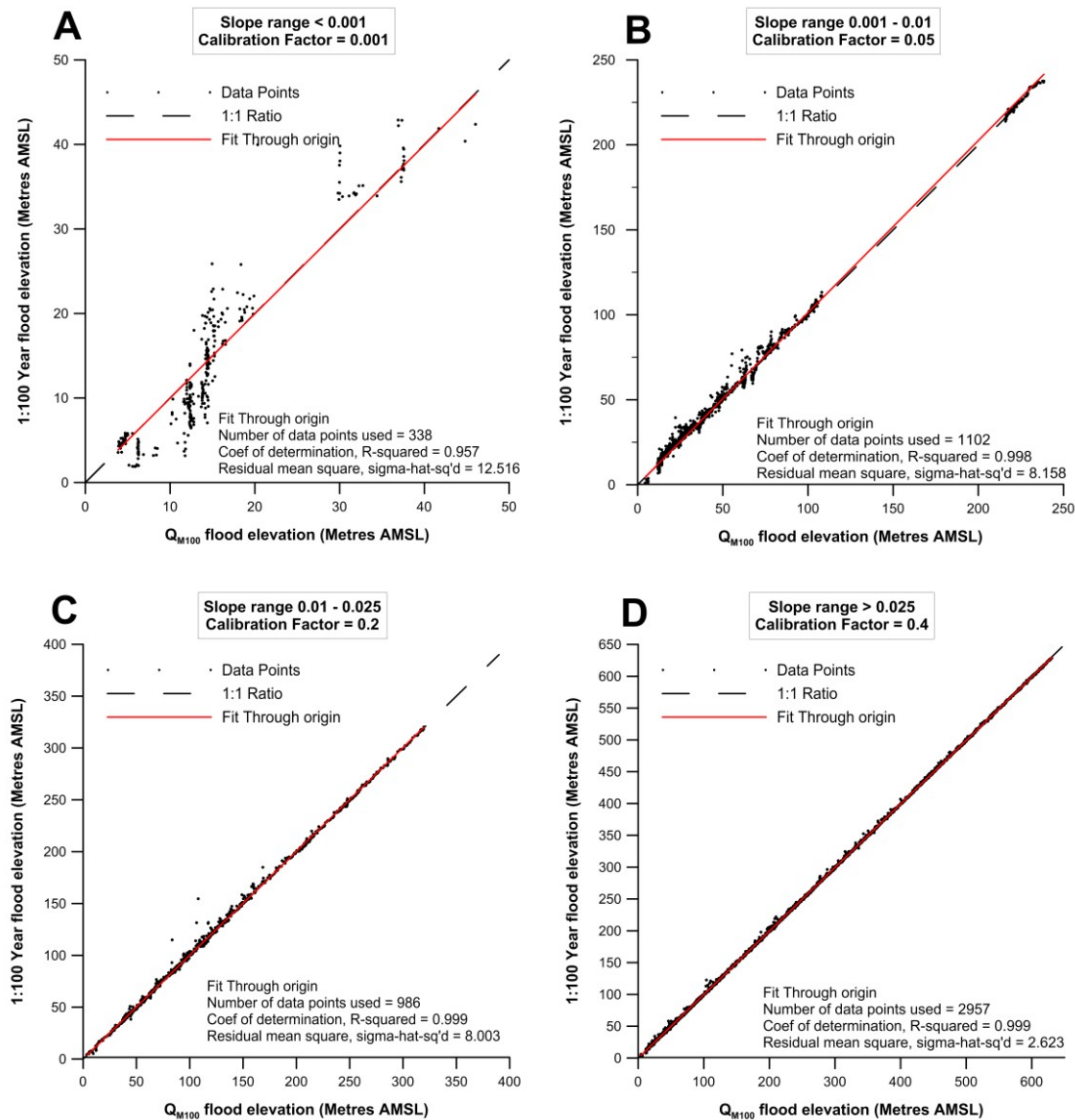


Figure 6.19. A. Plot of U20M quaternary catchment 1:100 year return period design floodline estimate elevations against Q_{M100} flood zone elevations with best fit through origin line for slope category < 0.001.

B. Plot of U20M quaternary catchment 1:100 year return period design floodline estimate elevations against Q_{M100} flood zone elevations with best fit through origin for slope category 0.001 – 0.01.

C. Plot of U20M quaternary catchment 1:100 year return period design floodline estimate elevations against Q_{M100} flood zone elevations with best fit through origin for slope category 0.01 – 0.025.

D. Plot of U20M quaternary catchment 1:100 year return period design floodline estimate elevations against Q_{M100} flood zone elevations with best fit through origin for slope category > 0.025.

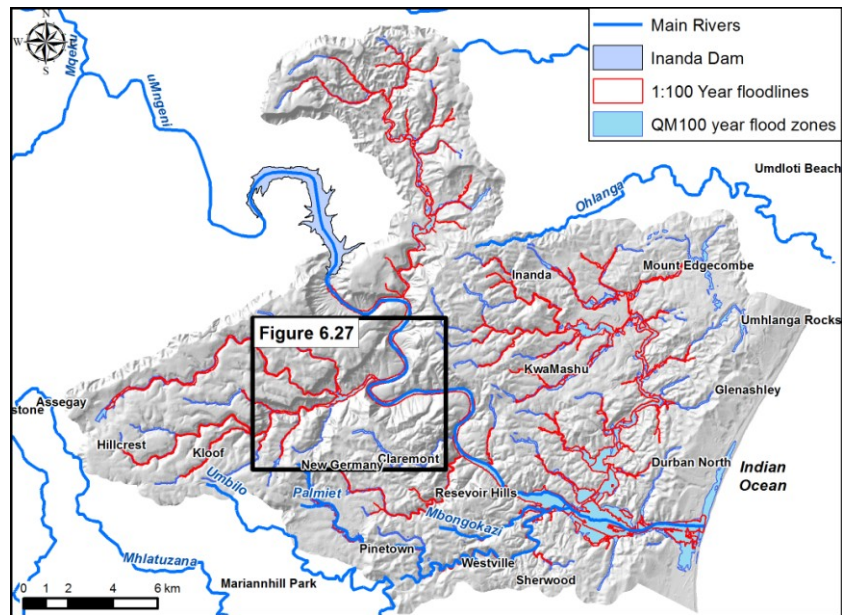


Figure 6.20. Map of the U20M quaternary catchment of the Mgeni River showing the comparison between the 1:100 year return period design floodline estimate and the Q_{M100} flood zones.

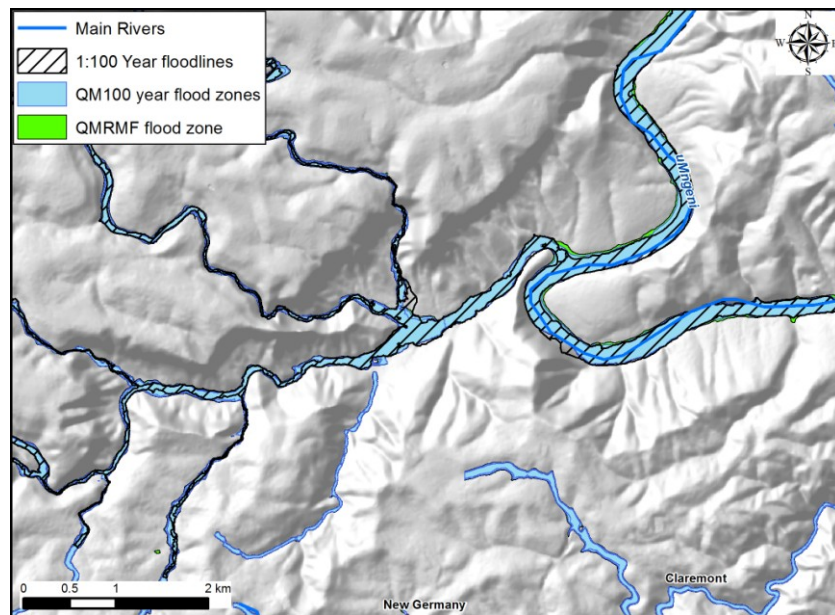


Figure 6.21. Detailed map of the central portion of the U20M catchment (Inset on Figure 6.26) showing the 1:100 year return period design floodline estimate, the Q_{M100} and Q_{MRMF} flood zones.

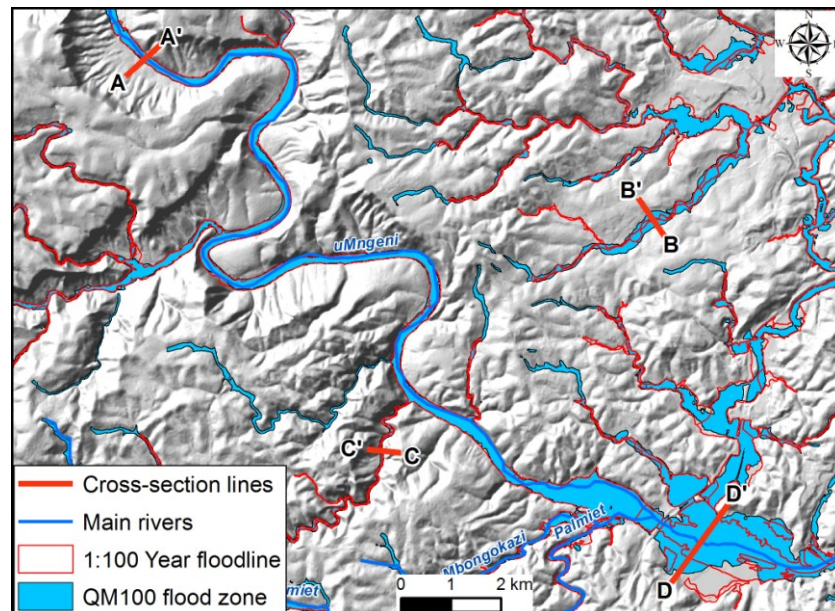


Figure 6.22. Map of a portion of the U20M Quaternary catchment showing positions of cross-sections.

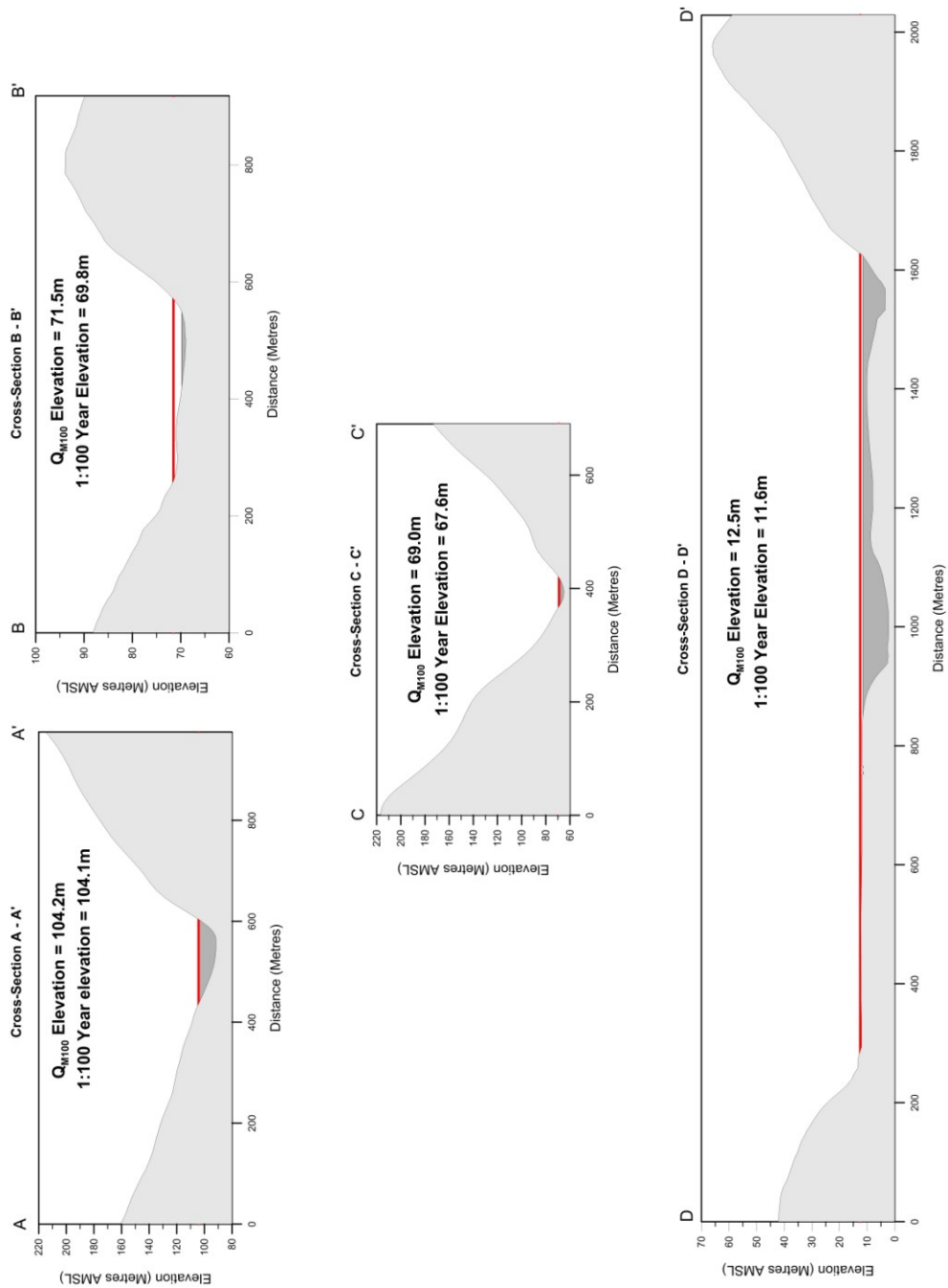


Figure 6.23. Cross-sections of quaternary catchment U20M comparing the modelled elevation surfaces with the data measurement sites. Red line – Q_{M100} modelled elevation. Medium grey – 1:100 year design floodline.

1.4. Discussion

According to Görgens (2002) the Regional Maximum Flood return periods (T) cannot easily be associated with the estimated flood peak. Although Kovács (1988) estimated $T > 200$ years, Görgens (2002) indicated that Kovács' (1988) method of determining the return periods was too simplistic and recommended that the 50 -, 100 - and 200 - year ratios must be factored down by 0.7, 0.8 and 0.9 respectively. Studies done by Pegram and Parak (2004) comparing Regional Maximum Flood to other flood determination methods found that the Regional Maximum Flood approximates to the 200 year return period. The point raised by Görgens (2002) was not found to be an issue in this study. Calibration using the same factor for Q_{MRMF} and Q_{M100} showed a similar high R^2 correlation.

The issue of over-inflating results was retested against the gauge station data used by Kovács (1988) to construct Regional Maximum Flood, with similar results. The quaternary catchment discharges do not contribute equally to the peak discharge, due to different times of concentration and timing of the flood peak. By reducing the area of the upstream catchments (main flow path) by a relatively small factor, and the inflowing subordinate quaternary catchments by a different larger factor, it was found that the summed discharges then produced similar values to the expected Regional Maximum Flood peak discharge. The reduction factors vary according to the Regional Maximum Flood K envelopes and catchment size. Using the reduction factors to reduce catchment area has the effect of reducing discharge. Reduction factors are applied on the basis that the main flow proportionally contributes to the bulk of the peak discharge and the inflowing subordinate quaternary catchments contributes a small portion.

For design flood estimations the roughness coefficient variation across the individual cross-sections for the overbanks or floodplains and channel is determined. Since this model is based on limited field data, it is impractical to apply this for all the river cross-sections in a quaternary catchment (*e.g.* U20M where 7435 cross-sections were used to construct the model). Instead, an assumption is made that a specific range of calibration factors can be applied across all the cross-sections in a reach, replacing the roughness coefficient.

The disadvantage of this approach is the loss of topographic detail, particularly along the river bed area. Where contour data with different intervals were compared, it was found that valley slopes with higher gradients showed marginal variation in detail between the 5 m /20 m and 1 m/2 m data. Broad valleys with shallow gradient and wide floodplains show greater variation in detail. It was also found that the fit between the modelled results and the design flood estimates improved with larger return periods. As larger return periods result in increased flood elevations, the improved fit is attributed to less variation between the various contour intervals on valleys slopes compared to the greater variation on the floodplains and river beds. The spatial similarity between the modelled results and the control data show that existing contour data can be used for flood hazard models. Contour data with the smallest intervals will improve the results.

Synthetic drainage lines produced by ArcHYDRO Tools[®] have two drawbacks that render them unusable in this process. Where the valleys are broad and the floodplains are flat, the tool that generates these lines will often produce parallel drainage lines that do not follow the correct river course. The second problem with the synthetic drainage lines is that they do not extend to the source point of the river in the sub-catchments. HEC-GeoRAS[®] uses river centrelines to calculate flow direction and cross-section intervals as part of the flood modelling process and if no river data are available, that portion of the sub-catchment cannot be modelled. This is resolved by using the Surveyor General river data that coincided with the synthetic drainage lines and incising these river courses into the DEM using an ArcHYDRO Tools[®] function. Highly detailed river centrelines are not required for any part of the flood routing calculations, making the SG 1:50 000 river feature class adequate for this application. Water body data from the SG 1:50 000 GIS data was modified where necessary. The smaller farm dam footprints generally matched satellite imagery. Dams constructed after the SG data were created, were captured. The large dam footprint did not always match the satellite imagery and these were recaptured.

Using the Regional Maximum Flood method to estimate discharges has many advantages for this modelling approach. Regional Maximum Flood only requires a geographic position from which the upstream catchment area is calculated. Once the area factor was adjusted, the Kovács (1988) Regional Maximum Flood formulae were used to calculate estimated discharges for a given quaternary catchment, the only input is the combined primary upstream and secondary

quaternary catchments areas. As Regional Maximum Flood was derived from gauge data, climatological and catchment characteristics do not need to be considered. A key component of this model is the assumption that flood deposits mapped in the field equate to Regional Maximum Flood. This correlation is very difficult to do with estimated return periods because successive floods have reworked sediments (Charlton 2007). Where the smaller flood deposits are identified relating them to a specific flood can only be done using age dating techniques.

Acknowledging that there is a level of uncertainty around the reliability of return period discharges derived from the Regional Maximum Flood, the unadjusted Kovács (1988) formulae were used because the modelled results closely matched the field observations and the control 1:100 year return period design floodline estimates when applying the same calibration factor. If the derived 1:100 year return discharge estimate was over reported by 20% (Görgens 2002), the Q_{RMF} modelled results would not match the field observations, the derived 1:100 year return modelled result would consistently plot above the control 1:100 year design floodline estimates, which was not the case. This issue may be accommodated by the calibration factors or averaged out due to the modelling process.

Estimating Manning n values or using Chezy or Darcy-Weisbach formulae to calculate roughness coefficients for cross-section across a quaternary catchment is a resource intensive task. Replacing the roughness coefficients with a calibration factor, which represents a best fit Manning based average value across a reach and associated slope, eliminates the need to determine roughness coefficients. The calibration factors also provide a means to raise or lower modelled results to match the control data. Application of the calibration factors across 15 quaternary catchments that produced consistently high R^2 fit coefficients for both the field data/ Q_{MRMF} relationship and Q_{M100} derived discharge/design 1:100 floodline estimates shows that they are independent of geographic location. Similarly, these quaternary catchments cover a range of Regional Maximum Flood K envelopes indicating that the calibration factors are also independent of these. Any quaternary catchment's flood zones could then be desktop modelled, as demonstrated for U20M.

When comparing the modelled flood extents for Q_{MRMF} and Q_{M100} (Figure 6.27) it can be seen that where the valley slopes is moderate to steep there is very little difference between the two

flood surfaces. Where slopes are moderate to shallow the difference between the surfaces are greater because small differences in elevation result in larger horizontal variation. For delineating flood risk zones the Q_{MRMF} flood elevation surface can be used as a conservative estimate. Should there be a need to generate 1:100 or 1:200 year Regional Maximum Flood return period derived estimates then it is recommended to use the Kovács (1988) formulae as is, and use it as a conservative estimate (Görgens 2002). Apart from the applications already described, the Flood Zone Model estimates can be used for pre-screening of developments and to highlight areas where design flood estimates should be carried out.

The advantages of the Regional Maximum Flood- and Modelling- based approach described here are thus:

- Existing GIS datasets produce sufficiently accurate DEM surfaces to create sub-catchments and reach drainage lines;
- Design peak discharges can be estimated for any quaternary catchment's location within the Regional Maximum Flood regions and applied to the sub-catchments under consideration;
- Can be applied to gauged and ungauged catchments;
- Reach slopes can be calculated by a GIS system and the defined river reach calibration factor values are comparable to the use of Manning's n -values used in HEC-RAS;
- Overall processing time for a quaternary catchment, depending on size and complexity of the drainage pattern is 20 – 25 hours;
- No or limited field work or detailed surveys are required to implement this approach; and

The disadvantages are:

- The model results are not as accurate as design floodline estimates and cannot be used for construction purposes.
- The technique requires advanced GIS software such as Spatial Analyst® and 3D Analyst®.
- If field verification is necessary, skilled personnel such as earth scientists or hydrologists are required.

CHAPTER 7 – FLASH FLOOD MODELLING

7. Introduction

The examination of historical data (Kovács 1988; SAWS 1991; van Bladeren 1992; Botes et al. 2010) shows that since the recording of flood records began in 1856 in KwaZulu-Natal (KZN), at least 144 localised (possibly flash) floods have been documented (average of 1 every 1.1 years) compared to 25 regional scale floods (average of 1 every 6.2 years). Historical records do not always distinguish between regional and flash floods (SAWS 1991), but indicate that every province in the Republic of South Africa has been subjected to flash flooding to some degree. Floods in general can have a large impact on the economy and the greater occurrence of flash flood events suggests that the cumulative damage may be greater than that of a regional flood.

During fieldwork for the development of the Flood Zone Model (FZM), it became apparent that in certain parts of catchment U20H, the distribution of some flood deposits were in excess of the regional maximum flood peak discharge (Q_{MRMF}). Discussions with local communities in the area also pointed out flood levels which exceeded that of the Q_{MRMF} estimation. Two important observations could be made from these survey results. Firstly, in plotting the GPS positions of the affected homesteads against the modelled Q_{M100} and Q_{MRMF} flood risk areas, it was found that most were located outside these zones and at elevations significantly higher than the estimated Q_{MRMF} (Fig. 7.1). Secondly, the timeframes indicated by the respondents did not correspond to the recorded long-rain flood events. These were most likely to instead correspond to a series of localised storm events in November 1999, January 2005 and February 2008 which produced flash flooding.

To account for the field observations and homestead survey results, the hydrological component of the Flood Zone Model was adapted by estimating peak discharges with a method better suited for small catchments. Using a semi-distributed modelling approach, a Flash Flood Model (FFM) was produced to emulate flash flood elevation surfaces. By processing both scenarios concurrently using the Flood Zone Model hydraulic flood routing component, it should then be possible to delineate flood zone and flash flood inundation data. The difference in magnitude and potential risk of these extreme events are compared to determine the rainfall and catchment characteristics which produced the inundation levels noted by field observations and survey respondents.

7.1. U20H quaternary catchment

The U20H (Fig. 5.11 and 5.15) is a 220 km² quaternary catchment divided into 59 sub-catchments with an elevation range of 784.5 m to 1603.5 m. This quaternary catchment, drained by the Slangspruit and Msunduze Rivers, has no inflowing rivers. The land cover is predominantly grasslands, with interspersed sparse to dense traditional settlement. AGIS (Schoeman et al. 2002) defines the soils as less than 100 mm thick with poor drainage capacity. The area is underlain by sandstones and shales of the Adelaide and Volksrust Formations with extensive dolerite sills which produce residual soils with a high clay content. The Slangspruit River experienced a flash flood on the 25th December 1995 which resulted in 154 deaths (Reliefweb 1996). For this catchment, the Regional Maximum Flood calculation predicted the regional maximum flood peak (Q_{MRMF}) at 1931 m³/s and a 1:100 year flood peak (Q_{M100}) of 1012 m³/s).

7.2. Results

Design rainfall data for the U20H quaternary catchment for 1 hour, 2 hour (storm) and 3 day (regional) rainfall durations are presented for various return periods as extracted from Hydrorisk (Smithers & Schulze 2003). These are shown in Tables 7.1, 7.2 and 7.3 and list the variable values and formulae used to calculate the rainfall intensity (i) (a from Table 7.1 and d, c from

Table 7.2) and the Rational Formula (RF) peak discharges (Q_i) (C, A from Table 7.3). An important point to note is the magnitude difference in rainfall depths, where a one hour storm can produce approximately 40% of the predicted three day rainfall for the equivalent return period (Table 7.1). Three U20H sub-catchments marked in Figure 7.2 are used to show the intensity calculations (Table 7.2) and discharges (Table 7.3). Table 7.4 compares discharges for both the regional and flash flood return periods.

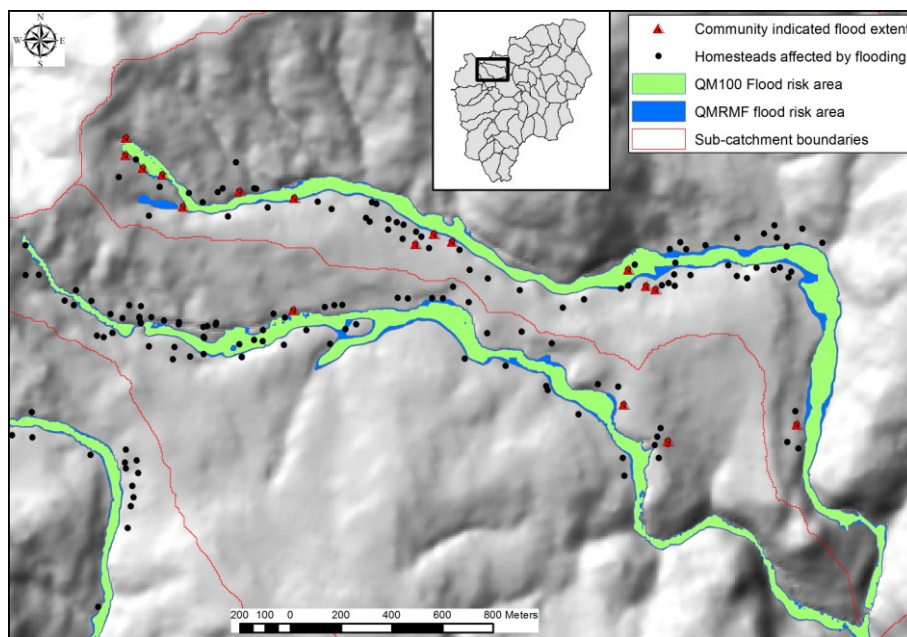


Figure 7.1. Detailed map of two U20H sub-catchments showing the Q_{M100} and Q_{MRMF} in comparison to the community reported flooded homesteads.

The lumped parameters used to determine the run-off coefficient for the semi-distributed flash flood model (Chapter 4), show very little variation. Catchment slopes for the area ranged between 10% and 26%, with a predominant grassland land cover. Overall soil infiltration is poor, with thin soils (< 100 mm deep) across the whole quaternary catchment. Based on the value ranges from Mark and Marek (2011), the run-off coefficient was determined to be 0.725 for all the sub-catchments within this quaternary catchment. Most sub-catchments have a time of concentration (T_c) between 1 – 2 hours (Figure 7.2).

A stepped series of calibration factors (CF) for the various reach slope categories were used to model flood elevation surfaces until the closest fit to the field data was found. Calibration factors were then refined to achieve a best fit across all reach slope categories. The calibration factors for the Flash Flood Model had to be significantly adjusted, particularly in the higher slope reaches to produce a best fit (Table 7.5). The results of the flash flood elevation modelling show that the surface with the closest fit to the control data (homestead data and GPS marked flood deposits) is the one derived from the FFM₂₀₀ estimated return period (Fig. 7.3). While the Flash Flood Model calibration factors produced consistent results within this catchment, the study needs to be extended to other quaternary catchments to verify if these can be also applied universally in the same manner as the Flood Zone Model calibration factors.

Table 7.1. Comparison for hourly and three day design rainfall depths for certain return periods (Extracted from Hydrorisk (Smithers & Schulze 2003)).

Rainfall Intensity	Return Period (Years)						
	a						
	2	5	10	20	50	100	200
1 Hour mm/hour	31	44	53	64	80	94	109
2 Hour mm/hour	38	53	65	78	96	113	131
3 Day (mm/day)	79	110	135	161	201	234	273

Table 7.2. The calculated values for three U20H sub-catchment variables are listed together with the rainfall intensity calculation results. See Figure 7.2.

Sub-catchment	Time of concentration	Power factor ³⁵	Rainfall Intensity, $i=ad^c$ (mm/hr)				
			Return Period (Years)				
	d	c	10	20	50	100	200
u20h_10b,1	1.4	-0.762	50.1	60	74.7	87.3	101.4
u20h_11,1	1.4	-0.762	51.5	61.7	76.8	89.7	104.3
u20h_10,1	2.2	-0.762	35.5	42.5	52.9	61.9	71.9

Table 7.3. Variables and calculations used for the RF calculations for the three selected U20H sub-catchments. See Figure 7.2.

Sub-catchment	Area km ²	Run-off coefficient	Rational Formula $Q_t = CiA/3.6$ (m ³ /s)				
			Return Period (Years)				
	A	C	10	20	50	100	200
u20h_10b,1	2.01	0.725	20	24	30	35	41
u20h_11,1	5.19	0.725	54	65	80	94	109
u20h_10,1	10.12	0.725	72	86	108	126	146

Table 7.4. Comparison of regional and flash flood discharges for various return periods.

Sub catchment	Regional Flood Return Period (Years)				Flash Flood Return Period (Years)			
	Area	Q_{M100}	Q_{M200}	Q_{MRMF}	20	50	100	200
	km ²	m ³ /s	m ³ /s	m ³ /s	m ³ /s	m ³ /s	m ³ /s	m ³ /s
U20H_10b,1	2.01	9	11	18	24	30	35	41
U20H_11,1	5.19	24	30	46	65	80	94	109
U20H_10,1	10.12	47	58	89	109	135	158	184

Spatially the estimated flash flood 200 year return period (FFM₂₀₀) flood risk area can be considerably larger than the Q_{M100} and Q_{MRMF} flood risk areas (Fig. 7.3). A relatively small flash flood in the U20H quaternary catchment can affect upward of 700 homesteads whilst a regional flood may only affect 100 homesteads (Table 7.6). From Figure 7.3, the modelled FFM₂₀₀ surface matches the survey respondent control quite closely.

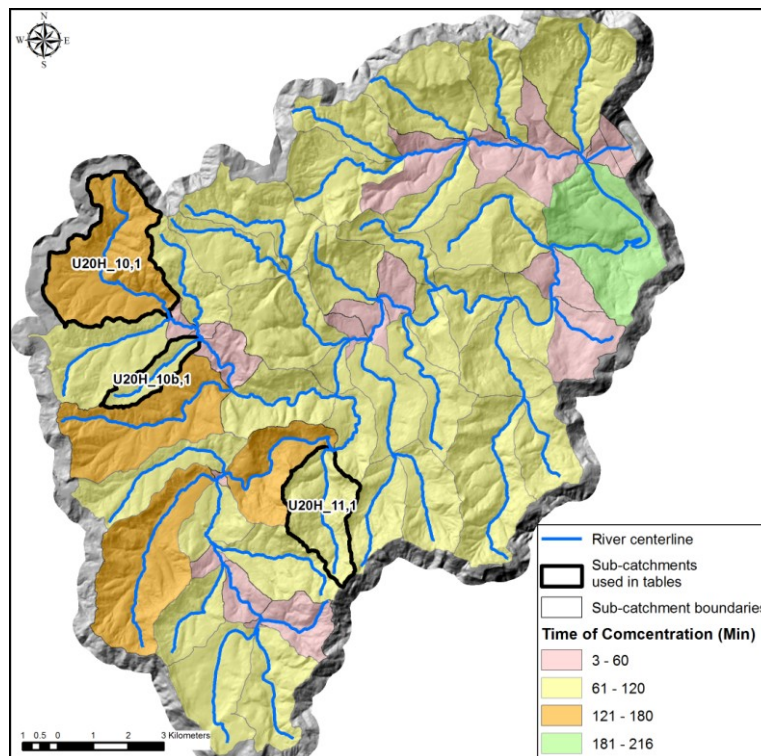


Figure 7.2. Map of the U20H quaternary catchment showing the sub-catchment time of concentration (T_c). The sub-catchments used in the tables as examples are also marked.

Table 7.5. Characteristics of floodplain slope categories and comparison of defined slopes categories for the Flood Zone (FZM) and Flash Flood Models (FFM).

Slope category	FZM Calibration factor applied	FFM Calibration factor applied	Floodplain characteristics
< 0.001	0.001	?	Reaches with very little or no elevation change. Valleys tend to be broad. Rivers tend to meander within the flood plain. Primarily major rivers. Common on coastal flood plains
0.01 – 0.001	0.05	0.3	Low relief. Valleys tend to be broad. Rivers tend to meander within the flood plain. Primarily major rivers.
0.01 - 0.025	0.2	1.2	Intermediate phase between the low relief drainage and the steep drainage.
> 0.025	0.4	6	High relief with steep sided valleys incised into the topography. Narrow floodplains.

Table 7.6 List of community reported flooded homesteads and estimated current homesteads at risk in quaternary catchment U20H for selected flash flood and regional flood return periods.

Estimated flood return period	Flooded homesteads	Current homesteads at risk
FFM ₂₀	328	753
FFM ₅₀	343	870
FFM ₁₀₀	357	969
FFM ₂₀₀	371	1069
Q _{M100}	31	74
Q _{MRMF}	44	104

The comparison between the data measurement sites and the modelled elevation surfaces for U20H is presented in Figures 7.4 and 7.5.

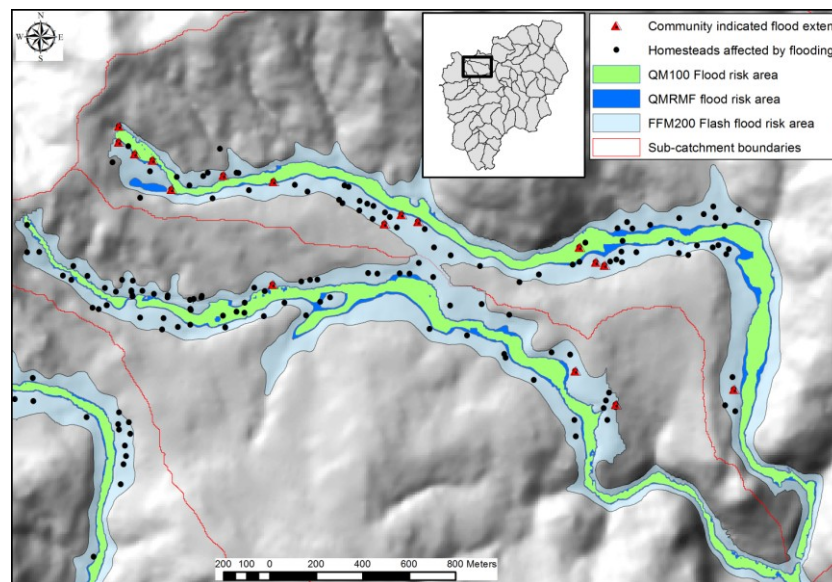


Figure 7.3. Detailed map of two U20H sub-catchments showing the Q_{M100} and Q_{MRMF} and FFM₂₀₀ flood risk areas in comparison to the community reported flooded homesteads.

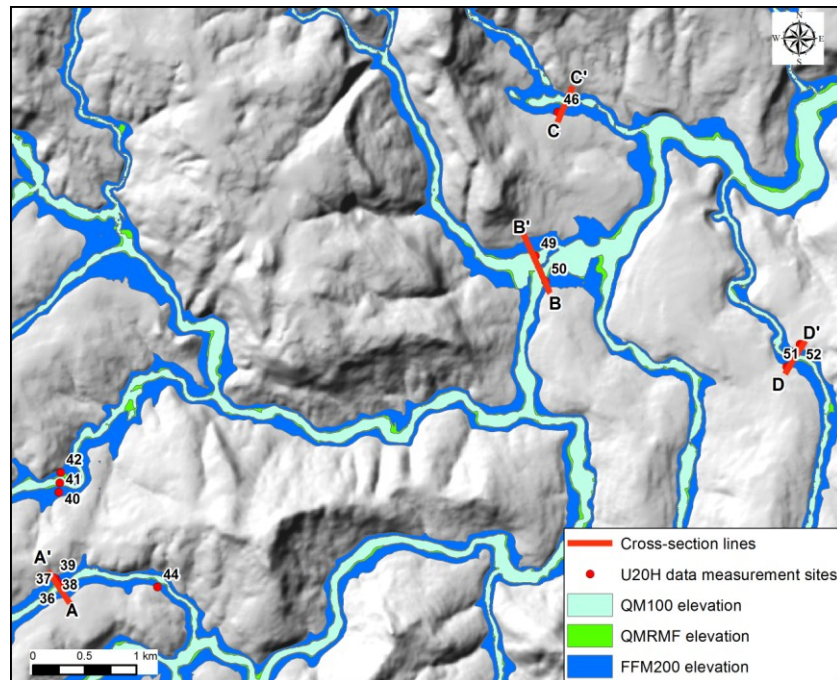


Figure 7.4 Map of the U20H Quaternary catchment showing positions of cross-sections in relation to the various modelled flood elevations.

Comparison of the cross-sections in Figure 7.5 shows that the difference in elevation between that of the Q_{MRMF} and the FFM_{200} can be at least nine metres. Spatially this has a significant impact on areas demarcated as flood risk areas (Figs. 7.3 and 7.4).

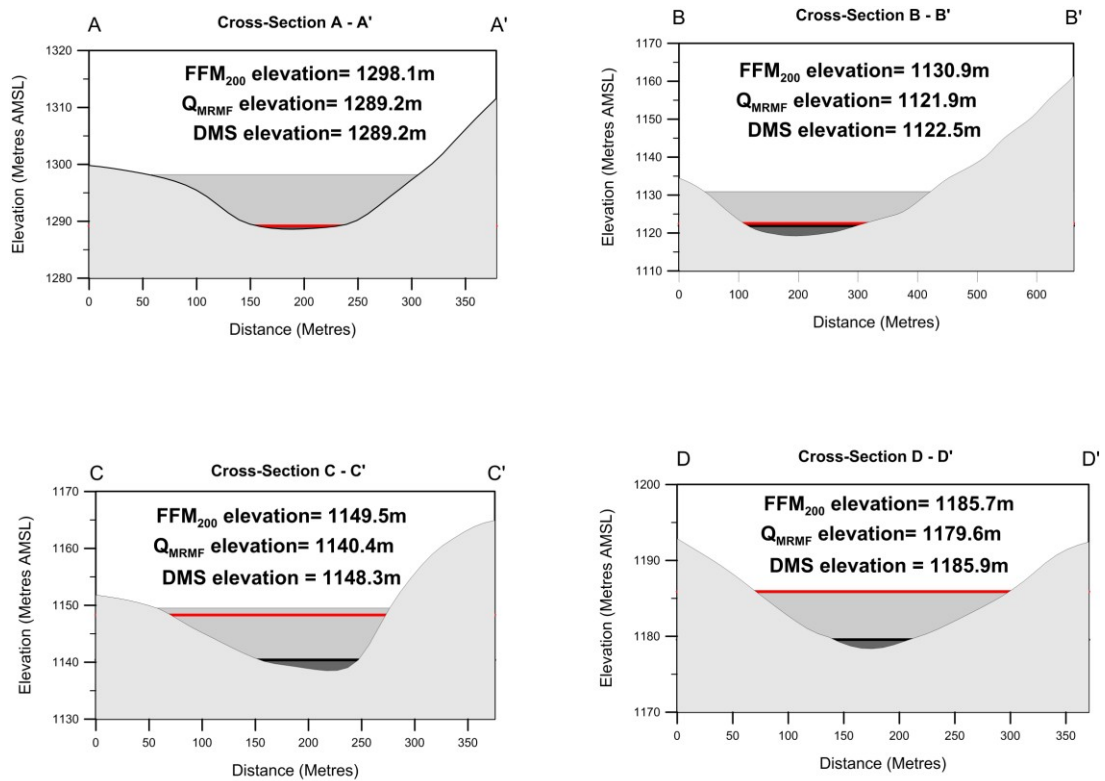


Figure 7.5. Cross-sections of quaternary catchment U20H comparing the modelled elevation surfaces with the data measurement sites. Red line (DMS) – data measurement site elevation from GPS field data. Dark grey – Q_{MRMF} modelled elevation. Medium Grey – FFM₂₀₀ flash flood elevation surface.

7.3. Discussion

The results show that the GIS based hydraulic and flood routing base data developed for the Flood Zone Model can be used to delineate flash flood risk areas. Sufficient information can be derived from existing GIS data sources to determine the variables for a semi-distributed model using the Rational Formula. The differences in calibration factor values between the Flood Zone Model and Flash Flood Model are attributed to the relatively rapid development of peak

discharge. Rapid flow will most likely result in greater turbulent flow thus increasing the internal flow resistance (Yen 2002; Jothityangkoon & Sivapalan 2003), with the net effect of increasing the relative surface roughness coefficient (Bridge 2003).

Converting rainfall depth to peak discharge indicates that flash floods in small catchments can produce nearly three times the discharges in hours compared to regional floods measured over days. Once again this indicates the hazard posed by such events that are often not catered for by conventional flood modelling. No published materials have been found that compare flash flood risk areas with design floodlines for the same river. This study further supports this by showing that field observations of the 1:100 estimated design floodlines and the Q_{MRMF} regional flood risk areas are inadequate with respect to defining risk areas for flash floods.

Post flood surveys amongst affected communities, as promoted by Gaume & Borga (2008), in combination with geologically mapped evidence of flash floods, are an important means for calibrating flood elevation simulations. Creation of a post flood database will be invaluable, especially in small catchments, for discharge estimates (Marchi et al. 2010). Such a resulting database of post flood records helps in distinguishing the prevalent flood risk types for an area, a key factor in an early warning system. Such early warning systems, as promoted by the South African Weather Service's Flash Flood Guidance System, are clearly needed. However these need to be implemented in conjunction with delineated inundation zones provided by the model described here for maximum efficacy in flood management.

CHAPTER 8 – STORM SYSTEMS

8. Introduction

As regional flooding and flash flooding are the results of both the duration and intensity of storm systems (Merz & Blöschl 2003), historical weather data can be used to reconstruct the spatial patterns of past storms systems. However, there are only limited examples in the literature of this. For example, storm footprints, have been used to determine historical landfall of tropical cyclones (Dettinger et al. 2011), and also compared to selected precipitation events (e.g. Viglione et al., 2010). Researchers have rather tended to concentrate on other factors such as the frequency of storms (Diodato 2004; Evan & Camargo 2010; Bothe et al. 2012), comparisons between selected events (Andrews et al. 2004; Viglione & Blöschl 2009) and the impacts of tropical cyclones (e.g. Easterling et al. 1999; Elsner et al. 2008; Coumou & Rahmstorf 2012; Booth et al. 2013). Zwiers et al. (2013) point out that there is a need to use historical weather data as *in situ* observations that allow the identification of trends and spatial distributions. One of the prime reasons for the limited use of such data is that it is in hardcopy format, and thus difficult to extract (Zwiers et al. 2013). Recently, radar satellite platforms have been used to capture precipitation data and identify rainfall characteristics and spatial patterns (Biasutti & Yuter 2012; Paschalis et al. 2013). While radar satellite data will provide a useful tool in the future, the short timeframe of available data will be of limited use without augmenting it with historical data.

The only reference sources to historical flooding in the Republic of South Africa (Kovács 1988; SAWS 1991; van Bladeren 1992) record the results of storms but do very little to determine the responsible storm characteristics. Only in the case of very large floods did the Department of Water Affairs carry out more detailed investigations into the related storm systems, e.g. 1984 and 1987 (Kovács et al. 1988; van Bladeren & Burger 1989). Studying the South African Weather Services (SAWS) publication of notable weather events (SAWS 1991), the impression is given that it is only the floods that resulted in loss of life, or significant damage to

infrastructure, that have been recorded. This raises two concerns. Firstly there appears to a limited understanding of the geographic distribution of floods; and secondly, there is an over emphasis on extreme flooding in the historical records (SAWS 1991; van Bladeren 1992). This implies that the historical flood records may not portray a complete picture of flooding, leaving lesser flood events unrecorded. By using rainfall station records, this chapter aims to produce a series of storm distribution footprints of recorded flood events, and by proxy, make use of similar storm events with similar patterns, to map out storm footprints for the last 110 years.

8.1. Methodology

Rainfall data were extracted for 2439 rainfall stations from the Daily Rainfall Extractor program database produced by Lynch (2003). These included data from 1856 to 2001. Only data between 1890 and 2000 were used as the earlier records were sparse and the post 2000 records were incomplete. Stations were selected to ensure that their spatial distribution extended beyond the drainage basins of KwaZulu-Natal in order to ensure a full coverage of the province.

Rainfall data were then interrogated for any station which recorded ≥ 50 mm per day from which a daily raster grid was produced with Spatial Analyst[®] using a 500 m cell resolution. Three types of patterns were then targeted, (1) regional storm events (RSE) which covered large geographic areas where two or more successive daily raster grids had areas exceeding the 75 mm isohyets and covering the same general geographic area (Table 8.1). (2) regional storm events associated with the extreme floods identified by van Bladeren (1992) and termed extreme flood-associated regional storm events (Table 8.1). (3) Local storms events (LSE) where only single daily raster grids exceeding the 50 mm isohyets covered by small localised geographic areas (Table 8.1). Where regional storm events were identified by this study, the preceding and successive two days around the regional storm event were also gridded.

Table 8.1. Summary of storm type patterns targeted for identification from the gridded rainfall data.

Storm type	Context	Definition
Regional storm event (RSE)	Regional	Where two or more rainfall stations recorded ≥ 75 mm rainfall depths for two or more successive days in the same general geographic area. Equates to 1:5 year design rainfall return period. Rainfall depths should result in sufficient run-off for water levels to exceed riverbanks.
Extreme flood-associated RSE	Regional	Same as regional storm event, but storm is associated with a recorded extreme flood event as listed by van Bladeren (1992).
Local storm event (LSE)	Local	Where a single rainfall station recorded ≥ 50 mm rainfall depths in a single day. Equates to 1:2 - 1:5 design rainfall return period.

The regional storm event cut-off value of ≥ 75 mm is based on the design rainfall return depths which equated to the 1:5 year return period rainfall in Hydrorisk (Smithers & Schulze 2003). A regional storm which produces rainfalls depth of ≥ 75 mm per day over two or more consecutive days, over the same general geographic area, should produce sufficient run-off for river water levels to exceed the riverbanks, thus producing some level of flooding. The demand for land, especially around urban centres in KwaZulu-Natal has resulted in settlement on floodplains, in some cases structures have been erected within metres of the riverbanks. Any regional storm event that results in water levels exceeding riverbanks places these settlements at risk to flooding. As such, the 1:5 year design rainfall return period (≥ 75 mm per day) is used as a *minimum threshold* for regional storm events. For each regional storm event, the start and end date, number of storm days and general geographic positions were recorded. The regional storm event area, highest recorded and mean rainfall depths were determined using the zonal statistics tool in ArcGIS[®] Spatial Analyst (ESRI 2002). The zonal statistics tool is used to summarise areas in a raster grid that have the same input value (zone). From this, the mean depth/duration values were calculated. The local storm event cut-off of ≥ 50 mm is also based on Hydrorisk (Smithers & Schulze 2003) as the approximate 1:2 – 1:5 year return period for a single day event. It is estimated that rainfall depths that are ≥ 50 mm can result in urban or flash flooding under certain conditions such as extensively paved areas, thin clayey soils and relatively short times of concentration for sub-catchments.

8.2. Results

The complete results of the regional storm events identified in this study are listed in Appendix IV together with the regional storm event footprints for each event. Figure 8.1 shows the daily regional storm footprints for the September 1987 floods as examples of an extreme flood-associated regional storm event. Gridded regional daily rainfall data were subdivided into 13 categories so that targets areas with high to very high rainfall (Rainfall depths > 75 mm) could be distinguished from areas with mid-range rainfall depths (Rainfall depths 6 – 10 mm, 11 – 20 mm, 21 – 50 mm and 51 – 75 mm) and limited or no rainfall (Rainfall depths, 0 mm, 1 mm, 2 – 5 mm). An example of a local storm event is shown in Figure 8.2.

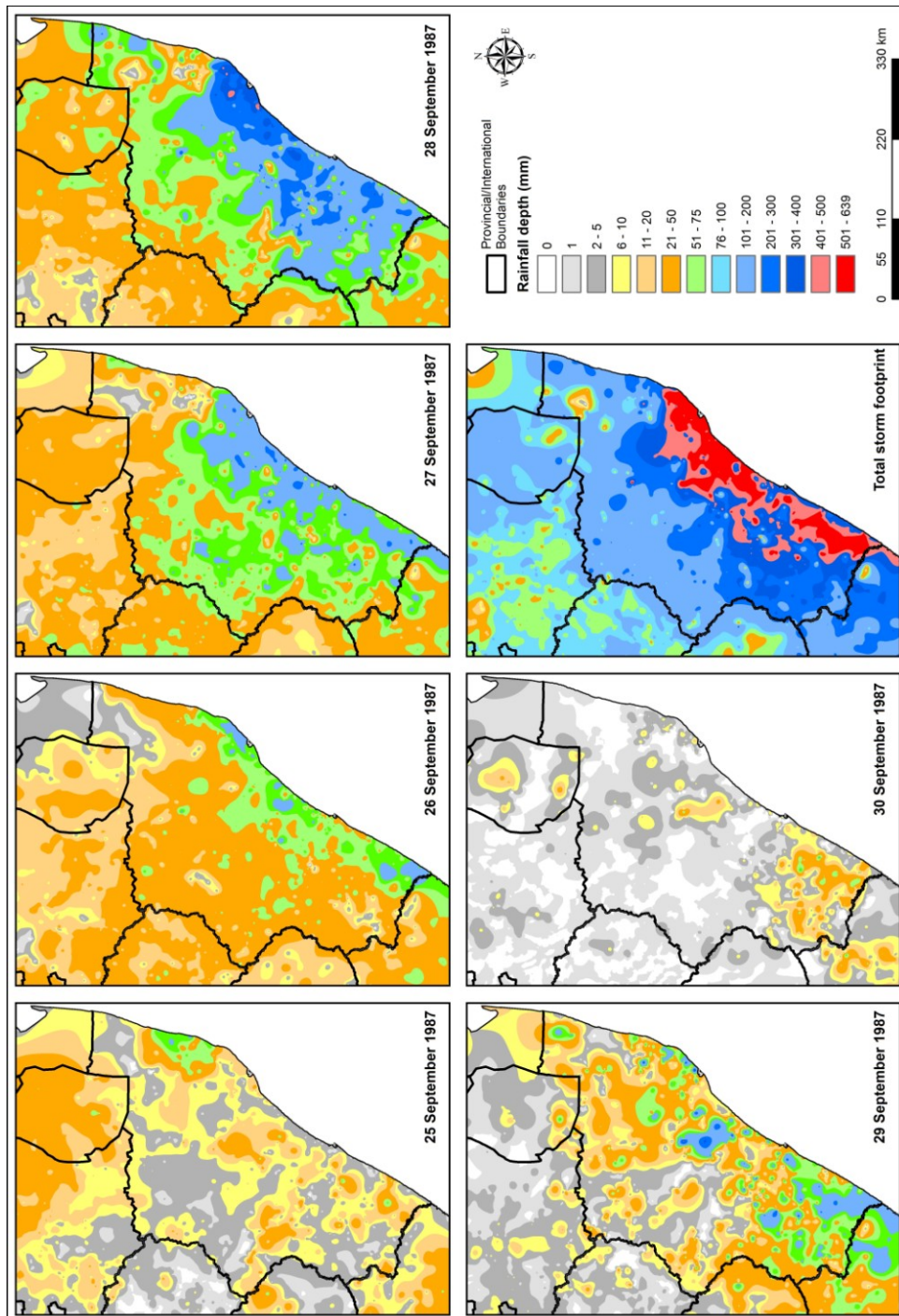


Figure 8.1. Example of daily regional storm footprints and the extreme flood-associated regional storm event footprint for the 26th September – 29th September 1987 floods. The pre- and post- storm day footprints are also shown.

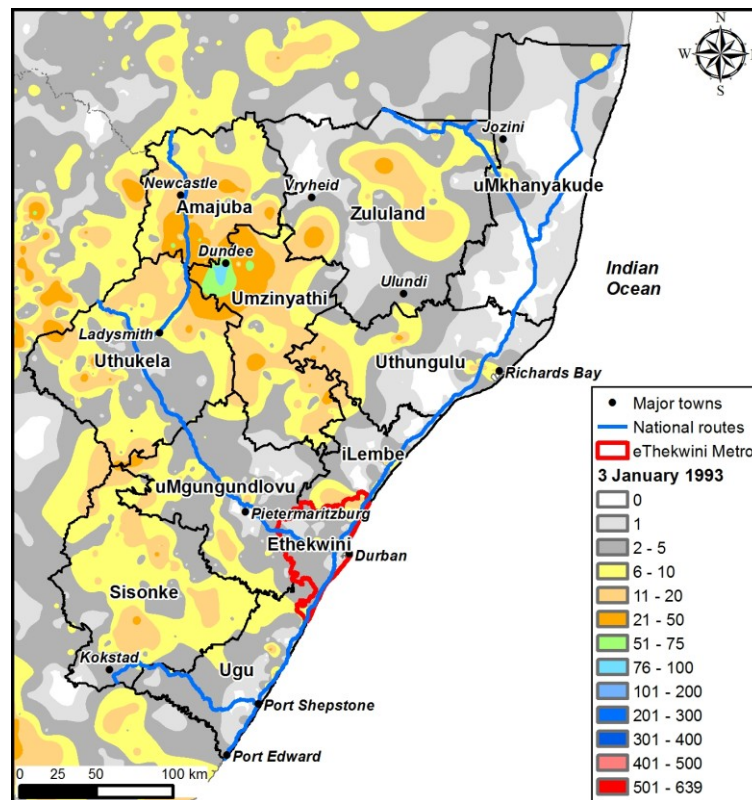


Figure 8.2. Example of a daily gridded isohyet map showing a local storm event (LSE) near Dundee.

8.2.1. Regional storm event footprints

Inspection of the extreme flood-associated regional storm events reveals there are clearly defined geographic areas affected by the storms (Fig. 1 - 18, Appendix IV). Comparison between these extreme flood-associated storm footprints indicate that extreme floods have occurred at a range of areas and rainfall depths in the past. While the March 1925, January 1984 and September 1987 storms (Fig. 8.3B, D, E) covered large portions of the study area with total rainfall depths exceeding 500 mm; the March 1913, February 1974 and April 1978 extreme flood event storms (Fig. 8.3F, H, I) showed smaller geographic spread with total rainfall depths varying between 200 - 300 mm. When comparing the regional storm footprints identified in this study, most of which were not specifically associated with any one particular extreme flood event, (Fig. 8.3J - M) to those that have a definite association (Fig. 8.3 F, H, I), it can be seen that their footprints are comparable in size to those in Figures 8.3B, D, E with total rainfall

depths up to the 300 – 400 mm range (and thus equitable to depths that have produced extreme floods before). The data thus indicate that there are likely to have been many other storms which have exceeded the areal extent and rainfall depths of some recorded extreme flood-associated events and as such would have had posed a significant flood hazard to communities within the footprints.

8.2.2. Regional storm event characteristics

Overall, 228 regional storm events were identified in the dataset, the footprint areas and rainfall depths of which are summarised in Table 8.2. Plotting the regional storm event durations shows that these storms can last up to 14 days with the bulk of the regional storm event lasting between two to four days. The mean duration is 3.45 days (Fig. 8.4). Extreme flood-associated regional storm events have larger footprints than those of the regional storm events. The maximum rainfall depths for the extreme flood-associated regional storm events are higher than those of the regional storm events (Table 8.2). In terms of mean rainfall depth and mean depth/duration, the regional storm events values are higher than those of the extreme flood-associated regional storm events. When comparing the mean values between the extreme flood-associated regional storm events and other regional storm events identified in this study, they are of the same general magnitude except the areal extent which is larger for the former.

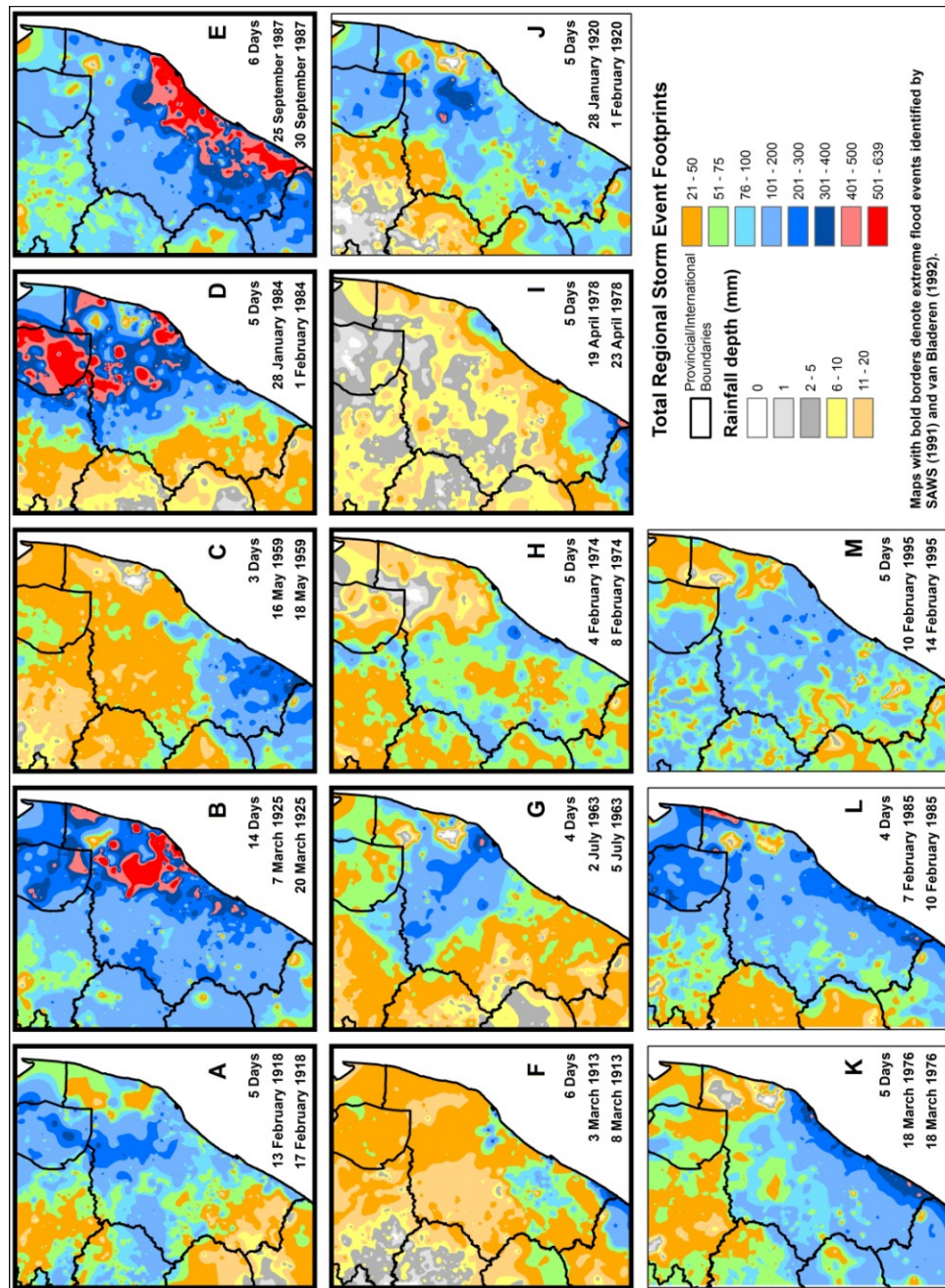


Figure 8.3. Comparison between extreme flood-associated regional storm events and other regional storm events identified in this study. A - I examples of extreme flood-associated regional storm events. J - K examples of identified regional storm events.

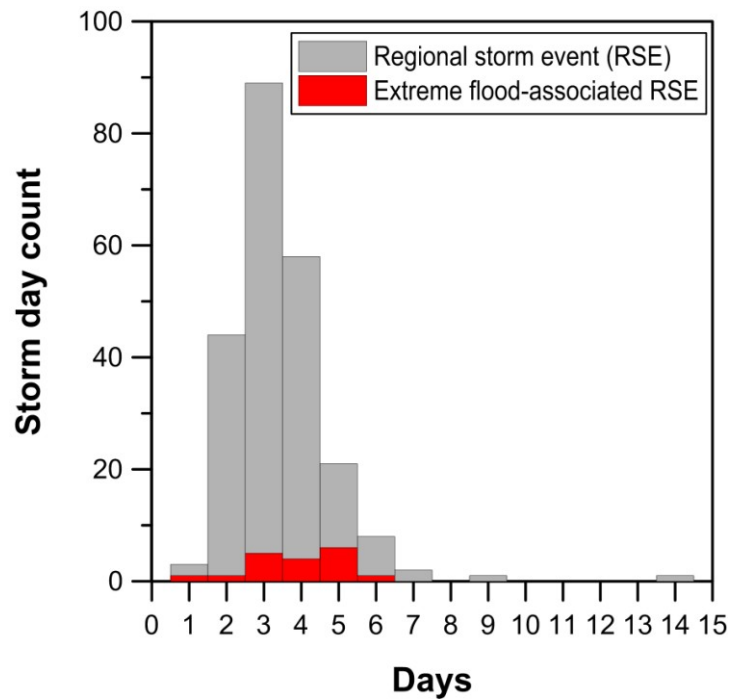


Figure 8.4. Plot of the regional storm event and extreme flood-associated regional storm event daily duration showing the predominance of the 3 – 4 day storms.

Table 8.2. Summary of regional storm events compared to extreme flood-associated regional storm events.

Parameter	Regional storm events (RSE)			Extreme flood-associated RSE			Total RSE		
	Min.	Max.	Mean	Min.	Max.	Mean	Min.	Max.	Mean
Area km ²	722	75634	14355	26	115306	47658	26	115306	17167
Max Rainfall Depth (mm)	120	1257	298	99	1560	550	99	1560	322
Mean Rainfall Depth (mm)	52	299	117	81	287	152	52	299	120
Mean Depth/Duration	15	95	39	17	81	40	15	95	39

8.2.3. Regional storm event distribution in time

Plotting the frequency of regional storm events per annum, together with extreme flood-associated regional storm events, shows that a potential flood producing storm has occurred nearly every year, with more than one occurring in some years (Fig. 8.5). Some years have recorded multiple regional storms with peak counts in 1893 (5), 1932 (6) and 1963 (9). The period from 1890 to 1943 show only 78 regional storm events having occurred. The period between 1943 - 1953 experienced the least amount of regional storm events with only four events. Regional storm events increased from 1953 to 2000 (146) with only four years during this period experiencing no regional storm events. By comparison the extreme flood events identified by van Bladeren (1992) occur in years with multiple regional storm events. Extreme flood events occurring in years with multiple regional storm events correspond to the years 1893, 1932, 1940, 1974, 1977, 1978, 1984, 1985 and 1987.

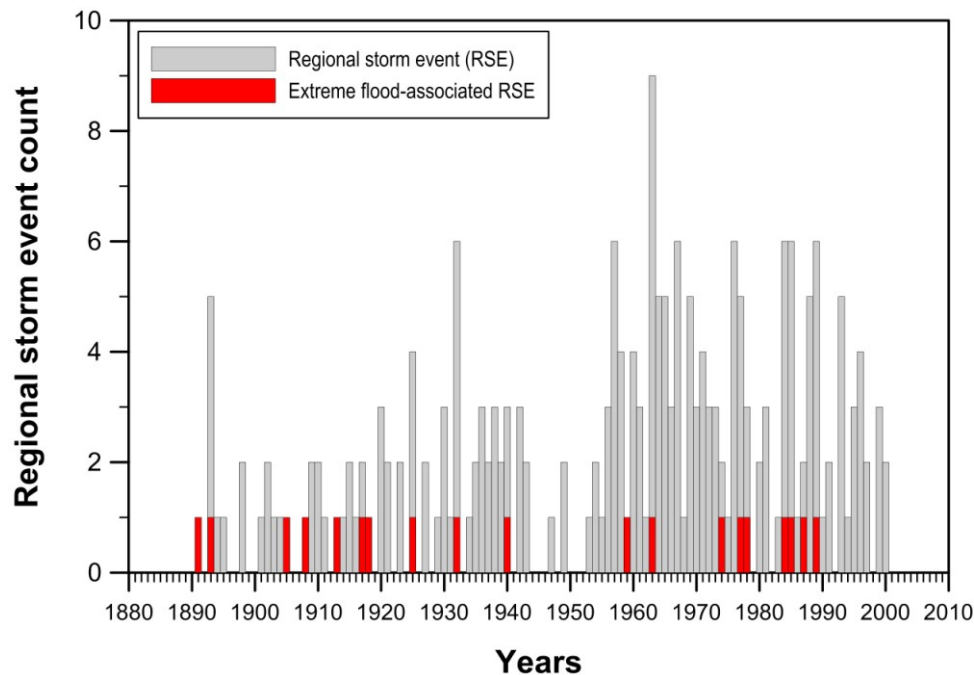


Figure 8.5. Regional storm event and extreme flood-associated regional storm event distribution from 1891 - 2000. Note the variation in the number of regional storm events that have occurred in various years and the periods of increased/decreased annual regional storm event counts.

Plotting the monthly frequency for the 228 regional storm events shows that no month is immune to potential flooding (Fig. 8.6). The peak risk period is between January to April; with September to December open to medium risk of flooding and June to August exposed to the lowest risks. No extreme flood events were recorded for June, August and December, these events thus being predisposed more to seasonality than the regional storm events.

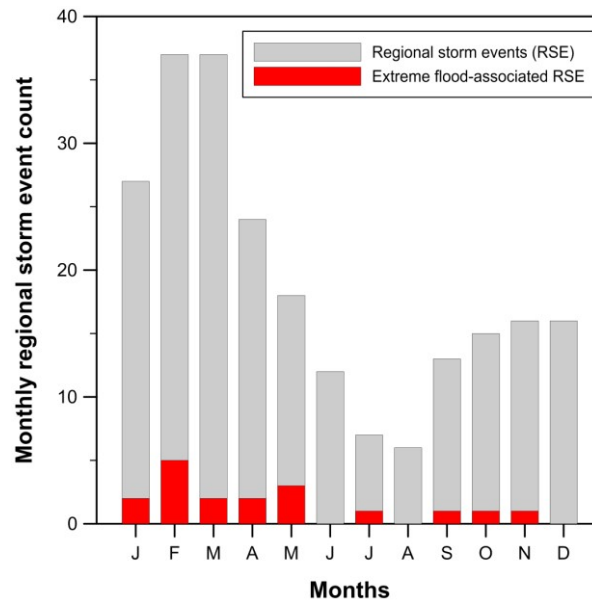


Figure 8.6. Regional storm event and extreme flood-associated occurrences per month showing increased regional storm event counts for the January – April period and reduced counts for the June – August period. Note the higher extreme flood-associated regional storm event counts for the January – May period.

Using a bubble plot to compare mean rainfall depth per year, and regional storm event footprint areas, this indicates that the storms are generally constrained by a mean rainfall envelope of approximately 80 to 185 mm. All but three of the extreme flood-associated regional storm events and two regional storm events plot outside this envelope. The extreme flood-associated regional storm events generally do not plot separately from the other regional storm events but all plots within the defined envelope.

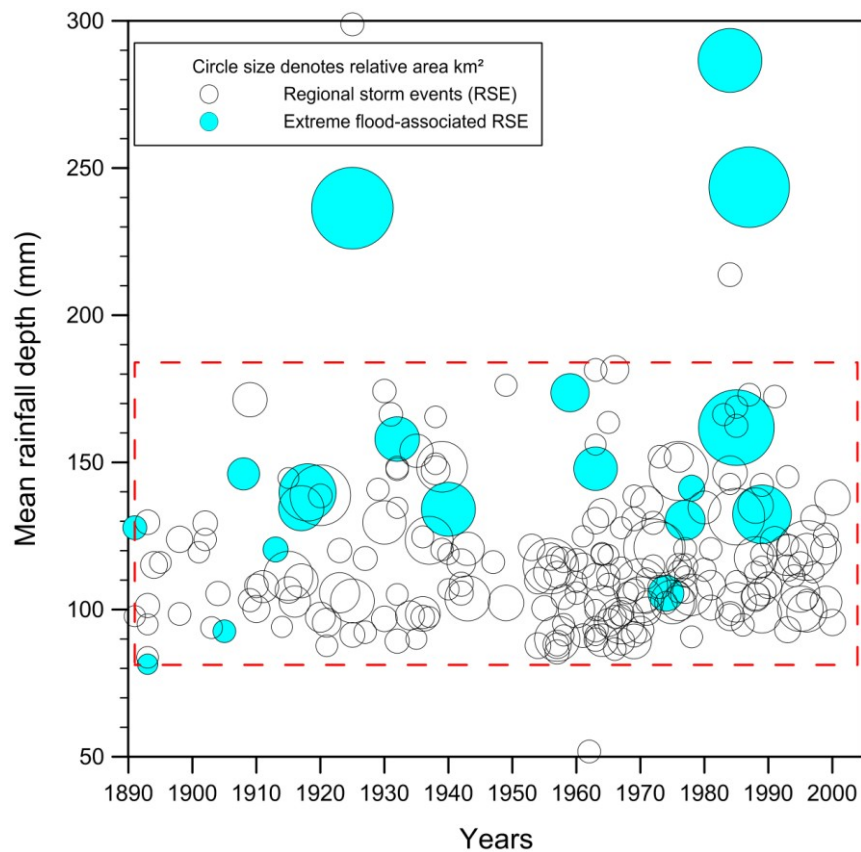


Figure 8.7. Bubble plot comparing mean rainfall depth and footprint area over time. The size of the bubble represents the footprint area of a regional storm event. The red dashed rectangle represents the 80 – 185 mm mean rainfall depth envelope.

8.2.4. Regional storm system event spatial distribution

Overlaying and summing the regional storm event footprints determines the number of times a storm has occurred at a specific geographic location (Fig. 8.8). Only 225 of the 228 regional storm event events can be plotted because the 1868 to 1891 extreme flood events did not have sufficient rainfall data to produce a footprint.

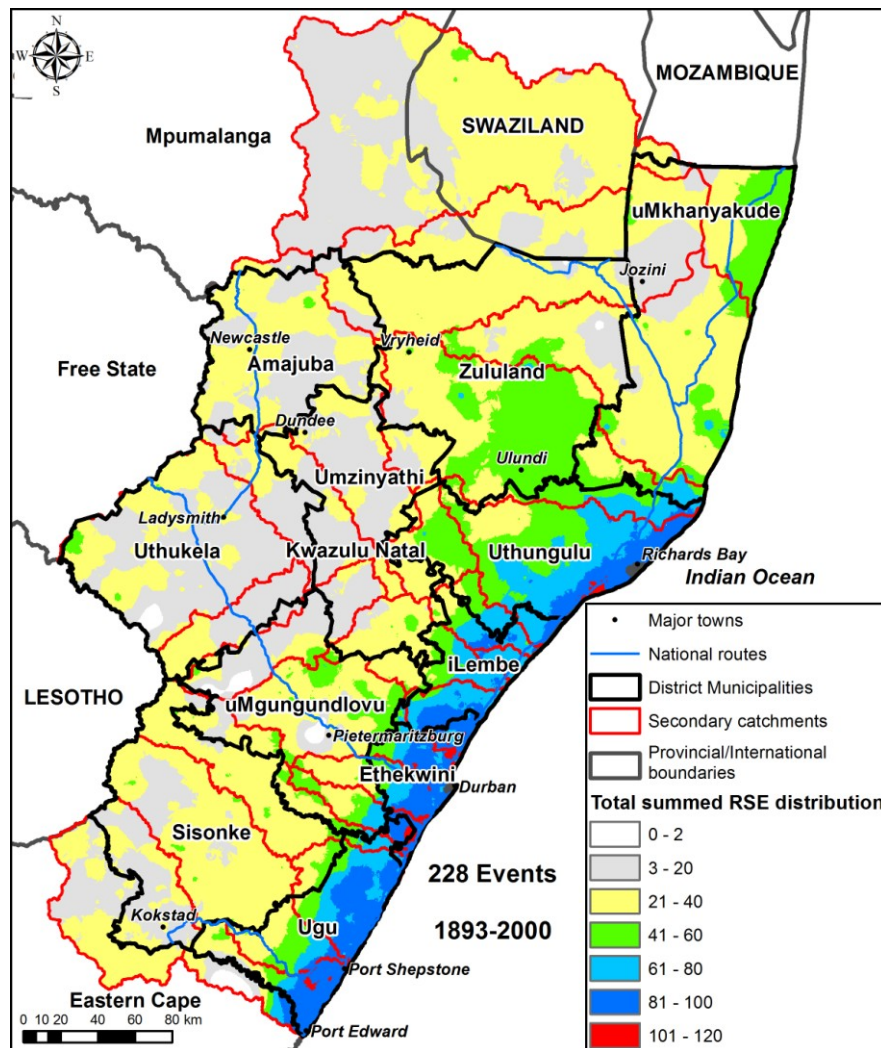


Figure 8.8. Geographic distribution of totalled regional storm events. Note the coast parallel zones that decrease in regional storm event count away from the coast.

It is clear that every part of the study area has been affected by regional storm events. The area with the highest occurrence of regional storm events is the coastal margin which has received between 80 - 120 regional storm events since 1893. The regional storm event count forms coast parallel bands reducing in count away from the coastline. In the Sisonke and Zululand District Municipal areas the 21 to 40 count band extends further inland than in other areas. The lowest count areas (1 - 20) are located as inliers within the 21 - 40 band particularly in the Uthukela/Umzinyathi and Sisonke District Municipal areas and into the Mpumalanga Province.

8.2.5. Local storm events (LSEs)

Using the methodology described in section 8.1, 1326 local storm events were identified. Together with the 24 events listed by van Bladeren (1992), this indicates that there have been at least 1350 local storm events which may have resulted in flash flooding above bank-full stage at the local scale during the 1893 - 2000 period (Appendix V).

8.2.6. Local storm event distribution in time

A plot of local storm event count per annum shows that excluding 1900, 1902 and 1999 every year during the 1893 to 200 period generally experienced multiple local storms (Fig. 8.9). Peak counts occurred in 1943 (29) and 2000 (29). Lesser peak per annum local storm event counts occurred in 1914 (13), 1938 (26), 1939 (20), 1942 (27), 1953 (24), 1958 (25), 1966 (18), 1973 (24), 1974 (26), 1975 (24), 1976 (26), 1981 (20), 1984 (25), 1988 (26) and 1997 (23). There are only 222 local storm events from 1891 to 1937, whereas for the period 1938 to 2000, 1128 local storm events were identified. There is an apparent cyclicity to the annual counts with peaks at 1914, 1925, 1943, 1958, 1974 1984 and 2000.

Monthly local storm event frequency for the 1893 to 2000 period (Fig. 8.10), shows that the bulk of the storms occur in the December to March period (881) while in the April to November months only 469 local storm event occurred. The highest count is in January (262) and the lowest in June (26).

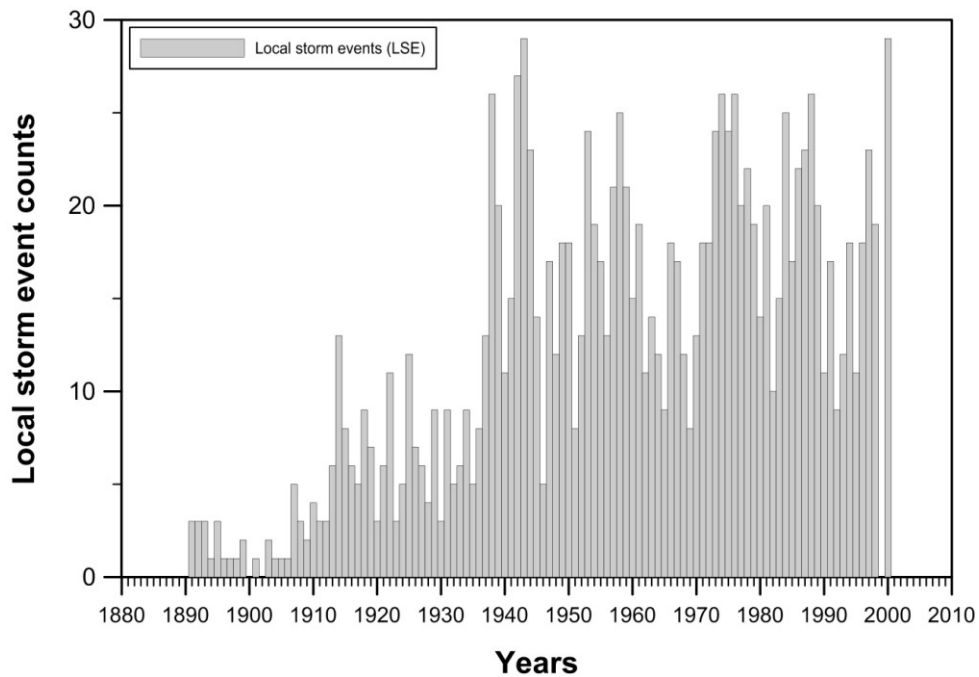


Figure 8.9. Local storm event frequency per annum from 1893 to 2000. Note the variations in annual counts and periods of increased/decreased annual counts.

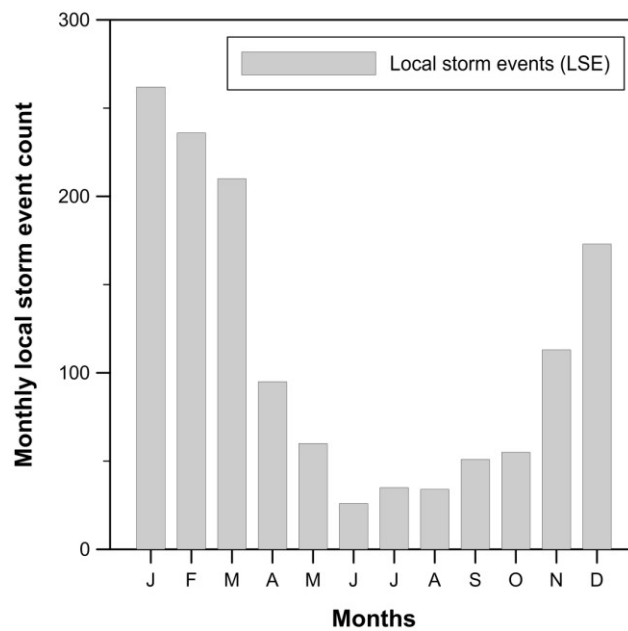


Figure 8.10. Local storm event occurrence per month. Note the higher monthly occurrences for the November – March period and lower occurrences for the April – October period.

8.2.7. Local storm system event spatial distribution

Summing local storm event footprints (Fig. 8.11) to determine the geographic reoccurrence of these storms indicate that the coastal belt has the highest occurrence, particularly in the Port Edward, Durban, Richards Bay – St Lucia and Mbazwana – Manguzi areas. In the interior of the study area, the higher local storm event counts tend to occur as scattered pockets, particularly Sani Pass and north of Franklin (Sisonke), east of Curry's Post (Umgungundlovu), Little Switzerland (Uthukela), Biggersberg (Umzinyathi), between Newcastle and Volksrust (Amajuba), Nkandla (Uthungulu), Nongoma – Ulundi – Pongola, Vryheid area (Zululand) and the Ingwavuma area (Umkhanyakude).

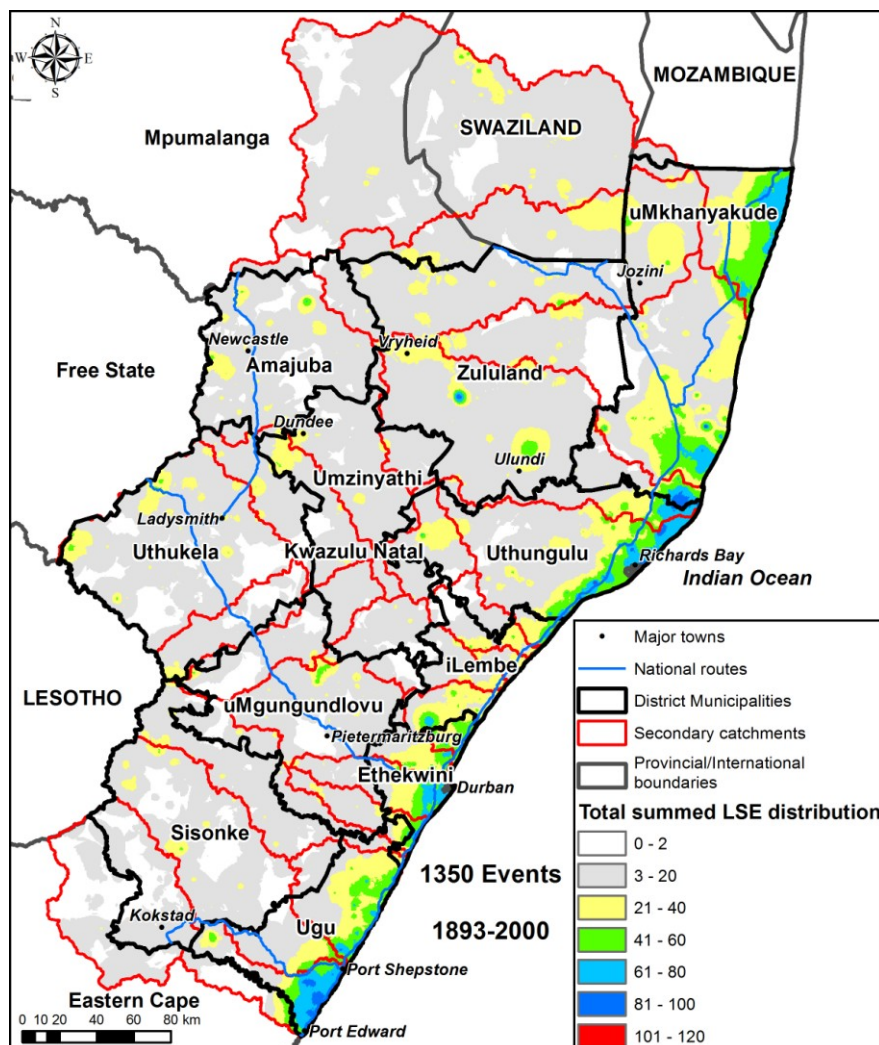


Figure 8.11. Geographic distribution of totalled Local storm events showing the concentration of the highest local storm event counts along the coastal margin.

8.3. Discussion

Inspection of the spatial distribution of the summed regional and local storm events categories shows some geographic commonality. The summed regional storm event categories (Fig. 8.08) have a larger geographic extent than that of the local storm events (Fig. 8.11) due to the difference in footprint size between the two storm types. The coastal margins of both the regional and local storm events record the highest number of storm events. Within the study area interior, the scattered distribution of the 21 – 60 local storm event count categories, coincide with the regional storm event distribution for the same categories. This indicates that there are parts of the study area that are more likely to be affected by storms irrespective of storm size.

Comparison between the extreme flood-associated regional storm events and that of the other regional storm events indentified in this study, indicate that these regional storm events would have resulted in flooding. Noting that van Bladeren (1992) based his selection of extreme floods on the six highest discharges for the major rivers in the study area, this does not mean that the seventh highest and lesser discharges did not result in significant flooding. The other point to note is that there is an overlap between the extreme flood-associated regional storm events and regional storm events (Fig. 8.3 and Fig. 8.7), particularly in terms of mean rainfall depths. Applying a best-fit line through the regional storm event data points of Figure 8.7, results in a mean regional storm event rainfall depth of 119 mm (Fig. 8.12), and which this thesis will use as a cut off to define a newly recognised set of extreme storm events (ESE). Comparing the extreme storm events to the extreme flood-associated regional storm events shows that the extreme storm events can account for all but three of van Bladeren's (1992) extreme flood events. Reasons why these three extreme flood events fall below the 119 mm mean rainfall depth is unclear. The 1893 and 1905 events may be a result of insufficient rainfall station data over that period and that the extreme storm event footprints may have been much larger. For the 1974 extreme flood event it appears that the scattered nature of the extreme storm event footprint (See Appendix IV, Fig. 12) produced, a lower mean rainfall depth but produced sufficient runoff in a catchment to be included in van Bladeren's (1992) list.

Regional storm system events are caused by weather systems that affect Southern Africa. One of the systems related to flooding are the intense westerly cut-off lows which have been associated with some of the most extreme flood events recorded (Singleton & Reason 2007). Severe weather and heavy rainfall has also been attributed to systems that range from local thunderstorms to mesoscale convection systems (Preston-Whyte & Tyson 1997; Blamey & Reason 2009). Overlaying a compilation of the weather system frequency (Tyson, 1986) and regional storm events show that there is a correlation between the frequency of the various weather systems and the amount of regional storm events occurring in a given month (Fig. 8.13). The seasonal variation in the predominance of either easterly or westerly wave systems is mirrored by the regional storm event count.

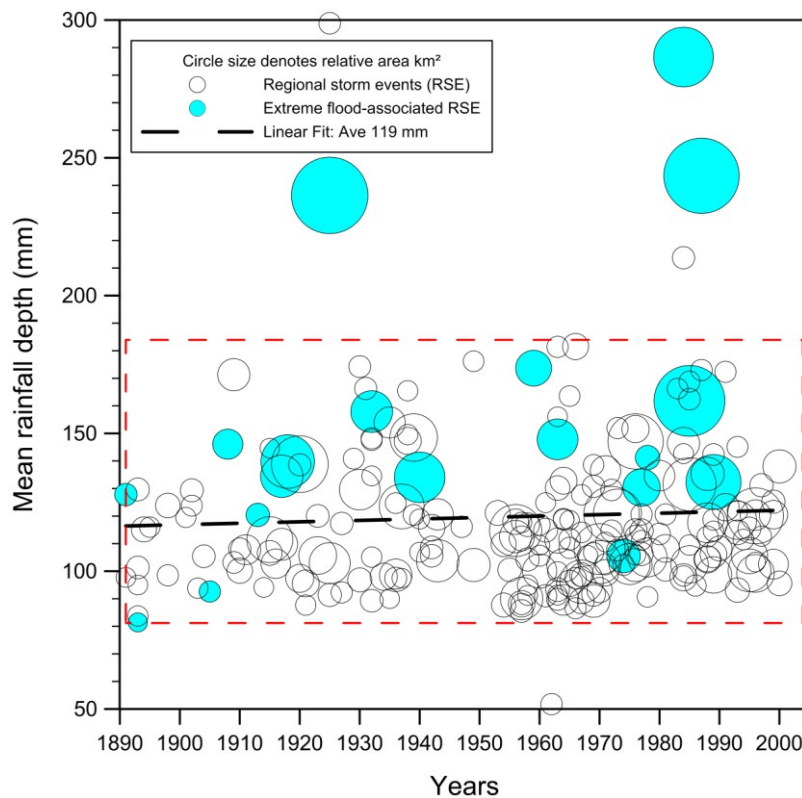


Figure 8.12. Bubble plot comparing mean rainfall depth and footprint area over time with a best fit mean curve to the regional storm events. The size of the bubble represents the footprint area of a regional storm event. Note that all but three of the extreme flood-associated regional storm event plot above the mean 119 mm rainfall depth line.

In overlaying the two data sets (Fig. 8.13), it is clear that from January to April the easterly systems predominate with some influence from westerly lows, and is strongly linked to the period of highest regional storm event counts. The westerly cut-off lows are dominant in the winter/spring months from April to November, particularly April/May and September and are most likely responsible for the flood producing regional storm events during this period. From November to December, both the westerly cut-off lows and the easterly lows are responsible for the regional storm events. Westerly anticyclones and lows thus appear to play a very small role in the flooding experienced in the study area.

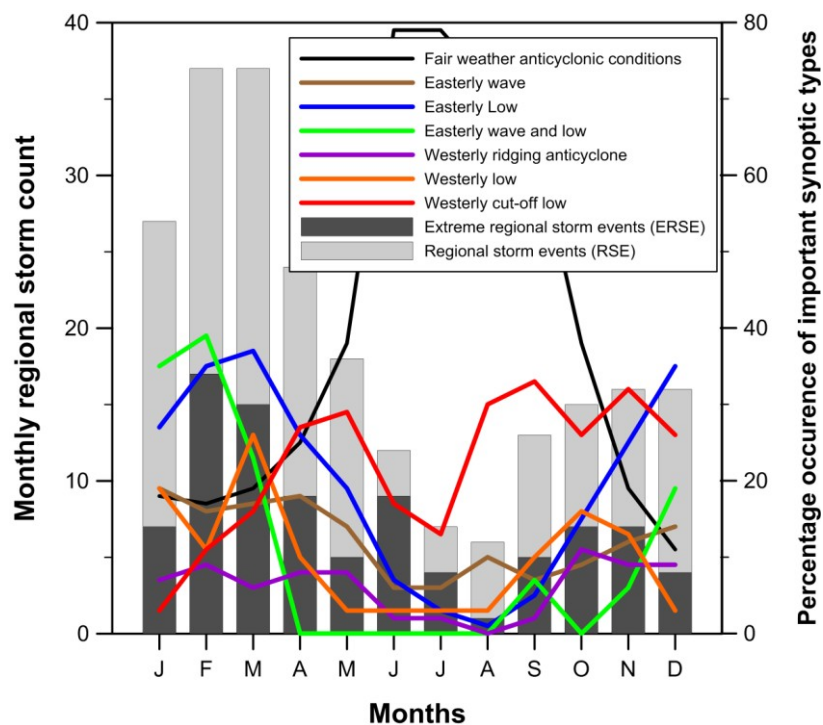


Figure 8.13. Monthly synoptic system frequency comparison with regional storm events and extreme regional storm events monthly frequency showing the positive correlation between the easterly synoptic systems and higher regional storm event and extreme storm event counts for the period December – April and the positive correlation between the westerly cut-off lows and regional storm event/extreme storm event counts for the period May – November.

Comparing the extreme storm events to the regional storm events and weather system frequencies, it can be seen that a similar trend exists and that cut-off lows that can produce intense rainfall and hence extreme flooding are not the dominant flood producing weather system as previously thought (Preston-Whyte & Tyson 1997). Rather this indicates that easterly weather systems are more likely to produce flooding during the spring/summer rainfall cycle.

From Figure 8.4 it is clear the regional storm events generally have a residence (transit) period of 3 – 4 days across the study area. The general upper limit is 4 – 5 days. This implies that any storm which lasted longer has been stalled and trapped by external weather systems.

Tropical cyclones/storms have also been a contributor to heavy rainfall events in the past (Dyson & Heerden 2002). Although these weather events are not common, on average 10 tropical cyclones a year occur in the South West Indian Ocean (SWIO) (Dunn 1984). According to Kovács (1985) 10 tropical cyclones have affected the study area (1956 to 1985). During the 1893 – 2000 period, Tropical Storm Domoina (1984) had the highest rainfall associated with a tropical cyclone (Kovács et al. 1985). A storm in March of 1925, thought to be a tropical cyclone, produced flooding greater than that attributed to Tropical Storm Domoina (van Heerden & Swart 1986).

To determine the areas affected by tropical cyclone/storms, regional storm event patterns were selected that were definitely associated with tropical cyclones/storms or if their footprints were restricted to northern KwaZulu-Natal, Swaziland or Mozambique. Overlaying these regional storm events, it becomes clear that it is not just northern KwaZulu-Natal that may be affected by these storms (Fig. 8.14). The whole coastal margin of the study area has been affected by at least three tropical cyclones/storms (1925 - unconfirmed, 1984 - Domoina and Imboa). This places densely populated areas such as Durban within the risk area, an observation also made by van Heerden & Swart (1985). Table 8.3 lists the tropical cyclones/storms that have affected rainfall in South Africa. From this list only four tropical cyclones/storms have had a trajectory along a path sufficiently southerly to have affected the study area during the 1956 – 1984 period. Extreme storm events in January 1909, February 1937 and February 1967 (Fig. 8.14) identified as a possible tropical cyclone/storm is not listed in Table 8.3 but fits all the other characteristics of the tropical cyclone/storm regional storm events. The trend for tropical cyclone activity in the SWIO appear to be mixed with decreasing numbers for the 1980 – 2007 period but with increasing numbers for the 1952 – 2007 period (Mavume et al. 2010).

The rise in global sea surface temperatures have been linked to increased tropical cyclone intensity and number (Elsner et al. 2008; Mann et al. 2009) which may result in future increased tropical cyclone activity in the study area. According to Henderson-Sellers et al. (1998), there is no validity in the general belief that cyclone belts will move away from the equator with increased global warming. Henderson-Sellers et al. (1998) do point out that due to other climatic factor there may be changes in the cyclone belt positions at a regional scale. In the case of Southern Africa, a shift from the current predominate land fall of 20 – 23° S to 25 – 28 ° S will place Richards Bay and Durban directly into the land fall path for tropical cyclones/storms.

During periods where weather and climatic conditions result in multiple regional storm events it would be anticipated that such conditions are more likely to produce extreme flooding. The extreme floods identified by van Bladeren (1992) do not reflect this (Fig. 8.5). Comparing the extreme storm events with the overall annual regional storm event count (Fig. 8.15) indicates a greater likelihood of extreme events occurring in years with multiple regional storm events. The only anomaly is the 1954 – 1958 period where 16 regional storm events occurred with no extreme storm events.

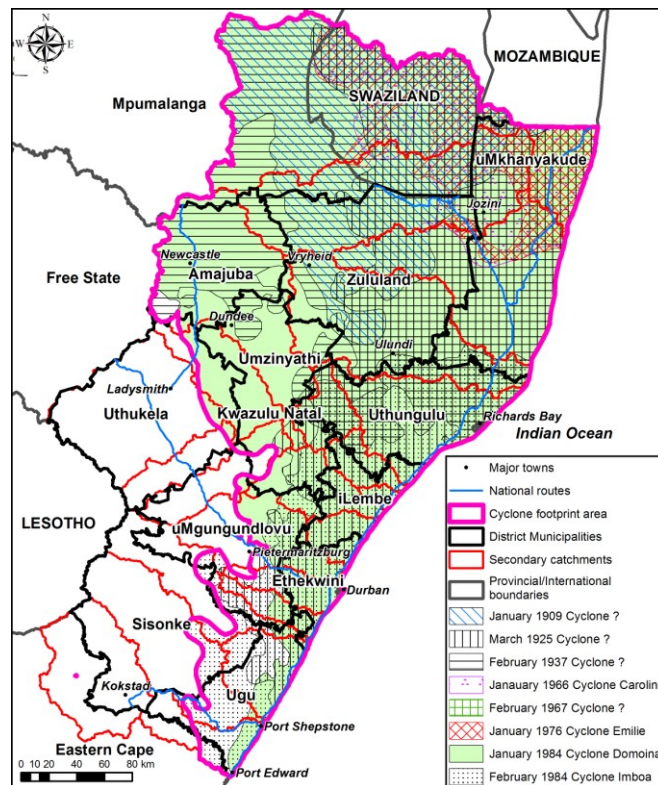


Figure 8.14. Geographic distribution of tropical cyclones-associated regional storm events (4) and possible cyclone regional storm events (4) with similar characteristics to that of cyclone-associated regional storm events. The distribution indicates that major towns such as Durban and Richards Bay can be affected by cyclones.

Although both the regional storm event and local storm event counts (Figs. 8.6 and 8.10) show a similar peak occurrence during the summer rainfall period, there is a poor correlation between their annual counts (Fig. 8.9). This suggests that there may be two different mechanisms responsible for these events. Plotting the distribution of regional storm events and local storm events over years and months (Fig. 8.16) reinforces the observation that the summer rainfall period has the highest occurrence of storm events. The number of regional storm events (228) compared to the local storm events (1350) for the 1893 – 2000 period indicate that the risk from flash flooding is far greater than that from regional flooding. There is a suggestion of fewer events prior to approximately 1910.

Table 8.3. List of tropical cyclones/storms that have affected South Africa (After Darlow 1990)

Tropical Cyclone	Dates	Impact on KZN
A ?	11 - 16 February 1956	No
Astrid	December 1957 - January 1958	No
Brigitte	24 December 1957 - 2 January 1958	No
Claude	30 January - 1 February 1960	No
Caroline	30 December 1965 - 5 January 1966	Yes
Eugenie	4 - 13 February 1972	No
Danae	5 - 22 February 1972	No
Emilie	31 - 30 January 1976	Yes
Domoina	26 January - 1 February 1984	Yes
Imboa	17 - 19 February 1984	Yes

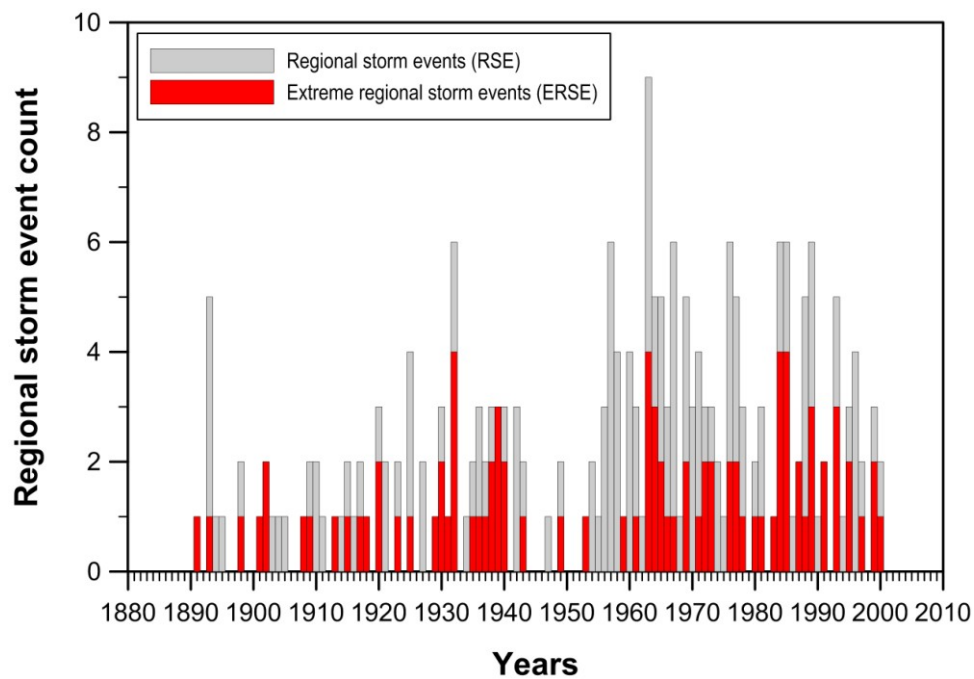


Figure 8.15. Regional storm event and extreme storm event distribution from 1891 to 2000. Note the increased number of extreme storm events in years with multiple regional storm events.

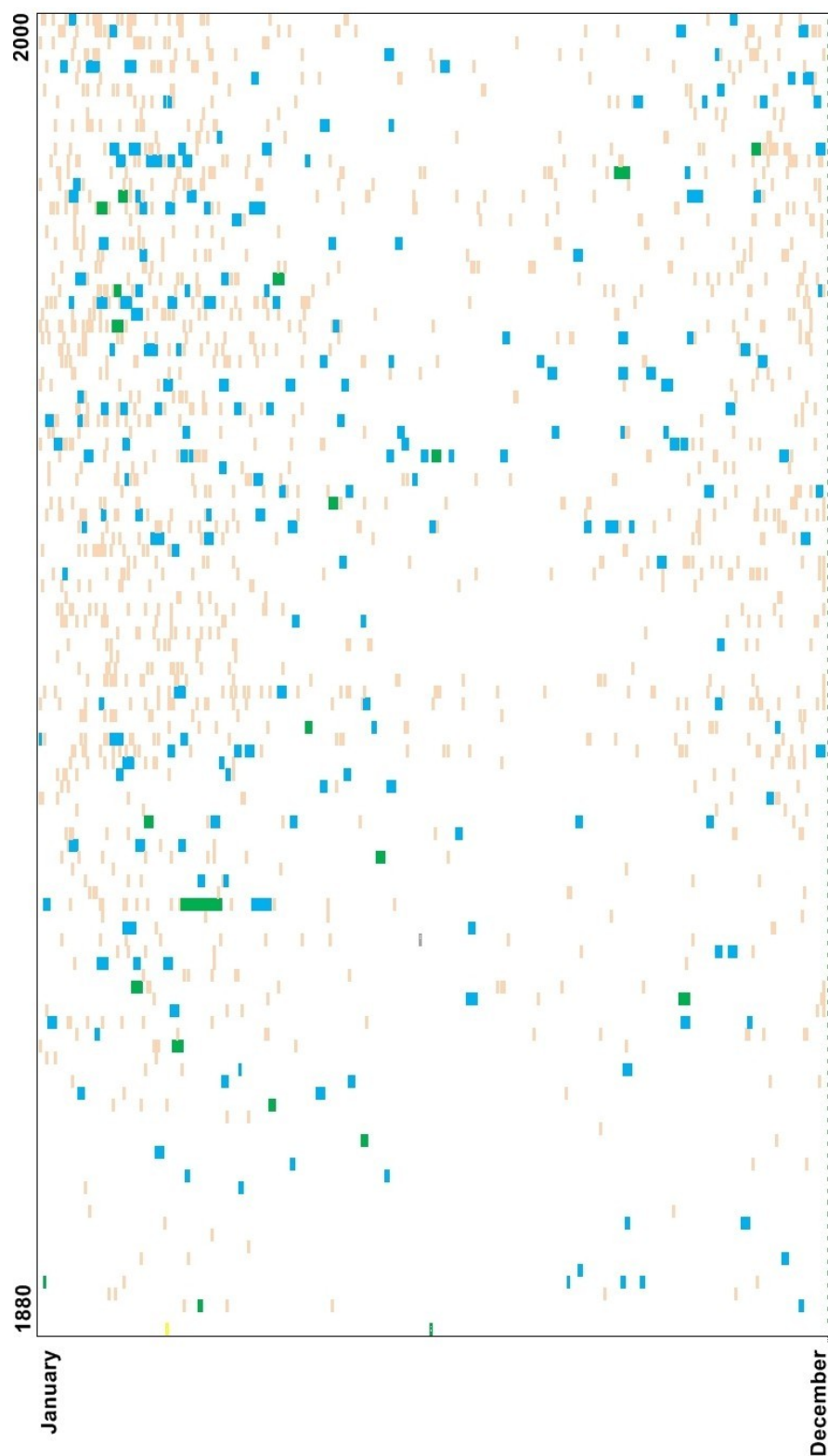


Figure 8.16. Distribution of both regional and local storm events in time from 1880 – 2000. Blue blocks are regional storms, orange blocks are local storms and green blocks are extreme flood-associated events. Note that most events occur during the summer rainfall period (November – April).

An important component of investigating natural hazards is the ability to produce maps delineating areas and levels of risk. This issue has received some attention in the literature (e.g. Viljoen et al. 2001; Plate 2002; Thieken et al. 2006; Marchi et al. 2010; Meyer et al. 2012) with these approaches primarily based on statistical design return period flood lines. Applying these methods to the study area has limited value due to the lack of available design flood lines (as discussed previously).

Due to the lack of data, other approaches have been used at attempting flood hazard mapping. The South African Risk and Vulnerability Atlas (SARVA, 2010) contains a map showing areas susceptible to flooding in South Africa, taken from the National Department of Agriculture's AGIS Land Capability System (Schoeman et al. 2002) (Fig. 8.17). The delineation of flood prone areas was based on terrain and soil types (Schoeman et al. 2002). The SARVA (2010) map suggests that only the northeastern portion of KwaZulu-Natal and some scattered areas are susceptible to flooding.

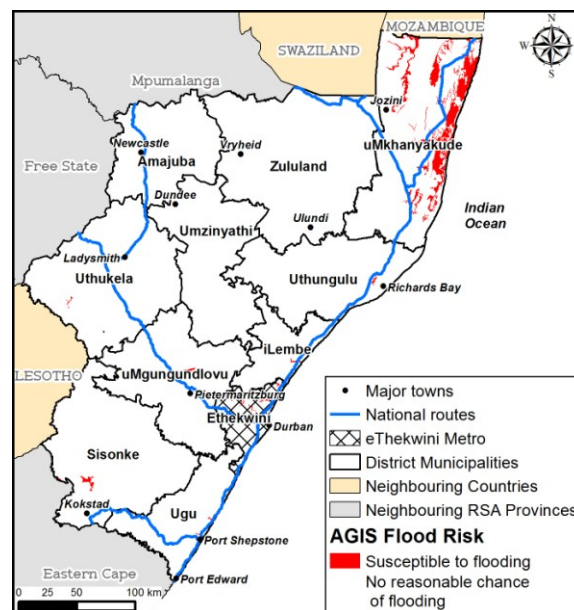


Figure 8. 17. Extract from the South African Risk and Vulnerability Atlas showing areas susceptible to flooding (After SARVA 2010).

The World Health Organization (WHO) has produced an eAtlas of global flood hazard distribution (El Abidine El Morjani 2011) (Fig. 8.18) and is a GIS classified weighted hazard map based on statistical analysis of causal factors (land cover, elevation, soils, geology, flow accumulation, precipitation and historical floods). For KwaZulu-Natal the WHO eAtlas indicates that all major rivers generally have the same (medium) flood risk, with some scattered areas with high to highest flood risk. The greatest concentration of high to highest flood risk areas is located around the northeastern coastal lake systems.

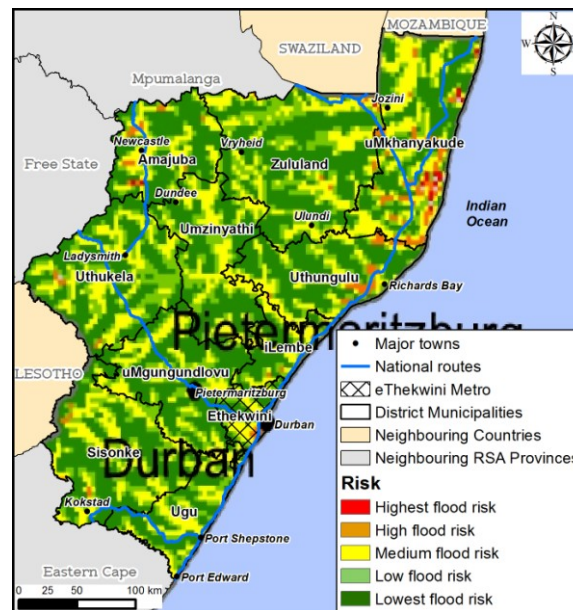


Figure 8.18. Extract from the WHO flood risk atlas (After El Morjani (2011)) showing the relative risk for rivers in KwaZulu-Natal.

The summed regional storm event footprints (Fig. 8.8) define areas where there are variations in the number of regional storm event that have occurred in the past. This indicates that areas with higher regional storm event counts have a greater likelihood of being affected by similar storms and hence have a greater flooding hazard. By converting the summed regional storm event map to a percentage risk map, depicting the historical distribution of regional storm events, a flood hazard map is produced (Fig. 8.19). This map shows that there is a well-defined spatial distribution to these data. It is significant to note that flooding has occurred at least once everywhere within KwaZulu-Natal. The study area can be divided into five distinct geographic zones based on the percentage distribution of regional storm events (Fig. 8.19).

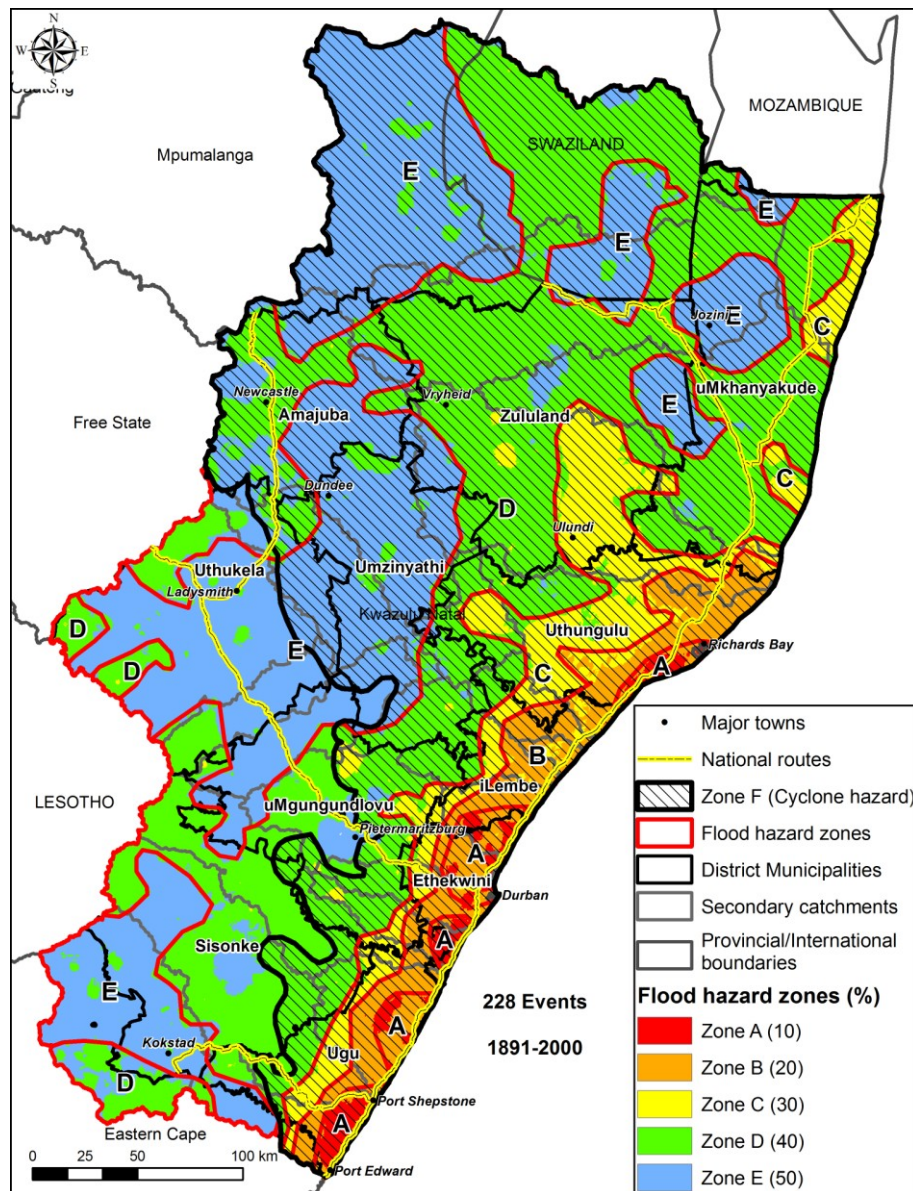


Figure 8.19. Flood hazard map for KwaZulu-Natal showing the general coast parallel zones of potential flood hazard risk. Explanation for Zones A – F are presented in Table 8.4.

Zone A consists of scattered zones located along the coastal margin extending from Port Edward to north of Durban with an outlier around the Mtunzini area. Zone B extends along the coastal margin from Port Edward in the south to St Lucia in the north. Zone C is located inland of the coastal margin with a similar trend to that of Zone B, except that it extends inland along four corridors with the best defined being along the Mfolozi River. Some outliers of Zone C are located along the northern coastal belt. Zone D is mainly located in the central midlands portion of the province and also occurs along the escarpment on the western border of KwaZulu-Natal.

Zone E predominantly covers the western portion of KwaZulu-Natal with some scattered outliers towards the east. Zone F represents the area impacted by tropical storms and cyclones. The southern and western extent is an approximate line between Durban and Newcastle and north into Swaziland and Mozambique.

The potential hazard based on 110 years of regional storm events is summarized in Table 8.4. While Zone A exhibits the highest risk, storm events over this area will not result in extreme events. Extensive localized flooding, especially in the urban environment represents a significant risk. Storm systems that affect Zones B and C can produce extensive flooding in the coastal catchments. Zone D represents areas where storm systems can produce extreme or near extreme flood events. Although Zone E represents the lowest risk area, storm systems that cover this area are the most likely to produce extreme flood events. Tropical storms and cyclones that affect Zone F have a low risk but these will generally produce extreme events.

Table 8.4. Flood hazard zone descriptions for KwaZulu-Natal (KZN) as per Fig. 8.19)

Flood Hazard Zone	Probability	Spatial Distribution	Hazard
A	50%	Coastal belt from Port Edward to Richards Bay. Patchy distribution up to approximately 300 m elevation	Very high risk, mainly from cut-off lows. Localised flooding
B	40%	Coast parallel band from Port Edward to St Lucia up to approximately 500 m elevation.	High risk, mainly from cut-off lows. Flooding at sub-basin level
C	30%	Similar to Zone B but well defined corridor over the Mfolozi Valley and outliers along the northern coastline. Elevation up to approximately 1000 m	Medium risk, mainly from cut-off lows. Flooding at sub-basin level
D	20%	Central midland belt and escarpment. 0 to 3200 m elevation.	Low risk. Medium to Extreme flood events
E	10%	Predominantly western portion of KZN with outliers along northern KZN. Predominantly over 1000 m elevation	Very low risk. Medium to extreme flood events
F	10%	Coastal and Northern KZN	Tropical storms and cyclones. Low risk. Medium to Extreme flood events

Comparing the SARVA (2010) flood susceptibility map (Fig. 8.17) with the flood hazard map (Fig. 8.19) shows two very different pictures. While the SARVA (2010) map indicates that the northeastern portion of KwaZulu-Natal is the most susceptible to flooding, the flood hazard map shows that the southern KwaZulu-Natal coastal margin has been subjected to the most storms and has a greater flood risk (Zone A and B, Fig. 8.19). The SARVA (2010) map is based on the distribution of a particular soil form associated with alluvial deposits and is a large scaled product that can only demarcate large areas of a particular soil form. This product is not of sufficient scale to be applied to settlements and it creates a false impression of flood risk in KwaZulu-Natal. Having the flood susceptibility areas of SARVA (2010) based on a soil form distribution mean that cannot provide any form of risk quantification. The flood hazard map's risk delineation is based on the historical distribution and repeatability of regional storms which provides a more accurate spatial risk distribution which is quantifiable.

The WHO eAtlas (El Abidine El Morjani 2011) (Fig. 8.18) is an improvement on the SARVA (2010) map (Fig. 8.17) but still lacks detail due to the scale and only provides the risk relative to all South African rivers making it difficult to apply at municipal scale. The other concern is that only major rivers have been modeled and they generally have the same medium risk suggesting that all rivers in KwaZulu-Natal have the same flood risk, and by extension that the storms which produced them have the same spatial distribution. This has been shown not to be the case by the flood hazard map (Fig. 8.19). Using the extreme flood data compiled by van Bladeren (1992) show that eight major rivers in primary catchments T and U in southern KwaZulu-Natal (Fig. 3.4B) recorded extreme discharges, while 11 such events were recorded for northern KwaZulu-Natal in primary catchments V and W (Fig. 3.4B). With primary catchments T and U having a combined area of 32 558 km² and V and W having a combined area of 85 261 km² indicates that the smaller catchment area (T and U) produced more extreme floods per km² than that of the larger catchment (V and W). This indicates that not all the rivers in KwaZulu-Natal have the same risk. Interrogation of the flood hazard map (Fig. 8.19) shows that the flood hazard zones are not evenly distributed across KwaZulu-Natal and that zones that have been subjected to more storms have a greater risk to flooding.

CHAPTER 9 – CLIMATIC INFLUENCES ON FLOODING IN KWAZULU-NATAL

9. Introduction

Climate cycles tend to operate on a planetary scale (e.g. El Niño Southern Oscillation - ENSO) (van Oldenborgh & Burgers 2005; Luo et al. 2010) and it has been well documented that climate cycles affect local and regional weather systems by means of teleconnections (e.g. Preston-Whyte & Tyson 1997; van Oldenborgh & Burgers 2005; Philippon et al. 2011). This results in large variations in rainfall at decadal time scales and associated variations in discharge (Trenberth 2010; Carey et al. 2013). Variation in rainfall patterns have been attributed to a number of climate cycles (Trenberth 2010; Booth et al. 2013; Willems 2013), some have attributed changes in rainfall intensities to global warming (Henderson-Sellers et al. 1998; Alley et al. 2007; Trenberth 2010; Booth et al. 2013) and increased in extreme events (Cai et al. 2014; Wuebbles et al. 2014). The variation and periodicity of South African weather systems are affected by global atmospheric circulation (Preston-Whyte & Tyson 1997) and hence the temporal and spatial distribution of regional storm events (RSE) can be said to be similarly affected.

Climate cycles can generally be grouped together based on sea surface temperature measurements (Hansingo & Reason 2009) or atmospheric measurements (Viles & Goudie 2003; Rouault & Richard 2003). Climatic cycles based on sea surface temperature variations have been identified for the Atlantic, Pacific and Indian Oceans. These include the Indian Ocean Dipole (IOD), the Atlantic Multi-decadal Oscillation (AMO), the Pacific Decadal Oscillation (PDO) and the Inter-decadal Pacific Oscillation (IPO). Climate cycles based on atmospheric pressure variations because of sea surface temperature changes such as the Southern Oscillation Index (SOI), El Niño Southern Oscillation (ENSO) and the Antarctic Oscillation (AAO) have also been recognised. Other climate cycles have been related to sunspots (Keeling & Whorf 1997; Hathaway 2010) or the lunar cycle (Currie 1984; Yndestad 2006; Copeland & Watts 2011). In the South African context regional climatic cycles have also been identified

based on mean annual precipitation (MAP) (Dyer & Tyson 1977). This chapter briefly discusses the climatic cycles that affect the Republic of South Africa and compares them to regional storm event (RSE) and extreme storm event (ESE) (Table 8.1) temporal distributions in order to investigate the relationships between them.

9.1. Results

Two aspects of the data concerning regional storm events have been used in the comparison to climatic cycles namely, the annual regional storm event count and the estimated regional storm event discharges. Regional storm event discharges were estimated using the Rational Formula (as discussed in Chapter 2 and 7) as a basic measure for comparison purposes. Climate data and descriptions used for comparison with the regional storm events are all sourced from public domain datasets (Appendix VI). These datasets vary in record length depending on how the data is collected (satellite observation, physical measurements or proxy data).

The general regional storm event count (Fig 9.1) displays a periodicity over the years, with three peak periods at 1893, 1932 and 1963, with intervals of 39 and 31 years respectively. From 1964 – 1989, a period of alternating occurrences has occurred forming an apparent plateau. After 1989, there is a general downward trend in the regional storm event annual count. extreme storm events follow a similar trend to that of the regional storm event annual count but with shorter interval peaks at 1902, 1920, 1932, 1939, 1963 and 1984/1985 with intervals of 18, 12, 7, 23 and 21 years respectively. The major peaks occur at 1932, 1963 and 1984/1985 with intervals of 31, 23 and 21 years respectively.

The general regional storm event discharge trend (Fig 9.2) shows nine peaks at 1908, 1920, 1932, 1940, 1949, 1959, 1976, 1987 and 1996 with intervals of 12, 12, 8, 9, 18, 11 and 9 years respectively. The general trend for the extreme storm events show a very similar trend to that of the regional storm event discharge trend except for the regional storm event peak at 1949 and more pronounced dips at 1966.

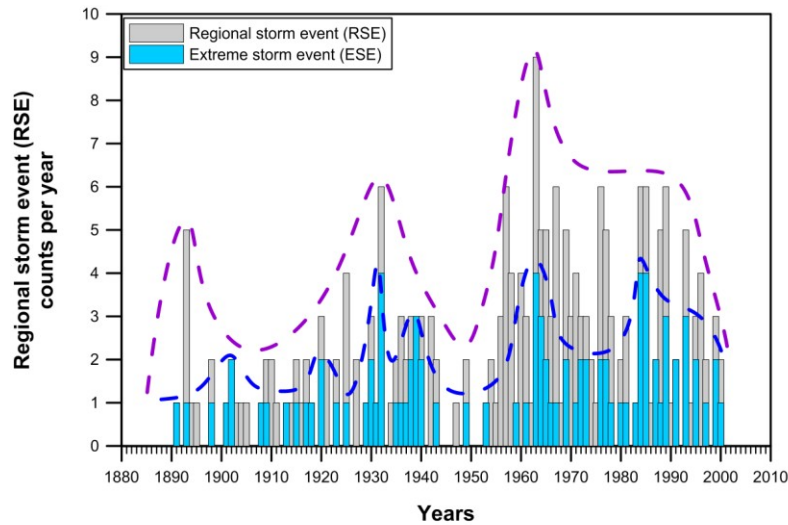


Figure 9.1. Annual regional storm event and extreme storm event count showing manually interpreted general trends. The regional storm events have peaks at 1893, 1932 and 1963. The extreme storm events have major peaks at 1932, 1963 and 1985 and minor peaks at 1902, 1920 and 1939. Purple dash line – manually interpreted general regional storm event count trend. Blue dashed line – manually interpreted general extreme storm event count trend.

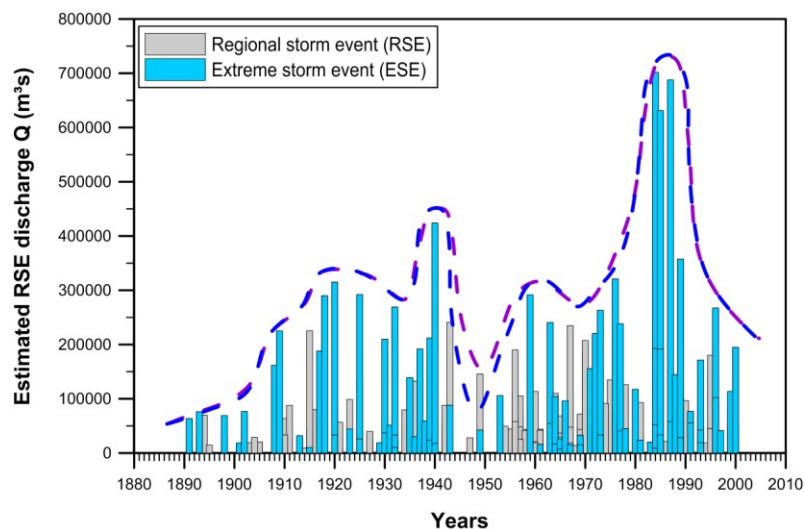


Figure 9.2. Annual regional storm event and extreme storm event manually interpreted discharge trends. Purple dash line – manually interpreted general regional storm event discharge trend. Blue dashed line – manually interpreted general extreme flood event discharge trend.

9.1.1. Mean annual precipitation and Wet/Dry Cycles

Comparing the mean annual precipitation with the regional storm event annual count shows some correlation where periods of higher mean annual precipitation values tend to coincide with periods of higher regional storm event counts (Fig 9.3). However, there does not appear to be any direct correlation between the magnitude of mean annual precipitation and the occurrences of regional storm events. For example, the 1942 mean annual precipitation value is larger than the 1963 mean annual precipitation value but three regional storm events occurred in 1942 while there were nine regional storm events in 1963. Positive correlations with the five-year running average mean annual precipitation only occur for the periods 1934 – 1961 and 1977 – 1992.

When comparing the extreme storm event years with the mean annual precipitation, a general correlation is apparent. However years with the highest mean annual precipitation do not coincide with years that have multiple extreme storm events. In the case of the five-year running average mean annual precipitation, only the 1963 and 1984/1987 periods have a positive correlation.

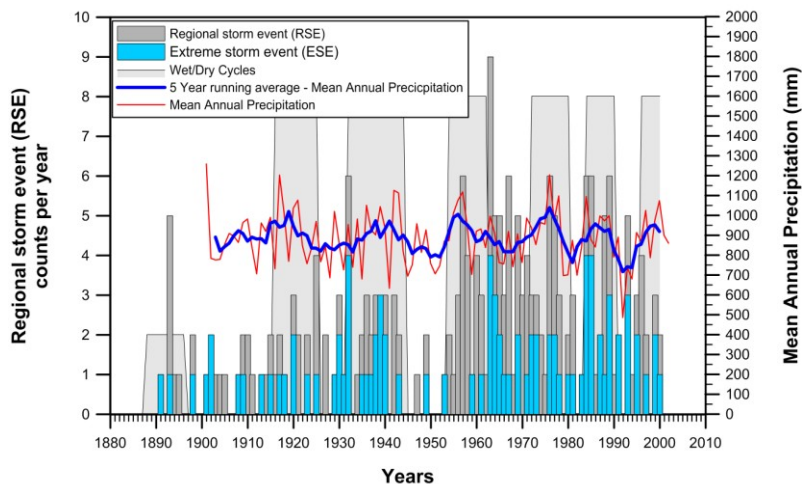


Figure 9.3. Annual regional storm event and extreme storm event count comparison to mean annual precipitation and Wet/Dry Cycles. Note that the mean annual precipitation and Wet/Dry Cycles have a good correlation. In general Wet Cycle periods have higher regional storm event occurrences than Dry Cycle periods.

(Dyer & Tyson 1977) recognised that there were decadal mean annual precipitation cycles, when the summer rainfall regions of Southern Africa were wetter and dryer. He attributed the wetter periods to the strengthening, and the dryer periods to the weakening, of the Tropical Easterly waves and Lows. Bredenkamp (2000) also identified wet and dry cycles using groundwater and lake levels that have similar periodicity as those of Dyer & Tyson (1977). Using proxy data Tyson et al. (2002) showed that the quasi – 18.6 year wet/dry cycle goes back at least 600 years. In Figure 9.3 the strong correlation between the five year running average mean annual precipitation and the Dyer & Tyson (1977) Wet and Dry Cycles can be seen. There is good correlation between the Wet/Dry Cycles and regional storm event/extreme storm event counts. Wet Cycles have higher regional storm event/extreme storm event counts, while Dry Cycles have fewer counts (Table 9.1). There are two anomalous periods (1897 - 1915 and 1963 – 1971) where the Dry Cycle regional storm event/extreme storm event counts are comparable to that of the Wet Cycles (Table 9.1). The anomalous regional storm event/local storm event (LSE) counts and distribution for the Wet/Dry cycles are shown in Figures 9.4 and 9.5 as maps of totalled regional storm events/local storm events per cycle period. Wet periods characterised by regional storm events exhibit a larger spatial distribution across the study area than the Dry cycles. Dry Cycle periods are characterised by relatively low counts and limited spatial distribution. The anomalous Dry cycles of 1897 – 1915 and 1963 – 1971 show all the characteristics of a wet cycle, having similar spatial distributions and higher regional storm event counts (Fig. 9.4). The 1963 – 1971 Dry Cycle period has the highest regional storm event count (42) for any of the Wet/Dry Cycles from 1891 – 2000. The local storm event counts show similar correlations to the Wet/Dry Cycles as the regional storm events counts (Fig. 9.5). The local storm events do not reflect the 1963 - 1971 anomaly but instead show an anomaly for the 1945 – 1953 Dry Cycle period (Fig. 9.5).

Table 9.1. Regional storm event (RSE) and extreme storm event (ESE) counts per Wet/Dry Cycles. The grey shading highlights the anomalous regional storm event/extreme storm event counts compared to other Dry Cycle periods.

Period	Wet/Dry Cycle	RSE count	ESE count
1887 - 1896	Neither	9	2
1897 - 1915	Dry	19	8
1916 - 1925	Wet	15	7
1926 - 1931	Dry	7	4
1932 - 1944	Wet	27	15
1945 - 1953	Dry	4	2
1954 - 1962	Wet	25	2
1963 - 1971	Dry	42	14
1972 - 1980	Wet	24	10
1981 - 1983	Dry	4	2
1984 - 1990	Wet	27	14
1991 - 1995	Dry	11	5
1996 - 2000 +	Wet	11	6

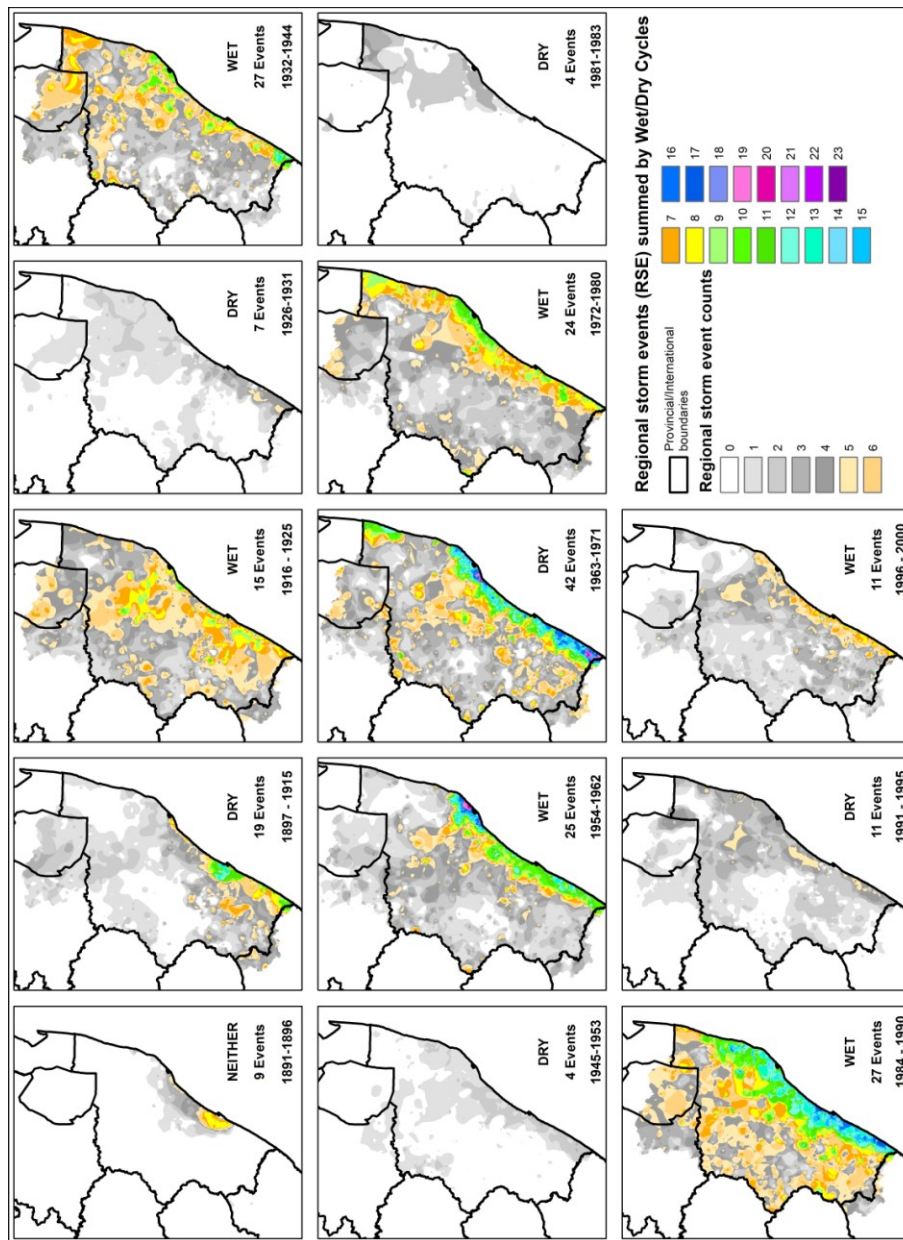


Figure 9.4. Maps showing totalled regional storm events (RSE) per Wet and Dry Cycle periods. Wet Cycles periods have increased counts of regional storm events and larger distributions while Dry Cycle periods have reduced regional storm event counts and generally smaller distributions. The 1897 – 1915 and 1963 – 1971 Dry Cycle periods have anomalous counts and distributions that resemble Wet Cycle periods.

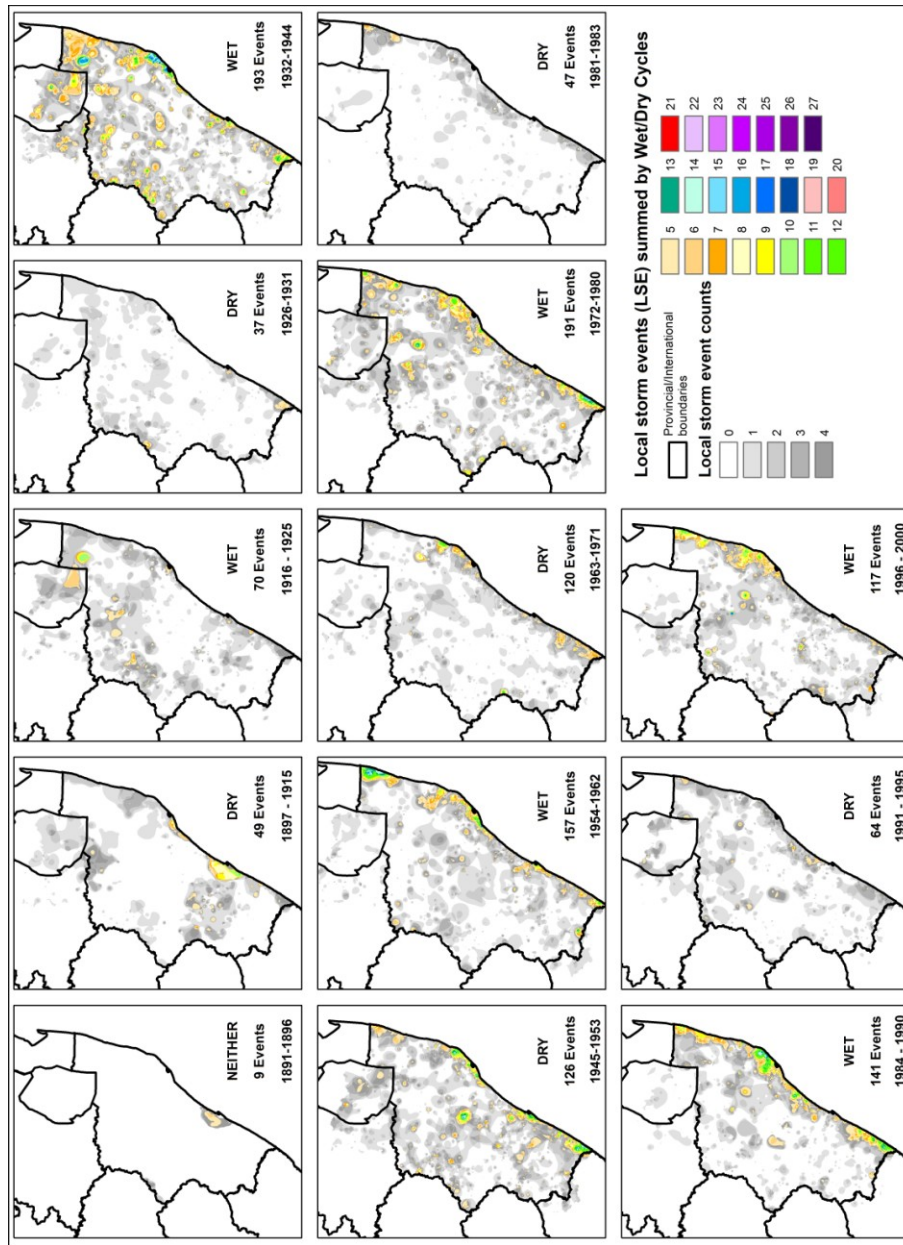


Figure 9.5. Maps showing totalled local storm events (LSEs) for the Wet and Dry cycles. Wet cycle periods have increased counts of local storm events and larger distributions. Dry Cycle periods have fewer local storm event counts and smaller distribution patterns. The 1945 – 1953 Dry Cycles period has anomalous local storm event counts and a spatial distribution similar to a Wet Cycle period.

Examination of regional storm event discharges and the mean annual precipitation (Fig 9.6) show that in general, larger discharges occurred in years with elevated mean annual precipitation but there is no correlation between mean annual precipitation and absolute estimated discharge magnitude. The five-year running average mean annual precipitation has a good correlation with the regional storm event estimated discharges. Extreme storm events show similar correlations for mean annual precipitation and the five-year running average mean annual precipitation as that of the estimated regional storm event discharges.

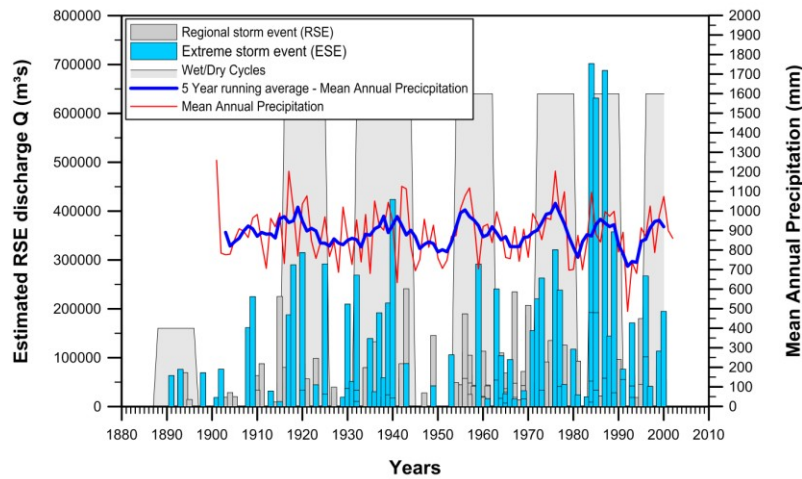


Figure 9.6. Annual regional storm event and extreme storm event estimated discharge comparison to mean annual precipitation and Wet/Dry Cycles. Note that generally larger regional storm event discharges occur in years with elevated mean annual precipitation but there is no correlation between discharge magnitude and mean annual precipitation or Wet/Dry Cycles.

9.1.2. Solar and lunar influences

Sunspots are the result of intense magnetic activity on the sun's surface (Elsner & Jagger 2008), with a positive correlation between the number of sunspots and solar radiation (Hathaway 2010). The increase and decrease of sunspot activity follows an approximate 11 year cycle (Schwabe Cycle) (Herman & Goldberg 1978; Hathaway 2010). The Schwabe cycle is half of the 22 year Hale cycle which results from the sun regularly switching magnetic polarity every 11 years (Herman & Goldberg 1978).

Sunspot and rainfall correlation appears varied with a good correlation at the equator, but elsewhere there may be a weak or non-existent correlation (Herman & Goldberg 1978). Correlations can vary seasonally, for example Clayton (1932) found that Cape Town had a positive correlation in winter but a negative correlation in summer. In general there is more rainfall in years with maximum sunspot activity particularly along the equatorial belt and latitudes below 40° and less so between latitudes 20 – 40° (Herman & Goldberg 1978). Similar variations are noted for temperature and weather pressure systems (Herman & Goldberg 1978). There is an indication that sunspot activity may affect storm tracks and that during sunspot maximum years, cyclone tracks shift towards the equator (Herman & Goldberg 1978). In some cases rainfall data correlated better with the 22 year Hale Cycle, especially drought periods in the northern hemisphere (Herman & Goldberg 1978).

There is evidence of the waxing and waning output of solar energy having an effect on global climate change over millennial cycles. A recent example is the Maunder Minimum (1645 – 1715) during the Little Ice Age, where sunspot development was virtually zero (Hathaway 2010). Although some researchers indicate that there is not enough evidence of sunspot influence on weather (Preston-Whyte & Tyson 1997), there have been links established for hurricanes (Elsner & Jagger 2008). In the RSA, Alexander (2007) showed that the Vaal River discharge is linked to the 11 year Schwabe cycle. Using selected South African rivers Alexander (2007) showed that there was a correlation between sunspot numbers and increased discharge. With regards lunar influences, as the moon orbits the earth in a lunar month (29.53 days), it also has a precessional wobble that lasts 18.6 years where the axis tilt (declination) varies between 18.3° and 28.6° (Shaw & Tsimplis 2010). Termed the Lunar Nodal Cycle (LNC), this perturbation controls the 18.6 year tidal cycle (Mazumder & Arima 2005; Gratiot et al. 2008; Eliot, Matt, Pattiaratchi 2009; Shaw & Tsimplis 2010).

According to Bell (1981), Keeling & Whorf (1997) and Keeling & Whorf (2000), the effects of the Lunar Nodal Cycle periodicity on sea surface temperatures influences climate cycles. This occurs when the lunar influence on tides is strong, resulting in the mixing of warm surface water with colder deeper water (Bell 1981; Keeling & Whorf 1997; Keeling & Whorf 2000) cyclically altering the sea surface temperature. Most recognised climatic cycles such as the El Niño Southern Oscillation, the Southern Oscillation Index and the Pacific Decadal Oscillation are linked to changes in the sea surface temperature, suggesting a Lunar Nodal Cycle forcing of climate (Ray 2007). The periodicity for the Wet and Dry

cycles discussed previously is on average about 18 years which is similar to the Lunar Nodal Cycle of 18.6 years (Tyson 1986; Malherbe et al. 2014).

9.1.2.1. Sunspot, lunar nodal cycles and regional storm events correlation

Correlation between the Lunar Nodal Cycle and the Wet/Dry Cycles (Dyer & Tyson 1977) are varied (Fig 9.7). From 1890 – 1913 and 1983 – 2000 the Lunar Nodal Cycle and Wet/Dry cycles are out of phase. The correlation between the Lunar Nodal Cycle and regional storm event count is poor and only coincides from 1932 – 1963 and 1972 – 1981. Comparing the sunspot activity shows no correlation to the regional storm event count (Fig 9.8) but there does appear to be a general correlation with an increase in both regional storm event and sunspots from about 1890 – 1959 and decreasing 1959 – 2000. There is no obvious correlation between the Lunar Nodal Cycle and extreme storm event counts.

Comparison between the Lunar Nodal Cycle and the estimated discharges of the regional storm event and extreme storm event generally shows a good correlation, except for the period 1983 – 1990 where the two are in opposition (Fig 9.8). For the period 1890 – 1910 the correlation is also unclear. There is no apparent correlation between the sunspot cycle and the extreme storm event discharges.

9.1.3. Global temperatures

The variations in Southern hemispheric global temperature and sea surface temperature show a similar trend, with a cooling phase prior to 1880 – 1909 and a warming trend from 1909 – 1943 (Fig 9.9). A short cooling trend occurred from 1943 – 1949 followed by a warming trend to the present. The Keeling Curve (Atmospheric CO₂) shows a constant increase from 1959 - 2000 which is the same trend for temperature for the same period (Fig 9.9).

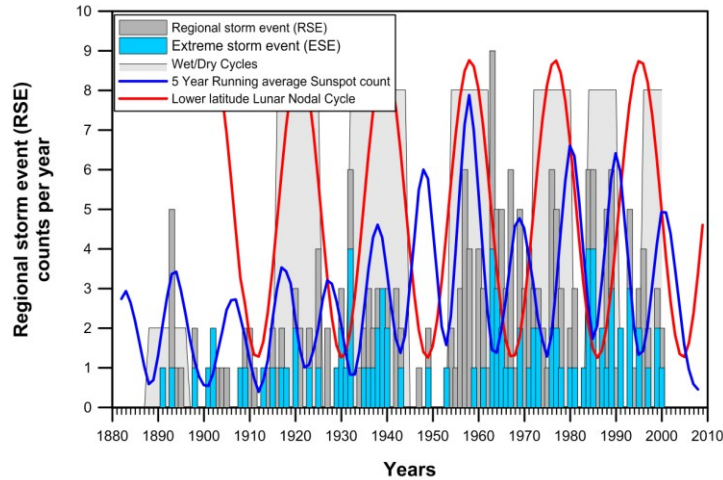


Figure 9.7. Annual regional storm event and extreme storm event count comparison to Sunspot count and the Lunar Nodal Cycle. Note the general correlation between Wet/Dry Cycles and the Lunar Nodal Cycle. There is a poor correlation between regional storm event/extreme storm event counts and the sunspot counts.

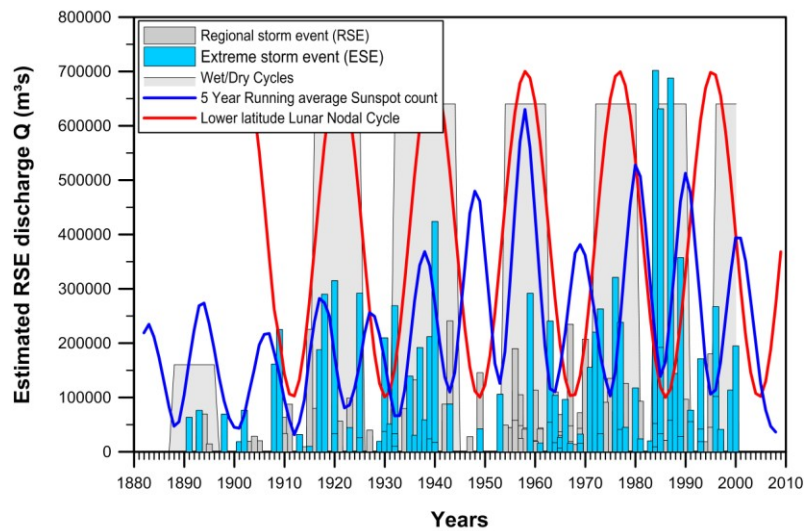


Figure 9.8. Annual regional storm event and extreme storm event estimated discharge comparison to Sunspot count and the Lunar Nodal Cycle. Note that there is no correlation between the Lunar Nodal Cycle and Sunspot counts and the regional storm event/extreme storm event counts.

There is weak correlation between regional storm event and extreme storm event counts and global temperatures (Fig 9.9). Three cooling periods around 1893, 1909 and 1963 – 1966 show increased occurrences of regional storm events, whereas the 1943 – 1949 cooling period recorded only a single regional storm event. The warming period from 1909 – 1932 showed a general increase in regional storm events, but this trend is not repeated in the warming period from 1949 – the present where the highest regional storm event counts remained fairly constant and started decreasing with increasing temperature since the early 1990s. There appears to be no correlation between atmospheric CO₂ and the number of regional storm events experienced.

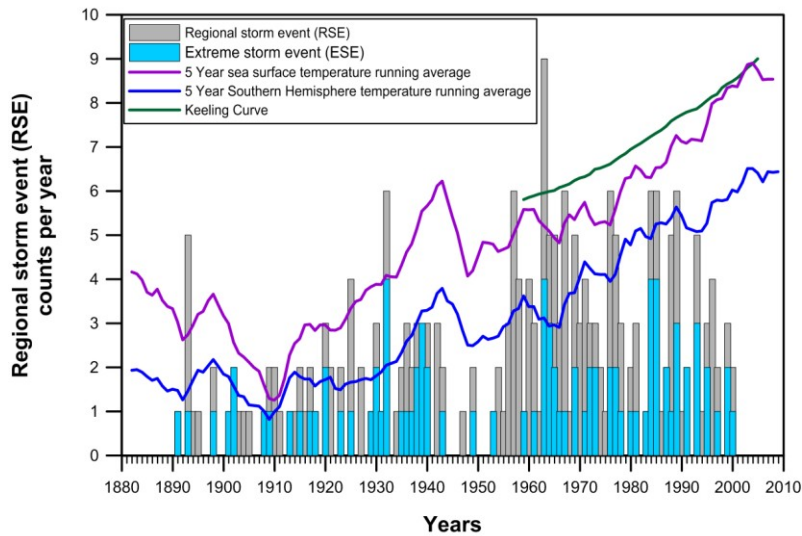


Figure 9.9. A comparison between annual regional storm event and extreme storm event counts comparison and atmospheric CO₂, Southern hemispheric global temperature and sea surface temperatures. Note the weak correlation between regional storm event/extreme storm event counts and Southern hemispheric global and sea surface temperature from 1890 – 1950. After 1950 there are no correlations.

There is a general correlation between global temperatures, sea surface temperature and regional storm event and extreme storm event discharges from 1911 – 1987 (Fig 9.10). From 1987 – 2000 there is no correlation. The correlation for the period from 1890 – 1910 is inconclusive. There is no correlation between atmospheric CO₂ and regional storm event discharges.

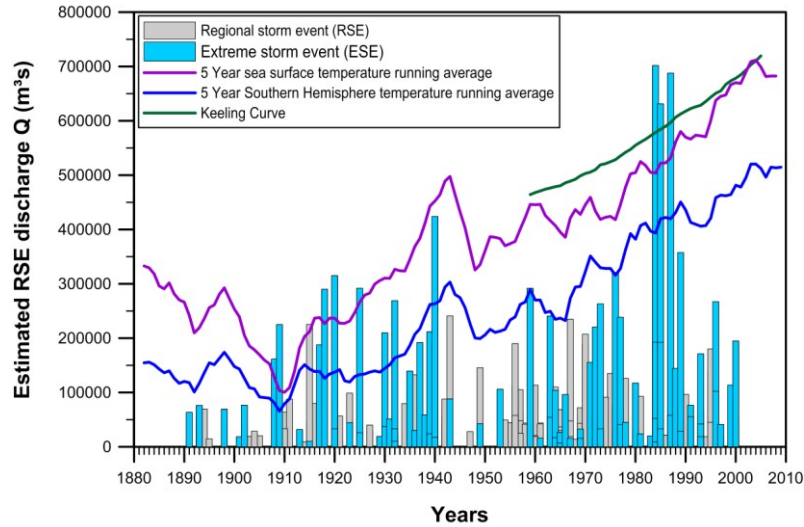


Figure 9.10. Annual regional storm event and extreme storm event estimated discharge comparison with atmospheric CO₂, Southern Hemisphere and sea surface temperatures. There is a general correlation from 1911 – 1987, after which there is no correlation.

9.1.4. Indian Ocean Dipole

The Indian Ocean Dipole (IOD) is restricted to the Indian Ocean where warmer sea surface temperatures along the western Indian Ocean lead to higher than average rainfall conditions over western Australia, East Africa, India and Indonesia (Ashok et al. 2003; Ummenhofer et al. 2009). Cooler sea surface temperatures occur along the eastern Indian Ocean. When the Indian Ocean Dipole reverses with cooler sea surface temperatures in the western Indian Ocean, it leads to below average rainfall in the areas previously noted (Ummenhofer et al. 2009). According to Rouault et al. (2010) there appears to be no correlation with the Indian Ocean Dipole to Southern African rainfall. There is no identifiable correlation between the regional storm event annual and extreme storm event counts with the Indian Ocean Dipole (Fig 9.11) or the associated estimated discharges (Fig 9.12).

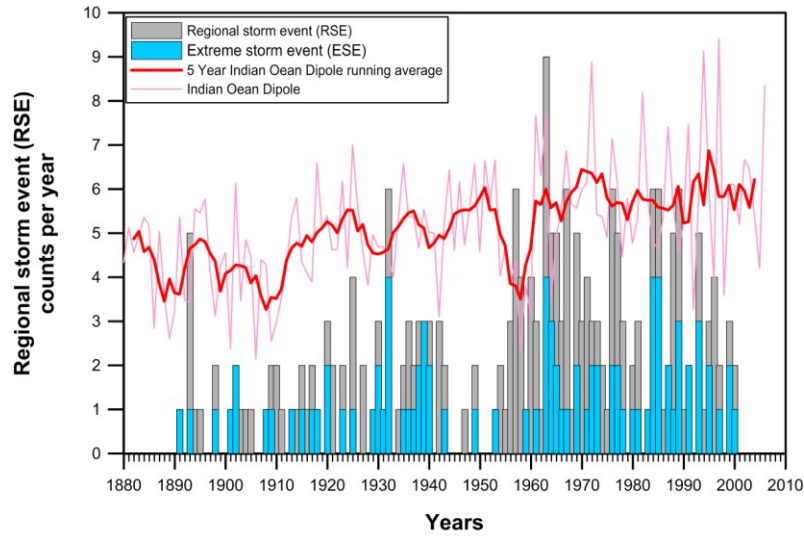


Figure 9.11. Annual regional storm event and extreme storm event annual counts comparison with the Indian Ocean Dipole. Note that there is no correlation.

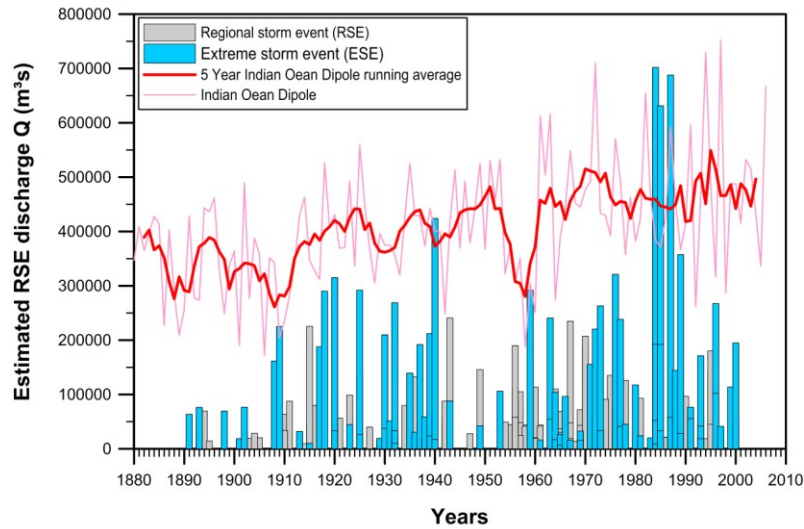


Figure 9.12. Annual regional storm event and extreme storm event discharges comparison with the Indian Ocean Dipole. Note that there is no correlation.

9.1.5. Atlantic Multi-decadal Oscillation

The Atlantic multi-decadal oscillation (AMO) is a cycle of sea surface temperature variance spanning approximately 65 - 70 years (Schlesinger & Ramankutty 1994; Enfield et al. 2001). It is associated with droughts and above average rainfall in the northern hemisphere (Sutton & Hodson 2005). The Atlantic Multi-decadal Oscillation only has an effect on North Africa (Sutton & Hodson 2005) and has little or no bearing on Southern African climate. There is no correlation between the regional storm event annual and extreme storm event counts with the Atlantic Multi-decadal Oscillation (Fig 9.13) or the associated estimated discharges (Fig 9.14).

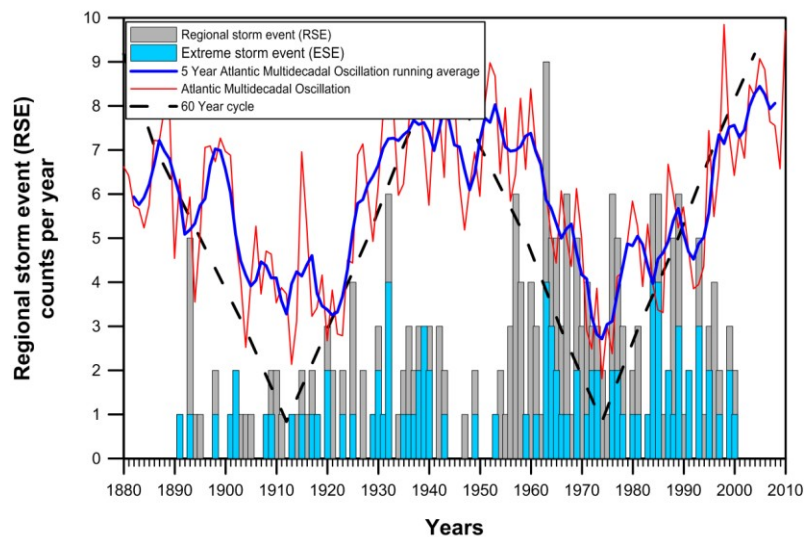


Figure 9.13. Annual regional storm event and extreme storm event annual counts comparison with the Atlantic Multi-decadal Oscillation. Note that there is no correlation.

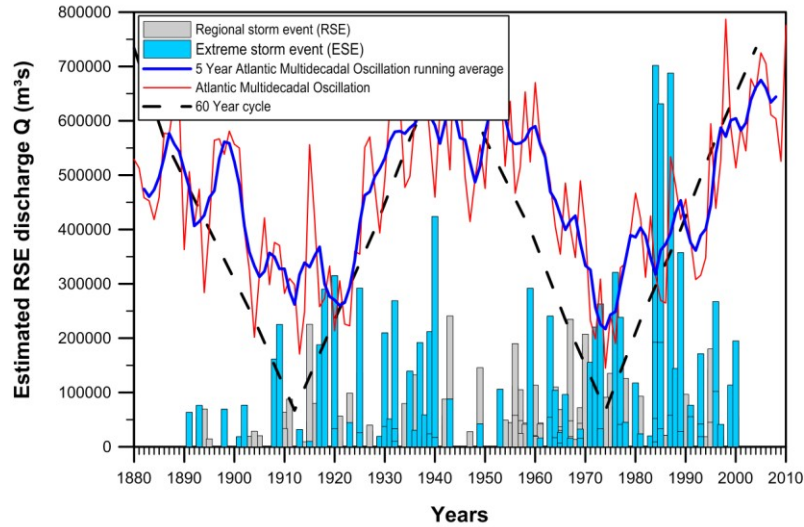


Figure 9.14. Annual regional storm event and extreme storm event discharge comparison with the Atlantic Multi-decadal Oscillation. Note that there is no correlation.

9.1.6. Pacific Decadal Oscillation

The Pacific Decadal Oscillation (PDO) has a major variable cycle of 15 - 25 years and 50 – 70 years (Mantua & Hare 2002). However, Shen et al. (2006) reconstructed the Pacific Decadal Oscillation cycle from 530 years of Chinese rainfall data and identified 11 - 12 year, 23 - 28 year, 35 - 45 year, 50 - 70 year and 75 - 115 year cycles. The Pacific Decadal Oscillation is identified by warmer and cooler sea surface temperatures in the eastern and western Pacific Ocean in a cycle similar to El Niño Southern Oscillation (Alexander & Bladé 2002; Newman et al. 2003). While the El Niño Southern Oscillation cycle variability is on an inter-annual scale, the Pacific Decadal Oscillation variability is on a multi-decadal scale. It is argued that El Niño Southern Oscillation and tropical forcing are responsible for the multi-dynamic origins of the Pacific Decadal Oscillation (Alexander & Bladé 2002; Newman et al. 2003; Schneider & Cornuelle 2005).

The Pacific Decadal Oscillation has an effect on climate variability around the planet (Newman et al. 2003). One result of the eastern Pacific warming is an increase in warming of the western Indian Ocean in

summer (Newman et al. 2003) which leads to more evaporation and moister air that can be transported by easterly wave weather systems over southern Africa. A positive Pacific Decadal Oscillation has been linked to increased precipitation in eastern Australia (Franks 2002; Mantua & Hare 2002), southern Africa, eastern Asia, northern South America and North America (Mantua & Hare 2002; Fauchereau et al. 2003; Dai 2012). There are no obvious correlations between the Pacific Decadal Oscillation and the regional storm event and extreme storm event annual counts (Fig 9.15). The regional storm event discharges and Pacific Decadal Oscillation show a very strong correlation from 1924 – 2000 (Fig 9.16). From 1900 - 1923 the correlation appears to have an inverse relationship. The extreme storm event discharges show a similar correlation to that of the regional storm event discharges.

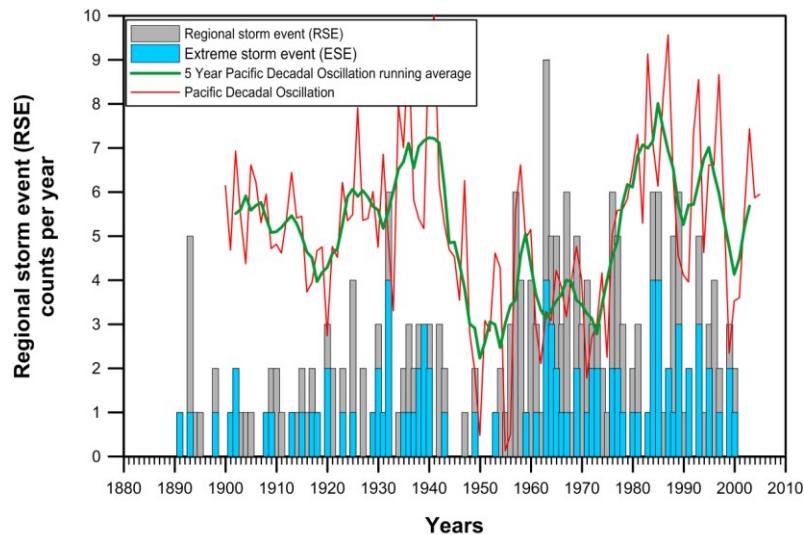


Figure 9.15. Annual regional storm event and extreme storm event annual counts comparison with the Pacific Decadal Oscillation. Note that there is no correlation.

9.1.7. Inter-decadal Pacific Oscillation

The Inter-decadal Pacific Oscillation (IPO) is a multi-decadal record of sea surface temperature changes similar to that of the Pacific Decadal Oscillation (Mantua & Hare 2002; Salinger et al. 2001; Folland & J. Renwick 2002; Folland 2008). While the Pacific Decadal Oscillation is a measure of sea surface temperature variation between the eastern and western Pacific Ocean, the Inter-decadal Pacific Oscillation is a measure of sea surface temperature across the whole Pacific Ocean between 55° N and 55° S (Folland 2008). The Pacific Decadal Oscillation and Inter-decadal Pacific Oscillation follow a similar cyclic trend, but the Inter-decadal Pacific Oscillation has broader, smoother periods similar to an average of the Pacific Decadal Oscillation variability.

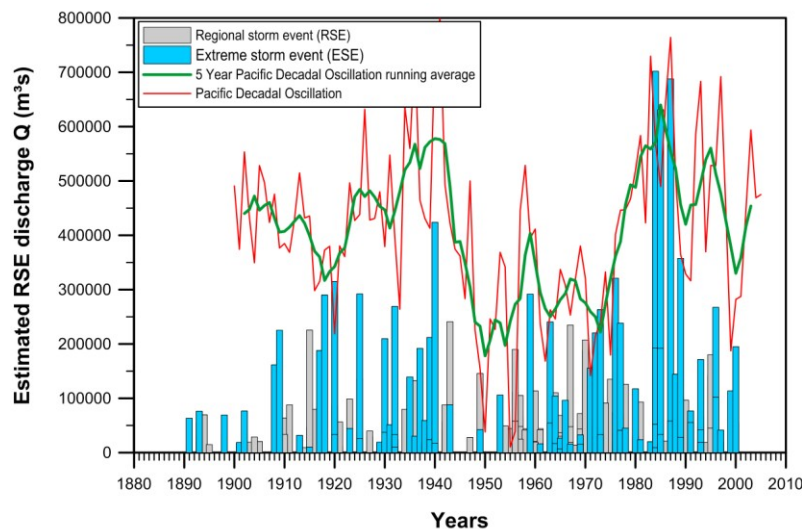


Figure 9.16. Annual regional storm event and extreme storm event discharge comparison with the Pacific Decadal Oscillation. The regional storm event/extreme storm event discharges and Pacific Decadal Oscillation show a very strong correlation from 1924 – 2000 with the 1900 – 1923 periods having a inverse relationship.

The Inter-decadal Pacific Oscillation shows a similar correlation to regional storm event/extreme storm event annual counts and discharges as the Pacific Decadal Oscillation, with no correlation between the Inter-decadal Pacific Oscillation and regional storm event/extreme storm event annual counts (Fig. 9.17). However, there is a strong correlation between the regional storm event/extreme storm event discharges

(Fig. 9.18). From 1940 – the present, there is a positive correlation between the Inter-decadal Pacific Oscillation and regional storm event/extreme storm event discharges. For the period 1891 – 1940, the correlation is inverse or inconclusive.

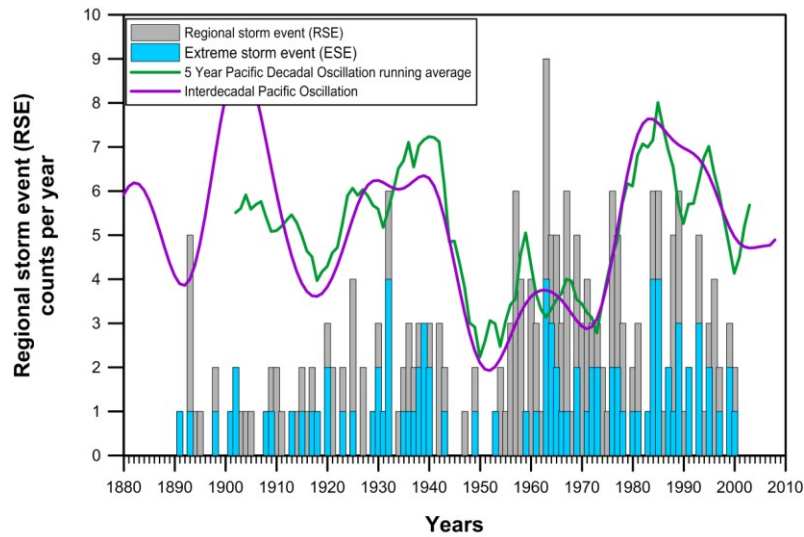


Figure 9.17. Annual regional storm event and extreme storm event counts comparison with the Pacific Decadal (PDO) and Inter-decadal Pacific Oscillation (IPO). Note that there is no correlation between the Inter-decadal Pacific Oscillation and regional storm event/extreme storm event counts.

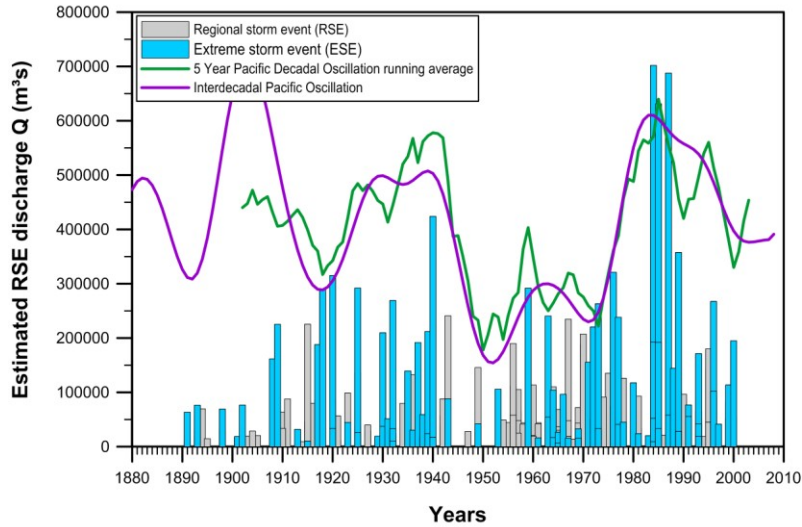


Figure 9.18. Annual regional storm event and extreme storm event discharge comparison with the Pacific Decadal (PDO) and Inter-decadal Pacific Oscillation (IPO). From 1940 – 2000 there is a strong correlation between the Inter-decadal Pacific Oscillation and regional storm event/extreme storm event discharges. From 1891 – 1940 the correlation is inconclusive or inverse correlative.

9.1.8. Southern Oscillation Index

The Southern Oscillation Index (SOI) is a measure of the pressure difference between Tahiti (in the eastern Pacific Ocean) and Darwin (in the western Pacific Ocean) (Können et al. 1998). The Southern Oscillation Index is the driver of the Walker Circulation and El Niño Southern Oscillation. As indicated by Preston-Whyte & Tyson (1997), mean annual precipitation and the Southern Oscillation Index show good correlation between 1900 – 1928 and in the period after 1948 – 2000. The period from 1928 – 1947 has a negative correlation. The correlation between the Southern Oscillation Index and the regional storm event annual count is weak (Fig 9.19). The previously identified anomalies (see section 9.1; Fig. 9.4) with mean annual precipitation and the wet/dry cycles (1897 – 1915, 1963 – 1971) are also present. The Southern Oscillation Index correlates with regional storm event discharge from 1890 – 1925, followed by an inverse correlation from 1925 – 1951 (Fig 9.20). From 1952 – 2000 the correlation is again positive.

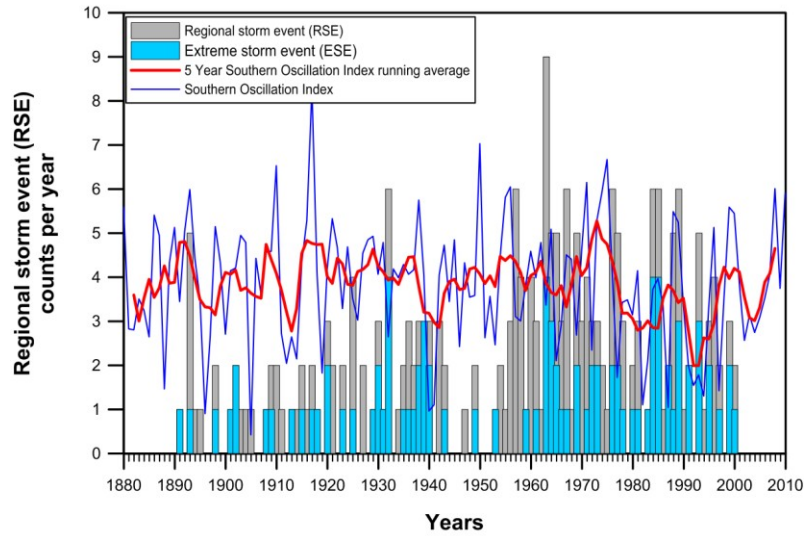


Figure 9.19. Annual regional storm event and extreme storm event counts comparison with the Southern Oscillation Index (SOI). There is a weak correlation between the Southern Oscillation Index and the regional storm event/extreme storm event counts.

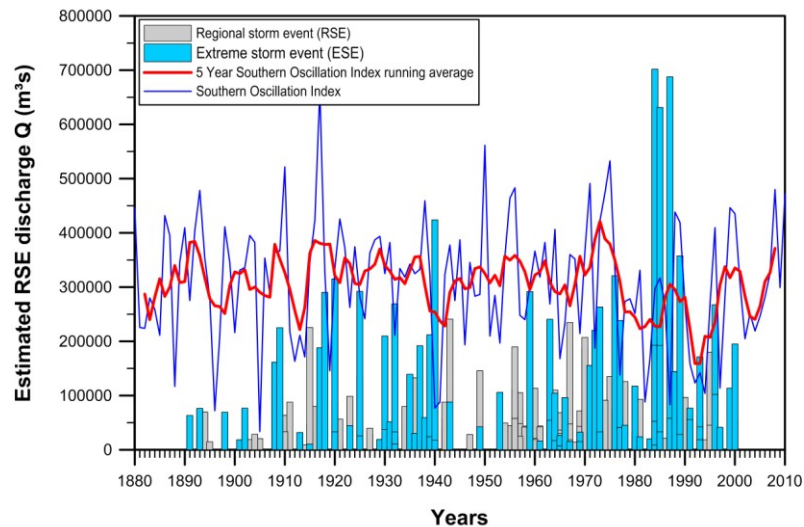


Figure 9.20. Annual regional storm event and extreme storm event discharge comparison with the Southern Oscillation Index (SOI). There is a general positive correlation between the Southern Oscillation Index and regional storm event/extreme storm event discharges during the periods of 1890 – 1925 and 1952 – 2000 with an inverse correlation for 1925 – 1951.

9.1.9. El Niño Southern Oscillation

The Southern Oscillation Index forms an integral part of the El Niño Southern Oscillation (ENSO) cycle. El Niño Southern Oscillation (Choudhury 1994; Andrews et al. 2004; van Oldenborgh & Burgers 2005; Klinman & Reason 2008; Philippon et al. 2011) is effectively the atmospheric response to the Southern Oscillation Index changing the Walker Circulation atmospheric cells (Lau & Yang 2002). The El Niño phase of the El Niño Southern Oscillation cycle represents the total reversal of the Walker Circulation to the negative phase (Preston-Whyte & Tyson 1997). The La Niña component of the El Niño Southern Oscillation cycle represents the positive phase of the Southern Oscillation Index producing the opposite effect to El Niño. A neutral phase of the El Niño Southern Oscillation cycle is when it changes phase from La Niña to El Niño or *vice versa*. The El Niño Southern Oscillation cycle can be complex with all three phases occurring in a single year. There is a second type of El Niño Southern Oscillation cycle called Modoki which occurs when there is warmer water in the central Pacific ocean but colder water in the western and eastern Pacific Ocean (Wang et al. 2012). As the El Niño Southern Oscillation and El Niño Southern Oscillation Modoki have similar trends (Figs. 9.21 and 9.22) only the El Niño Southern Oscillation cycle is discussed.

There is a varied correlation between the regional storm event/extreme storm event annual count and the El Niño Southern Oscillation (Fig 9.21). In general higher regional storm event/extreme storm event annual counts occur during periods when the El Niño Southern Oscillation cycle is in the La Niña or in neutral phase, changing to the La Niña phase. When the El Niño Southern Oscillation cycle is tending towards, or in the El Niño phase there are generally fewer regional storm event/extreme storm event annual counts. There is generally a negative correlation between regional storm event/extreme storm event annual counts and the La Niña/neutral phases for the periods 1894 – 1907, 1912 – 1915, 1927 – 1934, 1940 – 1945, 1972 – 1979 and 1992 – 2000 (total of 49 years). The correlation is generally positive for the periods 1891 – 1893, 1908 – 1911, 1916 – 1926, 1935 – 1939, 1946 – 1971 and 1980 – 1991 (total of 61 years).

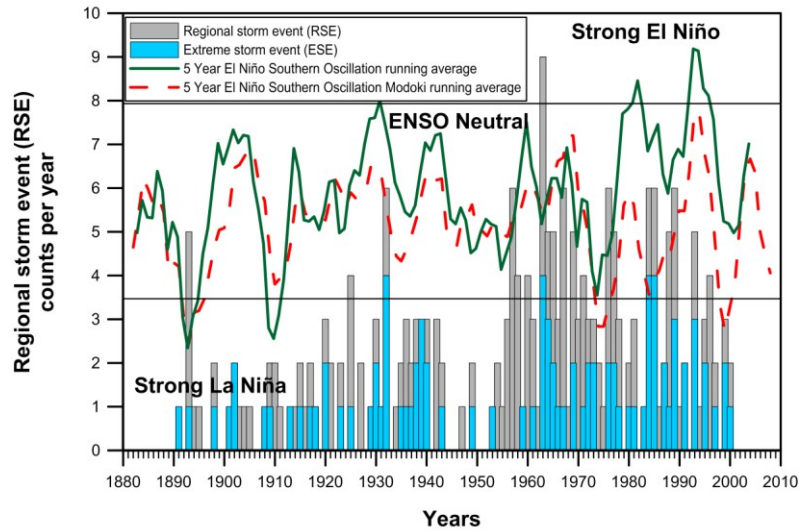


Figure 9.21. Annual regional storm event and extreme storm event annual counts comparison with the El Niño Southern Oscillation (ENSO) and ENSO Modoki. There is a varied correlation between the El Niño Southern Oscillation and the regional storm event/extreme storm event counts. Higher regional storm event/extreme storm event counts generally occur during the La Niña and the El Niño Southern Oscillation neutral phases.

Correlation between regional storm event/extreme storm event discharges and the El Niño Southern Oscillation cycles also varies (Fig. 9.22). There is generally a negative correlation between regional storm event/extreme storm event discharges and the La Niña/neutral phases for the period 1920 – 1969 (total of 50 years). There is generally a positive correlation between regional storm event/extreme storm event discharges and the La Niña/neutral phases for the periods 1891 – 1919 and 1970 – 2000 (total of 60 years). The magnitudes of the regional storm event/extreme storm event discharges show no correlation to the El Niño Southern Oscillation cycle peaks.

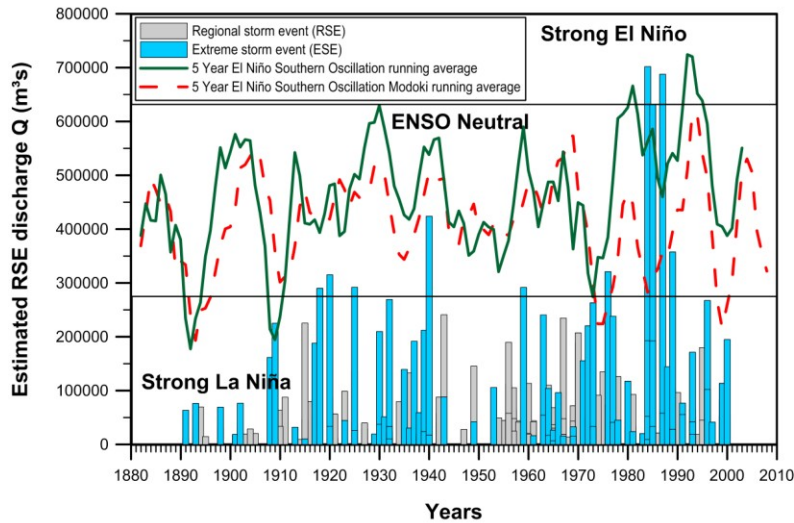


Figure 9.22. Annual regional storm event and extreme storm event discharge comparison with the El Niño Southern Oscillation (ENSO) and ENSO Modoki.
There is a varied correlation between the El Niño Southern Oscillation and regional storm event/extreme storm event discharges. In general there is marginally a positive correlation with the La Niña/El Niño Southern Oscillation neutral phases. There is no correlation between El Niño Southern Oscillation and discharge magnitude.

9.1.10. Antarctic Oscillation

Around the poles, below 20° south and north, there are zones of dominant tropospheric non-seasonal circulation (Reason & Rouault 2005). In the Antarctic this zone is called the Antarctic Oscillation (AAO) or Southern Annular Mode (Malherbe et al. 2014). This circulation is strongest in winter and takes the form of an annular ring between latitudes 20 – 45° (Thompson & Wallace 2000). This cycle has no reported effect on the south-eastern RSA but does have some influence over the winter rainfall of the south-western region of the RSA (Reason & Rouault 2005). According to Rouault et al. (2010) the Antarctic Oscillation has negligible influence on sea surface temperature along the south-east coast of the RSA. According to Malherbe et al. (2014), a positive Antarctic Oscillation driven by the Lunar Nodal Cycle results in increased summer rainfall over north-eastern Southern Africa. As can be seen from Figure 9.23 and Figure 9.24 there is no correlation between the Antarctic Oscillation and regional storm event count and discharge. The Antarctic Oscillation trends are instead similar to the sea surface temperature and Global temperature (Fig. 9.9 and Fig. 9.10).

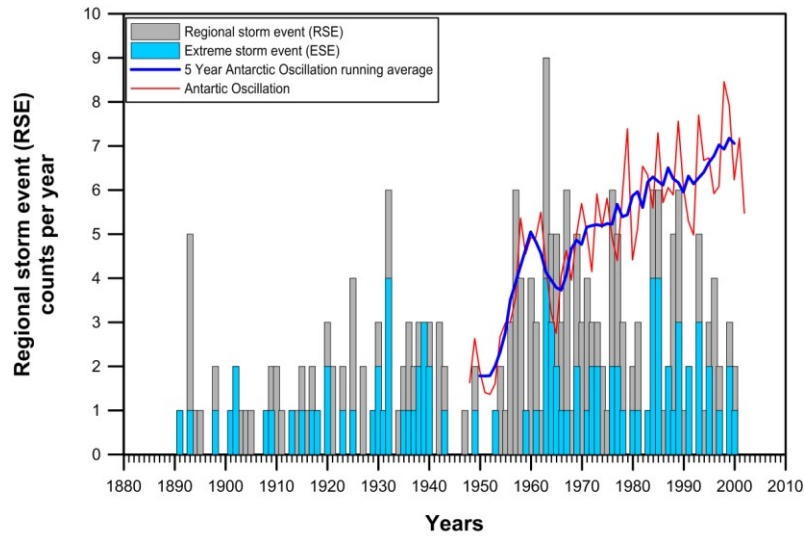


Figure 9.23. Annual regional storm event and extreme storm event counts comparison with the Antarctic Oscillation (AAO). Note that there is no correlation.

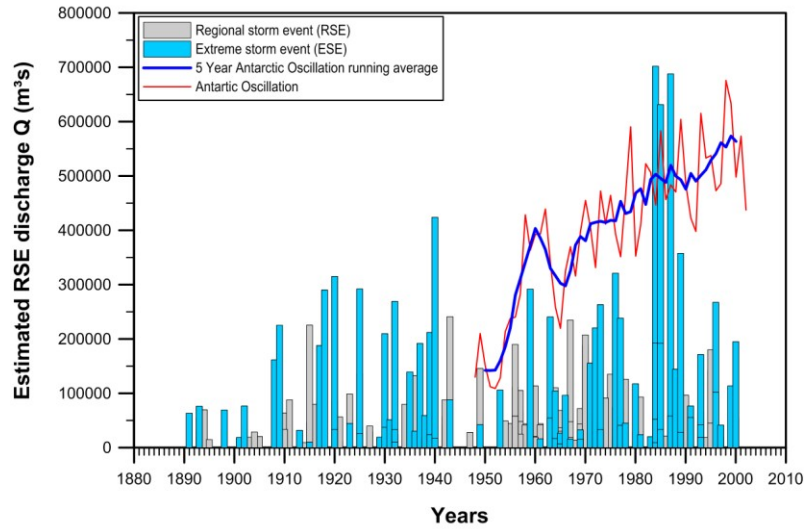


Figure 9.24. Annual regional storm event and extreme storm event discharge comparison with the Antarctic Oscillation (AAO). Note that there is no correlation.

9.2. Discussion

Examination of the temporal distribution of regional storm events indicates two factors that have to be accounted for namely, what controls the number of regional storm event events in a year and what controls the discharge magnitude for the regional storm events. As expected the correlation between mean annual precipitation (wet cycles) and the regional storm event count are generally positive with the result that wetter periods are more likely to produce a greater number of regional storm events (wet cycle = 62%, dry cycles = 38%). However, the dry cycle periods from 1897 – 1915, 1963 – 1971 and 1992 – 1995 which show higher regional storm event counts than other dry cycle periods (Fig. 9.4), indicate that mean annual precipitation is not the only climatic factor influencing regional storm event occurrences.

The gravitational effect of the moon on the earth's atmosphere and oceans by the Lunar Nodal Cycle have been recognised by a number of researchers (e.g. Tyson 1986; Yndestad 2006; Yasuda 2009; Malherbe et al. 2014). Currie (1984) linked the Lunar Nodal Cycle with the wet and dry rainfall cycles, Yasuda (2009) detected the 18.6 years Lunar Nodal Cycle's influence on the Pacific Decadal Oscillation and Malherbe et al. (2014) found that it influenced the Antarctic Oscillation. The Lunar Nodal Cycle influence has also been related to coastal erosion (e.g. Gratiot et al. 2008; Smith et al. 2010) and tidal sedimentary deposits (e.g. Ray 2007; Mazumder & Arima 2005). While the influence of the Lunar Nodal Cycle on climatic cycles are well documented there appears to be limited correlations with the regional storm events and extreme storm events. There is a correlation between the Lunar Nodal Cycle and Wet/Dry Cycles up to 1985, thereafter they occur out of phase. This indicates that the Wet/Dry Cycles may not necessarily only be affected by the Lunar Nodal Cycle. Cook et al. (2004) suggests that wet cycles may not necessarily consist of wetter periods but rather longer intense periods of wetness.

Sunspot cycles, global temperatures, sea surface temperature and atmospheric CO₂ appear to have no impact on the number of regional storm event annual counts or discharges. Comparison of climate cycles show that neither the Indian Ocean Dipole, Atlantic Multi-decadal Oscillation, El Niño Southern Oscillation, Antarctic Oscillation nor Pacific Decadal Oscillation have any correlation with the regional storm events annual count. The best correlation between the annual occurrences of regional storm events is with the Southern Oscillation Index. Apart from an anomalous period around 1940, the mean annual precipitation, wet/dry cycles, and the Southern Oscillation Index have a positive correlation. The

anomalous periods identified from the mean annual precipitation and wet/dry cycles 1963 – 1971 and 1992 – 1995 are also present in the Southern Oscillation Index but not the 1897 – 1915 anomaly. From the available data the most likely driver of the amount of the regional storm events is the teleconnection from the Southern Oscillation Index when sea surface temperature increases in the Pacific Ocean causing a shift in the Walker Circulation to positive as noted by Preston-Whyte & Tyson (1997).

While correlation with El Niño Southern Oscillation is not conclusive as the driver for regional storm event discharge magnitude, the correlation for regional storm event discharges and the Pacific Decadal Oscillation cycle is very good. In Chapter 3, Table 3.1 it was shown that the easterly wave systems dominate the summer rainfall (December – March) coinciding with the highest regional storm event count (Chapter 8). The easterly waves transport moist air from the south west Indian Ocean over the land and when sea surface temperatures increase over the south west Indian Ocean, these waves transport moister air resulting in wetter years (Washington & Preston 2006).

The decadal fluctuations of the Pacific Decadal Oscillation warming the south west Indian Ocean (Alexander & Bladé 2002) (Fig. 9.25) can account for the correlation of wet/dry cycles as a function of wetter and dryer years and the magnitude of regional storm event and extreme flood event discharges. An investigation of two periods which resulted in high magnitude regional storm event discharges during 1974 - 1976 (Washington & Preston 2006) and 1995 - 1996 (Rautenbach 1998) attribute these anomalous wet periods to increased sea surface temperature in the south west Indian Ocean and they correlation with the positive phase of the Pacific Decadal Oscillation. Ramsay & Cohen (1997) investigated a coral core taken from a site off the northeast coast of the study area, and identified fluorescent banding which they attributed to extreme flood discharges (1886, 1891, 1925, 1939, 1984, 1985, and 1987). There thus appears to be a strong correlation with the coral proxy dates and that of the Pacific Decadal Oscillation cycle peaks (Fig 9.26).

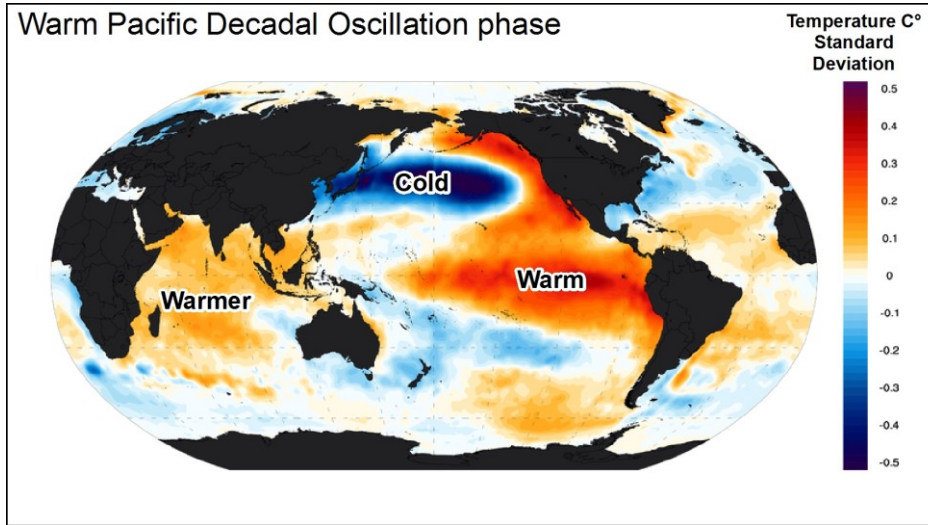


Figure 9.25. Map showing a positive Pacific Decadal Oscillation sea surface temperature distribution. Note the warm water in the eastern Pacific Ocean and associated cold water in the northern western Pacific Ocean and warmer water in the western Indian Ocean (Image: After Wikipedia Commons based on data from Hadley Met Office (HMO 2014))

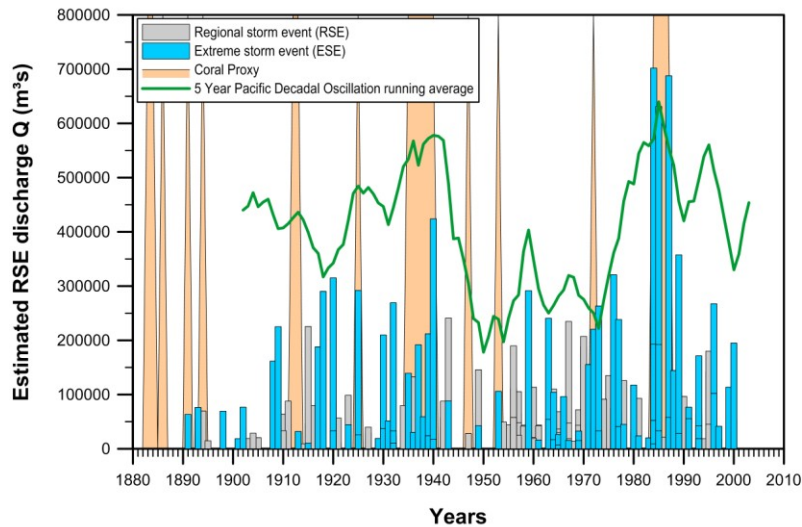


Figure 9.26 Annual regional storm event and extreme storm event discharge comparison with the Pacific Decadal Oscillation (PDO) and coral proxy data (Ramsay & Cohen 1997). Note the periods of increased sediment incorporation into the corals around 1885, 1937 and 1985. Also note the increased extreme storm event discharge magnitude correlation with the coral proxy periods.

According to Alexander & Bladé (2002) the sea - air interaction of the Southern Oscillation Index is the driver for El Niño Southern Oscillation and creates global teleconnections that can influence sea surface temperature around the world. El Niño Southern Oscillation is the forcing agent of the Pacific Decadal Oscillation causing variability over a decadal scale (Newman et al. 2003). The relationships between Southern Oscillation Index, El Niño Southern Oscillation and Pacific Decadal Oscillation and the teleconnections that result are complex, as can be seen from Figures 9.27 and 9.28. According to Preston-Whyte & Tyson (1997), the Southern Oscillation Index plays a major role in determining the southern African climate. The Southern Oscillation Index forcing of El Niño lags so that the Southern Oscillation Index and the El Niño Southern Oscillation are generally 180° out of phase. The El Niño Southern Oscillation forcing of the Pacific Decadal Oscillation has the same general trend. With El Niño causing dryer conditions and La Niña wetter conditions (Tyson et al. 2002). However warmer water in the eastern Pacific Ocean results in El Niño conditions which leads to less rainfall over southern Africa and Pacific Decadal Oscillation conditions that correlate with regional storm event discharges. This suggests that the El Niño Southern Oscillation forcing of the Pacific Decadal Oscillation creates a lag in the Pacific Decadal Oscillation or that the teleconnections from Pacific Decadal Oscillation are stronger than those of the El Niño Southern Oscillation.

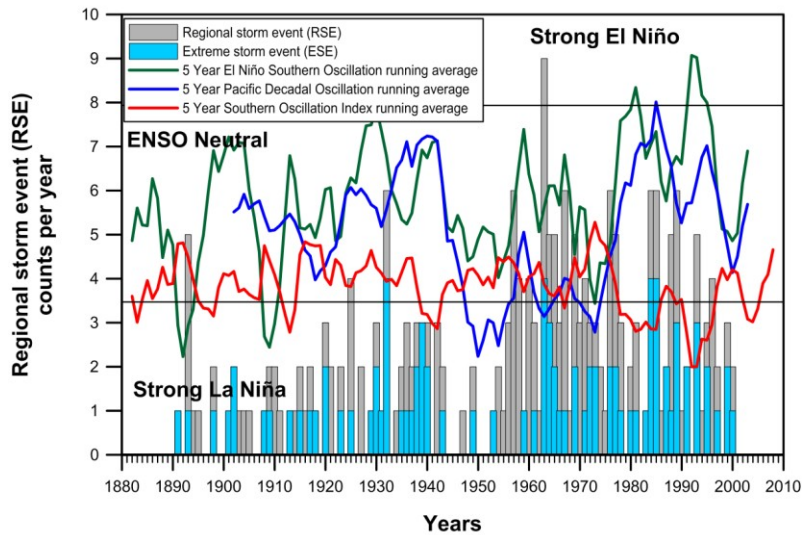


Figure 9.27. Annual regional storm event and extreme storm event annual count comparison with the El Niño Southern Oscillation, Southern Oscillation Index, and Pacific Decadal Oscillation. Note that the Southern Oscillation Index, which is seen as the driver for the El Niño Southern Oscillation, is generally 180° out of phase with the El Niño Southern Oscillation.

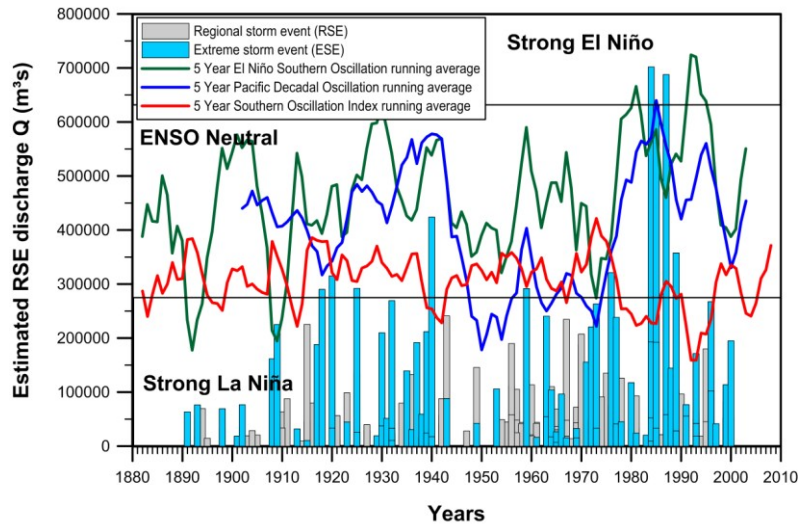


Figure 9.28. Annual regional storm event and extreme storm event discharge comparison with the El Niño Southern Oscillation, Southern Oscillation Index, and Pacific Decadal Oscillation.

Comparison of the various climate cycles show that they can be loosely divided into three time periods namely, 1880 - 1943 where the climate cycles are characterised by large variations, 1943 – 1975 where variations were relatively small and 1975 – present where there are large variations (Fig 9.27 and Fig. 9.28). There are more regional storm event counts per annum when the climate cycles show less variation and less regional storm events when the climate cycles show larger variations.

Investigation of the climate cycles have indicated periods where they change periodicity or undergo phase changes. When comparing climate cycles to the regional storm event counts and discharges two years experienced three such changes (1959, 1975) and one year (1942 - 1943) experienced five changes (Table 9.2, Fig 9.29). It would appear that minor climate phase changes occur at certain intervals, as listed in Table 9.2. However every 16 - 17 years these coincide to produce major climate phase changes that affect the regional storm events and by extension flooding in both a negative and positive manner.

Table 9.2. Climate change points identified from climate cycles.

Years	Wet/Dry cycle change point	Solar change point	Lunar change point compared to Wet/Dry cycles	Temperature Change point	Pacific Decadal Oscillation change point compared to regional storm event counts	El Niño Southern Oscillation change point compared to regional storm event counts	Temperature change point compared to discharge	SOI change point compared to discharge	El Niño Southern Oscillation change point compared to discharge	Pacific Decadal Oscillation change point compared to discharge	Number of change points
1910				X							1
1918									X	X	2
1925								X			1
1942								X			1
1943				X	X	X			X		4
1959		X						X	X		3
1967							X	X			2
1975					X	X			X		3
1981	X										1
1985			X				X				2
1993									X		1
1997							X				1

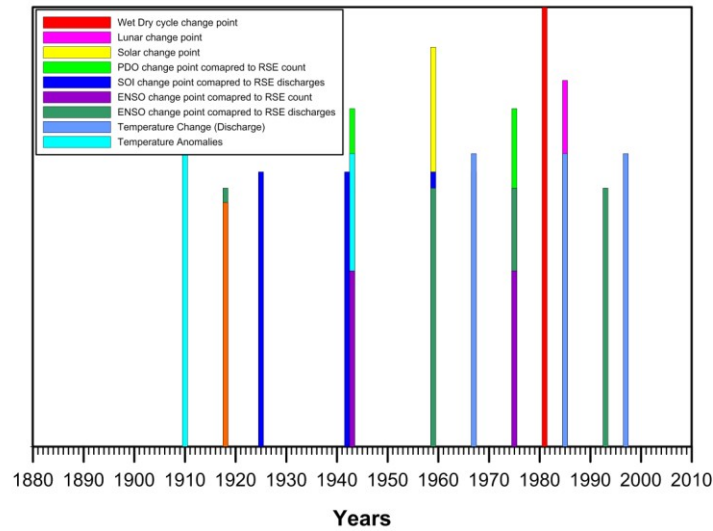


Figure 9.29. Climate change points identified from climate cycles. Note that there are a number of years when more than one climate cycle undergoes a phase shift or changes periodicity.

Global long-term variability in climate cycles have been repeatedly identified by researchers that range from annual (Jury & Majodina 1997) to multi decadal timeframes (Tyson et al. 2002). Of particular interest is the periodicity of those cycles that affect the study area. Given that the regional storm event count and regional storm event discharge variability appear to be driven by two or more different climatic cycles, any attempt at predicting future flooding needs to take this periodicity into account. The best correlation for the regional storm event count is the 18.6 year Wet/Dry Cycle and during the La Niña and the El Niño Southern Oscillation neutral phases. The periodicity of approximately 9 years of increased rainfall followed by approximately 9 years of reduced rainfall and has been shown to be in existence for at least the last 600 years (Tyson et al. 2002) and the trend should continue. The regional storm event discharge magnitude has the best correlation with the Pacific Decadal Oscillation cycle. Generally, the Pacific Decadal Oscillation peaks approximately every 50 years (1885, 1940, 1989) with minor peaks approximately every 15 - 25 years (1915, 1925, 1959).

Extrapolating the Pacific Decadal Oscillation cycle (Fig 9.30) and assuming it continues as it has in the past:

- It accounts for the floods during 2005 – 2007.
- It also suggests an increase in flooding from 2010 – 2018. This accounts for the floods experienced from 2010.
- Reduced flood events during the 2020 – 2029 period.
- Extreme floods similar to those experienced during the 1984 – 1989 period, from 2033 – 2038.

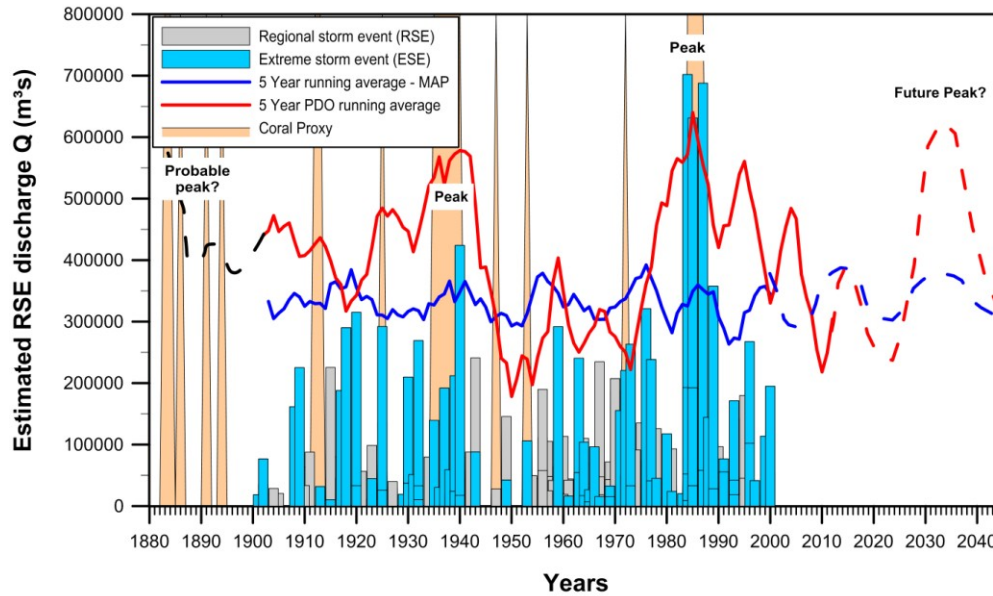


Figure 9.30. Projected future Pacific Decadal Oscillation, mean annual precipitation, Wet/Dry and regional storm event cycles. Note the positive correlation between the coral proxy data, extreme storm event discharge magnitude and the Pacific Decadal Oscillation periodicity. The coral proxy data suggests a probably major Pacific Decadal Oscillation peak around the 1880 – 1885 period. This indicates a 50 – 60 year major Pacific Decadal Oscillation peak periodicity (1885, 1940, 1889) and minor Pacific Decadal Oscillation peaks every 15 – 25 years (1915, 1925, 1959). Forward projecting the Pacific Decadal

The resultant variation in river discharges during wet/dry periods and the Pacific Decadal Oscillation cycle can affect return periods estimations as outlined by Franks (2002). He noted that climate cycles such as the Pacific Decadal Oscillation affected discharge magnitude and pointed out that return periods inferred without taking into account climate cycles will lead to under or over estimation of the flood risk.

CHAPTER 10 - CONCLUSIONS

The current lack of design floodlines, a detailed record keeping of flood events and a dearth of knowledge regarding flood footprints in both the spatial and temporal domain makes it difficult to adequately carry out disaster planning in the Republic of South Africa. The detailed information required to determine design floodlines is expensive and as a result there is limited funding to cover every river. The current settlement patterns close to rivers mean that the damage and death toll for a major flood is exacerbated. There is thus a need for flood extent determination to guide development and disaster planning in the Republic of South Africa.

Field observations of flooding are remarkably helpful in establishing previous flood elevations. Although flood marks can be preserved in the form of debris lines, flood marks on structures and vegetation scour, flood deposits provide the most accurate means of determining flood elevations. In the study area, there are sufficient flood deposits along the rivers studied to be used to map out maximum flood elevations. The complex relationship between flood deposits of the same and/or different flood events makes it difficult to assign these to any specific event. It is only the highest elevation flood clays that can be equated to the highest discharge.

This study has shown that suitable digital elevation model surfaces can be produced by using existing GIS datasets and data models. Combining these digital elevation model surfaces with a means to calculate maximum flood discharges such as the Regional Maximum Flood produces workable flood risk areas. By using field observations and measurements of flood deposits, the upper flood elevation surfaces can be determined. In addition, by using existing 1:100 year flood lines to calibrate the modelled data, model input can be adjusted in the form of a friction factor to produce flood elevation surfaces in close agreement with observations and previous delineations. Importantly, by using water discharges based on run-off and field data that effectively measure the spatial extent of run-off, factors such as soil conditions and land cover can be ignored. The results based on data spread over a wide geographic area produced are comparable to these using the same calibration factors. The implications are that any geographic area can be modelled, using the Flood Zone Model, with limited fieldwork to produce a first approximation dataset. This can be used for planning purposes and highlight critical areas for

detailed engineering flood line calculations. It appears that these calibration factors are independent of geographic location and Regional Maximum Flood K envelopes, thus any catchment can be modelled in theory given sufficiently high resolution digital elevation models. The Flood Zone Model presented, provides flood information as a guide without design flood data and to serve as a means to determine target areas for design flood studies.

Flash floods can produce nearly three times the discharge in hours compared to regional floods measured over days. This is supported by field observations indicating that estimated 1:100 year flood lines/flood zones can be inadequate with respect to defining risk areas for flash floods. The Flash Flood Model described here shows that sufficient information can be derived from existing data sources to calculate variables using the Rational Formula. By calibrating flood elevation simulations, realistic risk zones can be delineated for any quaternary catchment providing a rapid and cost effective solution for delineating flash flood risk zones.

Historical rainfall data have been used as a means to identify regional storm events, which can be related to flood events. The summed occurrences of regional storm events allowed for the development of a flood risk map for KwaZulu-Natal (Fig. 8.19, Table 8.4). The potential risk is zoned, based on a 110 years of regional storm events. While Zone A (Coastal belt from Port Edward to Richards Bay. Patchy distribution up to approximately 300 m elevation) exhibits the highest risk, storm events over this area will not result in extreme events. Extensive localized flooding, especially in the urban environment represents a significant risk. Storm systems that affect Zones B (Coast parallel band from Port Edward to St Lucia up to approximately 500 m elevation.) and C (Coast parallel band inland of Zone B but well-defined corridor over the Mfolozi Valley and outliers along the northern coastline. Elevation up to approximately 1000 m) can produce extensive flooding in the coastal catchments. Zone D (Central midland belt and escarpment up to 3200 m elevation) represents areas where storm systems can produce extreme or near extreme flood events. Although Zone E (Predominantly western portion of KwaZulu-Natal with outliers along northern KwaZulu-Natal, mainly above a 1000 m elevation) represents the lowest risk area, storm systems that cover this area are the most likely to produce extreme flood events. Tropical storms and tropical cyclones that affect Zone F (Coastal and Northern KwaZulu-Natal) present a low risk but these will generally produce the most extreme events.

It has been shown that the periodicity identified in the regional storm event data can be linked to climatic cycles. The number of regional storm event occurrences in a year is attributed to the Southern Oscillation Index and El Niño Southern Oscillation neutral/La Niña phases and the Dyer & Tyson (1977) Wet/Dry Cycles. The lunar influence on climatic cycles appears to be very important and needs to be taken into account in any study concerned with rainfall patterns. The regional storm event estimated discharge magnitudes, supported by coral proxy data, follows the Pacific Decadal Oscillation cycle. Assuming an unchanged Pacific Decadal Oscillation periodicity trend of approximately 50 years with minor Pacific Decadal Oscillation peaks approximately every 25 years, KwaZulu-Natal will experience a limited increase in flood events for the period 2010 – 2018 and extreme floods during the 2033 – 2038 period.

The flood delineation methods produced here are aimed at easily and rapidly producing flood hazard mapping for a quaternary catchment. The models are constrained by the available contour data. While there is a high level of confidence in maximum flood elevation surfaces and the hazard areas they delineate on a map, the lesser return period elevation hazard areas are strongly influenced by topographic form and can produce less accurate delineations. As stated previously only 1% of the river lengths in KwaZulu-Natal have floodline determinations. The resources required to carry out floodline determinations for the other 99% is beyond government to fund at this time. The model is a valid tool to produce maximum flood elevation hazard zones to guide placement of infrastructure. It is better to err on the side of caution by delineating a wider flood hazard zone than designing to a small return period and risk lives. However these models are not suitable for bridge design and dam failure determination.

REFERENCES

- Ahmad, U., Shabri, A. & Zakaria, Z., 2011. Flood frequency analysis of annual maximum stream flows using L-moments and TL-moments approach. *Applied Mathematical Sciences*, 5(5), pp.243–253.
- Alexander, M. & Bladé, I., 2002. The atmospheric bridge: The influence of ENSO teleconnections on air-sea interaction over the global oceans. *Journal of Climate*, 15, pp.2205–2231.
- Alexander, W., 2007. Development of a multi-year climate prediction model. *Water SA*, 31(2), pp.209–218.
- Alexander, W.J., 2002a. Statistical analysis of extreme floods. *Journal of the the South African Institution of Civil Engineering*, 44(1), pp.20–25.
- Alexander, W.J., 2002b. The standard design flood. *Journal of the South African Institute of Civil Engineering*, 44(1), pp 26-30.
- Alexander, W.J., 2002c. The Standard Design Flood - theory and practice (c). *Ceres*, (March), p.12. (<http://www.up.ac.za/academic/civil/divisions/water/upflood.html>).
- Alley, R., Bernstein, T., Bindoff, N., et al., 2007. *IPCC Climate Change 2007 : The Physical Science Basis Summary for Policymakers Contribution of Working Group I to the Fourth Assessment Report of the IPCC*. <https://www.ipcc.ch/pdf/assessment-report/ar4/wg1/ar4-wg1-spm.pdf>.
- Andrews, E.D. & Antweiler, R.C., 2004. Influence of ENSO on Flood Frequency along the California Coast. *Journal of Climate*, 17(2), p.337.
- Anquetin, S., Braud, I., Vannier, O., et al., 2010. Sensitivity of the hydrological response to the variability of rainfall fields and soils for the Gard 2002 flash-flood event. *Journal of Hydrology*, 394(1-2), pp.134–147.
- Anquetin, S., Creutin, J. D., Delrieu, G., et al (2004). *Increasing the forecasting lead-time of Weather Driven Flash-floods. Environment* (pp. 1–47). Institute for Environment and Sustainability Joint Research Centre. H01/812/02/D9056/AG/ct.
- Arnold, J.G., Srivivasan, R., Muttiah, R.S., et al., 1998. Large Area Hydrologic Modeling And Assessment Part 1: Model Development. *Journal of the American Water Resource Association*, 34(1), pp.73–89.
- Ashok, K., Guan, Z. & Yamagata, T., 2003. Influence of the Indian Ocean Dipole on the Australian winter rainfall. *Geophysical Research Letters*, 30(15), p.1821-1824.
- ASTER, 2010. ASTER GDEM. *NASA EODIS*. <https://earthdata.nasa.gov/>.

- Baker, V., 2008. Paleoflood hydrology: Origin, progress, prospects. *Geomorphology*, 101(1-2), pp.1–13.
- Balasch, J.C., Ruiz-Bellet, J.L. & Tuset, J. 2010. Reconstruction of the 1874 *Santa Tecla*'s rainstorm in Western Catalonia (NE Spain) from flood marks and historical accounts. *Natural Hazards and Earth System Science*, 10(11), pp.2317–2325.
- Bell, F. G. (1999). *Geological Hazards: Their assessment, avoidance and mitigation*. *Geology* (1st ed., p. 648). London: E & FN Spon (Routledge).
- Bell, F.G. & Mason, T.R., 1998. The problem of flooding in Ladysmith , Natal , South Africa. *Engineering Geology*, (July 2010), pp.3–10.
- Bell, P.R., 1981. The combined solar and tidal influence in climate. In *Variations of the Solar Constant*. NASA. Goddard Space Flight Center, pp. 241–255.
<http://adsabs.harvard.edu/abs/1981vsc..conf..241B>
- Benjamin, M.A., 2008. *Analysing urban flood risk in low-cost settlements of George, Western Cape, South Africa : Investigating physical and social dimensions*. Cape Town. Unpublished M.Soc.Sci. Thesis, Department of Environmental and Geographical Science. University of Cape Town.
- Beven, K., 2004. Robert E. Horton's perceptual model of infiltration processes. *Hydrological Processes*, 18(17), pp.3447–3460.
- Biasutti, M. & Yuter, S.E., 2012. Very high resolution rainfall patterns measured by TRMM precipitation radar : seasonal and diurnal cycles. *Climate Dynamics*, 39, pp.239–258.
- Biondić, D., Barbalić, D. & Petraš, J., 2007. Creager and Francou-Rodier envelope curves for extreme floods in the Danube River basin in. *Predictions in Ungauged Basins: PUB Kick-off (Proceedings of the PUB Kick-off meetings, Brazil, November 2002, IAHS Publication, 309, pp.20–22*.
- Blamey, R.C. & Reason, C.J.C., 2009. Numerical simulation of a mesoscale convective system over the east coast of South Africa. *Tellus A*, 61(1), pp.17–34.
- Blazkova, S. & Beven, K., 2004. Flood frequency estimation by continuous simulation of subcatchment rainfalls and discharges with the aim of improving dam safety assessment in a large basin in the Czech Republic. *Journal of Hydrology*, 292(1-4), pp.153–172.
- Bloschl, G., Reszler, C. & Komma, J., 2008. A spatially distributed flash flood forecasting model. *Environmental Modelling & Software*, 23(4), pp.464–478.
- Booth, J.F., Wang, S. & Polvani, L., 2013. Midlatitude storms in a moister world : lessons from idealized baroclinic life cycle experiments. *Climate Dynamics*, 41, pp.787–802.
- Borga, M., Gaume, E., Creutin, J.D., et al., 2008. Surveying flash floods : gauging the ungauged extremes. *Bulletin of the American Meteorological Society*, (June), pp.3–5.

- Botes, Z.A., Smith, A.M. & Uken, R., 2010. A New Spatial Planning Tool for the Delineation of Flood Risk Areas. In *Planning Africa 2010 Conference, South African Planning Institute*. pp. 1–12.
- Botes, Z.A., Smith, A.M. & Uken, R., 2011. The Application of GIS Data Models for First Order Regional Flood Risk Determination in Ungauged Catchments for KwaZulu-Natal, South Africa. In *AfricaGeo. Developing Geomatics for Africa* (pp. 1–15). Cape Town. Available from http://www.africageodownloads.info/065_botes_smith_uken.pdf.
- Bothe, O., Fraedrich, K. & Zhu, X., 2012. Precipitation climate of Central Asia and the large-scale atmospheric circulation. *Theoretical and applied climatology*, 108, pp. 345–354.
- Bredenkamp, D.B., 2000. *Groundwater monitoring: A critical evaluation of groundwater monitoring in water resources evaluation and management*. Water Research Commission Report, Pretoria, RSA. WRC 838/1/00. p76
- Bridge, J.S., 2003. *Rivers and floodplains: forms, processes, and sedimentary record*. p491 Malden, USA: Wiley-Blackwell.
- Brunner, G., 2008. HEC-RAS River Analysis System. US Army Corps of Engineers, Insitute for Water Resources, Hydrologic Engineering Center. p 411. Davis, California. Available at: <http://www.hec.usace.army.mil/software/hec-ras/>.
- Brunner, G., 2010. *HEC-RAS River Analysis System User 's Manual*. US Army Corps of Engineers, Insitute for Water Resources, Hydrologic Engineering Center. p582. Davis, California. Available at: <http://www.hec.usace.army.mil/software/hec-ras/>.
- Büchele, B., Kreibich, H., Kron, A., et al., 2006. Flood-risk mapping: contributions towards an enhanced assessment of extreme events and associated risks. *Natural Hazards and Earth System Science*, 6(4), pp.485–503.
- Cai, W., Borlace, S., Lengaigne, M., et al., 2014. Increasing frequency of extreme El Niño events due to greenhouse warming. *Nature Climate Change*, 5(1), pp.1–6.
- Cameron, D.S., Beven, K.J., Tawn, J., et al., 1999. Flood frequency estimation by continuous simulation for a gauged upland catchment (with uncertainty). *Journal of Hydrology*, 219(3-4), pp.169–187.
- Cameron, T. & Ackerman, P., 2011. *HEC-GeoRAS GIS Tools for Support of HEC-RAS using ArcGIS ® User 's Manual*, Davis, California. p508. Available at: <http://www.hec.usace.army.mil/software/hec-georas/>.
- Campbell, A., 1999. Rains pour on as floods claim 13 lives. *IOL*. Available at: <http://www.iol.co.za/news/south-africa/rains-pour-on-as-floods-claim-13-lives-1.23970#.VDqco2dxlhE>.
- Carey, S.K., Tetzlaff, D., Buttle, J., et al., 2013. Use of color maps and wavelet coherence to discern seasonal and interannual climate influences on streamflow variability in northern catchments. *Water Resources Research* , 49, pp.1–14.

- Carpenter, T. & Georgakakos, K., 2006. Intercomparison of lumped versus distributed hydrologic model ensemble simulations on operational forecast scales. *Journal of Hydrology*, 329(1-2), pp.174–185.
- Charlton, R.O., 2007. *Fundamentals of fluvial geomorphology* 1st ed. p234. New York: Routledge.
- Castellarin, A., Vogel, R.M. & Matalas, N.C., 2007. Multivariate probabilistic regional envelopes of extreme floods. *Journal of Hydrology*, 336(3-4), pp.376–390.
- Castellarin, A., Vogel, R.M. & Matalas, N.C., 2005. Probabilistic behavior of a regional envelope curve. *Water Resources Research*, 41(6), pp.1–13.
- Chetty, K. & Smithers, J., 2005. Continuous simulation modelling for design flood estimation in South Africa: Preliminary investigations in the Thukela catchment. *Physics and Chemistry of the Earth, Parts A/B/C*, 30(11-16), pp.634–638.
- Choudhury, A. M. (1994). Bangladesh floods, cyclones and ENSO. In *International Conference on Monsoon Variability and Prediction*. pp. 9–13. Trieste: International Centre for Theoretical Physics. Available from <http://streaming.ictp.trieste.it/preprints/P/94/078.pdf>
- Clayton, H., 1932. *World weather* : Cited in Herman, J. & Goldberg, R., 1978. *Sun, weather, and climate* , NASA US Government Printing Office., New York: MacMillan.
- Cook, C., Reason, C. & Hewitson, B., 2004. Wet and dry spells within particularly wet and dry summers in the South African summer rainfall region. *Climate Research*, 26 (March 2000), pp.17–31..
- Copeland, B. & Watts, A., 2011. Evidence of a Lunisolar Influence on Decadal and Bidecadal Oscillations In Globally Averaged Temperature Trends. *wattsupwiththat.com*. Available at: <http://wattsupwiththat.com/2009/05/23/evidence-of-a-lunisolar-influence-on-decadal-and-bidecadal-oscillations-in-globally-averaged-temperature-trends/>.
- Coumou, D. & Rahmstorf, S., 2012. A decade of weather extremes. *Nature Climate Change*, Online, pp1-6.
- CRU, 2010. University of East Anglia Climate Research Unit: Southern Oscillation Index. Available at: Research Unit <http://www.cru.uea.ac.uk/cru/data/soi/>.
- Creutin, J.D., Muste, M., Bradley, A.A., et al., 2003. River gauging using PIV techniques: a proof of concept experiment on the Iowa River. *Journal of Hydrology*, 277(3-4), pp.182–194.
- Currie, R.G., 1984. Periodic (18.6-year) and cyclic (11-year) induced drought and flood in western North America. *Journal of Geophysical Research*, 89(D5), pp.7215–7230.
- Dai, A., 2012. The influence of the inter-decadal Pacific oscillation on US precipitation during 1923–2010. *Climate Dynamics*, 41(3-4), pp.633–646.

- Darlow, T., 1990. The effects of sea surface temperature on tropical cyclones in the South West Indian Ocean. In *Student Geography Conference, University of Port Elizabeth*. Port Elizabeth, p. 1990.
- De Moel, H., van Alphen, J. & Aerts, J.C.J.H., 2009. Flood maps in Europe – methods, availability and use. *Natural Hazards and Earth System Science*, 9(2), pp.289–301.
- Dettinger, M.D., Ralph, F.M., Hughes, M., et al., 2011. Design and quantification of an extreme winter storm scenario for emergency preparedness and planning exercises in California. *Natural Hazards*. 60 (3). pp1085–1111.
- Diodato, N., 2004. Local models for rainstorm-induced hazard analysis on Mediterranean river-torrential geomorphological systems. *Natural Hazards and Earth System Science*, 4(3), pp.389–397.
- Dunn, P., 1984. *An investigation into tropical cyclones in the South West Indian Ocean*. Department of Water Affairs Flood Studies Technical Report No 1.
- Du Plessis, 2002. A review of effective flood forecasting, warning and response system for application in South Africa. *Water Sa*, 28(2), pp.129–138.
- Dyer, T.G.J. & Tyson, P.D., 1977. Estimating above and below normal rainfall periods over South Africa, 1972-2000. *Journal of Applied Meteorology*, 16, pp.145–147.
- Dyson, L.L., 2009. Heavy daily-rainfall characteristics over the Gauteng Province. *WaterSA*, 35(5), pp.627–638.
- Dyson, L.L. & Heerden, J. Van, 2002. A model for the identification of tropical weather systems over South Africa. *WaterSA*, 28(3), pp.249–258.
- Easterling, D.R., Evans, J.L. & Groisman, P.Y., 1999. Observed Variability and Trends in Extreme Climate Events : A Brief Review *. *Bulletin of the American Meteorological Society*, 81, 3, pp.417–425.
- El Abidine El Morjani, Z., 2011. *Methodology document for the WHO e-atlas of disaster risk . Volume 1 . Exposure to natural hazards Flood hazard modelling*, Available at: http://www.fpt.ac.ma/Publications/Methodology_flood_hazard.pdf.
- Eliot, Matt, Pattiaratchi, C., 2009. Inter-Annual Tidal Modulations Along the. In *5th Western Australian State Coastal Conference*. pp. 2017–2017.
- Elsner, J.B. & Jagger, T.H., 2008. United States and Caribbean tropical cyclone activity related to the solar cycle. *Geophysical Research Letters*, 35(18), pp.1–5.
- Elsner, J.B., Kossin, J.P. & Jagger, T.H., 2008. The increasing intensity of the strongest tropical cyclones. *Nature*, 455(7209), pp.92–5.
- Enfield, DB, Mestas-Nunez, AM, Trimble, P., 2001. The Atlantic multidecadal oscillation and its relation to rainfall and river flows in the continental US. *Geophysical Research Letters*, 28(10), pp.2077–2080.

- England Jr., J.F., Velleux, M.L. & Julien, P.Y., 2007. Two-dimensional simulations of extreme floods on a large watershed. *Journal of Hydrology*, 347(1-2), p.229–241.
- ESKOM, 2010. ESKOM Homestead GIS data. *ESKOM*, Megawatt Park.
- ESRI, 2002. ArcGIS 9: Using ArcGIS Spatial Analyst. *ESRI Software Manual*. pp.238.
- Evan, A. & Camargo, S.J., 2010. A Climatology of Arabian Sea Cyclonic Storms. *Journal of Climate*, 24, pp.140–158.
- Faber, R., 2006. *Flood Risk Analysis: Residual Risks and uncertainties in an Austrian context*. Unpublished P.hD. Thesis. Department of Water, Atmosphere and Environment Institute of Water Management, Hydrology and Hydraulic Engineering, University of Natural Resources and Applied Life Sciences, Vienna, p143.
- Fashuyi, M., Owolawi, P. & Afullo, T., 2006. Rainfall rate modeling for LOS radio systems in South Africa. *South African Institute of Electrical Engineer Journal*, 97(1), pp.74–81.
- Fauchereau, N., Trzaska, S., Rouault, M., et al., 2003. Rainfall variability and changes in southern Africa during the 20th century in the global warming context. *Natural Hazards*, 29, pp.139–154.
- Folland, C., 2008. Interdecadal Pacific Oscillation Time Series. *Met office Hadley Centre for Climate Change, Exeter, UK*, 29(July), p.8. Available at: www.iges.org/c20c/IPO_v2.doc.
- Folland, C. & Renwick, J., 2002. Relative influences of the interdecadal Pacific oscillation and ENSO on the South Pacific convergence zone. *Geophysical Research Letters*, 29(13), pp.2–5.
- Foody, G.M., Ghoneim, E.M. & Arnell, N.W., 2004. Predicting locations sensitive to flash flooding in an arid environment. *Journal of Hydrology*, 292, pp.48–58.
- Ford, D., Pingel, N. & DeVries, J., 2008. *Hydrologic Modeling System HEC-HMS Applications Guide*. CPD-74C. U.S. Army Corps of Engineers, Hydrologic Engineering Centre, Davis, California. http://www.hec.usace.army.mil/software/hec-hms/documentation/HEC-HMS_Applications_Guide_March2008.pdf
- Francou, J. & Rodier, J.A., 1967. Essai de classification des creus maximales. In *Proceedings, Leningrad Symposium on Floods and their Computation, UNESCO*. pp. 518 – 525. <http://unesdoc.unesco.org/images/0001/000143/014318mo.pdf>
- Franks, S.W., 2002. Identification of a change in climate state using regional flood data. *Hydrology and Earth System Sciences*, 6(1), pp.11–16.
- Franks, S. W. (2007). Integrating models , methods and measurements for prediction in ungauged basins. In *Predictions in Ungauged Basins: PUB Kick-off (Proceedings of the PUB Kick-off meeting)* (pp. 20–22). Brazilia: IAHS Publ. 309, 2007.
- Ganoulis, J., 2003. Risk-based floodplain management : A case study from Greece. *International Journal of River Basin Management*, 1(1), pp.41–47.

- Gaume, E., Gaal, L., Viglione, A., et al., 2010. Bayesian MCMC approach to regional flood frequency analyses involving extraordinary flood events at ungauged sites. *Journal of Hydrology*, pp.1–17.
- Gaume, E. & Borga, M., 2008. Post-flood field investigations in upland catchments after major flash floods: proposal of a methodology and illustrations. *Journal of Flood Risk Management*, 1(4), pp.175–189.
- Gericke, O. & Du Plessis, J., 2011. Evaluation of critical storm duration rainfall estimates used in flood hydrology in South Africa. *Water SA*, 37(4), pp.453–470.
- Gratiot, N., Anthony, E.J., Gardel, A., et al., 2008. Significant contribution of the 18.6 year tidal cycle to regional coastal changes. *Nature Geoscience*, 1(3), pp.169–172.
- Griffis, V. & Stedinger, J. (2007). Log-Pearson type 3 distribution and its application in flood frequency analysis. II: Parameter estimation methods. *Journal of Hydrologic Engineering*, (October), 492–500.
- Grunfest, E. & Ripps, A., 2000. Flash floods. Warning and mitigation efforts and prospects. In *Floods*. Available at: <http://www.uccs.edu/geogenvs/ecg/pdf/Parkerchapter.pdf>.
- Gupta, H., Sorooshian, S., Gao, X., et al., 2002. The challenge of predicting flash floods from thunderstorm rainfall. *Philosophical transactions. Series A, Mathematical, physical, and engineering sciences*, 360(1796), pp.1363–71.
- Hansen, J., Ruedy, R., Glascoe, J., et al., 1999. GISS analysis of surface temperature change. *Journal of Geophysical Research*, 104, pp.30997 – 31022.
- Hansingo, K. & Reason, C.J.C., 2009. Modelling the atmospheric response over southern Africa to SST forcing in the southeast tropical Atlantic and southwest. *International Journal of Climatology*, 1012(April), pp.1001–1012.
- Hathaway, D.H., 2010. The solar cycle. *Living Reviews Solar Physics*, 7(1). p65.
- Henderson-Sellers, A., Zhang, H., Berz, G., et al., 1998. Tropical cyclones and global climate change: A post-IPCC assessment. *Bulletin of the American Meteorological Society*. 79(1), pp.19–38..
- Herman, J. & Goldberg, R., 1978. *Sun, weather, and climate*, NASA US Government Printing Office. Available at: http://www.osti.gov/energycitations/product.biblio.jsp?osti_id=5465673.
- HMO, 2014. Met Office Hadley Centre observations datasets. Available at: <http://www.metoffice.gov.uk/hadobs/hadisst/data/download.html>.
- Hosking, J.R.M. & Wallis, J.R. 1997. *Regional frequency analysis: An approach based on L-Moments*. Cambridge University Press. UK. p224. cited by Kjeldsen, T.R., Smithers, J.C. & Schulze, R.E., 2001. Flood frequency analysis at ungauged sites in the KwaZulu-Natal Province, South Africa. *WaterSA*, 27(3), pp.315–324.

- HRC, 2012. Hydrological Research Centre. <http://www.hrc-lab.org/publicbenefit/the-project.html>.
- HRU1/72, 1972. *Design Flood Determination in South Africa*. Hydrological Research Unit Report No. 1/72. p 142. Department of Civil Engineering, University of the Witwatersrand.
- Hughes, D.A., 2004. Three decades of hydrological modelling research in South Africa. *South African Journal Of Science*, (December), pp.638–642.
- IPCC, 2014. Summary for Policy makers. In Field, C.B., Barros, V.R., Dokken, D.J., et al., ed. *Climate Change 2014: Impacts, Adaptation, and Vulnerability. Part A: Global and Sectoral Aspects. Contribution of Working Group II to the Fifth Assessment Report of the Intergovernmental Panel on Climate Change*. Cambridge University Press, Cambridge, United Kingdom and New York, NY, USA., p. 32.
- James, E.C.S. & King, J.M., 2010. *Ecohydraulics for South African Rivers A Review And Guide*. Water Research Commission Report, Pretoria, RSA. WRC TT 453/10. p294.
- JAMSTEC, 2012. Japan Agency for Marine-Earth-Science and Technology, SOI. Available at: [http://www.jamstec.go.jp/frcgc/research/d1/iod/HTML/Dipole Mode Index.html](http://www.jamstec.go.jp/frcgc/research/d1/iod/HTML/Dipole%20Mode%20Index.html).
- Javelle, P., Fouchier, C., Arnaud, P., et al., 2010. Flash flood warning at ungauged locations using radar rainfall and antecedent soil moisture estimations. *Journal of Hydrology*, 394(1-2), pp.267–274.
- JISAO, 2012. Joint Institute for the Study of the Atmosphere and Ocean. AAO. Available at: <http://www.jisao.washington.edu/data/ao/>.
- JISAO, 2013. PDO. Available at: <http://jisao.washington.edu/pdo/PDO.latest>.
- Johnson, D. & Miller, A., 1997. A spatially distributed hydrologic model utilizing raster data structures. *Computers & Geosciences*, 23(3), pp.267–272.
- Jothityangkoon, C. & Sivapalan, M., 2003. Towards estimation of extreme floods: examination of the roles of runoff process changes and floodplain flows. *Journal of Hydrology*, 281(3), pp.206–229.
- JTWC, 2014. Joint Typhoon Warning Centre. , p.2014. Available at: http://www.usno.navy.mil/NOOC/nmfc-ph/RSS/jtwc/best_tracks/shindex.php.
- Jury, M. & Majodina, M., 1997. Preliminary climatology of southern Africa extreme weather: 1973–1992. *Theoretical and applied climatology*, 112, pp.103–112.
- Jury, M. & Pathack, B., 1991. A study of climate and weather variability over the tropical southwest Indian Ocean. *Meteorology and Atmospheric Physics*, p.75.
- Kahn, M.E., 2003. The Death Toll From Natural Disasters: The Role of Income, Geography, and Institutions. *Review of Economics and Statistics*, 87(2), pp.271–284.

- Kajami, N., Gupta, H., Wagener, T., et al., 2004. Calibration of a semi-distributed hydrologic model for streamflow estimation along a river system. *Journal of Hydrology*, 298(1-4), pp.112–135.
- Keeling, C.D. & Whorf, T.P., 1997. Possible forcing of global temperature by the oceanic tides. *Proceedings of the National Academy of Sciences of the United States of America*, 94(16), pp.8321–8..
- Keeling, C.D. & Whorf, T.P., 2000. The 1,800-year oceanic tidal cycle: a possible cause of rapid climate change. *Proceedings of the National Academy of Sciences of the United States of America*, 97(8), pp.3814–9..
- Kendall, R., 2011. A soggy start to 2011. *iafrica.com*. Available at: <http://news.iafrica.com/features/701382.html>.
- Kim, E.S. & Choi, H. Il, 2011. Assessment of Vulnerability to Extreme Flash Floods in Design Storms. *International Journal of Environmental Research and Public Health*, 8(7), pp.2907–2922.
- Kirchner, J.W., 1993. Statistical inevitability of Horton's laws and the apparent randomness of stream channel networks. *Geology*, 21(7), p.591-594.
- Kjeldsen, T., Smithers, J. & Schulze, R., 2002. Regional flood frequency analysis in the KwaZulu-Natal province, South Africa, using the index-flood method. *Journal of Hydrology*, 255(1-4), pp.194–211.
- Kjeldsen, T.R., Smithers, J.C. & Schulze, R.E., 2001. Flood frequency analysis at ungauged sites in the KwaZulu-Natal Province, South Africa. *WaterSA*, 27(3), pp.315–324.
- Klinman, M. & Reason, C., 2008. On the peculiar storm track of TC Favio during the 2006–2007 Southwest Indian Ocean tropical cyclone season and relationships to ENSO. *Meteorology and Atmospheric Physics*, 100(1-4), pp.233–242.
- Knoesen, DM, Schulze, R, Pringle, C, et al., 2009. *Water for the future: Impacts of Climate Change on Water Resources in the Orange-Senqu River Basin*. Report to NeWater, a project funded under the Sixth Research Framework of the European Union. Institute of Natural Resources, Pietermaritzburg, South Africa. p 36.
- Kobiyama, M. & Goerl, R.F., 2007. Quantitative method to distinguish flood and flash flood as disasters. *SUISUI Hydrological Research Letters*, 1(May), pp.11–14.
- Kochel, R.C. & Baker, V.R., 1982. Paleoflood hydrology. *Science*, 215(4531), pp.353–361.
- Koltermann, C. & Gorelick, S., 1992. Paleoclimatic signature in terrestrial flood deposits. *Science*, 256, pp.1775–1782.
- Können, G., Jones, P.D., Kaltofen, M.H., et al., 1998. Pre-1866 extensions of the Southern Oscillation Index using early Indonesian and Tahitian meteorological readings. *Journal of Climate*, 11, pp.2325–2340.

- Kovács, Z., du Plessis, D.B., Bracher, P.R., et al., 1985. *Documentation of the 1984 Domoina Floods*. Department of Water Affairs Technical Report, TR122. pp149.
- Kovács, Z., 1988. *Regional maximum flood peaks in Southern Africa*. Technical Report TR 137, Department of Water Affairs and Forestry. p 91.
- Kovács, Z., 1985. Hydrology of the Mfolozi River. In *Sediment problems in the Mfolozi catchment assessment of research requirements*. U. Looser, ed. HRI Department of Water Affairs 34 - 54, p. 1985.
- Lee, J., Musiake, K. & Oka, Y., 1991. A Soil-Based Process-Conceptual Model for Hortonian Overland Flow and Infiltration. In *Proceedings of the Vienna Symposium*. pp. 207–216.
- Lumbroso, D., Ramsbottom, D. & Spaliveiro, M., 2008. Sustainable flood risk management strategies to reduce rural communities' vulnerability to flooding in Mozambique. *Journal of Flood Risk Management*, 1(1), pp.34–42.
- Lundquist, D.A.N., 2002. What is an extreme flood and for whom ? In *The extremes of the extremes: Extraordinary floods*. Reykjavik, Iceland: IAHS Publ. 271, pp. 367–371.
- Luo, J.J., Zhang, R., Behera, S.K., et al., 2010. Interaction between El Niño and Extreme Indian Ocean Dipole. *Journal of Climate*, 23(3), p.726.
- Lynch, S.D., 2003. *Development of a Raster Database of Annual, Monthly and Daily Rainfall for Southern Africa*. Water Research Commission Report, Pretoria, RSA. WRC 1156/1/03. p78.
- Maidment, D., 2002. *Arc Hydro: GIS for Water Resources* 1st ed. D. R. Maidment, ed., New York: ESRI Press. p 203.
- Makwananzi, N. & Pegram, G., 2004. *A flood Nowcasting System for the eThekweni Metro. Volume 2 : Modelling flood inundation in the Mlazi River under uncertainty*. Water Research Commission Report, Pretoria, RSA. WRC 1217/2/04. p153
- Malherbe, J., Engelbrecht, F. & Landman, W., 2014. Response of the Southern Annular Mode to tidal forcing and the bidecadal rainfall cycle over subtropical southern Africa. *Journal of Geophysical Research" Atmospheres*, 119, pp.2032–2049.
- Malherbe, J. Engelbrecht, F.A., Landman, W.A. and Engelbrecht, C.J., 2012. *Tropical systems from the southwest Indian Ocean making landfall over the Limpopo River Basin, southern Africa: a historical perspective*. Water Research Commission Report, Pretoria, RSA. WRC K5/1847. p43.
- Mann, M.E, Woodruff, J.D., Donnelly, J.P., et al., 2009. Atlantic hurricanes and climate over the past 1,500 years. *Nature*, 460(7257), pp.880–3.
- Mantua, N.J., Hare, S.R., Zhang, Y., et al., 1997. A Pacific Interdecadal Climate Oscillation with Impacts on Salmon Production. *Bulletin of the American Meteorological Society*, 78(6), pp.1069–1079.

- Mantua, N. & Hare, S., 2002. The Pacific decadal oscillation. *Journal of Oceanography*, 58(1), pp.35 – 44.
- Marchi, L., Borga, M., Preciso, E., et al., 2010. Characterisation of selected extreme flash floods in Europe and implications for flood risk management. *Journal of Hydrology*, 394(1-2), pp.118–133.
- Mark, A. & Marek, P.E., 2011. *Hydraulic Design Manual*. Texas Department of Transportation. <http://onlinemanuals.txdot.gov/txdotmanuals/hyd/hyd.pdf>
- Mavume, A., Rydberg, L., Rouault, M., et al., 2009. Climatology and landfall of tropical cyclones in the south-west Indian Ocean. *Western Indian Ocean Journal of Marine Science*, 8(1), pp.15–36..
- Mazumder, R. & Arima, M., 2005. Tidal rhythmites and their implications. *Earth-Science Reviews*, 69(1-2), pp.79–95.
- Medina, S., 2005. *Orographic enhancement of mid-latitude cyclone precipitation*. Unpublished P.hD. Thesis. Department of Atmospheric Sciences, University of Washington, p177.
- Mcenery, J., Ingram, J., Duan, Q., et al., 2005. NOAA’S Advanced Hydrologic Prediction Service: Building Pathways for Better Science in Water Forecasting. *Bulletin of the American Meteorological Society*, 86(3), pp.375–385.
- Merz, R. & Blöschl, G., 2003. Regional flood risk-what are the driving processes? In *Water Resources Systems - Hydrological Risk, Management and Development*. Sapporo: IAHS Publ. no. 281, pp. 49–58.
- Meyer, V., Kuhlicke, C., Luther, J., et al., 2012. Recommendations for the user-specific enhancement of flood maps. *Natural Hazards and Earth System Science*, 12(5), pp.1701–1716.
- Michele, C. & Salvadori, G., 2002. On the derived flood frequency distribution: analytical formulation and the influence of antecedent soil moisture condition. *Journal of Hydrology*, 262(1-4), pp.245–258.
- Morris, J., 2011. Pers. comm. Senior Consulting Engineer, SRK Consulting Durban.
- Mulder, V.L., de Bruin, S., Schaepman, M.E., et al., 2011. The use of remote sensing in soil and terrain mapping — A review. *Geoderma*, 162(1-2), pp.1–19.
- Mwakalila, S., 2003. Estimation of stream flows of ungauged catchments for river basin management. *Physics and Chemistry of the Earth, Parts A/B/C*, 28(20-27), pp.935–942.
- NASA, 2012. NASA Goddard Space Flight Center. Available at: <http://data.giss.nasa.gov/gistemp/>.
- NASA, 2013. NASA Marshall Space Flight Centre, Solar Physics. Available at: <http://solarscience.msfc.nasa.gov/SunspotCycle.shtml>.

- Naulet, R., Lang, M., Ouarda, T.B., et al., 2005. Flood frequency analysis on the Ardèche river using French documentary sources from the last two centuries. *Journal of Hydrology*, 313(1-2), pp.58–78.
- Neiff, J.J., Mendiando, E.M. & Depettris, C.A., 2000. ENSO floods on river ecosystems: from catastrophes to myths. In F. Toensmann & M. Koch, eds. *River flood defenses*. Kassel: Herkules Verlag, pp. F141–F152.
- Nel, W., 2008. Observations on daily rainfall events in the KwaZulu-Natal Drakensberg. *WaterSA*, 34(2), pp.271–274.
- Newman, M., Compo, G. & Alexander, M., 2003. ENSO-forced variability of the Pacific decadal oscillation. *Journal of Climate*, 16, pp.3853–3857..
- NOAA, 2013. ENSO – MEI Index (Multivariate ENSO Index) Extension. Available at: <http://www.esrl.noaa.gov/psd/enso/mei.ext/index.html>.
- NOAA, 2012. NOAA Climatic Data Center. SST. Available at: <http://www.ncdc.noaa.gov/ersst/#time>.
- NOAA/ESRLa, 2012. NOAA Earth System Research Laboratory. CO2. Available at: www.esrl.noaa.gov/gmd/ccgg/trends/; scrippsco2.ucsd.edu/.
- NOAA/ESRLb, 2012. Atlantic Multidecadal Oscillation (AMO). Available at: <http://www.esrl.noaa.gov/psd/data/climateindices/list/#AMO>.
- NOAA_ERSST_V3, 2012. SST. , p.3. Available at: <http://www.esrl.noaa.gov/psd/>.
- Norbiato, D., 2008. *Regional analysis of flooding and flash flooding*. Unpublished PhD Thesis. Università Degli Studi Padova, Dipartimento Territorio e Sistemi Agro-Forestali. p 162.
- Norbiato, D., Borga, M., Esposti, D.S., et al., 2008. Flash flood warning based on rainfall thresholds and soil moisture conditions: An assessment for gauged and ungauged basins. *Journal of Hydrology*, pp.274– 290.
- Ntelekos, A., Georgakakos, K.P. & Krajewski, W.F., 2006. On the Uncertainties of Flash Flood Guidance: Toward Probabilistic Forecasting of Flash Floods. *Journal of Hydrometeorology*, 7(5), pp.896–915.
- NWA, 1998. National Water Act 36 of 1998. *Republic of South Africa Government Gazette*, 398(19182). http://www.energy.gov.za/files/policies/act_nationalwater36of1998.pdf
- OCHA, 2011. *Southern Africa • Floods and Cyclones*. United Nations Office for the coordination of humanitarian affairs. Available at: http://reliefweb.int/sites/reliefweb.int/files/resources/Full_Report_1783.pdf.
- Oellermann, I., 1999. Residents clean up after flash flood. *IOL*, p.1999. Available at: <http://www.iol.co.za/news/south-africa/residents-clean-up-after-flash-flood-1.19860#.VDqb1mdxIhE>.

- Parak, M. & Pegram, 2006. The rational formula from the runhydrograph. *Water SA*, 32(2), pp.163–180.
- Paschalis, A., Molnar, P., Fatchi, S., et al., 2013. A stochastic model for high-resolution space-time precipitation simulation. *Water Resources Research*, 49, pp.8400–8417.
- Paudel, M., 2010. *An examination of distributed hydrologic modeling methods as compared with traditional lumped parameter approaches*. Unpublished PhD Thesis. Department of Civil and Environmental Engineering. Brigham Young University. p 174.
- Pegram, G. & Parak, M., 2004. A review of the regional maximum flood and rational formula using geomorphological information and observed floods. *WaterSA*, 30(3), pp.4738–4738.
- Pegram, G., Sinclair, S. & Parak, M., 2007. *National Flood Nowcasting System: Towards an integrated mitigation strategy*. Water Research Commission Report, Pretoria, RSA. WRC 1429/1/06, p.134.
- Perez-Pena, J.V., Azanon, J.M., Azor, A., et al., 2009. Spatial analysis of stream power using GIS: SLk anomaly maps. *Earth Surface Processes and Landforms*, 34, pp.16–25.
- Philippon, N., Rouult, M., Richard, Y., et al., 2011. The influence of ENSO on winter rainfall in South Africa. *International Journal of Climatology*, 32(15), pp.2333–2347.
- Plate, E.J., 2002. Flood risk and flood management. *Journal of Hydrology*, 267(1-2), pp.2–11.
- Prat, O.P. & Barros, A.P., 2010. Ground observations to characterize the spatial gradients and vertical structure of orographic precipitation – Experiments in the inner region of the Great Smoky Mountains. *Journal of Hydrology*, 391(1-2), pp.141–156.
- Preston-Whyte, R. & Tyson, P., 1997. *The atmosphere and weather of southern Africa* 4th ed., Cape Town: Oxford University Press, Inc. p 374
- Prinos, P., 2008. *Review of Flood Hazard Mapping*, FLOODSite Report T03-07-01, Rev 4_3_P01. Available at: http://www.floodsite.net/html/partner_area/project_docs/T03_07_01_Review_Hazard_Mapping_V4_3_P01.pdf.
- Ramsay, P. & Cohen, A., 1997. Coral paleoclimatology research on the southeast African shelf. *Proc. 8th Int. Coral Reef Symp.* Available at: <http://scholar.google.com/scholar?hl=en&btnG=Search&q=intitle:Coral+Paleoclimatology+research+on+the+Southeast+African+Shelf#0>.
- Rautenbach, C. de W., 1998. The unusual rainfall and sea surface temperature characteristics in the South African region during the 1995/96 summer season. *Water SA*, 24(3), pp.165–172.
- Ray, R.D., 2007. Decadal Climate Variability: Is There a Tidal Connection? *Journal of Climate*, 20(14), pp.3542–3560.
- Reason, C. J. C., R.M., 2005. Links between the Antarctic Oscillation and winter rainfall over western South Africa. *Geophysical Research Letters*, 32(7), p.L07705.

- Reed, S., Schaake, J. & Zhang, Z., 2007. A distributed hydrologic model and threshold frequency-based method for flash flood forecasting at ungauged locations. *Journal of Hydrology*, 337(3-4), pp.402–420.
- Reliefweb, 1996. *South Africa – Floods Information Report No. 2.*, Available at: <http://reliefweb.int/report/south-africa/south-africa-floods-information-report-no2>.
- Rouault, M., Pohl, B., Penven, P., et al., 2010. *Multidisciplinary Analysis of Hydroclimatic Variability at the Catchment Scale*. Water Research Commission Report, Pretoria, RSA. WRC 1747/1/10. p97.
- Rouault, M., Pohl, B. & Penven, P., 2010. Coastal oceanic climate change and variability from 1982 to 2009 around South Africa. *African Journal of Marine Science*, 32(2), pp.237–246.
- Rouault, M. & Richard, Y., 2003. Intensity and spatial extension of drought in South Africa at different time scales. *WaterSA*, 29(4), pp.489–500.
- Saji, N.H., Goswami, B.N., Vinayachandran, P.N., et al., 1999. A dipole mode in the tropical Indian Ocean. *Nature*, 401(6751), pp.360–3.
- Salinger, M.J., Renwick, J. a. & Mullan, A.B., 2001. Interdecadal Pacific Oscillation and South Pacific climate. *International Journal of Climatology*, 21(14), pp.1705–1721.
- SANRAL, 2013. *SANRAL Drainage Manual*. South African Roads Agency SOC Ltd, Pretoria, South Africa. p 464. www.sanral.co.za
- SARVA, 2010. *The South African Risk and Vulnerability Atlas*. p 52 CPD Print.
- SAWS, 1991. *SAWS: CAELUM: A history of notable weather events in South Africa, 1500-1991*. Government Printers, Pretoria.
- SCC, 2013. Sunshine Coast Council Flood Definitions. Available at: <http://www.sunshinecoast.qld.gov.au/sitePage.cfm?code=flood-definition>.
- Schlesinger, M. & Ramankutty, N., 1994. An oscillation in the global climate system of period 65-70 years. *Nature*, 367(6465), pp.723 – 726.
- Schneider, N. & Cornuelle, B., 2005. The Forcing of the Pacific Decadal Oscillation. *Journal of Climate*, 18, pp.4355–4373.
- Schoeman, J., van der Walt, M., Monnik, K.A., et al., 2002. *Development and application of a land capability classification system for South Africa*. ARC Institute for Soil, Climate and Water, Pretoria. GW/A/2000/57. p 61.
- Shaw, a. G.P. & Tsimplis, M.N., 2010. The 18.6yr nodal modulation in the tides of Southern European coasts. *Continental Shelf Research*, 30(2), pp.138–151.
- Shen, C., Wang, W., Gong, W., et al., 2006. A Pacific Decadal Oscillation record since 1470 AD reconstructed from proxy data of summer rainfall over eastern China. *Geophysical Research Letters*, 33(3), p.L03702.

- Singleton, a. T. & Reason, C.J.C., 2007. A Numerical Model Study of an Intense Cutoff Low Pressure System over South Africa. *Monthly Weather Review*, 135(3), pp.1128–1150.
- Sivapalan, M., Takeychi, K., Franks, S.W., et al., 2003. IAHS Decade on Predictions in Ungauged Basins (PUB), 2003–2012: Shaping an exciting future for the hydrological sciences. *Hydrological Sciences Journal*, 48(6), pp.857–880.
- Smith, A.M., 1992. Palaeoflood hydrology of the lower Umgeni River from a reach south of the Inanda Dam, Natal. *South African geographical journal*, 74(2), p.1992.
- Smith, A.M., Mather, A.A., Bundy, S.C., et al., 2010. Contrasting styles of swell-driven coastal erosion: examples from KwaZulu-Natal, South Africa. *Geological Magazine*, (May), pp.1–14.
- Smithers, J.C., 2011. Opportunities for design flood estimation in South Africa. *15th South African National Hydrology Symposium, 2011*. Available at: http://www.ru.ac.za/static/institutes/iwr/SANCIAHS/2011/the.pdf/files/JC_Smithers_Paper.pdf.
- Smithers, J.C., 2012. Issues in contemporary geographical hydrology. *Water SA*, 38(4), pp.633–646.
- Smithers, J.C. & Schulze, R., 2003. *Design rainfall and flood estimation in South Africa*. Water Research Commission Report, Pretoria, RSA. WRC 1060/1/03. p156.
- StatsSA. 2009. Mid-year population estimates: Statistics South Africa. P0302. Statistics South Africa, Pretoria. p17.
- Stomph, T.J., de Ridder, N., Steenhuis, T.S., et al., 2002. Scale effects of Hortonian overland flow and rainfall-runoff dynamics: laboratory validation of a process-based model. *Earth Surface Processes and Landforms*, 27(8), pp.847–855.
- Sutcliffe, J., 1978. *Methods of flood estimation: A guide to the flood studies report*, Institute of Hydrology, Natural Environment Research Council. Report 48 Available at: http://nora.nerc.ac.uk/5776/1/IH_049.pdf.
- Sutton, R.T. & Hodson, D.L.R., 2005. Atlantic Ocean forcing of North American and European summer climate. *Science*, 309(5731), pp.115–8.
- Taljaard, J.J., 1982. Cut-off lows and heavy rain over the Republic. *South African Weather Newsletter*. No 403. Cited by: Tyson, P.D. 1986. *Climate change and variability in Southern Africa*. Cape Town. Oxford University Press, Inc. pp 220., pp.155–156.
- Thieken, A., Merz, B., Kreibich, H., et al., 2006. Methods for flood risk assessment : Concepts and challenges. *International Workshop on Flash Floods in Urban Areas*, Muscat, Oman, pp.4–6.
- Thompson, D. & Wallace, J., 2000. Annular modes in the extratropical circulation. Part I: month-to-month variability. *Journal of Climate*, 13(1999), pp.1000–1017.

- Trenberth, K.E., 2010. Changes in precipitation with climate change. *Technical Conference on Changing Climate and Demands for Climate Services for Sustainable development, Turkey 2010*, pp.16–18.
- Tyson, P.D., 1986. *Climate Change and Variability in Southern Africa*, Cape Town: Oxford University Press, Inc. p 220.
- Tilman, D., Cassman, K. & Matson, P., 2002. Agricultural sustainability and intensive production practices. *Nature*, 418(August), pp.671–677.
- Tyson, P.D., Cooper, G.R.J. & McCarthy, T.S., 2002. Millennial to multi-decadal variability in the climate of southern Africa. *International Journal of Climatology*, 22(9), pp.1105–1117.
- UCAR, 2010a. *Flash flood early warning system reference guide*. University Corporation for Atmospheric Research under Award NA06NWS4670013 from the National Oceanic and Atmospheric Administration, U.S. Department of Commerce. Available at: http://www.meted.ucar.edu/hazwarnsys/haz_fflood.php.
- UCAR, 2010b. Unit Hydrograph Theory. *Unit Hydrograph Theory, University Corporation for Atmospheric Research*. Available at: http://stream2.cma.gov.cn/pub/comet/HydrologyFlooding/UnitHydrographTheoryInternationalEdition/comet/hydro/basic_int/unit_hydrograph/index.htm.
- Ummenhofer, C.C., England, M.H., McIntosh, P.C., et al., 2009. What causes southeast Australia's worst droughts? *Geophysical Research Letters*, 36(4), p.L04706..
- van Bladeren, D., 1992. *Historical flood documentation series No. 1: Natal and Transkei, 1848-1989*. p 179. Technical Report TR 147, Department of Water Affairs and Forestry.
- van Bladeren, D. & Burger, C., 1989. *Documentation of the September 1987 Natal floods*, p 198. Technical Report TR 139, Department of Water Affairs and Forestry.
- van Bladeren, D., Zawada, P.K. & Mahlangu, D., 2007. *Statistical based regional flood frequency estimation study for South Africa using systematic, historical and palaeoflood data*. Water Research Commission Report, Pretoria, RSA. WRC 1260/1/07. p254
- van Heerden, I. & Swart, D., 1986. Fluvial processes in the Mfolozi Flats and the consequences for St Lucia Estuary. *Proceedings, 2nd South African National Hydrology*, (22).
- van Oldenborgh, G. & Burgers, G., 2005. Searching for decadal variations in ENSO precipitation teleconnections. *Geophysical Research Letters*, (1), pp.2–5.
- Viglione, A., Chirico, G.B., Komma, J., et al., 2010. Quantifying space-time dynamics of flood event types. *Journal of Hydrology*. 394 (1-2), pp.213-229.
- Viglione, A. & Blöschl, G., 2009. On the role of storm duration in the mapping of rainfall to flood return periods. *Hydrology and Earth System Sciences*, 13, pp.205–216.
- Viles, H. & Goudie, A., 2003. Interannual, decadal and multidecadal scale climatic variability and geomorphology. *Earth-Science Reviews*, 61, pp.105–131.

- Viljoen, M.F., Plessis, L.A. & Booysen, H.J., 2001. Extending flood damage assessment methodology to include sociological and environmental dimensions. *WaterSA*, 27(4), pp.517–522.
- Vischel, T., Pegram, G., Sinclair, S., et al., 2008. Implementation of the TOPKAPI model in South Africa : Initial results from the Liebenbergsvlei catchment. *WaterSA*, 34(3), pp.331–342.
- Viviroli, D., Mittelbach, H., Gurtz, R., et al., 2009. Continuous simulation for flood estimation in ungauged mesoscale catchments of Switzerland – Part II: Parameter regionalisation and flood estimation results☆. *Journal of Hydrology*, 377(1-2), pp.208–225.
- Vowinckel, E., 1956. Ein beitrag zur Witterungsklimatologie des suedlichen Mozambiquekanals. *Miscelanea Geofisica Publicada Pelo Servico Meteorologico de Angola em Comemoracao de X Aniversario do Servico Metrologico Nacional, Luanda*. Cited by: Tyson, P.D. 1986. *Climate change and variability in Southern Africa*. Cape Town. Oxford University Press., pp.63–86.
- Wang, D., Qin, X., Xiao, X., et al., 2012. El Niño and El Niño Modoki variability based on a new ocean reanalysis. *Ocean Dynamics*, 62(9), pp.1311–1322.
- Warner, J.C., Brunner, G.W., Wolfe, B.C., et al., 2010. *HEC-RAS Applications Guide*. US Army Corps of Engineers, Insitute for Water Resources, Hydrologic Engineering Center. p 351. Davis, California. Available at: <http://www.hec.usace.army.mil/software/hecras/>.
- Washington, R. & Preston, A., 2006. Extreme wet years over southern Africa: Role of Indian Ocean sea surface temperatures. *Journal of Geophysical Research*, 111(D15), pp.1–15.
- Weingartner, R., Barben, M. & Spreafico, M., 2003. Floods in mountain areas—an overview based on examples from Switzerland. *Journal of Hydrology*, 282(1-4), pp.10–24.
- Willems, P., 2013. Adjustment of extreme rainfall statistics accounting for multidecadal climate oscillations. *Journal of Hydrology*, 490, pp.126–133.
- Wolter, K. & Timlin, M.S., 2011. El Niño/Southern Oscillation behaviour since 1871 as diagnosed in an extended multivariate ENSO index (MEI.ext). *International Journal of Climatology*, 31(7), pp.1074–1087.
- WSUD, 2012. *Water Sensitive Urban Design - Engineering Procedures for Stormwater Management in Southern Tansmania*. Derwent Estuary Program (Tas.). State of Tasmania. http://epa.tas.gov.au/documents/wsud_manual_2012.pdf.
- Wuebbles, D., Meehl, G., Hayhoe, K., et al., 2014. CMIP5 Climate Model Analyses, Climate Extremes in the United States. *American Meteorological Society*, (April), pp.571–583.
- Yasuda, I., 2009. The 18.6-year period moon-tidal cycle in Pacific Decadal Oscillation reconstructed from tree-rings in western North America. *Geophysical Research Letters*, 36(5), p.L05605.
- Xue, Y., Smith, T. & Reynolds, R., 2003. Interdecadal changes of 30-yr SST normals during 1871-2000. *Journal of Climate*, 16, pp.1601–1612.

- Yen, B., 2002. Open channel flow resistance. *Journal of Hydraulic Engineering*, 128(1), pp.20–39.
- Yndestad, H., 2006. The influence of the lunar nodal cycle on Arctic climate. *ICES Journal of Marine Science*, 63(3), pp.401–420.
- Zawada, P., Hattingh, J. & van Bladeren, D., 1996. *Paleoflood hydrological analysis of selected South African rivers*. Water Research Commission Report, Pretoria, RSA. WRC 509/1/96. p241.
- Zawada, P., 1997. Palaeoflood hydrology: method and application in flood-prone southern Africa. *South African Journal of Science*, 93, pp.111–132.
- Zhang, Y., Wallace, J. & Battisti, D., 1997. ENSO-like interdecadal variability: 1900-93. *Journal of climate*, 10, pp.1004–1020.
- Zwiers, F.W., Alexander, L.V., Hegerl, G.C., et al., 2013. Climate Extremes : Challenges in Estimating and Understanding Recent Changes in the Frequency and Intensity of Extreme Climate and Weather Events. *Climate Science for Serving Society: Research, Modelling and Prediction Priorities*. Eds Asrar, G.R. & Hurrell, J.W. Springer Science, Dordrecht. p484.

APPENDIX I – LIST OF HISTORICAL FLOODS

Historical flood records (1848 – 2000) compiled from(SAWS 1991), van Bladeren (1992), newspaper and internet sources. Grey shading represents the extreme floods identified by van Bladeren (1992).

Year	Month	Date	Location	Type	Notes	Reference
1848	April		Durban	?	No rainfall data	van Bladeren
1856	April	14-17	Durban	Flood	Also at Pietermaritzburg. Umgeni Changed channel	SAWS/van Bladeren
1868	August	28	Durban	Flood	420mm in Durban and 320mm in Pmb in 60 Hours	SAWS/van Bladeren
1886	January	23	Ladysmith	Flood		SAWS
1891	March	15-17	Durban, Richards Bay	Extreme flood		van Bladeren
1893	January	3	Durban	Extreme flood		van Bladeren
1895	May		Durban	Flood		SAWS/van Bladeren
1905	March	31 - 1	Durban & South Coast	Heavy Rains/Flooding/Extreme flood		SAWS/van Bladeren
1908	April	17 - 18	Durban	Extreme flood		SAWS/van Bladeren
1911	October	1	KZN Coast (Durban South ?)	Extreme flood		SAWS
1913	March	7	Scattered across Southern KZN	Extreme flood		van Bladeren
1914	February	1	Matatiele	Heavy Rains/Flooding		SAWS/van Bladeren
1915	October	26 - 27	KZN Coast	Flood		SAWS/van Bladeren
1916	February	25	Dundee	Heavy Rains/Flooding		SAWS/van Bladeren

Year	Month	Date	Location	Type	Notes	Reference
1916	March	28	Umbogintwini	Flood		SAWS/van Bladeren
1917	October	28	KZN	Extreme flood	Large scale flooding	SAWS/van Bladeren
1918	February	15	Zululand	Extreme flood	Umfolozi River	SAWS/van Bladeren
1923	February	12	Ladysmith	Flood		SAWS/van Bladeren
1923	July	20 - 22	Southern KZN	Flood		SAWS/van Bladeren
1925	March		Ladysmith	Flood		SAWS/van Bladeren
1925	March		Newcastle	Flood		SAWS/van Bladeren
1925	March		Tugela	Extreme flood		SAWS/van Bladeren
1925	March		Umvoti	Flood		SAWS/van Bladeren
1925	April	22	Estcourt	Heavy Rains/Flooding	Cyclone ?	SAWS/van Bladeren
1926	February	16	Newcastle	Heavy Rains/Flooding		SAWS/van Bladeren
1929	June	6 - 9	South Coast	Flood		van Bladeren
1930	January	15 - 17	Northern & Coastal KZN	Flood		van Bladeren
1930	March	6 - 8	South central KZN, Northern KZN	Flood		van Bladeren
1931	July	13 -15	South Coast	Flood		van Bladeren
1932	February	21	KZN North Coast	Extreme flood		SAWS/van Bladeren
1935	June	12	KZN Coast	Flood	Durban, Stanger, Mount Edgecombe	SAWS
1937	February	8 - 11	NE Tvl, Zululand, Swaziland	Flood		SAWS
1939	February	3 -8	Northern KZN	Flood		van Bladeren
1940	May	5	Mainly Zululand Coast	Extreme flood	Eshowe to Port Shepstone	SAWS/van Bladeren
1943	April	21 - 23	Scattered KZN	Flood		van Bladeren
1947	January	14	Pietermaritzburg	Heavy Rains/Flooding		SAWS
1947	February	25	Durban	Heavy Rains/Flooding		SAWS
1947	November	13	Winkelspruit	Heavy Rains/Flooding		SAWS
1948	April	19	Durban	Heavy Rains/Flooding		SAWS

Year	Month	Date	Location	Type	Notes	Reference
1949	April	29 - 30	Zululand	Flood		SAWS
1949	December	1	Durban	Heavy Rains/Flooding		SAWS
1953	January	12 - 13	Durban	Heavy Rains/Flooding		SAWS
1954	May	20 - 21	Eastern Cape/KZN	Heavy Rains/Flooding		SAWS
1956	February	25 - 27	Free State, KZN	Flood	Zululand	SAWS
1956	March	18 - 21	South Coast, Berg	Flood		van Bladeren
1956	December	19 - 22	KZN Coast	Flood	Port Shepstone to Mtubatuba	SAWS
1957	April	26 - 28	KZN Coast	Flood	Durban	SAWS
1957	June	1 - 3	Northern KZN	Flood		van Bladeren
1957	September	21 -26	Northern KZN	Flood		van Bladeren
1957	October	2 - 3	Rbay - Nongoma	Flood		van Bladeren
1958	April	13	KZN South Coast	Flood		SAWS/van Bladeren
1959	May	15 - 17	KZN South Coast	Extreme flood		SAWS/van Bladeren
1960	November	6	Richards Bay area	Flood		van Bladeren
1960	December	28	Pietermaritzburg	Flood		SAWS
1962	January	10	Weenen	Flood		SAWS
1963	March	13	Eastern Cape Southern KZN	Flood		SAWS
1963	July	4	Northern KZN	Extreme flood		SAWS/van Bladeren
1964	June	19	KZN South Coast	Heavy Rains/Flooding		SAWS
1964	October	22	Interior	Heavy Rains/Flooding	Western Free State, KZN, Southern Transvaal	SAWS
1966	January	4 - 7	Mkhathini area	Flood	Tropical Cyclone Claude	van Bladeren
1967	January	24	Ladysmith	Flood		SAWS
1967	February	8	Durban	Heavy Rains/Flooding		SAWS
1970	October	13	KZN South Coast	Flood		SAWS

Year	Month	Date	Location	Type	Notes	Reference
1971	May	12	KZN North Coast	Flood		SAWS
1972	February	19 - 24	KZN			van Bladeren
1973	September	30	Zululand	Flood		SAWS/van Bladeren
1974	February	4 - 9	Interior	Extreme flood	Vaal, KZN, Southern Free State, North Cape, Karro, Namibia	SAWS/van Bladeren
1974	March	11	Durban	Heavy Rains/Flooding		SAWS
1975	January	30	Ladysmith	Flood		SAWS
1975	February	13	Durban	Flood		SAWS
1975	April	21	Amanzimtoti	Heavy Rains/Flooding		SAWS
1976	January	27 - 30	Ladysmith	Flood		SAWS
1976	January	30 -31	Northern KZN	Flood	Tropical Cyclone Terry-Danae	SAWS
1976	March	20 -21	KZN Coast	Flood	Coastal Belt	SAWS/van Bladeren
1977	February	9	Eastern Transvaal Zululand	Extreme flood	Tropical Cyclone Emile	SAWS/van Bladeren
1977	March	4	Durban	Heavy Rains/Flooding		SAWS
1977	December	29, 30	Durban	Heavy Rains/Flooding		SAWS/van Bladeren
1978	January	23	KZN Coast	Flood		SAWS
1978	February	12	Pietermaritzburg	Heavy Rains/Flooding		SAWS
1978	April	20	Margate	Heavy Rains/Flooding/Extreme flood		SAWS/van Bladeren
1980	September	7, 8	KZN Coast	Flood		SAWS
1981	May	15 - 17	North Coast	Flood		van Bladeren
1983	December	25	Durban	Flood		SAWS
1984	January	28	Northeastern KZN	Extreme flood	Tropical Storm Domoina	SAWS/van Bladeren
1984	April	17	Durban	Heavy Rains/Flooding		SAWS
1985	February	7, 10	Eastern Transvaal, KZN	Extreme flood		SAWS/van Bladeren

Year	Month	Date	Location	Type	Notes	Reference
1985	October	29 - 4	South Coast, Scattered KZN	Flood		van Bladeren
1987	February	11	Ladysmith	Flood		SAWS
1987	February	13	Ladysmith	Flood		SAWS
1987	March	5	KZN South Coast	Flood		SAWS
1987	March	15	Pietermaritzburg	Heavy Rains/Flooding		SAWS
1987	March	22	Pietermaritzburg	Flood		SAWS
1987	September	27, 28	KZN	Extreme flood		SAWS/van Bladeren
1987	December	14	Vryheid	Heavy Rains/Flooding		SAWS
1988	February	8	KZN	Flood		SAWS
1988	March	1, 2	KZN	Heavy Rains/Flooding	Margate, Mooiriver	SAWS
1988	March	8, 9	KZN Coast	Heavy Rains/Flooding	South Coast?	SAWS
1988	March	8, 12	Central Interior	Flood	Ladysmith, Free State, W Tvl, N Cape	SAWS
1988	May	5	Durban	Heavy Rains/Flooding		SAWS
1988	December	8	Durban	Flood		SAWS
1989	February	14	Ladysmith	Flood		SAWS
1989	March	14	Amanzimtoti	Heavy Rains/Flooding		SAWS
1989	April	14,15	KZN South Coast	Flood		SAWS
1989	October	30	Pietermaritzburg	Heavy Rains/Flooding		SAWS
1989	November	28,30	KZN	Heavy Rains/Flooding/Extreme flood		SAWS/van Bladeren
1990	March	24,25	KZN	Heavy Rains/Flooding		SAWS
1991	May	9, 13	Zululand	Heavy Rains/Flooding		SAWS Updates
1993	October	7	Zululand	Flood		SAWS Updates
1993	October	17	Zululand	Flood		SAWS Updates
1993	December	27, 30	KZN	Heavy Rains/Flooding		SAWS Updates
1994	January	10	Durban	Flood		SAWS Updates

Year	Month	Date	Location	Type	Notes	Reference
1994	February	2	Ladysmith	Flood		SAWS Updates
1994	March	9	Durban	Heavy Rains/Flooding		SAWS Updates
1994	October	25	KZN Coast	Heavy Rains/Flooding	Durban Area	SAWS Updates
1995	January	14, 15	Pietermaritzburg	Flood		SAWS Updates
1995	March	22	Empangeni	Heavy Rains/Flooding		SAWS Updates
1995	March	22, 23	Durban	Heavy Rains/Flooding		SAWS Updates
1995	December	16, 18	Southern KZN	Flood		SAWS Updates
1995	December	25	Pietermaritzburg	Flood		SAWS Updates
1999	October	26	KZN	Flood		(IOL 1999)
1999	November	16	Pietermaritzburg	Heavy Rains/Flooding		(Oellermann 1999)
1999	December	22	Durban/Pmb	Heavy Rains/Flooding		(Campbell 1999)
2000	November	19, 20	Zululand	Heavy Rains/Flooding		SAWS Updates

APPENDIX II – FLOOD ZONE MODELLING

1. Modelling Methodology Software Programmes and Data Models

In this appendix the software and datasets used are discussed. A detailed data processing procedure that has been used to generate Q_{MRMF} and Q_{M100} flood zone areas.

1.1. Geographic Information Systems

Listed below are the primary software packages and applications used for processing the model. These are all commercial or public domain packages and copyright, usage rights and branding rests with the respective organisations.

1.1.1.1. Software

The philosophy in choosing these particular packages was:-

- A commonly used GIS system with a standard data format to do as much of the processing and data management as possible.
- Software that is widely available and easily accessible.
- User friendly interface on a Windows ® platform

1.1.1.2. ArcGIS® 10.1

This probably the most widely used GIS system. It is a commercial system distributed by ESRI®. Most GIS users are familiar with this software. Its shape file format has become an industry standard and all the datasets used and produced in this study are in this format.

1.1.1.3. Spatial Analyst®

Spatial Analyst is an ESRI® Extension package that is used to do raster/grid based spatial mathematical modelling. It is used extensively for catchment and water surface modelling and is the engine for HEC-RAS®, HEC-Georas® and Archydrotools®.

1.1.1.4. 3D Analyst®

3D Analyst® is an ESRI® Extension package that is in conjunction with Spatial Analyst® and HEC-RAS®, HEC-Georas® and Archydrotools® for cross-section viewing and manipulation.

1.1.1.5. ArcHYDRO Tools®

Archydrotools® is a freeware extension distributed by ERSI®. It is a collection of Spatial Analyst® Tools and hydrological modelling tools specifically designed to do catchment and watershed modelling. In this process it is used to produce a hydrological surface, sub-catchments and drainage lines.

1.1.1.6. ReGIS®

This is the author's preferred choice of CAD software. Any other CAD software can be used. Its main function is to clean the river datasets used in the GIS.

1.1.1.7. HEC-RAS[®]

HEC-RAS[®] is a river analyses software package released as public domain by the Hydrological Engineering Unit a sub unit of the Institute for Water Resources of the US Army Corps of Engineers (Brunner 2008; Brunner 2010; Warner et al. 2010). This is the software used to do the flow modelling for this project. It is a standalone package but has import and export capability to interface with ArcGIS[®].

1.1.1.8. HEC-Georas[®]

Also a release of the Hydrological Engineering Unit (Cameron & Ackerman 2011), this is a plug-in for ArcGIS[®] and allows the user to do all the data preparation and create the setup files in the GIS that is then exported for use in HECRAS[®]. Once the flow analysis is completed it allows for the import of the data back into the GIS where the final inundation data is produced.

1.1.2. Datasets

As the process is GIS driven and the products from the project must integrate with existing GIS datasets part of the exercise is to determine:-

- What datasets are needed to carry out the model processing, the aim being to use as many existing GIS datasets as possible.
- Which of these are readily available, preferably as public domain information?
- What is the integrity and completeness of the data and what refinement of the data will be required to bring it to the standard need for the modelling process?
- Which of the required datasets still need to be captured?

The minimum required datasets to carry out the modelling process are:-

- Rivers – to guide drainage line processing.
- Digital Elevation Models (DEM) – to develop a hydrological drainage surface.
- Cut lines or cross-sections across rivers to determine the drainage valley shape. These have to be captured as a new dataset.

Optional datasets include:-

- Bridges and culverts – This will be ignored as the modelling process requires very specific data that may not be available at this time.
- Ineffective flow areas – This is ignored. It relates primarily to flow around bridge structures and is very site specific.
- Ezemvelo KZN Wildlife land cover data (Fig. 1E).
- Obstructions – Relates to flood plain areas that remove flow area from the profiles. Site specific data which is not available and is ignored.
- In line structures – Requires structure specific information about dam walls and weirs and where this is available it will be applied.
- Levees – To be ignored.
- Lateral Structures – Primarily used to mark areas where flow will spill from the main flow into storage areas. To be ignored.
- Storage Areas – Areas of water retention adjacent to the main flow channel but not part of the floodplain and separated from it by a lateral structure. To be ignored.

Other datasets will be used for the overall project such as homestead positions, administrative boundaries, etc., that add informational value but are not part of the modelling process.

All the datasets used in this process are copyrighted and made available by the various national and provincial governments departments. Any modifications and alterations made were done to bring the data to the standard needed for the modelling process.

1.1.2.1. SG Rivers

Use is made of the Surveyor General (SG) 1:50 000 map vector dataset. This is effectively the river data as it appears on the 1:50 000 map series. This is a good dataset from an informational point of view but the vector lines tend to be fragmented and not always continuous, especially in areas that cover marshes and where they intersect with water bodies. Another deficiency of the data is the fact that the smaller rivers and streams were captured as vector lines and the larger rivers were captured as river polygon areas according to their flood plains. As the modelling process requires vector lines all the river areas has to be recaptured as vector lines (Fig. 1A).

1.1.2.2. Department of Water Affairs (DWA) Quaternary Catchments

To effectively manage the project the study area had to be subdivided into smaller units. As the project revolves around drainage and catchments the quaternary catchment dataset of DWA is used. There are 275 quaternary catchments that underlie the study area and a further 49 that directly influence water flow in it. This layer forms the foundation for all data processing.

1.1.2.3. SG Contours

Contour data form the basis for the DEM modelling. Again the source of this elevation data is the Surveyor General's 1:50 000 map series 20m contours. There are available for the whole of the study area. Where possible the 5m contours from the 1:10 000 map series is used, but this has not yet been captured for the everywhere within the study area. On the whole both datasets are good. The only problems encountered were some mislabelled elevation values which creates artefacts in the DEM interpolation and alignment discrepancies between the original map sheets that were transferred to the vector data.

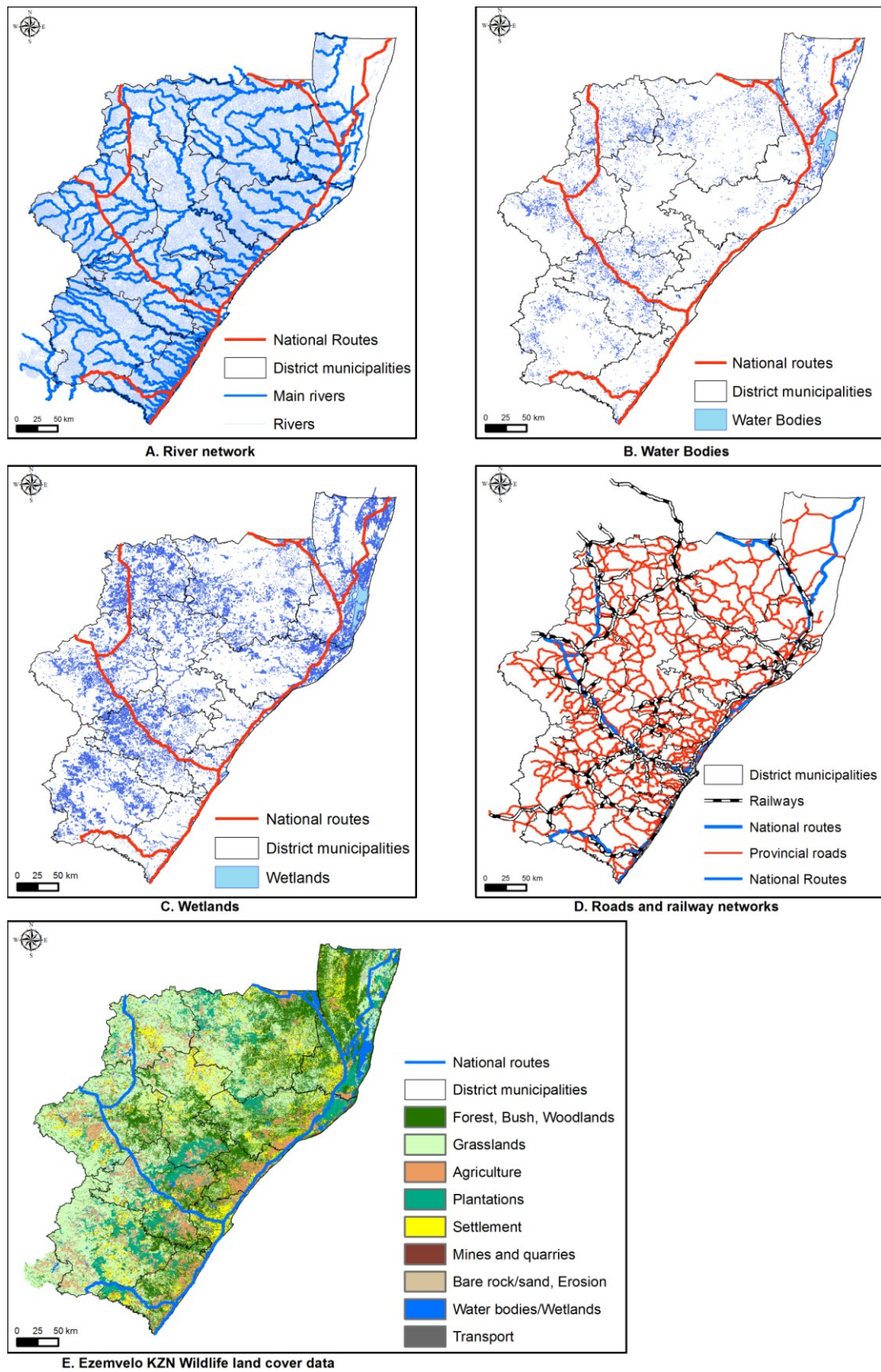


Figure 1. Example of datasets

1.1.2.4. ASTER GDEM Data

Within certain portions of the study area the SG Contour data proved to be unsuitable or not readily available. Initially the SRTM (Shuttle Radar Topographic Mission) 90 data was used for these areas but is replaced by the recently released ASTER (2010) (Advanced Spaceborne Thermal Emission and Reflection Radiometer, Global Digital Elevation Model (GDEM) (This data is applied to the low relief areas of the Makhathini Flats where the 20 m contour data is to sparse and there is not sufficient coverage of the 5m contours to produce reliable hydrological surfaces. ASTER data was also used to provide elevation data for quaternary catchments that fall outside the borders of South Africa.

1.1.2.5. Other Contour Data

In some cases the larger municipal structures have 2m contours available and are integrated into the DEM interpolation process.

1.1.2.6. SG Water bodies

This is also sourced from the Surveyor General (SG) 1:50 000 map vector dataset. The pans, lakes and dams are used to level out the hydrological surface where these features occur (Fig. 1B).

1.1.2.7. KZN DOT Roads

Road network data (Fig. 1D) is sourced from the Kwazulu-Natal Department of Transport. It is used to determine bridging points with the rivers. Further use of this data (other than as an information layer) will depend on the availability of engineering information for the bridge and culvert structures.

1.1.2.8. SG Rail

Sourced from the Surveyor General (SG) 1:50 000 map vector dataset this is also intended for use to determine bridging points with rivers (Fig. 1D). Again further use of this data (other than as an information layer) will depend on the availability of engineering information for the bridge and culvert structures. In certain locations, mainly along the coast this data will be used as an obstruction feature where the rail bed has been raised and creates a partial barrier across river mouths.

1.1.2.9. Ezemvelo KZN Wildlife Land Cover Data

This data forms the basis for evaluating sub-catchment land cover for flash flood determination. (Fig. 1E).

1.1.2.10. Ezemvelo KZN Wildlife Wetlands Data

This was not used directly in the modelling process other than what is delineated in the land cover dataset. This forms an addendum layer in the final product to indicate areas of potential water ponding, especially during flood events (Fig. 1C).

1.1.3. Spatial Referencing

Due to the large geographic extent of the project area and the fact that it extends over three Transverse Mercator meridians working in a geographic projection would have been preferable. Especially as the final product output will most likely be in this format to match other widely used datasets.

However, because of the way in which Spatial Analyst[®] processes data by using the mapping units for many of the calculations, problems are created when the expected calculation uses degrees instead of metres. For this reason all data has to be in a projected format. A Universal Transverse Mercator Projection (UTM 36S) was considered as it provided the best extent over the study area, but because it is probably an unfamiliar projection format for most GIS users this was rejected.

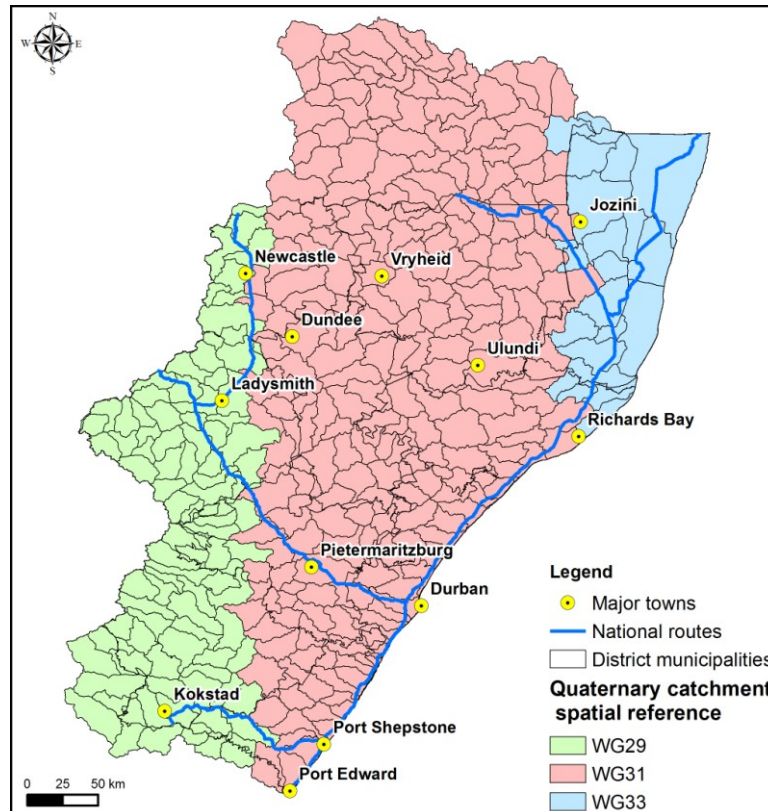


Figure 2. Spatial referencing

It was decided to instead use the Transverse Mercator projection and use the three standard meridians 29°, 31° and 33°. The geodetic surface used is the World Geodetic Surface (1984) with the Hartebeeshoek Tie Point. Hence all data was re-projected and all modelling calculations done using either the WG29, WG31 or WG33 projections. Quaternary catchments are assigned to the relevant projection and where they intersect more than one projection, assigned to that projection into which the bulk of the quaternary catchment falls (Fig. 2).

1.1.4. Data Processing

Producing flood risk area polygons from the basic datasets can be divided into eight processing steps. Each of these consists of a number of procedures to produce the output.

1.1.4.1. Quaternary Catchment Selection and Data Extraction

The quaternary catchments that directly underlie the study area were selected from its intersection with the District Municipality layer. Using the river layer as a guide the quaternary catchments surrounding the study area were inspected manually to see if they were part of a larger catchment whose water flowed into the study area. A polygon “envelope” was constructed around each quaternary catchment which forms the basis for all data extraction and modelling boundaries. Firstly the quaternary catchments from each projection band were selected and a 1000m buffer was constructed around each quaternary catchment. In turn a bounding polygon was created for each quaternary catchment using the buffered data as a base. The quaternary catchment envelope was assigned the same name as the original quaternary catchment. Each of the basic datasets used is clipped to the each quaternary catchment envelope and stored as part of the quaternary catchment data structure.

1.1.4.2. Catchment DEM Processing

In theory this is a three step process. Firstly extract the relevant contours; secondly interpolate these to a DEM; thirdly clip the DEM to the quaternary envelope. However, in reality it soon became apparent that such a simplified process was flawed by technical constraints and dataset problems. Processing data for large areas usually requires a trade-off between the size of the data block to be processed and the numbers of block to be processed to give the required result. As an example, interpolating the same block of contours to a 10m resolution DEM takes about 1 minute. The same block interpolated to 5m takes on average 5 minutes. At the same time, the desktop computer used for the processing, could interpolate a complete 1:50 000 block at 10m resolution it did not have enough memory to do the same process at a 5m resolution. The hydrological DEM is the foundation upon which the rest of the data modelling will be placed.

Hence, generating the best hydrologically precise DEM that could reasonably be produced from the available data had priority over processing time.

1.1.4.3. Elevation Data Extraction

Given that 74% of the study area was already covered by 5m contours and that in time the complete dataset will become available for the area it was decided to use this as the basis for elevation modelling (Fig. 3). Those areas that only had 20m contours available were interpolated with the same parameters used for the 5m contours. Spatial Analyst[®] Topo-to-Raster Tool is used for interpolation of the contour data with its emphasis on drainage enforcement and surface continuity to create the hydrological surface.

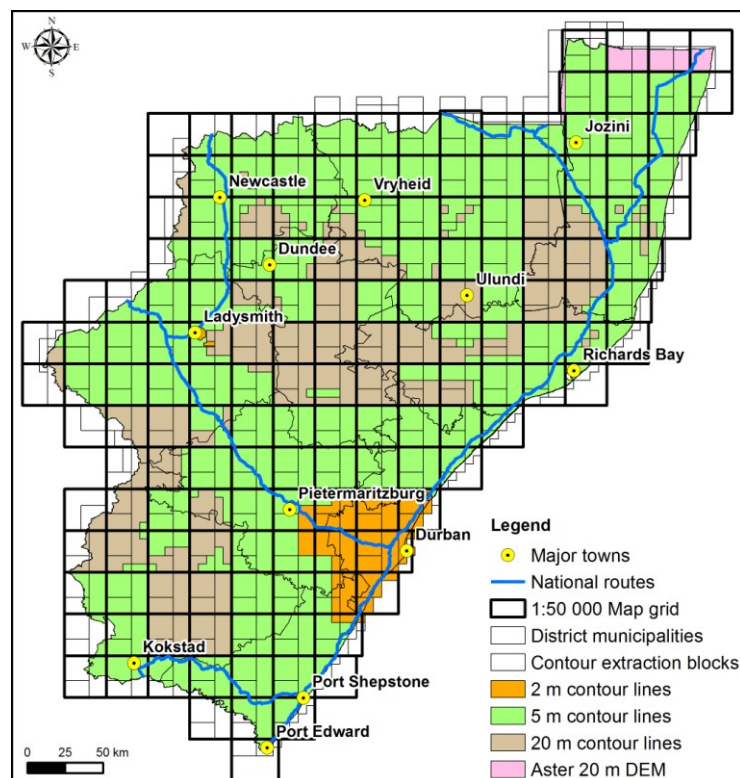


Figure 3. Contour interval distribution

To overcome the technical restraint of the data block size that the computer could process each 1:50 000 map was split into three blocks using the 1:10 000 grids as a guide. (Fig. 3). Using 1:50000 and 1:10000 map grids as a base have a number of advantages. Contour datasets available are not continuous lines but split along these mapping grids. As a result the relevant data can be selected via the database, making selection and extraction of contours faster than first block selecting the data, writing the selection out to a temporary layer and then clipping it to the desired boundaries. Where the 5m contours are available, they do not always cover a complete block and the block is then split and the 20m contours are then only extracted for the area not covered by the 5m contours. There are two geographic areas where this process was modified. Where 2m contours are available these have been used to replace the 5m/20m contour data (Fig. 3). The end product of this processing step is a 2m, 5m and 20m contour shape file per 1:50000 block where relevant.

1.1.4.4. Surface Interpolation

Using the Topo-to-Raster Interpolation Tool in Spatial Analyst[®] each of the 1:50 000 blocks was gridded and a DEM created. This is a tool specifically created by ESRI to interpolate contour data to a hydrologically correct surface. Each block was processed using the following parameters:-

- Output Surface Raster {[xxxx]_dem}
- Output Cell Size {5m}
- Margin in cells – {20}
- Drainage Enforcement – {Enforce}
- Primary Type of input data – {Contour}
- Other optional variable ignored.

Each DEM was then used to create a shaded pseudo 3D image using the Spatial Analyst[®] Hillshade Tool in with a 2 times vertical exaggeration. The Hillshade surface was then visually inspected for gridding artefacts. It was found that these were predominantly the result of incorrect elevation data in the database. Where this problem was encountered the contour data was corrected and the Topo-to-Raster Interpolation run again to produce a corrected DEM.

1.1.4.5. Quaternary Catchment Surface

To create a DEM surface for each catchment the catchment envelope layer and the 1:50000 block layer was used as a guide. By selecting a catchment envelope inspection showed which DEM blocks were needed to cover the catchment envelope. Using the ArcGIS® Mosaic-to-New Raster Tool these DEMs were mosaiced to create a temporary raster using the following parameters:-

- Coordinate System for the Raster – {Relevant projection band – WGx}
- Pixel type – {16 bit signed}
- Cell Size – {5}
- Mosaic Method – {Blend}

The temporary raster was then clipped (ArcGIS® Raster Processing Clip Tool) to the catchment envelope to produce the final catchment DEM. For the catchments that intersect the coast, the catchment envelope was split along the 0m contour and the offshore part of the DEM was blanked. This was done using the Spatial Analyst® Extract-by-Mask Tool using the onshore component of the catchment envelope as the mask.

1.1.5. Sub-catchment and Drainage Modelling

To determine the flow paths and sub-catchment boundaries, further manipulation of the DEM surface is required to produce a hydrologically correct surface before flow modelling can be carried out. All the processing steps below were carried out using ArcHYDRO Tools®. The output from a process step becomes the input for the next step (Fig. 4).

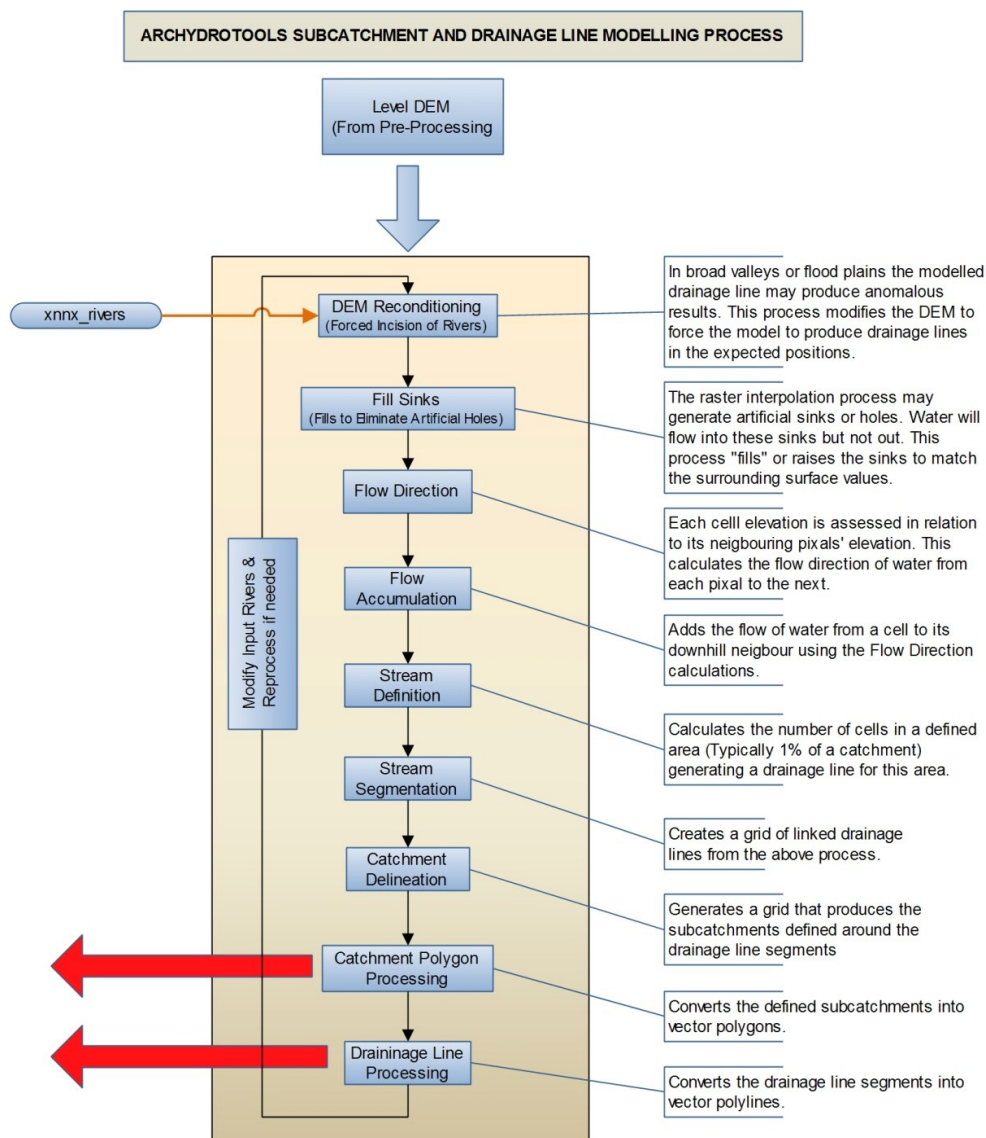


Figure 4 Archydrotools© Processing Flow Diagram

1.1.5.1. Level DEM

All water bodies (dams; lakes; pans) need to have their underlying pixel elevations levelled to the same value. The DEM interpolation does not necessarily take these features into account and this process will enforce these features onto the DEM. Due to the fact that the surface elevation

for most of the water body data is unknown; the fill elevation used is {None}. The software will then compute an average elevation for each water body and apply this when processing (Fig. 5).

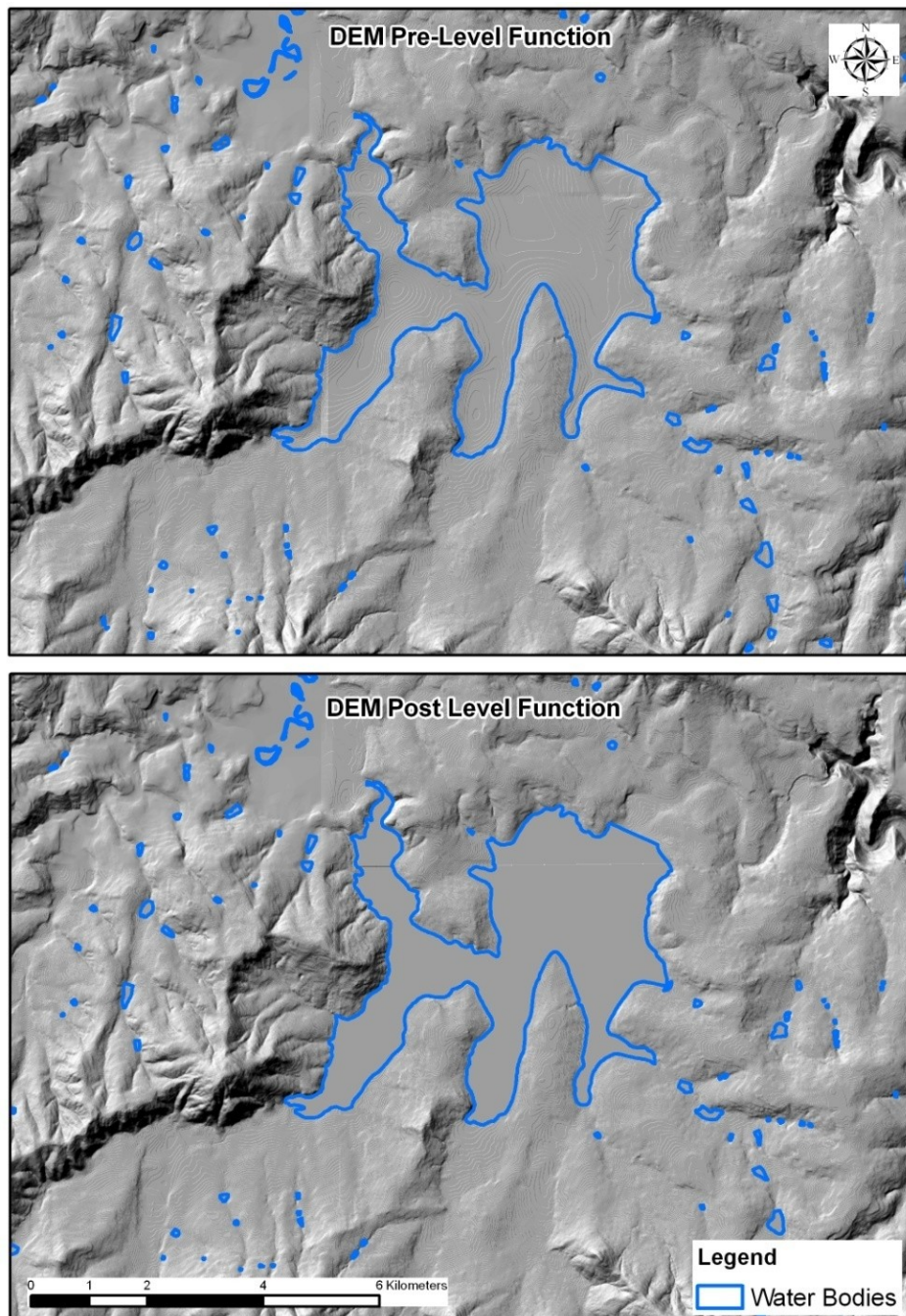


Figure 5. Level DEM

1.1.5.2. DEM Reconditioning

The positions of rivers and streams need to be imposed onto the DEM surface (Fig. 6). This tool modifies the DEM by over emphasising the known drainage lines, in effect creating very deep river channels to force the surface drainage to be consistent with the existing river vector data.

Three variables are applied to the DEM surface:-

- A river buffer zone to which the process will be applied. This is based on the DEM cell sizes and a value of {5} is used. Effectively a 25m buffer around each river.
- Smooth drop distance {10m} creates a gradual lowering of the DEM surface towards the river centreline.
- Sharp drop value {2000m} creates an incision into the DEM surface. This over emphasis is not only needed to enforce river positions but is necessary for the next process of sink filling. If the value used is too small the Sink Fill process will consider the incised drainage lines as sinks and remove them, negating the exercise of river enforcement.

1.1.5.3. Fill Sinks

During the DEM interpolation, Level and DEM reconditioning processes the modelling may create “Sinks” or holes where water will flow in but not necessarily flow out. This process eliminates these sinks.

1.1.5.4. Flow Direction

The software examines each cell and assigns it a value base on how many surrounding cells at a higher elevation flow into it. The output is a new surface displaying the flow direction of water on the hydrological surface (Fig. 7).

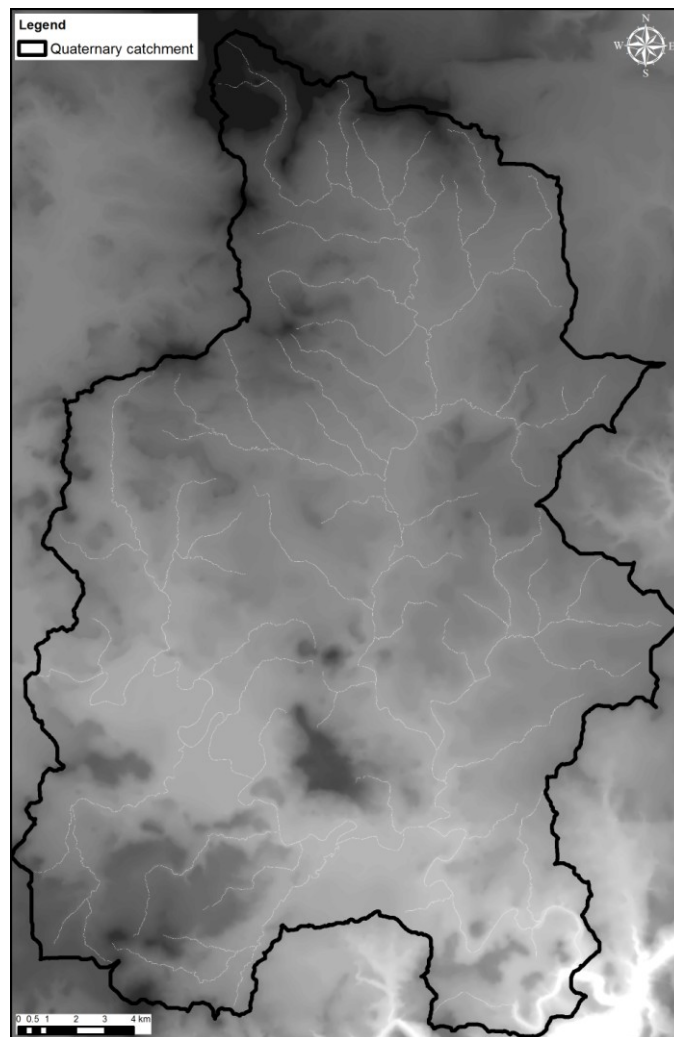


Figure 6. Example of river courses incised into the DEM.

1.1.5.5. Flow Accumulation

This process uses the Flow Direction Grid and calculated the flow accumulation from the upstream cells (Fig. 8).

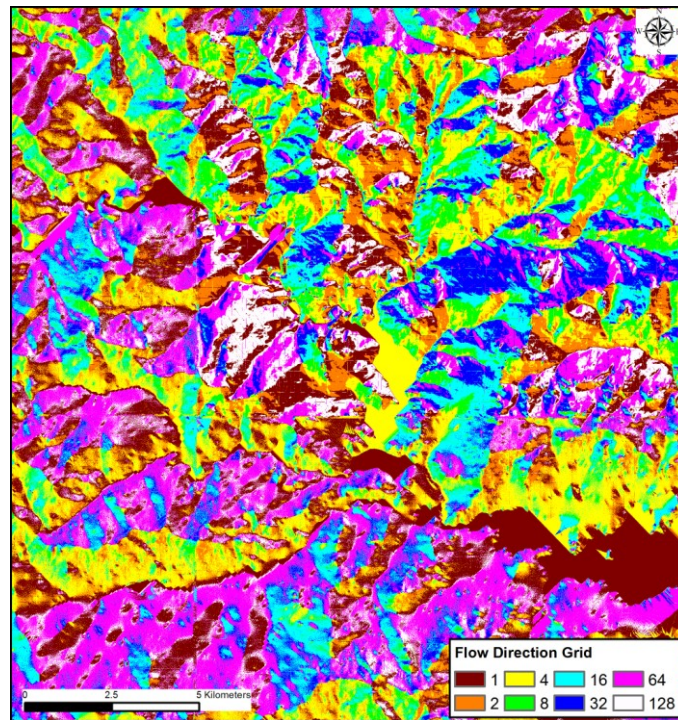


Figure 7. Flow direction model.

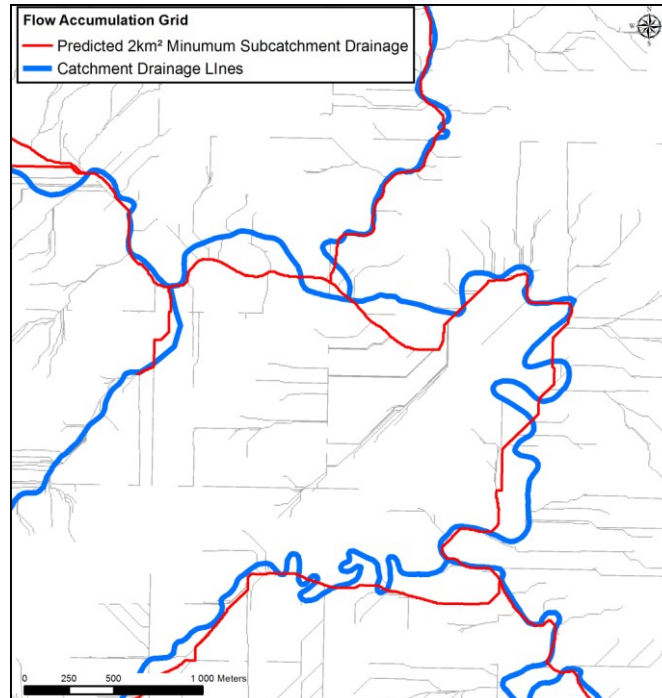


Figure 8. Difference between automated drainage and vector data.

1.1.5.6. Stream Definition

Using the Flow Accumulation Grid, a stream or river grid is created along the lines of highest flow accumulation. The number of streams created is a function of the user supplied variable that defines the minimum drainage area. It is recommended to use a value that is 1% of the overall model surface area.

Testing done using 1km², 2km² and 5km² sub-catchment areas were done (Fig. 9). This compares the various generated drainage lines based on sub-catchment areas, against the actual drainage lines (thick darker blue lines) used in the modelling process. As can be seen, the 5km² outputs (green lines) does not give sufficient coverage. The 1km² (orange lines) does not realistically add extra drainage lines other than some minor streams and mainly tends to extend the 2km² drainage lines (red lines).

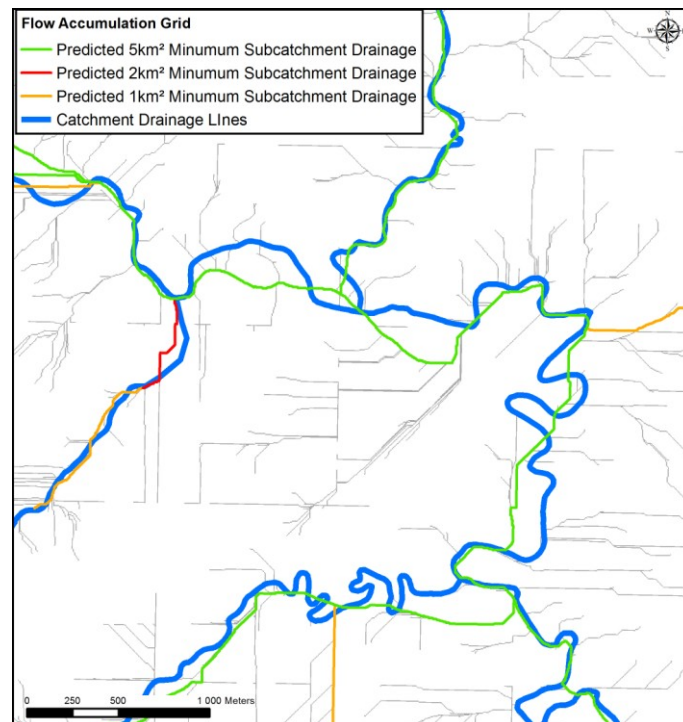


Figure 9. Comparison between drainage lines generated from various sub-catchments sizes.

It was decided to use a consistent value of 2km² across all the quaternary catchments. This value matched the recommended 1% in 67 catchments was less than 1% in 193 catchments and exceeded the 1% in 20 catchments.

1.1.5.7. Stream Segmentation (Linking)

This is an intermediate processing step, linking defined stream segments.

1.1.5.8. Catchment Grid Delineation

Unique values are assigned to cells that drain into the various associated linked stream segments, forming a subcatchments (Fig. 10).

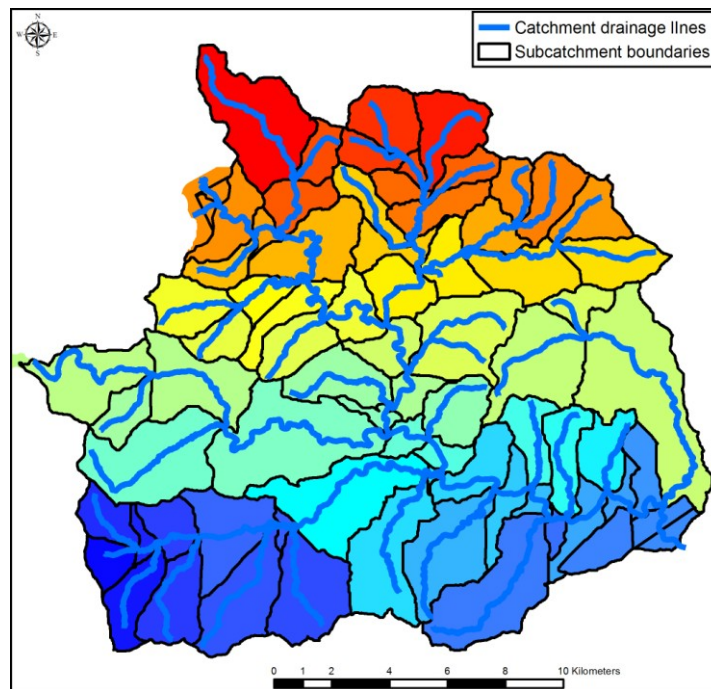


Figure 10. Subcatchment boundaries generated from a Stream Link Grid

1.1.5.9. Catchment polygon Processing

This process converts the raster grid into a series of sub-catchment polygon features. It is these polygons that are used to calculate water run-off values for the flow modelling process.

1.1.5.10. Drainage Line Processing

The process converts the stream segment grid into vector lines. These generated or synthetic drainage lines are used to check the selected river vector data and by extension that the number of sub-catchments matches the number of drainage lines within the quaternary catchment.

1.1.5.11. Drainage Line Pre-Processing

In doing a number of test models it became apparent that the river vector datasets (SG) were not suitable for use in their current state (Fig. 11). The fragmented and disconnected lines could not be used in the DEM reconditioning process with any confidence because the Sink Fill process identified these incised segments as sinks and removed them.

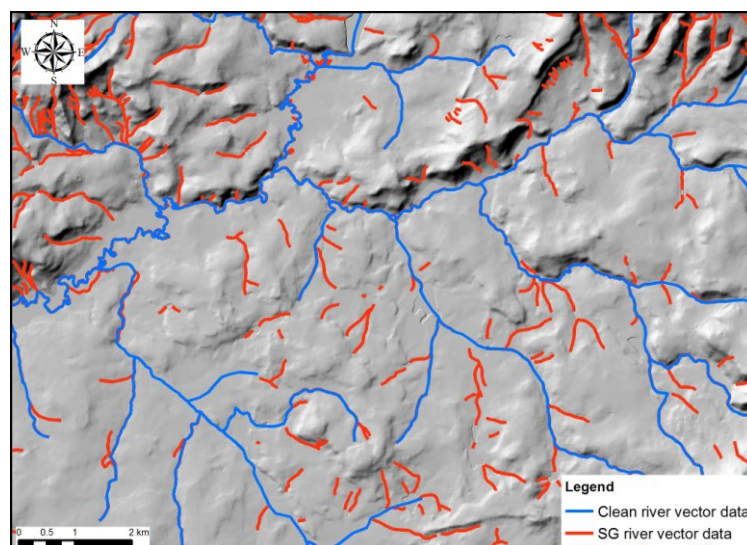


Figure 11. Drainage lines issues

The only solution was to clean up the vector data and to ensure that each line intersection was snapped to each other, that all fragmented/discontinuous lines were resolved and that rivers continued unbroken across water bodies. Not only is a coherent river dataset necessary to produce a correct hydrological surface, it is a crucial dataset for the flow modelling process.

To eliminate the need of spending a lot of pre-processing time (Fig. 12) cleaning every river and stream in the river datasets it was decided to process the hydrological surfaces by skipping the DEM reconditioning and catchment delineation steps. The drainage lines produced from this are then used as “predictor” drainage. Overlying the predictor drainage on the existing river datasets allows for only the necessary vector lines to be selected and extracted for cleaning.

The hydrological modelling process is then carried out as described above and the synthetic drainage lines checked against the cleaned data. Any variations are rectified and the process is carried out again. Iterations of this process is carried out until the cleaned river dataset matches the synthetic drainage lines.

1.1.6. River Analysis Geometry

Having generated a hydrological surface, delineated sub-catchments and generated the flow or drainage lines in a catchment, the next step is to create the river geometry that is used in the HECRAS[®] software to do the river analysis.

For this process ArcGIS[®] is used to capture the required data and HECGeoras[®] is used to create the required layers and populated databases that is exported to HECRAS[®].

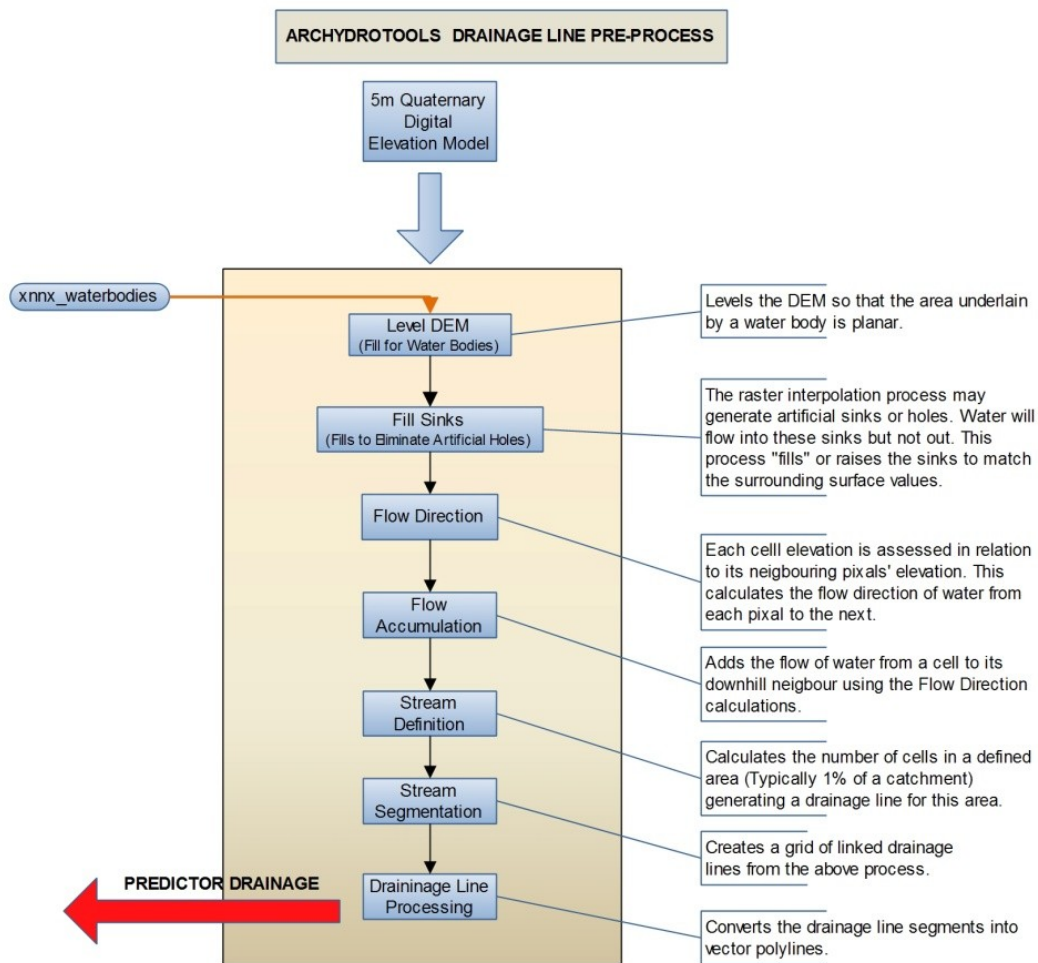


Figure 12. Archydrotools® Drainage Line Pre-processing

HECGeoras© generates four data types:-

- Required surface – Either a Raster or TIN model of the hydrological surface. A TIN surface seems to create less processing failures and hence the hydrological DEM is converted to a TIN surface using 3D Analyst®.
- Required Layers:-
- Stream Centreline – rivers/drainage lines created in the previous process. Each of these have specific information captured in the database
- XS Cut Lines – cross-section lines drawn at right angles to the drainage lines. These are used to extract data along the profiles that is used to model the drainage valleys.
- XS Cut Line Profiles – 3D version of the cut lines, where the z-value has been attributed.

Optional Layers – there are a number of optional layers that can be used to define the characteristics of the associated drainage lines. These include levees, land use, obstructions, inline structures, banks, bridges/culverts, lateral structures and storage areas. For this process only the layers listed below are used and some only where there is available data.

- Flow path – generated from the stream centreline data and used to define flow in HECRAS.
- Bridges/culverts – only used where the necessary engineering structure data is available
- Inline structures – only where the necessary dam/weir structure data is available.
- Lateral Structures - where this applied and the necessary structure data is available.
- Optional Tables - most of these relate to optional layers which are not being used.

1.1.6.1. River Processing

A stream centreline is created and the data from the drainage line layer is copied into this. The stream centreline has six values to be captured in order to populate the database table, River name, Reach name, From node, To node, From station and To station. Of these only the River and Reach Names are entered manually, the rest are auto-generated.

Each drainage line segment, that is, from the start of a river to a confluence point or sections between confluence points is coded with a unique identifier made up of the river name and the reach name. For example the Mgeni River is made up of a number of reaches (segments) and is coded as Mgeni-Reach1, Mgeni-Reach2 etc.

Certain rules apply to the river data layer.

- River vector lines must start on the upstream end and finish on the downstream end.
- Rivers must meet at a junction (confluence points).
- River segments must have unique identifiers.
- Rivers may not cross.

- Reach names must start on the highest up stream segment of a river and count in the downstream direction.

To ensure that these rules are adhered to, a function in XtoolsPro[®] called ‘Show Direction’ is used and this draws arrows on the river vector lines indicating the direction. If necessary the ‘Flip Line’ tool in Edit Tools[®] is used to correct the line direction.

In this project, the geographical names of the rivers were ignored because only the larger rivers were named and many of the smaller tributaries are unnamed or have names duplicated in different parts of the province. To ensure that river and reach names are unique, an alphanumeric coding based on the catchment names is used instead. Using the V12G catchment as an example, the naming convention is as follows (Fig. 13) :-

- The primary drainage line is named ‘V12G’ and the first reach ‘1’, the second reach ‘2’. Starting at the upstream point the river is coded V12G_1, V12G_2 V12G_3 etc. By convention the longest drainage line in the catchment is taken to be the primary river. This situation applies to those catchments on the periphery which are situated at the highest elevation and has no rivers flowing into them. Where water flows from one catchment to another, the relevant drainage line is designated the primary drainage line even if it is not the longest drainage line in the catchment.
- Drainage lines that junction onto the primary drainage line (secondary drainage) is designated ‘a’, ‘b’, ‘c’ etc and sequentially labelled in the upstream direction. The longest series of connected river segments is considered to be the secondary drainage line. The first upstream intersecting river is then coded V12Ga_x, the second V12Gb_x etc.
- Similarly, rivers that junction onto secondary drainage lines are considered to be tertiary drainage and coded V12Ga1_x, V12Ga2_x sequentially in an upstream direction. Again the longest series of connected river segments is designated as the tertiary drainage lines.

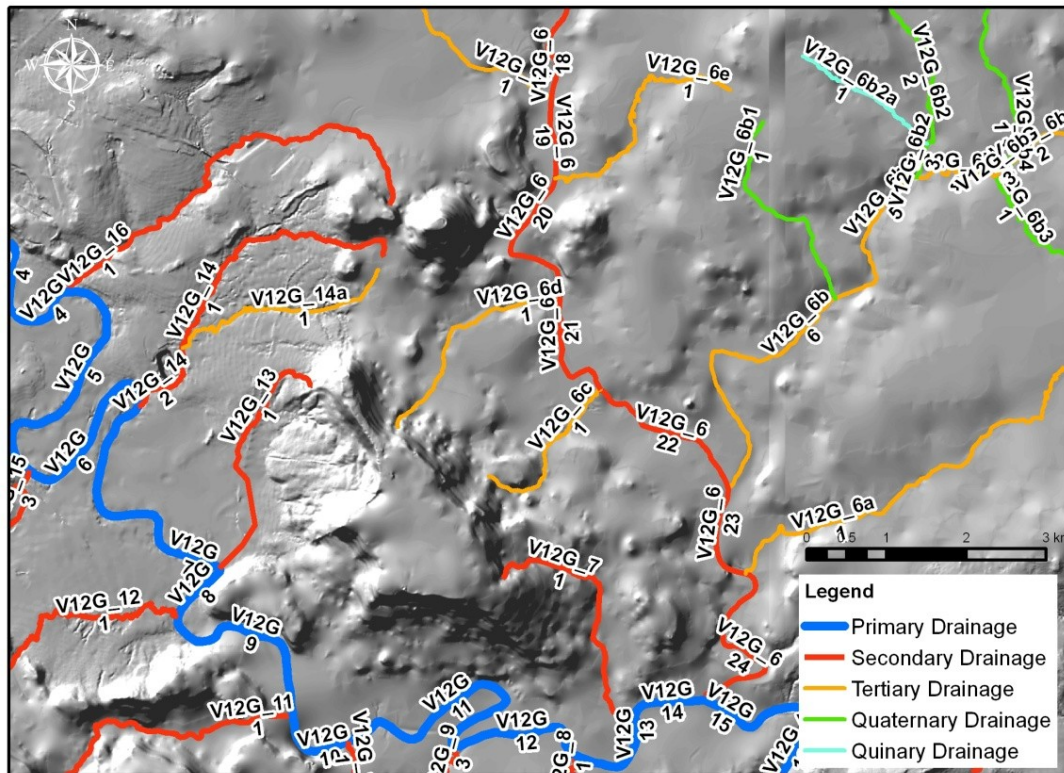


Figure 13. Example of river order and reach labelling.

The same procedure is applied to the quaternary and quinary drainage lines and coded V12G1a1_x, V12G1a2_x etc. and V12G1a1a_x, V12G1a1b_x etc., respectively. Again the longest series of connected river segments is designated the quaternary and quinary drainage lines respectively.

As a rule, the existing state (perennial/non-perennial) or status (1st, 2nd, 3rd order etc.) of a river is ignored in this nomenclature convention. This is deemed immaterial because under conditions of heavy rainfall the longer the river, the more sub-catchments it will intersect and hence will accumulate a greater volume of water.

Once all the drainage line segments have been coded, the Stream Topology Tool is run. This creates a node assignment process at the start and end of each river reach and populates the From Node and To Node fields in the table.

The Lengths/Station Tool populates the From Station and To Station fields, the starting and ending distance between nodes based on river/reach coding.

1.1.6.2. Cross-Section Processing

To model the behaviour of water surfaces in a drainage valley, the shape and spatial characteristics of the valley must be known. This is done by creating a series of cross-sections (cut lines) at right angles to the drainage line (Fig. 14).

In generating the cross-sections, certain rules have to be applied:-

- Cut lines have to start on the left bank and stretch to the right bank when facing downstream.
- Cut lines have to be perpendicular to the flow path.
- Cut lines may not intersect.
- Cut lines may only cross a drainage line once
- Cut lines may not extend past the edge of the hydrological surface.
- Cut lines should long enough to extend over river banks far enough to extend past the expected flood extents.

The automatic cut line generation tool is used to create lines at {500m} intervals and line lengths of {500m} giving a 250m extent on either side of the drainage centreline. These are used as guides for the manual placement of the extra cut lines.

Processing test data block of flood level water extents have shown that where rivers tend to be straight the cut lines generated by the automatic tool produce acceptable results for the shape of the water extent polygons. However, where the rivers bend, at confluences and areas with broad valleys the automatic cut lines need to be augmented with manual cut line placement else there is a tendency for the output to be squared-off or truncated before the expected water extent is reached.

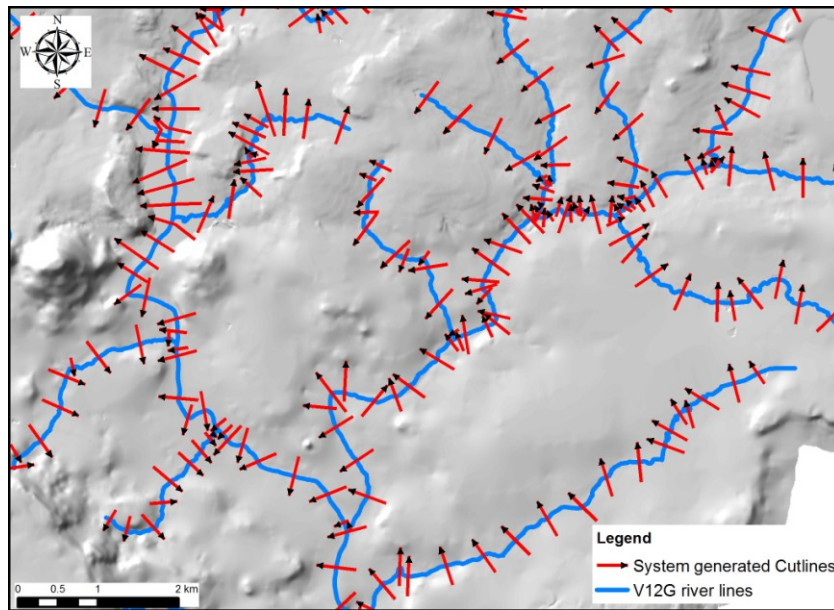


Figure 14. Cutlines

To check that the cut lines are pointing in the correct direction, the XtoolsPro[®] function ‘Show Direction’ is used. If necessary the ‘Flip Line’ tool in Edit Tools[®] is used to correct the line direction.

Cross-sections were generally placed at approximately 50 m intervals perpendicular to flow. Closer spacing either resulted in very long processing times or the data generated exceeded the processing capacity of the HEC-GeoRAS[®] software. Where there are road crossings (guided by KZN DOT roads data), railway crossings (SG 1:50 000 railway feature class) and dam walls (taken from satellite and aerial imagery) cross-sections were placed across these features. Visual inspection of a hillshade model, produced from the hydrological DEM surface, was used to place additional cross-sections on steeper slopes. This was done where there were marked changes in slope, channel width and any other geographical features that may affect flow such as wetlands (EKZN Wildlife data). The sub-catchments and their coinciding reaches are used for flood routing modelling.

Once the cut lines are created the database fields are automatically populated by using the ‘Cut Line Attributes Tool’ to populate the “River”, “Reach”, “Station” and “Chainage Length” fields in the database table. The ‘Elevation Tool’ creates the 3D Cut lines layer by assigning z-value along a cut line from the hydrological surface.

1.1.6.3. Optional Layers

Currently none of the data required to populate these fields are available and will not be discussed here in detail. Should data become available during the course project the document will be reviewed. Suffice to say that the optional layers are created in a similar way to the Cut Line data.

1.1.6.4. GIS Data Export

Once all the available data has been captured and correctly assigned in the “Layer Setup Tool”, HECGeoras[®] extracts the data from the various layers and creates a .xml export file that can be read by HECRAS[®].

1.1.7. Catchment Regional Maximum Flood Modelling (RMF)

Calculating the amount of water that can fall within a catchment or sub-catchment needs to be determined because it is this discharge that is applied to the flow modelling to produce the water surface extents in a drainage line during flood conditions. The target is to calculate at least three predicted water surfaces namely, the maximum flood conditions (Q_{RMF}) the statistical 100 (Q_{1M100}) and 200 (Q_{M200}) year reoccurrence intervals.

Using existing recorded maximum rainfall figures will not necessarily equal the highest possible rainfall. At the same time each catchment does not have a recording station so there is no standard maximum rainfall dataset available per catchment.

A means to calculate the maximum rainfall per catchment is needed, that can be applied to each catchment in a consistent manner. For this the Regional Maximum Flood Peaks Model is selected (See Chapter 6).

1.1.8. River Analysis and Modelling

The .xml GIS export file generated by HECGeoras© is imported into HECRAS© where river flow modelling processing takes place. A series of modules are used to do the hydraulic (water flow) computations.

1.1.8.1. Flow Geometric Editor

Once a new project file is created in the main HECRAS© interface, the exported .xml file can be imported into the Geometric Editor (Fig. 15). This procedure imports the drainage flow lines, cross-section (cut lines) and any other spatial features created in ArcGIS© and exported from HECGeoras©.

The geometric interface can be used to capture or edit data and generally allows for the management of spatial data.

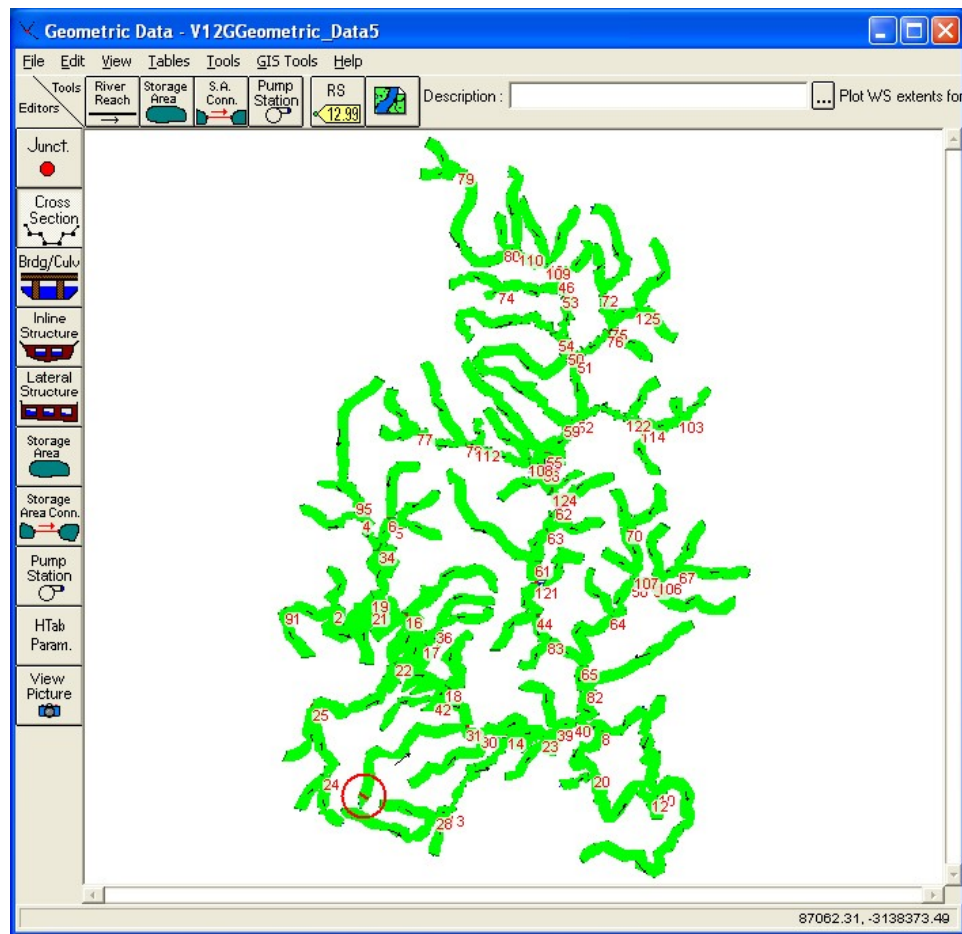


Figure 15. Screen shot of the Geometric Editor

1.1.8.2. Steady Flow Editor

HECRAS can compute two type of flow analysis, Steady Flow and Unsteady Flow. For this process Steady Flow (Fig. 16) is used and although a less complicated process the data required for the computation is easily obtained or created in the context of this exercise, while data for Unsteady flow is not available on a provincial scale.

In the Steady Flow Editor creates a table which lists all the river reaches to be analysed in the catchment. The first task is to select the number of water surfaces profiles to be calculated. Once

this has been done the RMF sub-catchment water flow volumes (as calculated in 2.7) is entered into the table for the corresponding River Reaches.

The boundary conditions need to be set for each upstream portion of the river reaches. Boundary conditions are essentially the starting water level. As these are unknown the 'Critical Depth' option is used which allows the software to automatically calculate a water depth value based on given data.

The screenshot shows the 'Steady Flow Data - v12g_Steady_Flow_Data1' window. It includes a menu bar (File, Options, Help), a text field for 'Enter/Edit Number of Profiles (25000 max):' with the value '3', and buttons for 'Reach Boundary Conditions ...' and 'Apply Data'. Below this is a section for 'Locations of Flow Data Changes' with dropdowns for 'River:' (v11_50) and 'Reach:' (1), and a 'River Sta.:' field (34.89212). There are also buttons for 'Add Multiple...' and 'Add A Flow Change Location'. The main part of the window is a table with two main sections: 'Flow Change Location' and 'Profile Names and Flow Rates'. The table has columns for River, Reach, RS, RMF100, RMF200, and RMF. The data is as follows:

Flow Change Location			Profile Names and Flow Rates		
River	Reach	RS	RMF100	RMF200	RMF
1 v11_50	1	34.89212	2233	1476	4060
2 V12G	1	47155.95	90	108	164
3 V12G	2	44454.27	155	186	281
4 V12G	3	39635.47	26	31	47
5 V12G	4	39040.81	88	106	161
6 V12G	5	35990.96	89	107	162
7 V12G	6	32776.75	55	66	100
8 V12G	7	30516.16	98	117	178
9 V12G	8	27148.46	32	38	58
10 V12G	9	26375.97	108	130	197
11 V12G	10	23783.93	52	63	95
12 V12G	11	22783.93	115	138	209
13 V12G	12	19374.81	61	74	112
14 V12G	13	17513.74	71	85	128
15 V12G	14	16283.93	42	51	77
16 V12G	15	15281.32	84	101	153
17 V12G	16	13519.36	116	139	210
18 V12G	17	9826.02	159	191	289
19 V12G	18	4084.64	41	49	74
20 V12G	19	3687.46	123	148	223
21 V12G_1	1	7341.79	171	206	311

At the bottom of the window, there is a text field with the label 'Edit Steady flow data for the profiles (m3/s)'.

Figure 16. Screen shot of the Flow Data Editor

1.1.8.3. Steady Flow Analysis Computation

Once all the data has been entered, the Steady Flow Computation Interface is used to select the flow regime. For this process all calculation are done as Supercritical, i.e. flood conditions. The computation is executed and if there are any errors or missing data values the system lists them

for correction. If no errors are encountered the water surface extents are calculated for the water surface profiles as listed in the Steady Flow Editor. Extra cut lines can now be interpolated automatically between earlier defined cut lines imported from the GIS. For this a distance of 10m is used. The Steady Flow Computation is re-computed for these additional cut lines.

1.1.8.4. Cross-section Viewer

This viewer is used to inspect individual cut line profiles (Fig. 17). It is used to visually check the output water surfaces and to check the positioning of the cut line in relation to the water extent. If corrections or alterations need to be carried out the Steady Flow Computation must be re-applied. Once this has been completed the data can be exported from HEC-RAS[®].

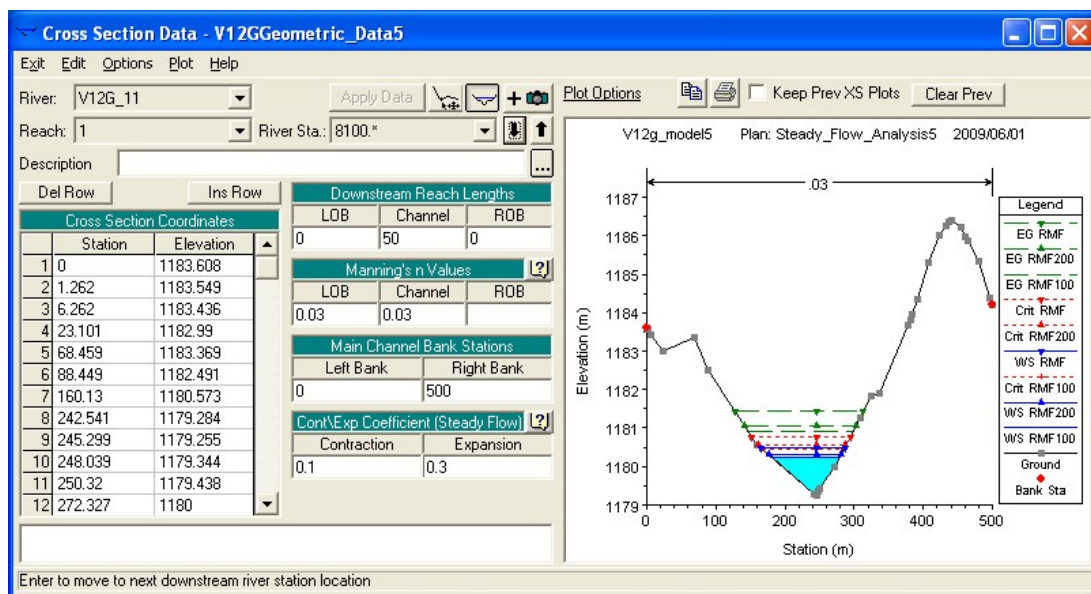


Figure 17. Screen shot of the Cross-section Editor

1.1.9. Flood Extent Mapping

Using the HECGeoras[®] extension in ArcGIS[®], the export file from HECRAS[®] is first converted to a .xml format using the 'Import RAS SDF File' converter, which can be read by HECGeoras[®].

To produce a water surface polygon, the first step is to set up an analysis with its import parameters. This is done from the Layer Setup interface on the RAS Mapping Menu. In most cases this will be a new analysis. The analysis is given a name, the converted export file from HECRAS[®] is selected and the TIN surface generated earlier is selected. An output directory and name for the analysis files is required. The final variable required is the raster grid cell size. As all the DEM surfaces are created at 5m the same value is used here.

Using the ‘Read RAS GIS Export File’ option is imported into a new data frame in ArcGIS[®]. The water surface extents must then be calculated using ‘Water Surface Generation’. Each water surface profile is then calculated and added to the data frame.

The last step is to do a ‘Floodplain Delineation using Rasters’ procedure. This is done for each water surface profile. GIS polygons are created and added to the data frame. The polygons are the flood inundation extents or boundaries are the “Flood Zone Areas” which is the final output for this part of the project.

An overview of the overall processing steps are presented in Figure 18.

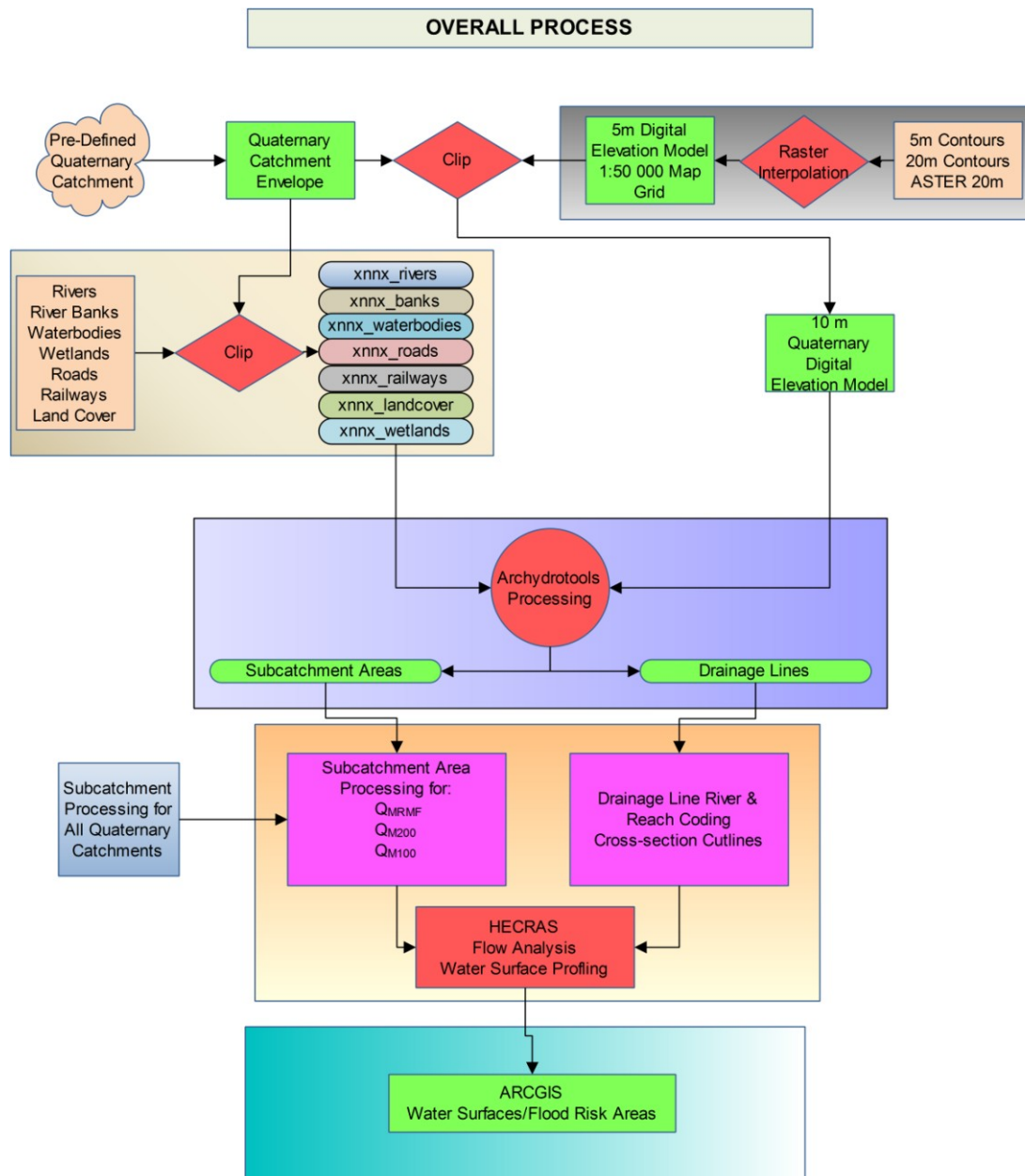


Figure 18. Data Processing Flow Chart

APPENDIX III – COMMUNITY SURVEYS

The results of four of the five representative areas are presented in Table 1. In quaternary catchment W23A there were no settlements found with the flood zone. This is probably community experience of the extent of the floods resulting from Tropical Storm Domoina in 1984. Although post-flood surveys (Borga et al. 2008) are most effective when conducted directly after a flood event, the process applied here was aimed at gathering any local knowledge of past flood events. An important observation was that some homesteads recorded flood levels which were located significantly higher than flood elevation levels estimated from the RMF (See Chapter 7).

Table 1. Summary of homestead surveys for the representative areas

T40G = 822 Respondents		T52D = 459 Respondents	
Timeframe	Respondents	Timeframe	Respondents
>1	119	>1	84
>5	16	>5	17
>10	4	>10	72
Total	139	Total	173
Damage	Respondents	Damage	Respondents
Lost everything	2	Lost everything	8
Major	33	Major	33
Minor	65	Minor	49
Minimal	39	Minimal	83
Total	139	Total	173
Flood marks	Respondents	Flood marks	Respondents
Yes	73	Yes	82
No	66	No	91
Total	139	Total	173

U20H = 960 Respondents		V12G = 409 Respondents	
Timeframe	Respondents	Timeframe	Respondents
>1	449	>1	155
>5	45	>5	16
>10	46	>10	0
Total	540	Total	171
Damage	Respondents	Damage	Respondents
Lost everything	45	Lost everything	4
Major	67	Major	14
Minor	104	Minor	22
Minimal	324	Minimal	131
Total	540	Total	171
Flood marks	Respondents	Flood marks	Respondents
Yes	100	Yes	8
No	440	No	163
Total	540	Total	171

APPENDIX IV – REGIONAL STORM EVENT DATA

Regional storm events identified from storm footprints.

ZAB – Author, vB - van Bladeren (1992), (SAWS 1991) – South African Weather Services. Grey blocks mark extreme flood events as identified by van Bladeren (1992).

Year	Month	Start Date	End Date	Days	Geographic Area	Note	Source	Area km ²	Max Rainfall Depth (mm)	Mean Rainfall Depth (mm)	Mean Depth/Duration
1848	April	?	?	?	Durban Area	No rainfall data	vB	?	?	?	0.0
1856	April	12 April 1856	15 April 1856	4	Durban PMB St Lucia	No rainfall data	vB, SAWS, ZAB	?	709		0.0
1868	August	29 August 1868	30 August 1868	2	Durban Area	No rainfall data	vB, SAWS, ZAB	?	420		0.0
1891	March	15 March 1891	16 March 1891	2	Durban, Rbay		vB, SAWS, ZAB	6619	314	128	63.9
1891	December	20 December 1891	21 December 1891	2	Durban		ZAB	1505	171	98	48.9
1893	January	3 January 1893	3 January 1893	1	Durban		vB, SAWS, ZAB	26	99	81	81.4
1893	March	3 March 1893	3 March 1893	1	Durban		ZAB	1267	160	95	95.0
1893	September	2 September 1893	3 September 1893	2	Durban, Mtunzini		ZAB	2463	120	84	83.8
1893	September	28 September 1893	29 September 1893	2	Durban, Mtunzini		ZAB	7289	179	101	50.7
1893	October	7 October 1893	8 October 1893	2	Durban, St Lucia		ZAB	7842	317	130	64.8
1894	September	7 September 1894	9 September 1894	3	Durban to RBay		ZAB	12099	260	115	38.4
1895	December	12 December 1895	14 December 1895	3	Durban to Mtunzini, Ixopo		ZAB	2533	233	116	38.7
1898	September	30 September 1898	1 October 1898	2	Durban to Mtunzini		ZAB	4296	187	99	49.3
1898	November	23 November 1898	26 November 1898	4	South Coast		ZAB	11189	255	124	41.3

Year	Month	Start Date	End Date	Days	Geographic Area	Note	Source	Area km ²	Max Rainfall Depth (mm)	Mean Rainfall Depth (mm)	Mean Depth/Duration
1901	April	03 April 1901	04 April 1901	2	Durban Area		ZAB	2074	245	120	59.8
1902	February	09 February 1902	10 February 1902	2	Durban to Mtunzini		ZAB	3817	306	124	61.9
1902	June	10 June 1902	11 June 1902	2	South Coast		ZAB	7899	284	129	64.7
1903	April	27 April 1903	28 April 1903	2	South Coast		ZAB	2720	149	94	46.9
1904	February	24 February 1904	27 February 1904	4	Mainly Durban to Mtunzini, Kokstad, Noodsberg, Newcastle		ZAB	7266	297	105	26.4
1905	May	30 May 1905	01 June 1905	3	South Coast, Durban to Rbay		vB, SAWS, ZAB	4438	173	93	30.9
1908	April	17 April 1908	19 April 1908	3	South Coast, Durban to Rbay		vB, SAWS, ZAB	22121	577	146	48.7
1909	January	19 January 1909	21 January 1909	3	Northern KZN	Cyclone ?	ZAB	26289	634	171	57.1
1909	May	09 May 1909	12 May 1909	4	Coastal Belt		ZAB	5370	215	103	25.8
1910	March	26 March 1910	28 March 1910	3	South Coast		ZAB	6189	193	108	36.0
1910	May	24 May 1910	26 May 1910	3	Durabn to Port Edward		ZAB	12707	220	100	33.4
1911	September	29 September 1911	02 October 1911	4	Southern KZN		ZAB	21720	327	108	26.9
1913	March	03 March 1913	08 March 1913	6	Scattered across Southern KZN		vB, SAWS, ZAB	8818	373	120	24.1
1914	January	27 January 1914	28 January 1914	2	Kokstad		ZAB	1332	162	94	47.1
1915	January	05 January 1915	08 January 1915	4	Underberg, Newcastle, Rbay, North Coast		ZAB	11573	283	107	26.7
1915	October	26 October 1915	29 October 1915	4	KZN		ZAB	53937	483	111	27.9
1915	November	26 November 1915	27 November 1915	2	Hluhluwe		ZAB	944	381	145	72.3
1916	March	02 March 1916	05 March 1916	4	Northern KZN		ZAB	20754	310	103	25.7
1917	July	18 July 1917	22 July 1917	5	Central coastal		ZAB	25363	392	110	22.0
1917	October	25 October 1917	29 October 1917	5	Southern KZN		vB, SAWS, ZAB	46594	471	134	26.9
1918	February	13 February 1918	17 February 1918	5	KZN		vB, SAWS, ZAB	69171	400	140	28.0
1920	January	28 January 1920	01 February 1920	5	Most of KZN		ZAB	75634	604	139	27.8
1920	February	14 February 1920	16 February 1920	3	Central and Coastal KZN		ZAB	17894	284	97	32.5
1920	February	28 February 1920	02 March 1920	4	Maputuland		ZAB	6404	355	139	34.7
1921	November	11 November 1921	13 November 1921	3	South Coast - Coastal		ZAB	2595	141	88	29.2

Year	Month	Start Date	End Date	Days	Geographic Area	Note	Source	Area km ²	Max Rainfall Depth (mm)	Mean Rainfall Depth (mm)	Mean Depth/Duration
1921	November	17 November 1921	20 November 1921	4	Northern KZN		vB, ZAB	15811	181	96	23.9
1923	February	09 February 1923	14 February 1923	6	Scattered across KZN		ZAB	37358	275	106	17.6
1923	July	19 July 1923	21 July 1923	3	Southern KZN		ZAB	7417	278	120	40.0
1925	January	03 January 1925	05 January 1925	3	South Coast to Ulundi		ZAB	8474	180	91	30.5
1925	March	07 March 1925	20 March 1925	14	South to North KZN		vB, SAWS, ZAB	115306	1560	236	16.9
1925	March	21 March 1925	25 March 1925	5	South to North KZN		vB, SAWS, ZAB	44143	238	103	20.6
1925	April	09 April 1925	17 April 1925	9	Hluhluwe		ZAB	5178	1257	299	33.2
1927	March	15 March 1927	17 March 1927	3	South Coast		ZAB	6800	307	117	39.1
1927	March	27 March 1927	28 March 1927	2	South Coast - Mtunzini		ZAB	4246	208	92	46.2
1929	June	06 June 1929	09 June 1929	4	South Coast		vB, ZAB	3633	329	141	35.2
1930	January	15 January 1930	18 January 1930	4	Northern & Coastal KZN		vB, ZAB	43159	437	130	32.4
1930	February	15 February 1930	18 February 1930	4	Makhathini Flats		ZAB	5717	338	174	43.6
1930	March	06 March 1930	08 March 1930	3	South central KZN, Northern KZN		vB, ZAB	9929	238	97	32.3
1931	July	13 July 1931	15 July 1931	3	South Coast		vB, ZAB	6173	571	166	55.4
1932	February	19 February 1932	22 February 1932	4	KZN		vB, SAWS, ZAB	45450	476	158	39.5
1932	March	07 March 1932	10 March 1932	4	Scattered across KZN		ZAB	7346	163	89	22.3
1932	March	22 March 1932	25 March 1932	4	Hluhluwe		ZAB	4264	295	148	36.9
1932	April	27 April 1932	29 April 1932	3	Mtubatuba Area		ZAB	4467	405	148	49.4
1932	September	07 September 1932	09 September 1932	3	Port Edward area		ZAB	1548	255	135	44.9
1932	November	07 November 1932	09 November 1932	3	Port Edward area		ZAB	2633	185	105	35.0
1934	December	05 December 1934	07 December 1934	3	Scattered KZN		ZAB	16266	236	98	32.7
1935	May	11 May 1935	13 May 1935	3	South Coast		ZAB	1007	152	90	30.0
1935	June	11 June 1935	14 June 1935	4	South Coast, Durban to Rbay		ZAB	24137	465	154	38.5
1936	February	06 February 1936	08 February 1936	3	Southern KZN		ZAB	5980	300	97	32.5
1936	March	28 March 1936	29 March 1936	2	Ulundi area		ZAB	3247	362	125	62.3
1936	May	22 May 1936	24 May 1936	3	Scattered KZN		ZAB	26920	268	99	32.8

Year	Month	Start Date	End Date	Days	Geographic Area	Note	Source	Area km ²	Max Rainfall Depth (mm)	Mean Rainfall Depth (mm)	Mean Depth/Duration
1937	February	09 February 1937	13 February 1937	5	Northern KZN	Cyclone ?	ZAB	51770	410	124	24.7
1937	March	25 March 1937	26 March 1937	2	Rbay area		ZAB	722	186	97	48.7
1938	March	01 March 1938	03 March 1938	3	Jozini area		ZAB	2390	539	165	55.2
1938	April	06 April 1938	09 April 1938	4	Jozini area		ZAB	2592	427	150	37.4
1938	December	28 December 1938	01 January 1939	6	Northern KZN		ZAB	16050	471	147	24.6
1939	February	03 February 1939	08 February 1939	6	Northern KZN		vB, ZAB	57086	508	149	24.8
1939	March	07 March 1939	09 March 1939	3	Makhathini area		ZAB	4002	252	120	40.1
1940	May	04 May 1940	06 May 1940	3	South Coast, Central KZN		vB, SAWS, ZAB	63241	475	134	44.7
1940	June	04 June 1940	05 June 1940	2	Makhathini area		ZAB	1966	217	119	59.5
1940	December	09 December 1940	10 December 1940	2	Hluhluwe area		ZAB	1744	179	107	53.5
1942	January	29 January 1942	30 January 1942	2	Makhathini area		ZAB	7281	172	106	52.8
1942	May	31 May 1942	02 June 1942	3	Jozini area		ZAB	15175	227	116	38.6
1942	November	11 November 1942	13 November 1942	3	South Coast & Kosi Bay area		ZAB	7370	276	109	36.2
1943	March	04 March 1943	08 March 1943	5	KZN Coast		ZAB	24311	372	121	24.1
1943	April	21 April 1943	24 April 1943	3	Scattered KZN		vB, ZAB	46446	251	104	34.6
1947	November	12 November 1947	14 November 1947	3	South Coast		ZAB	4833	267	116	38.7
1949	April	28 April 1948	30 April 1948	3	Northern KZN		ZAB	28501	437	102	34.1
1949	May	30 May 1949	31 May 1949	2	Makhathini area		ZAB	3205	360	176	88.1
1953	January	12 January 1953	13 January 1953	2	South Coast and other scattered regions in KZN		ZAB	11657	365	121	60.6
1954	May	20 May 1954	22 May 1954	3	Scattered regions in KZN		ZAB	10117	192	88	29.2
1954	October	15 October 1954	18 October 1954	4	South Coast		ZAB	11996	274	110	27.5
1955	March	03 March 1955	05 March 1955	3	South Coast		ZAB	8872	316	101	33.5
1956	February	22 February 1956	27 February 1956	6	Scattered regions in KZN		ZAB	66178	287	115	19.1
1956	March	18 March 1956	21 March 1956	4	South Coast, Berg		vB, ZAB	26421	338	113	28.2
1956	December	21 December 1956	24 December 1956	4	Rbay, South Coast		ZAB	13089	393	118	29.5
1957	January	21 January 1957	22 January 1957	2	Hluhluwe area		ZAB	2821	258	118	58.8

Year	Month	Start Date	End Date	Days	Geographic Area	Note	Source	Area km ²	Max Rainfall Depth (mm)	Mean Rainfall Depth (mm)	Mean Depth/Duration
1957	April	26 April 1957	29 April 1957	4	Coast Port Edward to Rbay		ZAB	11493	293	112	28.0
1957	July	01 July 1957	03 July 1957	3	Northern KZN		vB, ZAB	4832	162	88	29.4
1957	September	11 September 1957	13 September 1957	3	Central KZN		ZAB	14685	229	88	29.4
1957	September	21 September 1957	26 September 1957	6	Northern KZN		vB, ZAB	46754	240	90	15.0
1957	October	02 October 1957	03 October 1957	2	Rbay - Nongoma		vB, SAWS, ZAB	7378	135	86	42.8
1958	January	30 January 1958	31 January 1958	2	Durban to Rbay		ZAB	2929	158	95	47.5
1958	February	15 February 1958	17 February 1958	3	KZN Coast		ZAB	8421	257	104	34.8
1958	March	19 March 1958	20 March 1958	2	South Coast		ZAB	1698	167	91	45.6
1958	April	11 April 1958	14 April 1958	4	South Coast		vB, ZAB	9529	389	117	29.2
1959	May	16 May 1959	18 May 1959	3	Southern KZN		vB, SAWS, ZAB	33595	552	174	57.9
1960	April	22 April 1960	24 April 1960	3	Rbay area		ZAB	3953	215	106	35.2
1960	May	23 May 1960	25 May 1960	3	Rbay area		ZAB	1649	221	109	36.5
1960	November	06 November 1960	09 November 1960	4	Rbay area		vB, ZAB	4361	268	117	29.2
1960	December	27 December 1960	30 December 1960	4	Scattered Northern KZN		ZAB	30255	306	100	25.0
1961	February	10 February 1961	11 February 1961	2	Central KZN		ZAB	6457	229	91	45.6
1961	April	10 April 1961	13 April 1961	4	South Coast		ZAB	9779	193	115	28.7
1961	June	23 June 1961	24 June 1961	2	Rbay area		ZAB	1728	211	125	62.4
1962	March	25 March 1962	27 March 1962	3	South Coast		ZAB	4563	211	52	17.3
1963	January	22 January 1963	25 January 1963	4	Scattered KZN		ZAB	12369	329	111	27.8
1963	March	07 March 1963	09 March 1963	3	South Coast		ZAB	5613	171	90	29.9
1963	March	11 March 1963	12 March 1963	2	South Coast		ZAB	1373	295	156	78.0
1963	June	11 June 1963	13 June 1963	3	Northern KZN		ZAB	9481	245	93	31.1
1963	June	27 June 1963	29 June 1963	3	Durban to Rbay		ZAB	1950	173	100	33.3
1963	July	02 July 1963	05 July 1963	4	Northern KZN		vB, SAWS, ZAB	43401	440	148	37.0
1963	July	10 July 1963	11 July 1963	2	South Coast		ZAB	1476	142	91	45.7
1963	August	03 August 1963	05 August 1963	3	Hluhluwe area		ZAB	4479	535	181	60.5

Year	Month	Start Date	End Date	Days	Geographic Area	Note	Source	Area km ²	Max Rainfall Depth (mm)	Mean Rainfall Depth (mm)	Mean Depth/Duration
1963	December	11 December 1963	14 December 1963	4	South Coast		ZAB	11145	375	130	32.5
1964	January	08 January 1964	11 January 1964	4	KZN		ZAB	28752	305	102	25.5
1964	February	09 February 1964	11 February 1964	3	Hluhluwe area		ZAB	3288	359	119	39.6
1964	June	18 May 1964	20 May 1964	3	South Coast		ZAB	15678	401	133	44.3
1964	October	21 October 1964	24 October 1964	4	South Coast		ZAB	3810	306	119	29.7
1964	October	26 October 1964	28 October 1964	3	North and Central KZN		ZAB	22980	153	90	29.9
1965	March	08 March 1965	10 March 1965	3	Mkhathini area		ZAB	3239	766	164	54.5
1965	June	16 June 1965	18 June 1965	3	Southern KZN		ZAB	14345	250	96	31.9
1965	August	27 August 1965	29 August 1965	3	Northern KZN Coast		ZAB	5406	265	112	37.2
1965	September	28 September 1965	29 September 1965	2	St Lucia Area		ZAB	790	248	119	59.3
1965	October	18 October 1965	19 October 1965	2	Northern KZN		ZAB	4491	193	108	54.2
1966	January	04 January 1966	07 January 1966	4	Mkhathini area	Cyclone ?	vB, ZAB	14150	562	182	45.4
1966	January	19 January 1966	20 January 1966	2	Scattered KZN		ZAB	4144	203	87	43.3
1966	May	19 May 1966	21 May 1966	3	South Coast		ZAB	4737	208	98	32.5
1967	January	30 January 1967	01 February 1967	3	KZN		ZAB	48794	182	96	32.1
1967	February	08 February 1967	10 February 1967	3	South Coast and N Zululand		ZAB	9672	211	99	32.9
1967	February	24 February 1967	26 February 1967	3	Maputoland	Cyclone ?	ZAB	3279	200	114	38.0
1967	April	01 April 1967	03 April 1967	3	Rbay area		ZAB	2024	148	98	32.7
1967	April	16 April 1967	18 April 1967	3	Rbay area		ZAB	2428	225	128	42.6
1967	November	16 November 1967	19 November 1967	4	Scattered KZN		ZAB	12560	173	89	22.3
1968	January	19 January 1968	21 January 1968	3	Durban north coast		ZAB	2644	196	106	35.2
1969	February	28 February 1969	02 March 1969	3	Coastal belt		ZAB	9442	198	92	30.5
1969	March	25 March 1969	28 March 1969	4	North Coast		ZAB	6638	306	131	32.7
1969	April	25 April 1969	28 April 1969	4	St Lucia Area		ZAB	2956	337	139	34.7
1969	May	21 May 1969	23 May 1969	3	South Coast		ZAB	2440	216	107	35.6
1969	October	16 October 1969	21 October 1969	5	North Coast		ZAB	26903	180	89	17.8

Year	Month	Start Date	End Date	Days	Geographic Area	Note	Source	Area km ²	Max Rainfall Depth (mm)	Mean Rainfall Depth (mm)	Mean Depth/Duration
1970	August	25 August 1970	28 August 1970	4	Southern KZN		ZAB	12363	174	93	23.3
1970	September	27 September 1970	30 September 1970	4	KZN		ZAB	48545	241	103	25.8
1970	October	08 October 1970	13 October 1970	5	KZN		ZAB	63957	373	108	21.6
1971	May	11 May 1971	13 May 1971	3	KZN		ZAB	22783	507	136	45.5
1971	June	12 June 1971	13 June 1971	2	St Lucia Area		ZAB	1173	275	111	55.3
1971	June	20 August 1971	22 August 1971	3	South Coast		ZAB	4129	238	103	34.2
1971	December	01 December 1971	04 December 1971	4	Coastal & Berg		ZAB	14827	217	99	24.9
1972	February	03 February 1972	04 February 1972	2	Makhathini area		ZAB	5152	245	129	64.7
1972	February	19 February 1972	24 February 1972	6	KZN		vB, ZAB	73025	359	121	20.1
1972	November	23 November 1972	26 November 1972	4	South Coast, St Lucia area		ZAB	5195	264	115	28.7
1973	August	04 August 1973	06 August 1973	3	North Coast		ZAB	5732	232	108	35.9
1973	September	27 September 1973	30 September 1973	4	KZN		vB, SAWS, ZAB	57935	390	121	30.3
1973	October	29 October 1973	31 October 1973	3	Hluhluwe area		ZAB	4365	263	152	50.6
1974	February	04 February 1974	08 February 1974	5	Scattered Localities, KZN		vB, SAWS, ZAB	28835	362	106	21.1
1974	May	17 May 1974	19 May 1974	3	Coastal Belt		ZAB	4217	199	102	34.1
1975	February	13 February 1975	17 February 1975	5	KZN		ZAB	43891	217	103	20.5
1976	January	15 January 1976	16 January 1976	2	Hluhluwe area		ZAB	2348	209	106	53.0
1976	January	28 January 1976	01 February 1976	5	Maputoland	Cyclone	ZAB	16378	569	152	30.3
1976	February	08 February 1976	12 February 1976	5	KZN		ZAB	28083	251	102	20.4
1976	March	01 March 1976	04 March 1976	4	Southern KZN, Hluhluwe area		vB, SAWS, ZAB	8638	305	115	28.7
1976	March	18 March 1976	22 March 1976	5	South Coast		ZAB	72732	475	147	29.4
1976	April	19 April 1976	21 April 1976	3	Mkhathini area		ZAB	1751	245	113	37.7
1977	February	05 February 1977	07 February 1977	3	Coastal Belt		vB, SAWS, ZAB	36566	383	130	43.5
1977	February	15 February 1977	17 February 1977	3	North Coast		ZAB	8556	261	115	38.2
1977	March	09 March 1977	10 March 1977	2	North Coast		ZAB	4551	221	121	60.3
1977	April	15 April 1977	16 April 1977	2	St Lucia Area		ZAB	1649	227	111	55.6

Year	Month	Start Date	End Date	Days	Geographic Area	Note	Source	Area km ²	Max Rainfall Depth (mm)	Mean Rainfall Depth (mm)	Mean Depth/Duration
1977	December	29 December 1977	30 December 1977	2	Southern KZN		vB, ZAB	8565	284	106	53.1
1978	January	18 January 1977	22 January 1977	5	KZN scattered locations		ZAB	39978	308	105	21.0
1978	March	26 March 1978	28 March 1978	3	South Coast		ZAB	3026	182	91	30.2
1978	April	19 April 1978	23 April 1978	5	South Coast		vB, SAWS, ZAB	10637	594	141	28.2
1980	February	17 February 1980	19 February 1980	3	Mkhathini area		ZAB	5263	236	114	37.8
1980	September	06 September 1980	09 September 1980	4	Coastal Belt		ZAB	23252	356	135	33.7
1981	January	29 January 1981	01 February 1981	4	Scattered KZN		ZAB	8855	209	101	25.2
1981	May	15 May 1981	17 May 1981	3	North Coast		vB, ZAB	17194	420	108	36.1
1981	June	15 June 1981	17 June 1981	3	Hluhluwe area		ZAB	3963	241	121	40.2
1983	March	31 March 1983	03 April 1983	4	Mkhathini area		ZAB	3244	499	166	41.6
1984	January	28 January 1984	01 February 1984	5	Northern KZN	Cyclone	vB, SAWS, ZAB	81641	1171	287	57.3
1984	February	17 February 1984	19 February 1984	3	Coastal Belt	Cyclone	ZAB	26324	623	146	48.8
1984	February	29 February 1984	03 March 1984	4	Hluhluwe Area		ZAB	6527	692	214	53.4
1984	March	18 March 1984	20 March 1984	3	Mkhathini area		ZAB	2690	164	98	32.8
1984	April	08 April 1984	10 April 1984	3	KZN, Coastal Belt		ZAB	16251	212	98	32.6
1984	April	11 April 1984	14 April 1984	4	Makhathini		ZAB	1702	321	143	35.7
1985	January	15 January 1985	18 January 1985	4	KZN		ZAB	36629	238	102	25.6
1985	February	07 February 1985	10 February 1985	4	KZN		vB, SAWS, ZAB	104031	602	162	40.5
1985	February	15 February 1985	16 February 1985	2	Hluhluwe area		ZAB	3136	170	110	54.8
1985	March	10 March 1985	13 March 1985	4	Mkhathini area		ZAB	5049	378	162	40.6
1985	October	29 October 1985	04 November 1985	7	South Coast, Scattered KZN		vB, ZAB	68209	501	132	18.8
1985	November	29 November 1985	01 December 1985	3	Mkhathini area		ZAB	3939	423	169	56.3
1986	January	17 January 1986	19 January 1986	3	Coastline		ZAB	4501	238	95	31.6
1987	September	25 September 1987	30 September 1987	6	KZN		vB, SAWS, ZAB	112983	979	243	40.6
1987	October	28 October 1987	29 October 1987	2	Hluhluwe Area		ZAB	4478	412	173	86.5
1988	February	06 February 1988	09 February 1988	4	Coastal Belt		ZAB	28423	410	135	33.8

Year	Month	Start Date	End Date	Days	Geographic Area	Note	Source	Area km ²	Max Rainfall Depth (mm)	Mean Rainfall Depth (mm)	Mean Depth/Duration
1988	February	20 February 1988	26 February 1988	7	KZN		ZAB	41513	325	118	16.8
1988	March	01 March 1988	03 March 1988	3	South Coast		ZAB	13770	312	104	34.8
1988	March	08 March 1988	11 March 1988	4	South Coast, Central KZN, North Coast		ZAB	16044	245	104	26.1
1988	May	04 May 1988	05 May 1988	2	South Coast		ZAB	3910	323	113	56.3
1989	February	03 February 1989	06 February 1989	4	KZN		ZAB	15262	304	106	26.5
1989	February	12 February 1989	16 February 1989	5	KZN		ZAB	34812	255	99	19.7
1989	March	06 March 1989	08 March 1989	3	Maputoland		ZAB	2482	203	115	38.2
1989	April	14 April 1989	16 April 1989	3	South Coast		ZAB	4455	293	119	39.6
1989	November	28 November 1989	01 December 1989	4	KZN		vB, SAWS, ZAB	72029	440	132	33.1
1989	December	28 December 1989	31 December 1989	4	Mkhathini area		ZAB	5298	316	142	35.6
1990	March	24 March 1990	25 March 1990	2	Coastal Belt		ZAB	11896	238	108	54.1
1991	May	11 May 1991	14 May 1991	4	North Coast		ZAB	16598	436	123	30.8
1991	June	12 June 1991	13 June 1991	2	North Coast		ZAB	4307	362	172	86.2
1993	February	28 February 1993	02 March 1993	3	Mkhathini area		ZAB	11368	327	114	38.0
1993	October	04 October 1993	07 October 1993	4	Northern KZN		ZAB	38558	367	119	29.6
1993	November	05 November 1993	06 November 1993	2	Hluhluwe Area		ZAB	3867	346	145	72.6
1993	December	02 December 1993	04 December 1993	3	South Coast		ZAB	3057	260	122	40.6
1993	December	27 December 1993	29 December 1993	3	Northern KZN		ZAB	10851	199	93	31.0
1994	November	12 November 1994	14 November 1994	3	Hluhluwe Area		ZAB	3340	276	111	37.2
1995	April	09 April 1995	11 April 1995	3	Coastal Belt		ZAB	7830	242	115	38.5
1995	December	15 December 1995	17 December 1995	3	KZN		ZAB	34079	444	106	35.2
1995	December	22 December 1995	26 December 1995	5	Scattered KZN		ZAB	47263	360	100	20.1
1996	January	11 January 1995	13 January 1995	3	Coastal Belt		ZAB	1217	177	103	34.4
1996	January	23 January 1995	28 January 1995	6	KZN		ZAB	37093	250	99	16.5
1996	February	10 February 1995	14 February 1995	5	KZN		ZAB	74212	311	120	24.0
1996	July	06 July 1995	09 July 1995	4	Southern KZN		ZAB	22607	326	120	30.1

Year	Month	Start Date	End Date	Days	Geographic Area	Note	Source	Area km ²	Max Rainfall Depth (mm)	Mean Rainfall Depth (mm)	Mean Depth/Duration
1997	June	10 June 1997	13 June 1997	4	South Coast		ZAB	8430	425	131	32.8
1997	November	11 November 1997	12 November 1997	2	Kosi Bay area		ZAB	2203	245	113	56.4
1999	February	03 February 1999	05 February 1999	3	Coastal Belt		ZAB	8433	335	125	41.7
1999	October	24 October 1999	27 October 1999	4	Coastal Belt		ZAB	18855	424	121	40.2
1999	December	20 December 1999	23 December 1999	4	Coastal Belt		ZAB	21429	353	103	25.6
2000	January	15 January 2000	17 January 2000	3	Coastal Belt		ZAB	11322	232	96	31.9
2000	November	18 November 2000	20 November 2000	3	North Coast		ZAB	28240	488	138	46.0

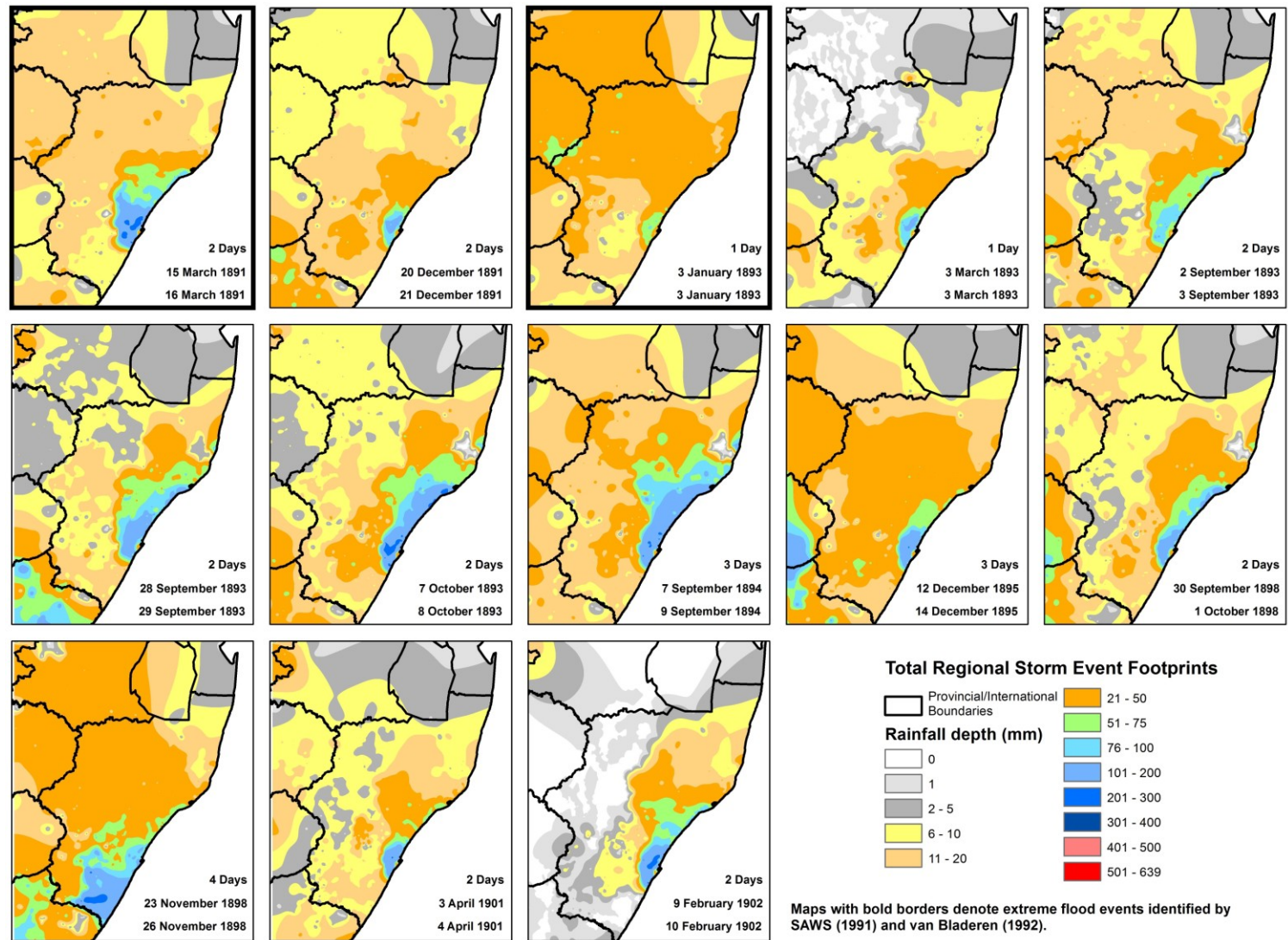


Figure 1. Total regional storm event footprints 15 March 1891 – 9 February 1902.

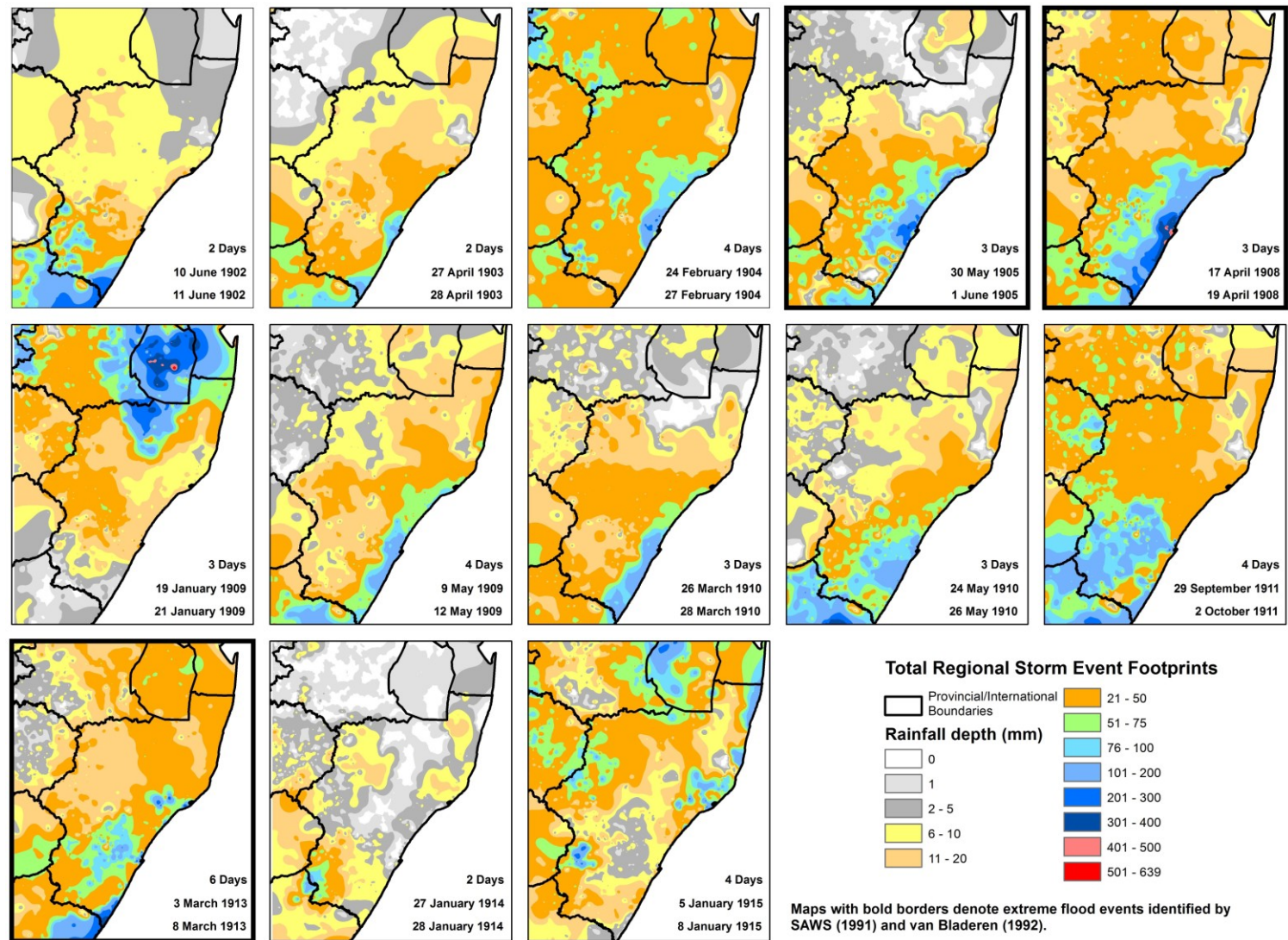


Figure 2. Total regional storm event footprints 10 June 1902 – 8 January 1915.

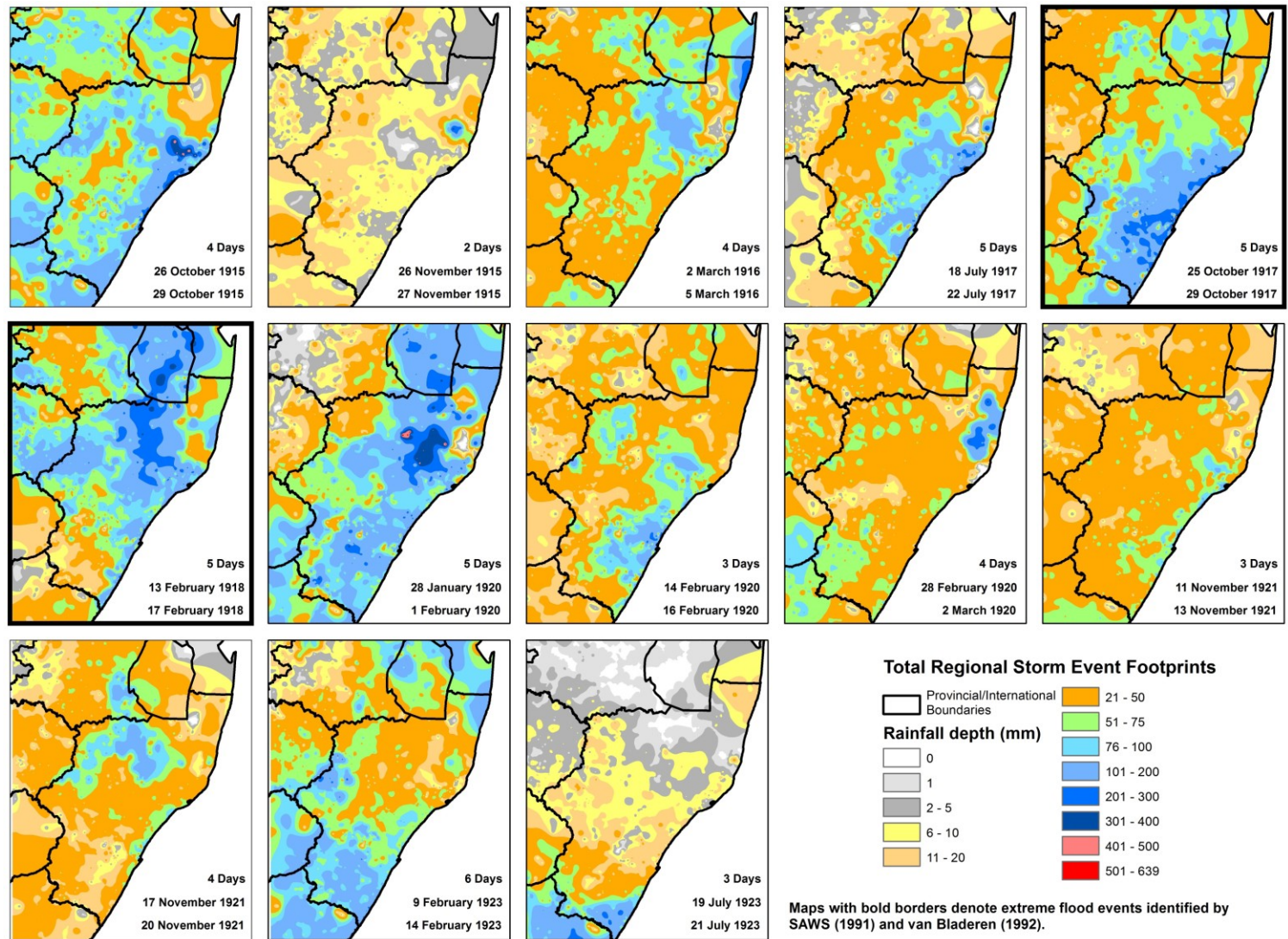


Figure 3. Total regional storm event footprints 26 October 1915 – 21 July 1923.

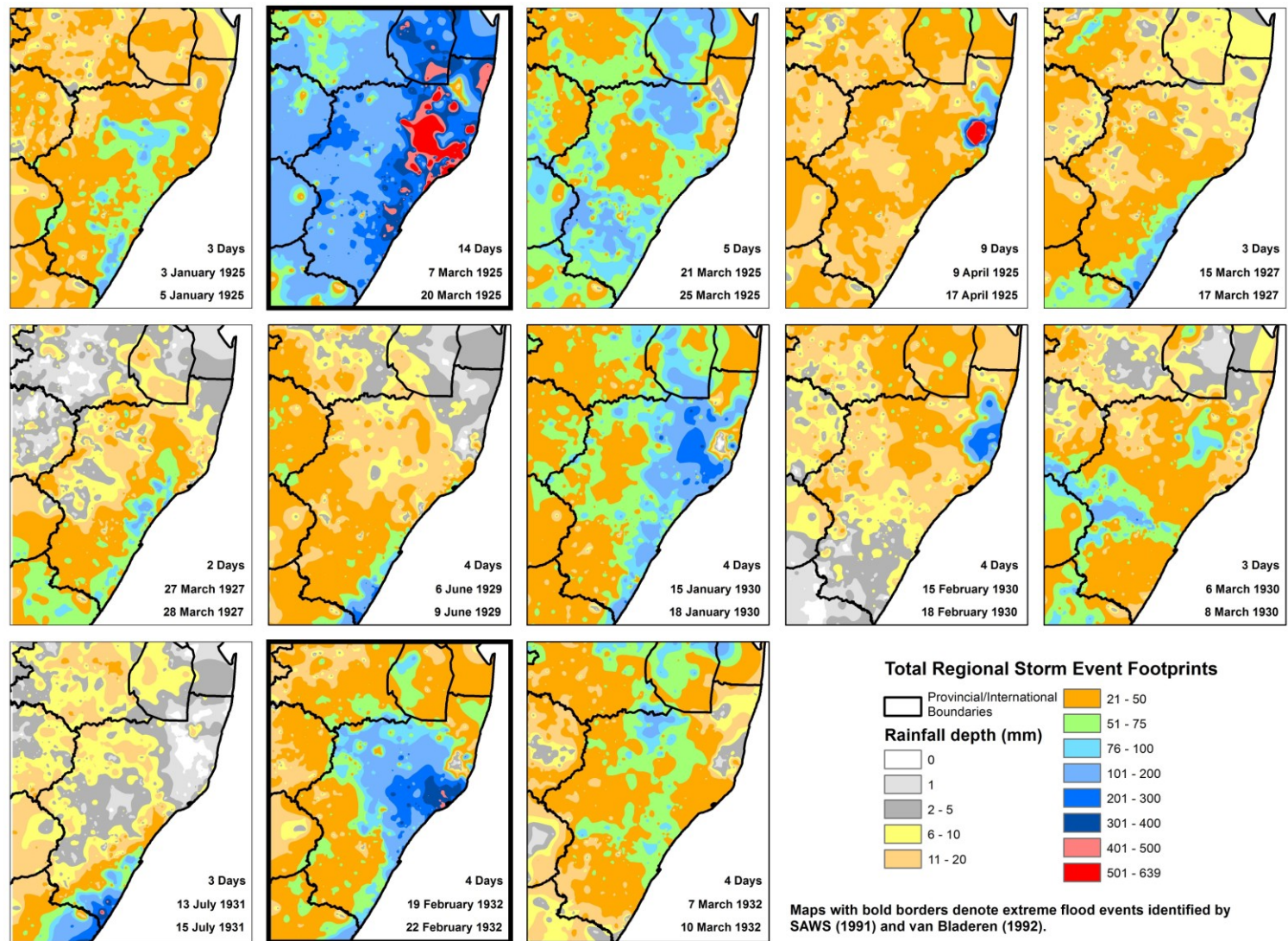


Figure 4. Total regional storm event footprints 3 January 1925 – 7 March 1932.

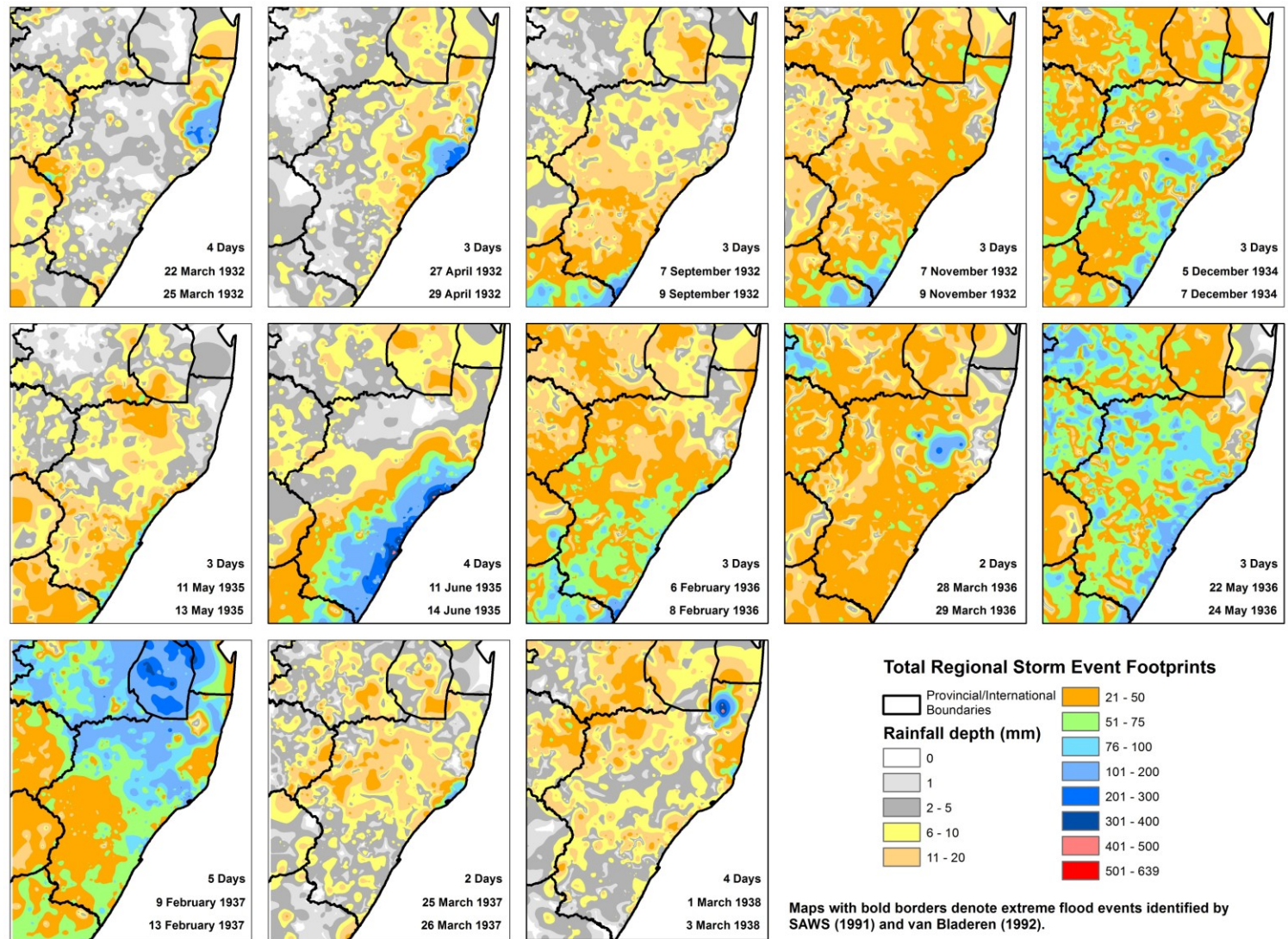


Figure 5. Total regional storm event footprints 22 March 1932 – 3 March 1938.

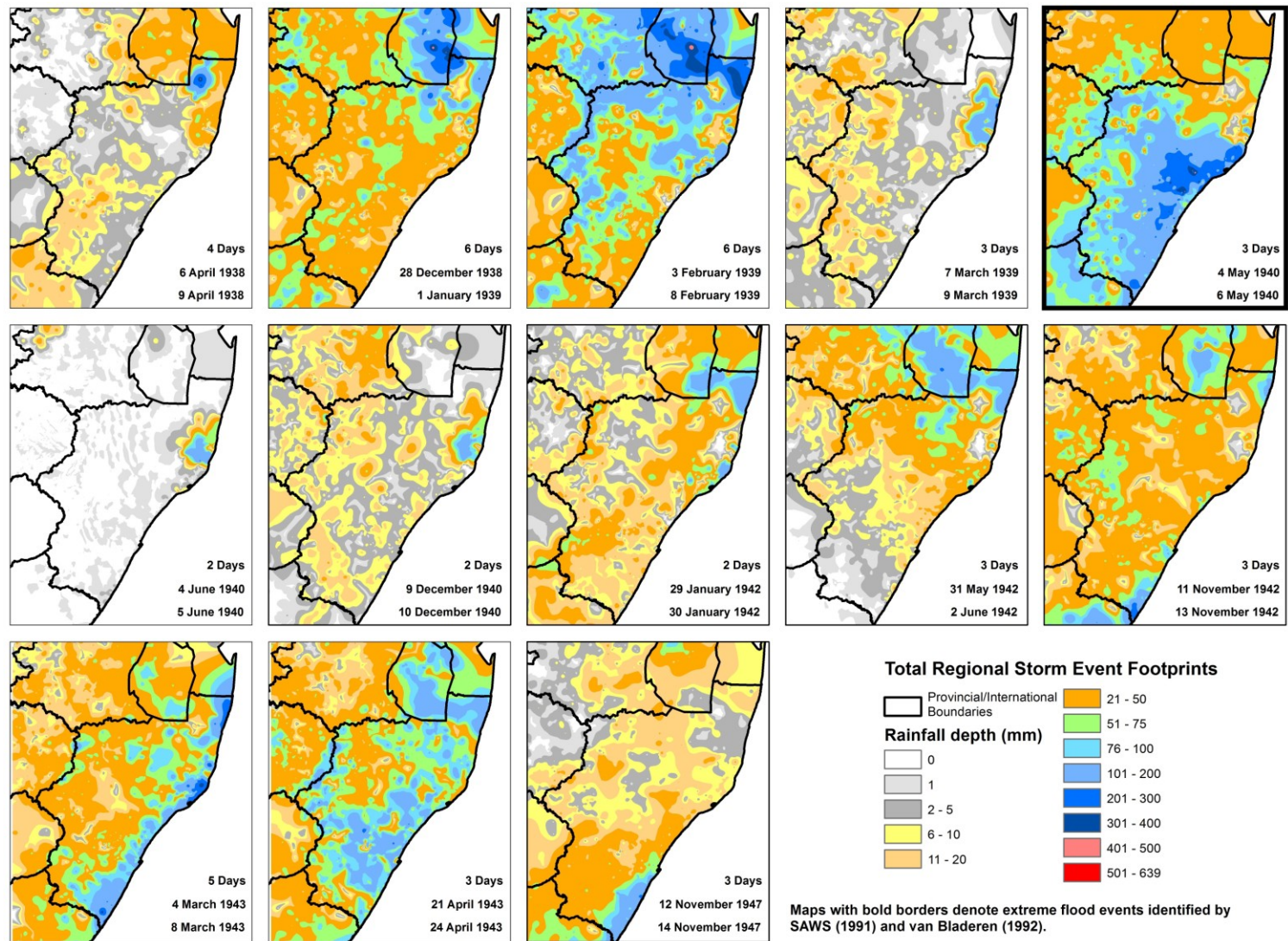


Figure 6. Total regional storm event footprints 6 April 1938 – 14 November 1947.

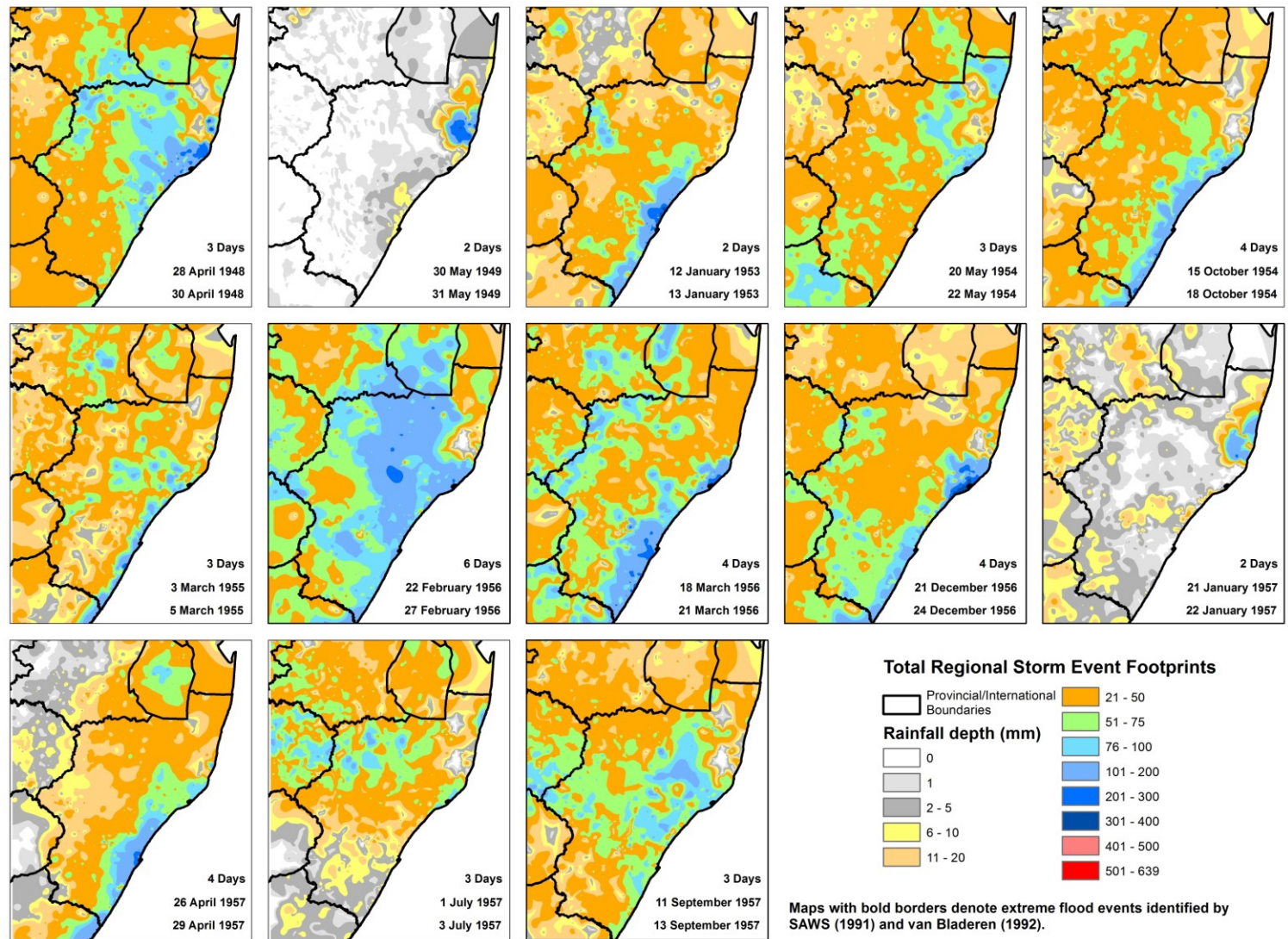


Figure 7. Total regional storm event footprints 28 April 1948 – 13 September 1957.

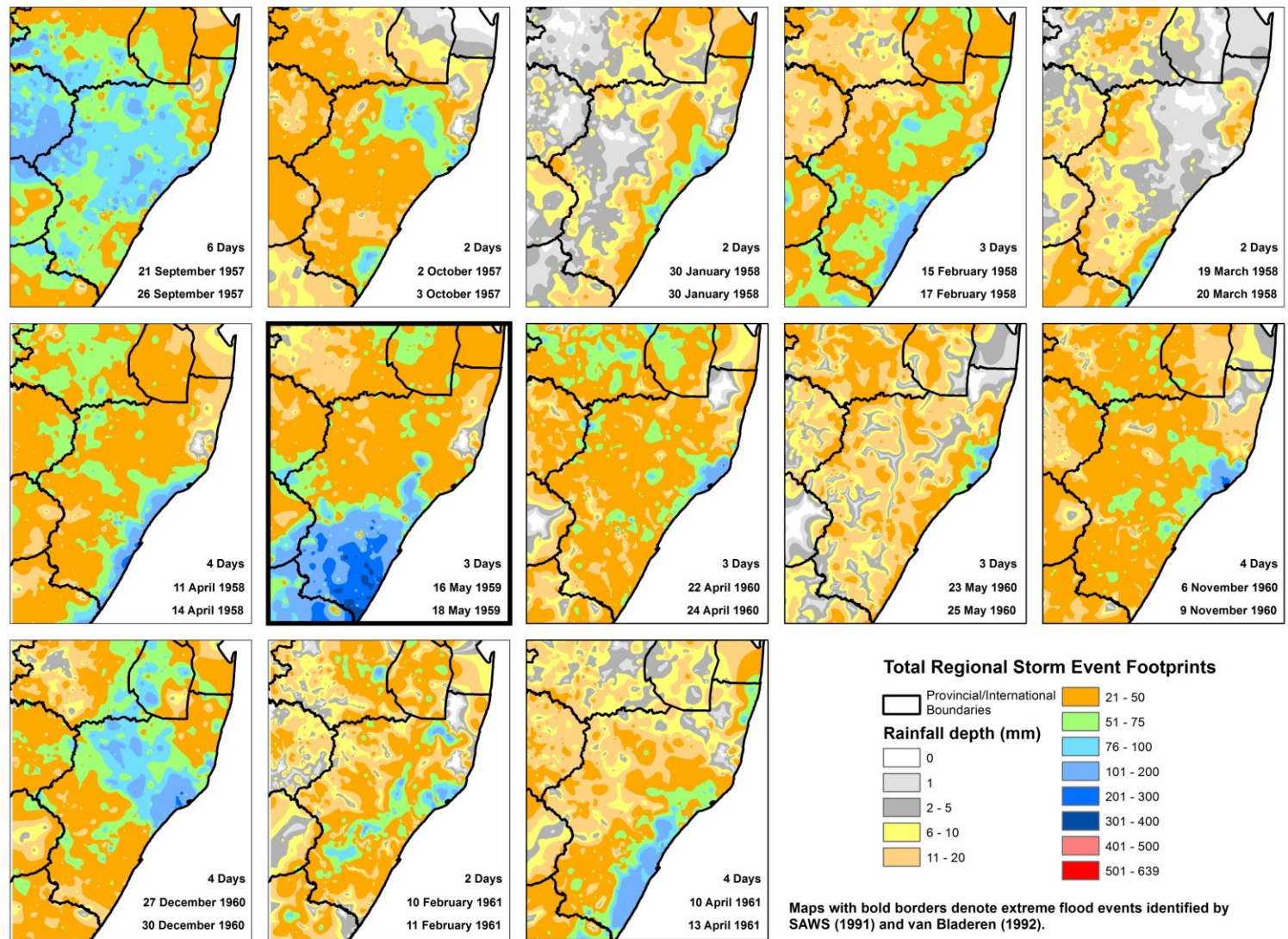


Figure 8. Total regional storm event footprints 21 September 1957 – 13 April 1961.

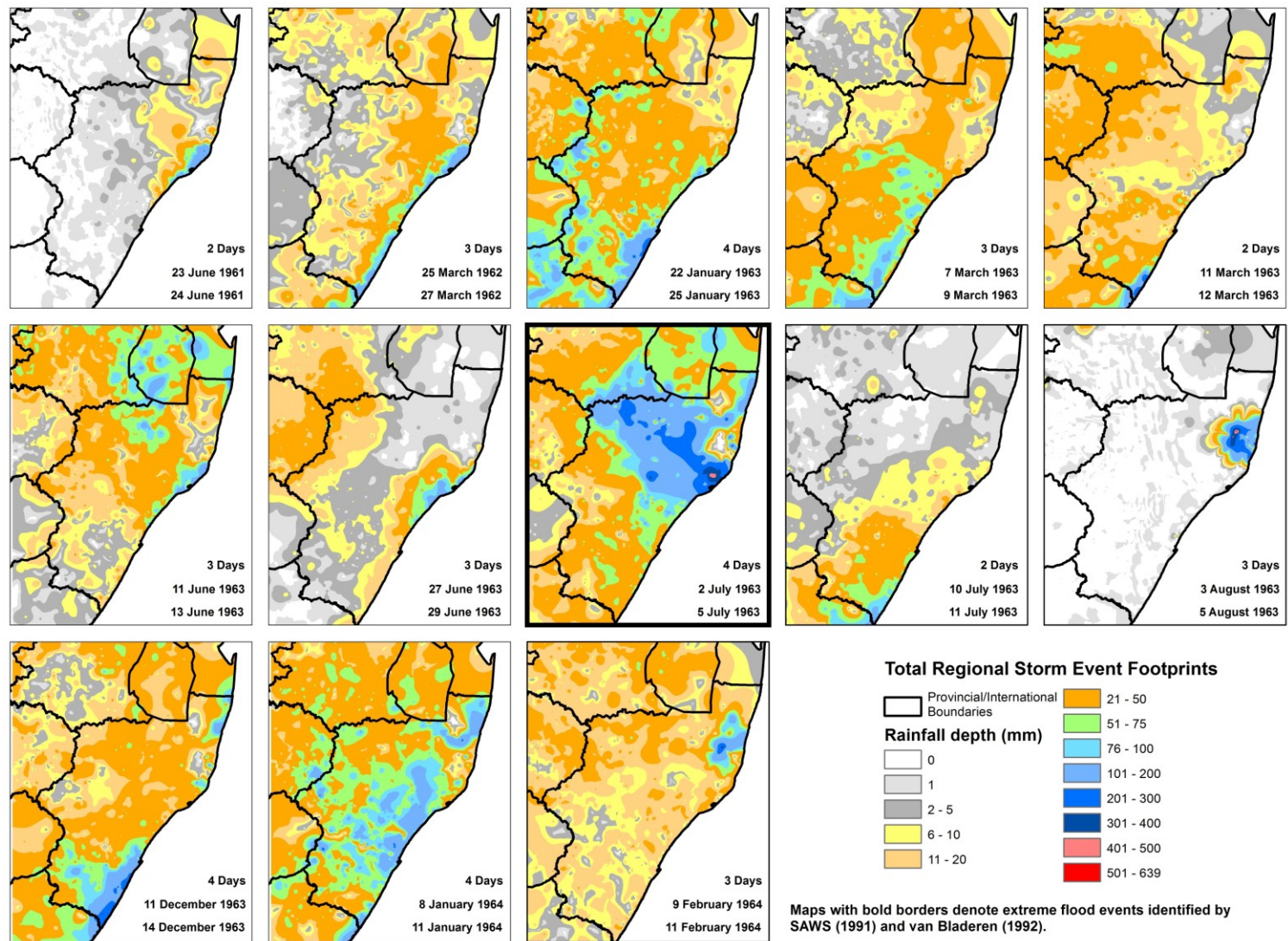


Figure 9. Total regional storm event footprints 23 June 1961 – 11 February 1964.

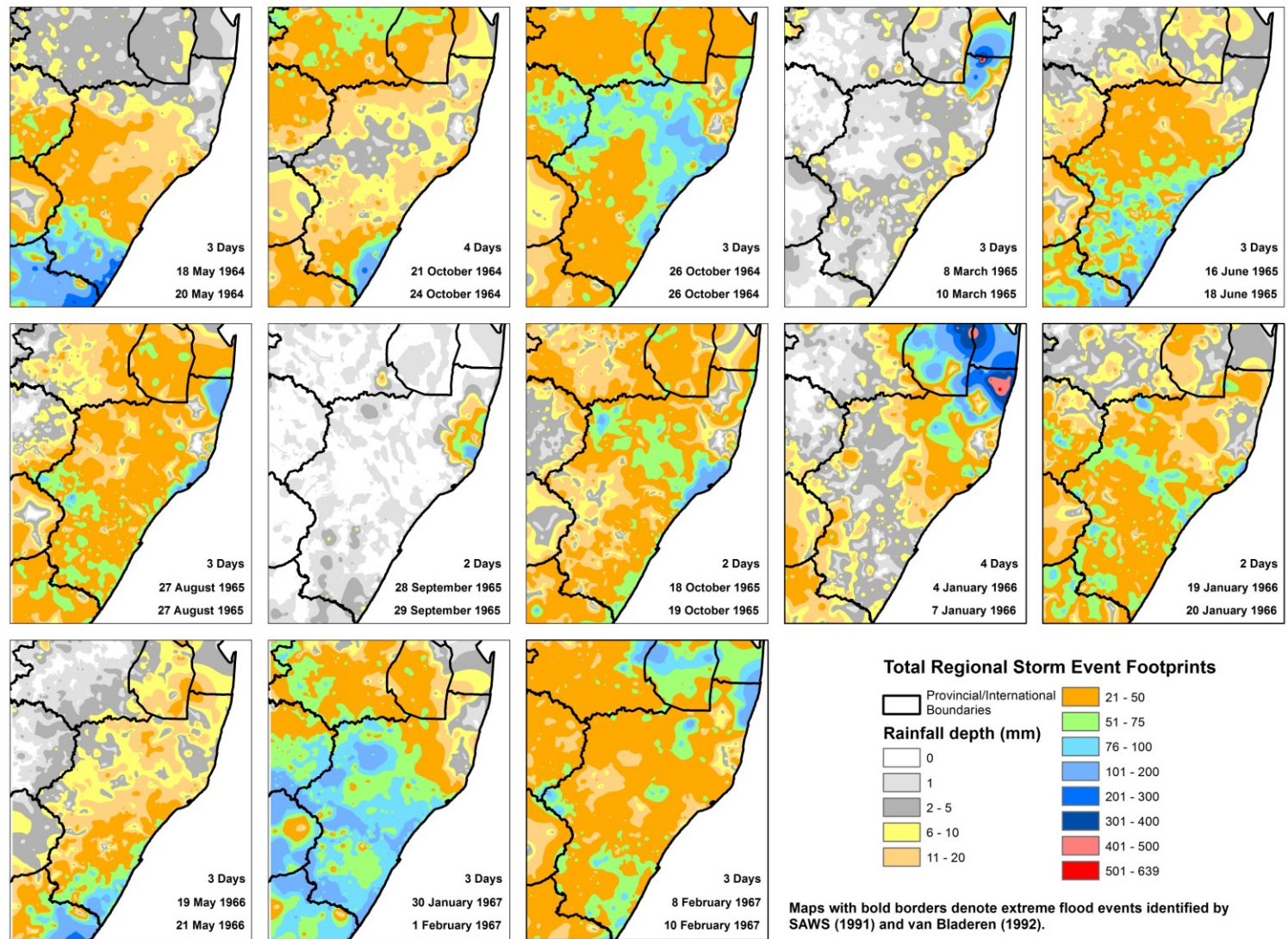


Figure 10. Total regional storm event footprints 18 May 1964 – 10 February 1967.

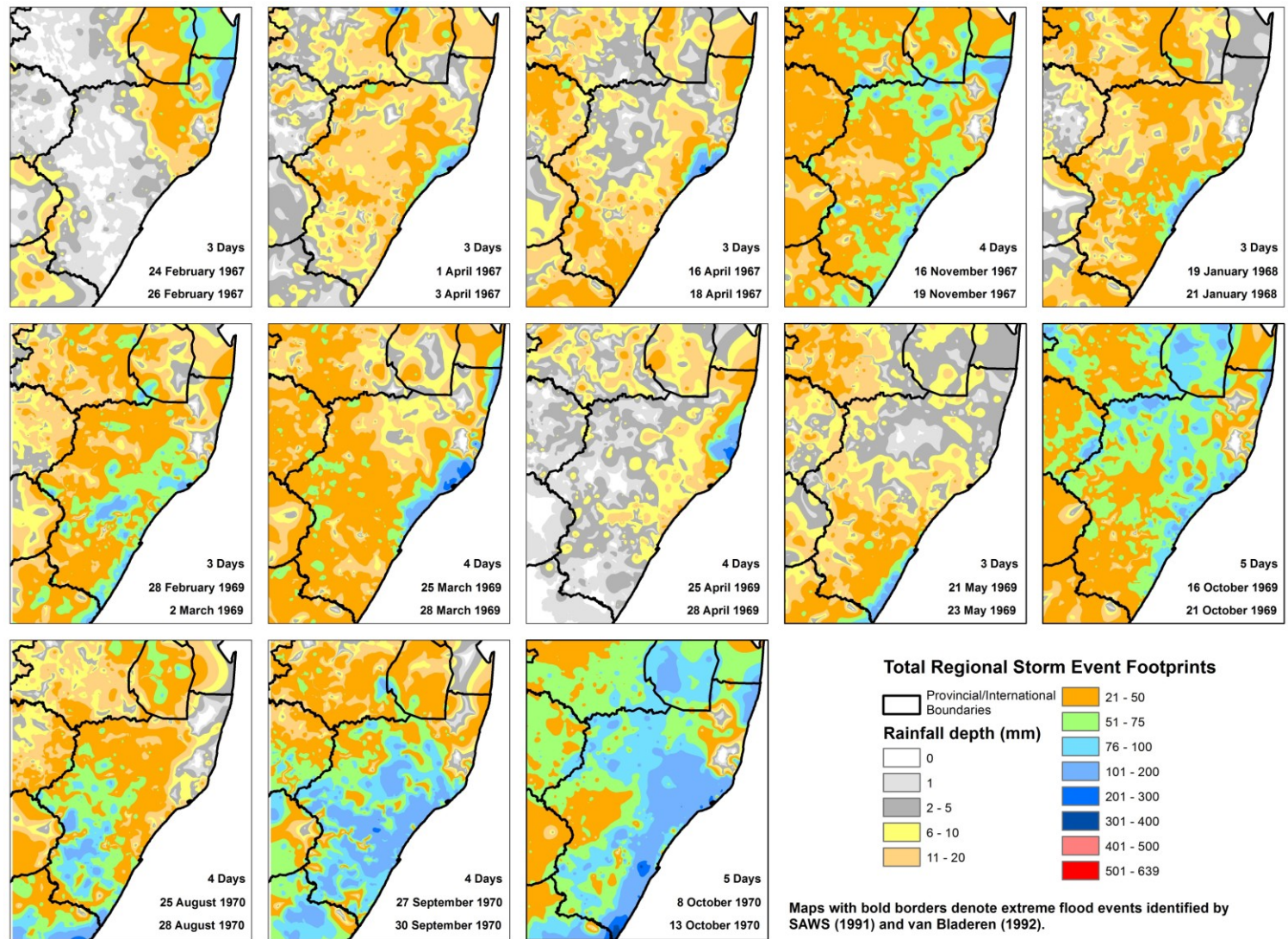


Figure 11. Total regional storm event footprints 24 February 1967 – 13 October 1970.

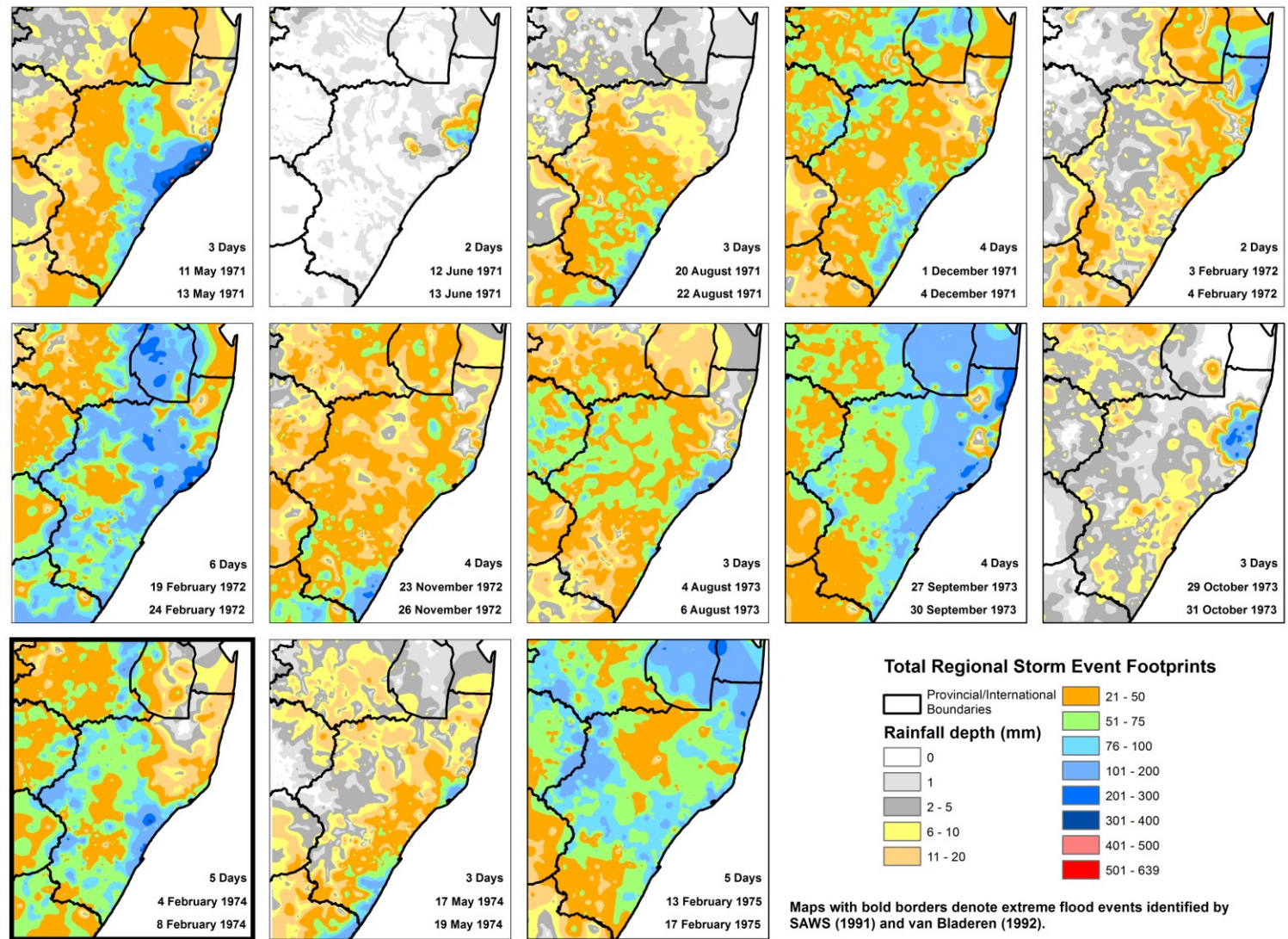


Figure 12. Total regional storm event footprints 11 May 1971 – 17 February 1975.

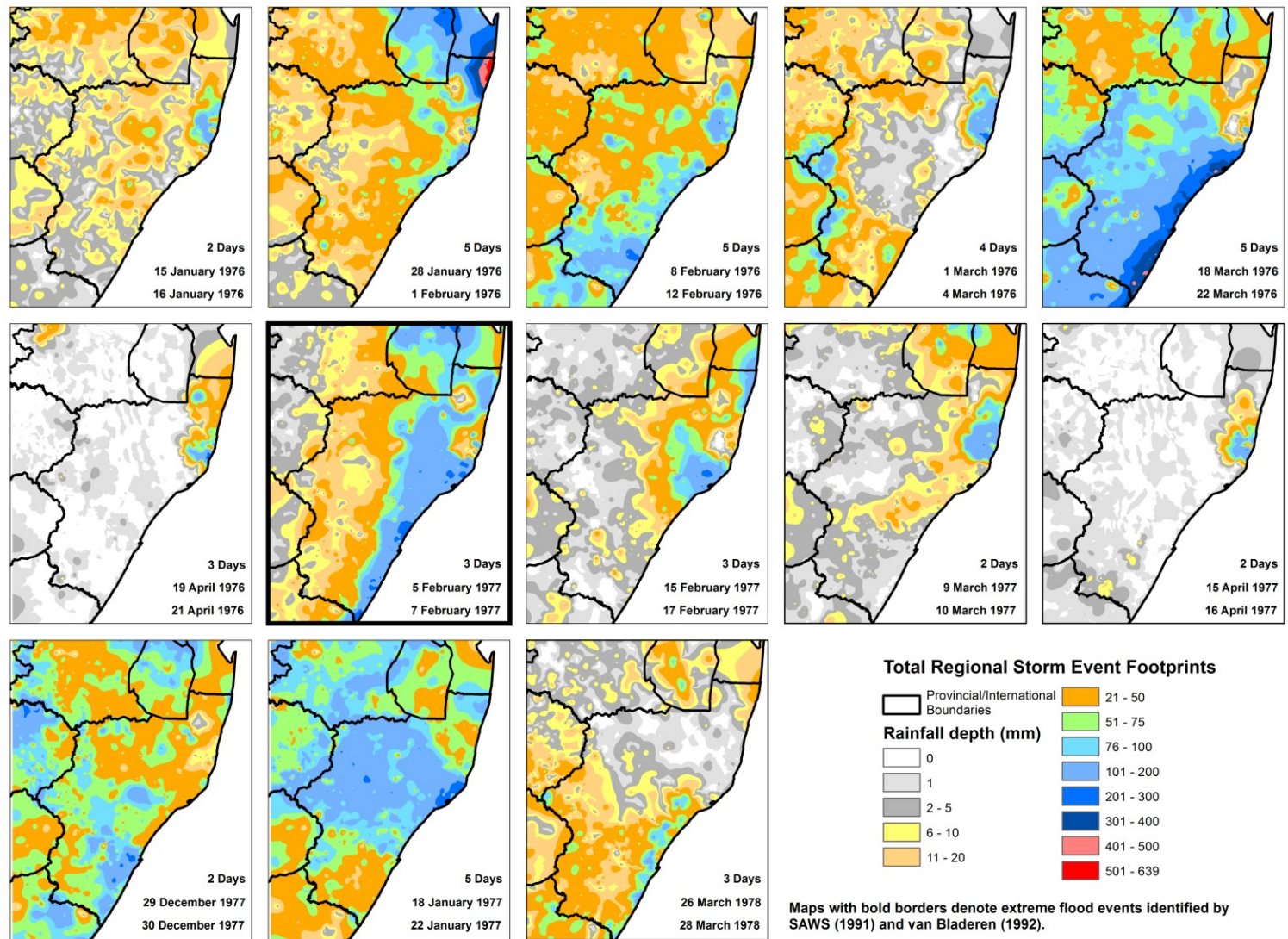


Figure 13. Total regional storm event footprints 15 January 1976 – 28 March 1978.

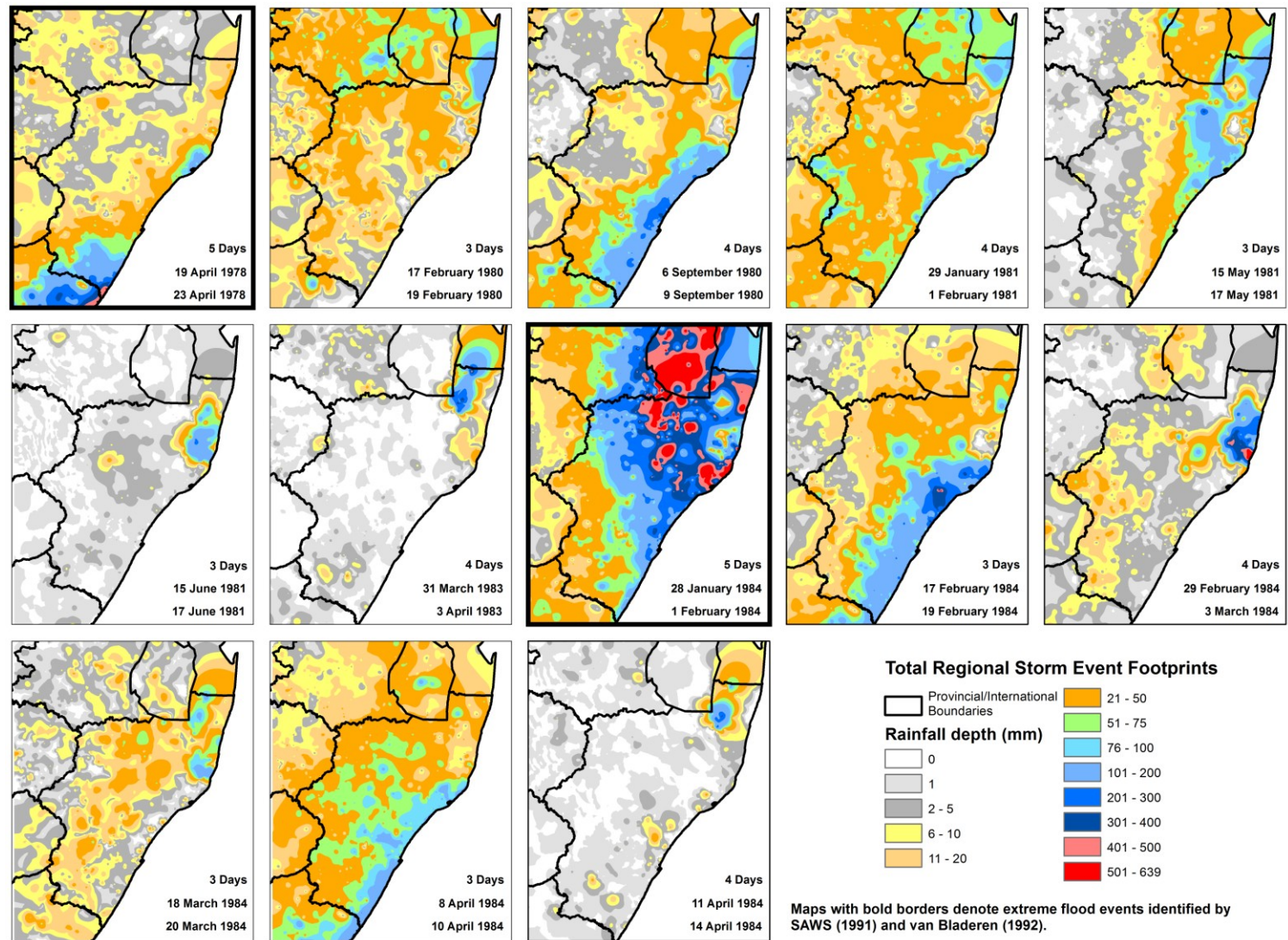


Figure 14. Total regional storm event footprints 19 April 1978 – 14 April 1984.

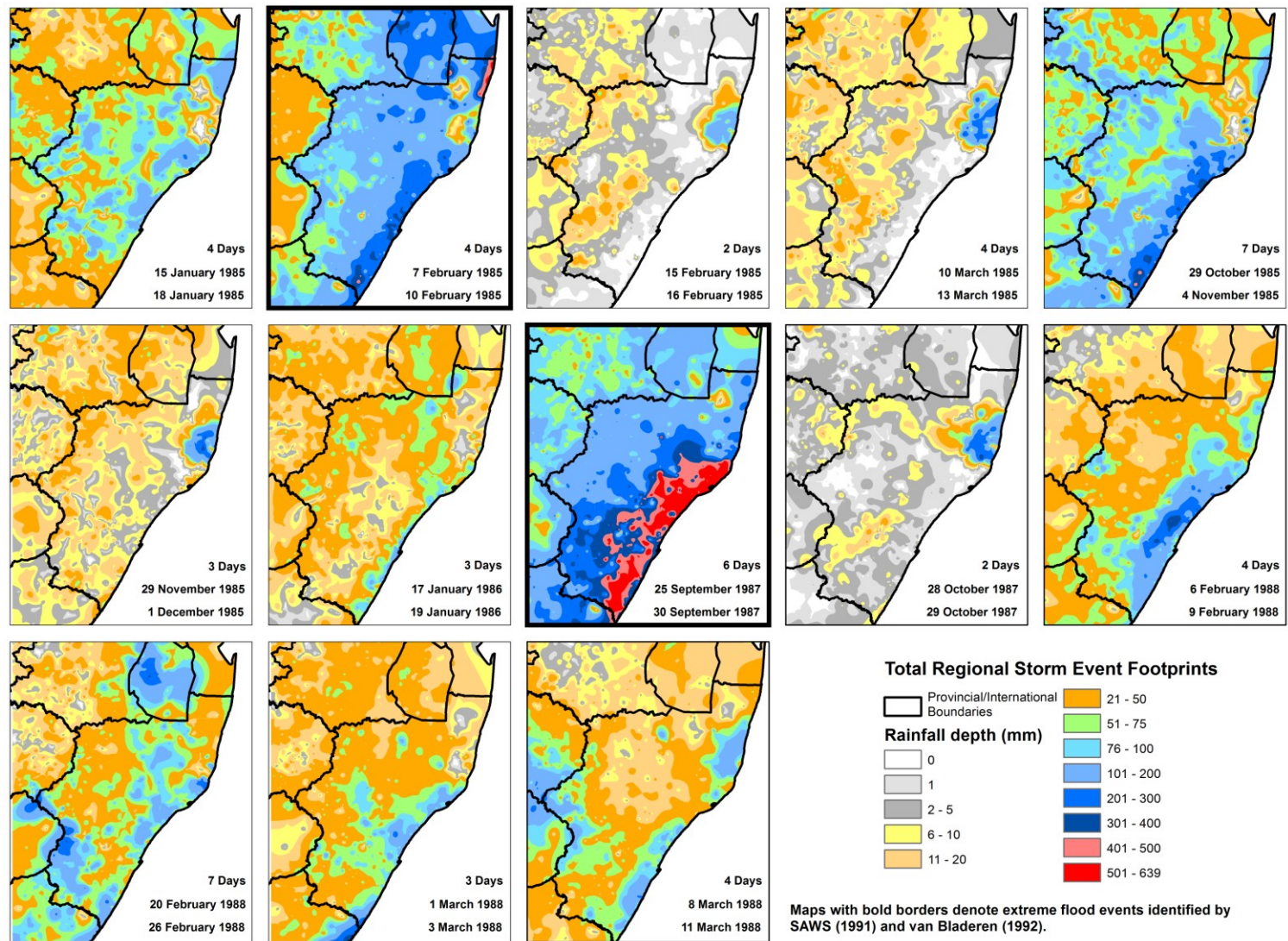


Figure 15. Total regional storm event footprints 15 January 1985 – 11 March 1988.

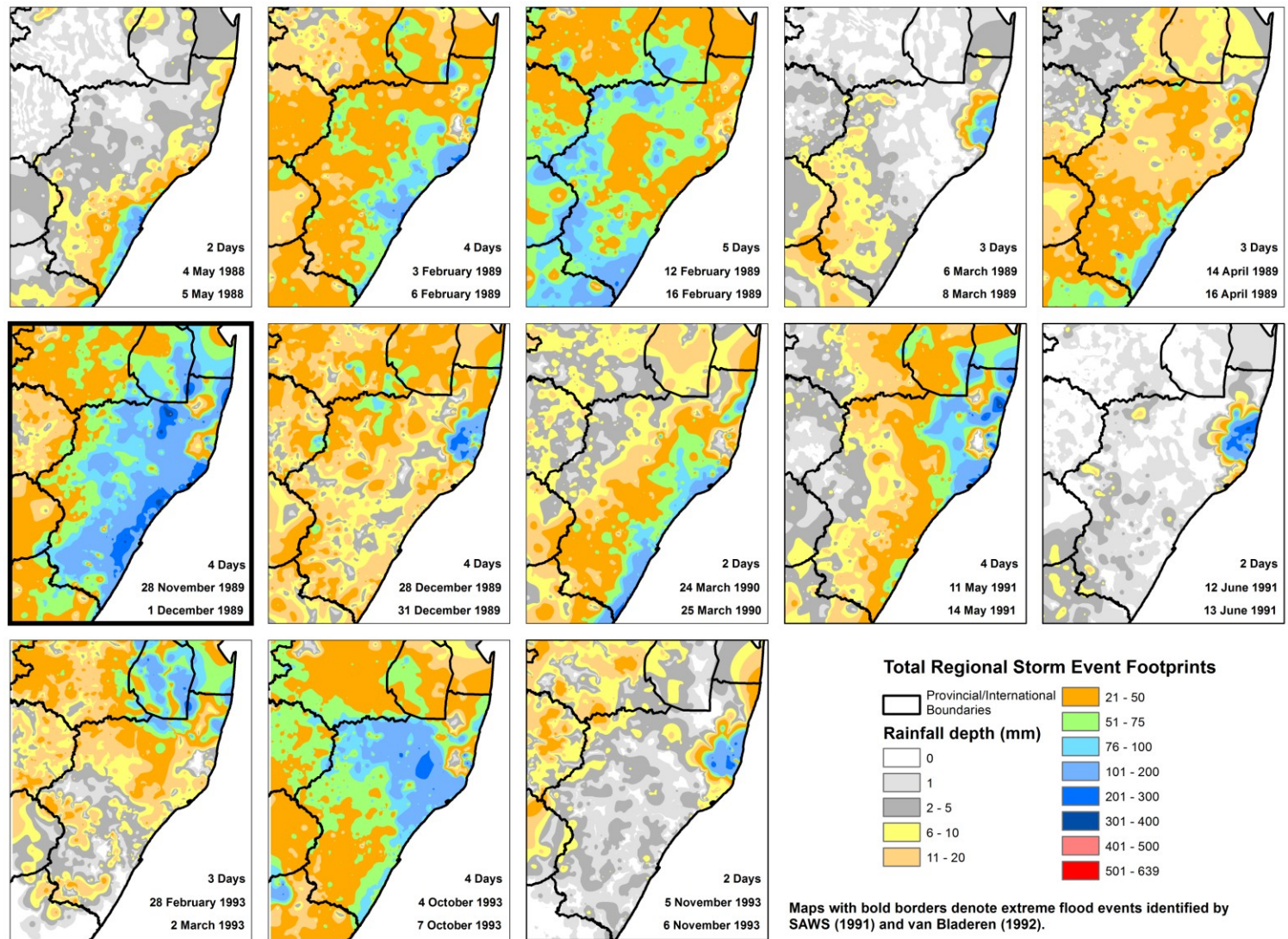


Figure 16. Total regional storm event footprints 4 May 1988 – 6 November 1993.

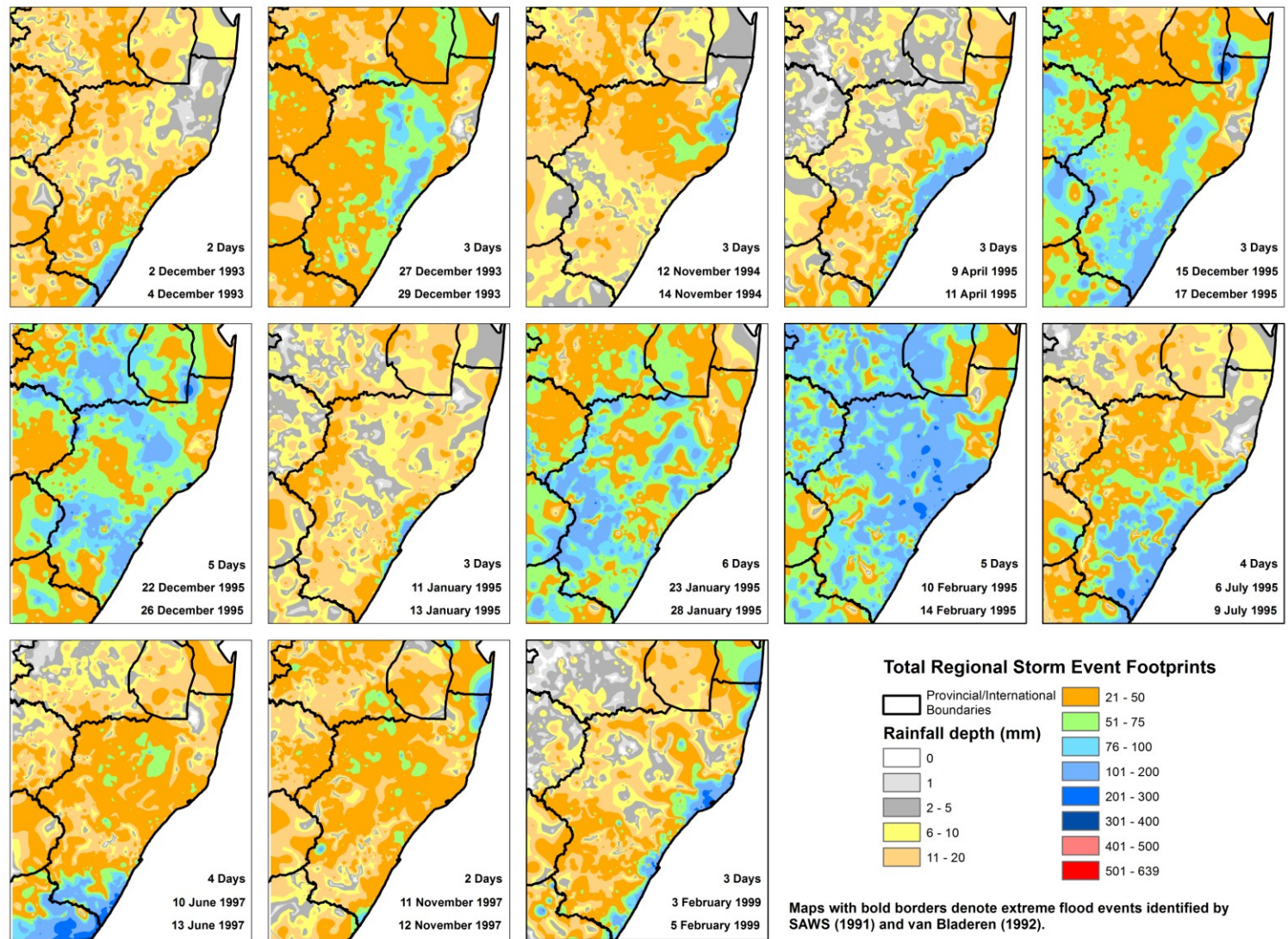
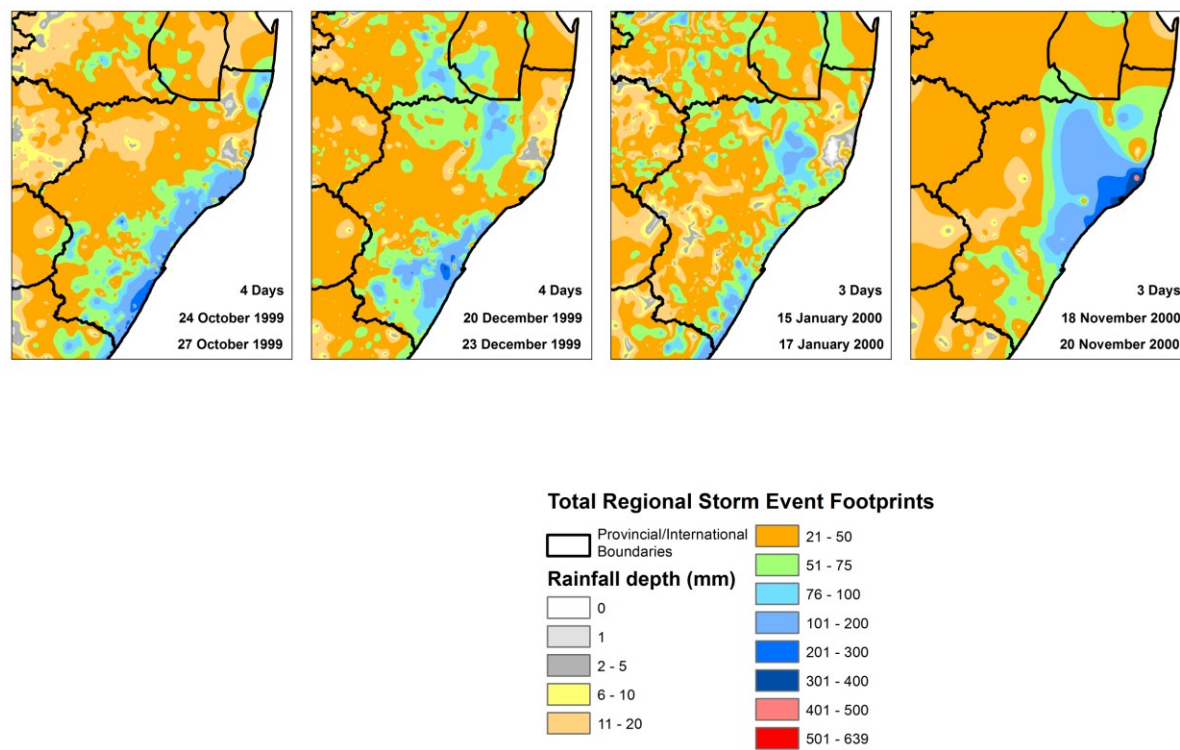


Figure 17. Total regional storm event footprints 2 December 1993 – 5 February 1999.



Maps with bold borders denote extreme flood events identified by SAWS (1991) and van Bladeren (1992).

Figure 18. Total regional storm event footprints 24 October 1999 – 20 November 2000.

APPENDIX V – LOCAL STORM EVENT DATA

Local storm events identified from storm footprints.

ZAB – Author, vB - van Bladeren (1992)

Year	Month	Date	Geographic Area	Source
1891	March	8 March 1891	Durban	ZAB
1891	March	28 March 1891	Van Reenens	ZAB
1891	May	16 May 1891	Durban	ZAB
1892	February	2 February 1892	Durban	ZAB
1892	February	5 February 1892	Drakensberg	ZAB
1892	November	20 November 1892	Ixopo	ZAB
1893	February	9 February 1893	Durban	ZAB
1893	November	22 November 1893	Drakensburg - Bloukrans River	vB
1893	November	30 November 1893	Drakensberg	ZAB
1894	March	05 March 1894	Ladysmith	vB
1895	February	17 February 1895	Durban	ZAB
1895	March	10 March 1895	Durban	ZAB
1895	May	9 May 1895	Durban	vB
1896	April	7 April 1896	Durban	ZAB
1897	March	21 March 1897	Durban	ZAB
1898	February	28 February 1898	Durban	ZAB
1899	January	24 January 1899	Durban	ZAB
1899	October	22 October 1899	Durban	ZAB
1901	January	22 January 1901	Wartburg	ZAB
1903	November	28 November 1903	Durban	ZAB
1903	December	23 December 1903	Durban	ZAB
1904	January	22 January 1904	Drakensburg - Bloukrans River	vB
1905	December	09 December 1905	Pmb - Mooi River	ZAB
1906	September	18 September 1906	Greytown to Pmb	ZAB
1907	January	18 January 1907	Durban Area	vB
1907	February	28 February 1907	Empangeni	vB
1907	March	28 March 1907	Ixopo Area	ZAB
1907	April	07 April 1907	Durban Area	ZAB
1907	November	28 November 1907	Empangeni	vB
1908	February	04 February 1908	Scottburgh	ZAB
1908	February	17 February 1908	Mooi River Area	ZAB
1908	February	29 February 1908	Estcourt Area	ZAB
1909	February	09 February 1909	Drakensberg	ZAB
1909	September	02 September 1909	Scottburgh	ZAB
1910	January	16 January 1910	Wartburg	ZAB
1910	February	11 February 1910	Port Shepstone Area	vB
1910	December	06 December 1910	Durban Area	ZAB
1910	December	29 December 1910	Ixopo Area	ZAB
1911	February	19 February 1911	Port Shepstone Area	ZAB
1911	March	02 March 1911	Midlands	vB
1911	March	07 March 1911	Drakensburg	ZAB
1912	January	04 January 1912	Paulpietersburg area	ZAB
1912	January	08 January 1912	Paulpietersburg area	ZAB

Year	Month	Date	Geographic Area	Source
1912	February	24 February 1912	Underberg area	ZAB
1913	January	01 January 1913	Port Edward area	ZAB
1913	February	23 February 1913	Pmb - Durban	ZAB
1913	February	24 February 1913	Berg area	ZAB
1913	February	25 February 1913	Port Edward area	ZAB
1913	April	29 April 1913	Mtunzini area	ZAB
1913	September	30 September 1913	Port Edward area	ZAB
1914	January	18 January 1914	Ladysmith - Dundee	ZAB
1914	January	30 January 1914	Kwambonambi	ZAB
1914	March	05 March 1914	Dundee	ZAB
1914	April	15 April 1914	Mtunzini area	ZAB
1914	April	16 April 1914	Durban	ZAB
1914	August	18 August 1914	Rbay area	ZAB
1914	September	18 September 1914	Hluhluwe area	ZAB
1914	November	25 November 1914	Paulpietersburg area	ZAB
1914	November	26 November 1914	Nongoma	ZAB
1914	December	02 December 1914	Ladysmith	vB
1914	December	03 December 1914	Van Reenens	ZAB
1914	December	22 December 1914	Northern KZN	ZAB
1914	December	23 December 1914	Berg area	ZAB
1915	January	14 January 1915	Rbay area	ZAB
1915	January	15 January 1915	Pongola area	ZAB
1915	January	23 January 1915	Kosi Bay	ZAB
1915	January	30 January 1915	Underberg area	ZAB
1915	February	08 February 1915	St Lucia Area	ZAB
1915	February	18 February 1915	North coast	ZAB
1915	March	21 March 1915	North coast	ZAB
1915	June	01 June 1915	North coast	ZAB
1916	January	04 January 1916	Dundee	ZAB
1916	March	16 March 1915	Durban Area	vB
1916	March	28 March 1916	Scottburgh	ZAB
1916	April	04 April 1916	Cape Vidal	ZAB
1916	December	28 December 1916	Dundee	ZAB
1916	December	31 December 1916	Underberg Mooiriver	ZAB
1917	February	23 February 1917	Ladysmith	vB
1917	April	16 April 1917	Jozini	ZAB
1917	August	20 August 1917	Hluhluwe area	ZAB
1917	December	30 December 1917	South of Vryheid	ZAB
1917	December	31 December 1917	Nkandla area	vB
1918	February	20 February 1918	North of Pmb	ZAB
1918	February	21 February 1918	Rbay area	ZAB
1918	April	21 April 1918	Jozini	ZAB
1918	August	01 August 1918	Berg area	ZAB
1918	August	03 August 1918	South Coast to Pmb	ZAB
1918	August	04 August 1918	Port Edward area	ZAB
1918	August	31 August 1918	Port Edward area	ZAB
1918	October	08 October 1918	Vryheid area	ZAB
1918	December	31 December 1918	Weenen	ZAB
1919	February	18 February 1919	North Coast	ZAB
1919	March	08 March 1919	Durban coast	ZAB
1919	March	10 March 1919	Durban area	ZAB
1919	March	21 March 1919	Hluhluwe area	ZAB
1919	April	01 April 1919	Tembe	ZAB
1919	April	02 April 1919	Jozini	ZAB

Year	Month	Date	Geographic Area	Source
1919	May	24 May 1919	Jozini	ZAB
1920	January	17 January 1920	Berg area	ZAB
1920	March	22 March 1920	Rbay & Maputuland	ZAB
1920	October	28 October 1920	Estcourt	ZAB
1921	February	06 February 1921	Ladysmith area	ZAB
1921	February	11 February 1921	Durban	ZAB
1921	February	19 February 1921	Dundee	ZAB
1921	March	22 March 1921	Ulundi area	ZAB
1921	September	09 September 1921	Dundee	ZAB
1921	November	28 November 1921	Newcastle Area, Durban - Pmb, Empangeni Area	ZAB
1922	January	11 January 1922	Ladysmith area	ZAB
1922	January	29 January 1922	Underberg area	ZAB
1922	February	10 February 1922	Ulundi area	ZAB
1922	February	26 February 1922	Ladysmith area	ZAB
1922	March	25 March 1922	Newcastle area	ZAB
1922	April	15 April 1922	Jozini area	ZAB
1922	May	02 May 1922	Jozini area	ZAB
1922	May	15 May 1922	Jozini area	ZAB
1922	June	?	Umzimkhulu	vB
1922	August	06 August 1922	Vryheid area	ZAB
1922	October	31 October 1922	South Coast	ZAB
1923	February	24 February 1923	Van Reenens	ZAB
1923	December	07 December 1923	Ixopo	ZAB
1923	December	08 December 1923	Jozini area	ZAB
1924	January	30 January 1924	Ladysmith - Dundee area	ZAB
1924	March	18 March 1924	Tembe	ZAB
1924	May	14 May 1924	Jozini area	ZAB
1924	September	23 September 1924	Jozini area	ZAB
1924	December	21 December 1924	Jozini area	ZAB
1925	January	15 January 1925	Kosi Bay area	ZAB
1925	January	29 January 1925	Ladysmith area	ZAB
1925	January	30 January 1925	Volksrust area	ZAB
1925	February	09 February 1925	Scattered KZN	ZAB
1925	February	10 February 1925	Rbay area	ZAB
1925	February	15 February 1925	Sodwana area	ZAB
1925	February	20 February 1925	Ladysmith - Dundee	ZAB
1932	March	02 March 1932	Northern KZN	ZAB
1925	March	06 March 1925	Rbay & Jozini	ZAB
1925	March	30 March 1925	Lebombo	ZAB
1925	April	19 April 1925	Sodwana	ZAB
1925	May	14 May 1925	Rbay area	ZAB
1925	June	14 June 1925	Hluhluwe area	ZAB
1926	January	24 January 1926	Ladysmith area	ZAB
1926	January	26 January 1926	North of Greytown	ZAB
1926	January	27 January 1926	Ladysmith area	ZAB
1926	March	24 March 1926	Port Edward area	ZAB
1926	September	03 September 1926	Van Reenens - Dundee	ZAB
1926	September	04 September 1926	Ladysmith - Vryheid area	ZAB
1926	December	22 December 1926	Kwambonambi	ZAB
1927	January	22 January 1927	Somkhele	ZAB
1927	February	11 February 1927	Newcastle area	ZAB
1927	February	17 February 1927	Nkandla area	ZAB
1927	March	26 March 1927	Van Reenens	ZAB
1927	October	31 October 1927	Kokstad area	ZAB

Year	Month	Date	Geographic Area	Source
1927	December	01 December 1927	Van Reenens area	ZAB
1928	January	16 January 1928	Paulpietersburg area	ZAB
1928	February	04 February 1928	Mtunzini	ZAB
1928	April	22 April 1928	Jozini area	ZAB
1928	September	30 September 1928	Mooiriver area	ZAB
1929	January	11 January 1929	Dundee area	ZAB
1929	January	19 January 1929	Empangeni area	ZAB
1929	January	30 January 1929	Mooiriver area	ZAB
1929	February	19 February 1929	Pongola area	ZAB
1929	March	02 March 1929	Hibberdene area	ZAB
1929	March	19 March 1929	Jozini area	ZAB
1929	March	22 March 1929	Makhathini area	ZAB
1929	April	06 April 1929	Port Edward area	ZAB
1929	July	09 July 1929	South Coast	ZAB
1930	January	14 January 1930	Sani Pass area	ZAB
1930	February	26 February 1930	Nongoma area	ZAB
1930	March	22 March 1930	Durban area	ZAB
1931	January	13 January 1931	Ixopo Area	ZAB
1931	January	15 January 1931	Nkandla area	ZAB
1931	January	16 January 1931	Melmoth area	ZAB
1931	February	01 February 1931	Van Reenen - Newcastle	ZAB
1931	February	11 February 1931	Ladysmith area	ZAB
1931	July	03 July 1931	South Coast	ZAB
1931	November	19 November 1931	Mtubatuba Area	ZAB
1931	November	20 November 1931	St Lucia Area	ZAB
1931	December	20 December 1931	St Lucia Area	ZAB
1932	March	19 March 1932	Port Edward	ZAB
1932	April	23 April 1932	Pongola area	ZAB
1932	May	29 May 1932	Mtubatuba Area	ZAB
1932	December	17 December 1932	Vryheid area	ZAB
1933	January	18 January 1933	Pongola area	ZAB
1933	February	18 February 1933	Jozini area	ZAB
1933	November	09 November 1933	Hibberdene area	ZAB
1933	November	11 November 1933	Dundee area	ZAB
1933	December	13 December 1933	Nongoma - Vryheid	ZAB
1933	December	23 December 1933	Stanger Area	ZAB
1934	January	01 January 1934	Berg - Ladysmith area	vB
1934	January	02 January 1934	Ladysmith area	ZAB
1934	January	09 January 1934	Ladysmith - Newcastle area	ZAB
1934	February	11 February 1934	Ladysmith area	ZAB
1934	April	04 April 1934	Mbazwana area	ZAB
1934	April	05 April 1934	Ladysmith area	ZAB
1934	November	18 November 1934	Estcourt Area	ZAB
1934	December	09 December 1934	Van Reenens area	ZAB
1934	December	10 December 1934	Port Edward area	ZAB
1935	January	11 January 1935	Volsrust area	ZAB
1935	January	14 January 1935	Durban area	ZAB
1935	May	18 May 1935	Mtunzini	ZAB
1935	November	01 November 1935	Berg area	ZAB
1935	December	19 December 1935	Vryheid area	ZAB
1936	January	09 January 1936	Newcastle - Vryheid area	ZAB
1936	January	11 January 1936	Jozini area	ZAB
1936	January	12 January 1936	Jozini area	ZAB
1936	January	18 January 1936	Scattered Nothern KZN	ZAB

Year	Month	Date	Geographic Area	Source
1936	March	01 March 1936	Scattered Nothern KZN	ZAB
1936	March	31 March 1936	Mtubatuba Area	ZAB
1936	November	10 November 1936	Scattered KZN	vB
1936	November	19 November 1936	Dundee area	ZAB
1937	January	15 January 1937	Port Edward area	ZAB
1937	January	23 January 1937	Port Edward area, Dundee area	ZAB
1937	February	04 February 1937	Ladysmith, Nqutu	ZAB
1937	February	19 February 1937	Scattered Central KZN axis	ZAB
1937	February	20 February 1937	Kokstad, Port Edward	ZAB
1937	February	23 February 1937	Jozini area	ZAB
1937	February	24 February 1937	Kokstad area	ZAB
1937	March	31 March 1937	St Lucia Area	ZAB
1937	August	03 August 1937	South Coast	ZAB
1937	December	07 December 1937	Hluhluwe area	ZAB
1937	December	15 December 1937	Berg area	ZAB
1937	December	17 December 1937	St Lucia Area	ZAB
1937	December	22 December 1937	Pongola area	ZAB
1938	January	16 January 1938	Nqutu area	ZAB
1938	January	17 January 1938	Dundee & Hluhluwe area	ZAB
1938	January	21 January 1938	Van Reenens area	ZAB
1938	January	22 January 1938	Port edward & Jozini area	ZAB
1938	January	29 January 1938	St Lucia Area	ZAB
1938	February	04 February 1938	Jozini area	ZAB
1938	February	07 February 1938	Eshowe area	ZAB
1938	February	10 February 1938	Jozini area	ZAB
1938	February	14 February 1938	Durban area	ZAB
1938	February	16 February 1938	Eshowe area	ZAB
1938	March	11 March 1938	Newcastle area	ZAB
1938	April	13 April 1938	Port Edward area	ZAB
1938	June	20 June 1938	Rbay area	ZAB
1938	July	07 July 1938	Port Edward area	ZAB
1938	July	09 July 1938	Stanger Area	ZAB
1938	July	19 July 1938	Mtunzini area	ZAB
1938	October	05 October 1938	Berg area	ZAB
1938	October	25 October 1938	Vryheid area	ZAB
1938	October	26 October 1938	Durban area	ZAB
1938	October	28 October 1938	Dundee area	ZAB
1938	November	30 November 1938	Ulundi area	ZAB
1938	December	01 December 1938	Van Reenens area	ZAB
1938	December	09 December 1938	Port Edward area	ZAB
1938	December	10 December 1938	Port Edward & Pongola area	ZAB
1938	December	16 December 1938	Ladysmith area	ZAB
1938	December	22 December 1938	Dundee area	ZAB
1939	January	03 January 1939	Hluhluwe area	ZAB
1939	January	20 January 1939	Utrecht area	ZAB
1939	January	22 January 1939	Underberg area	ZAB
1939	January	31 January 1939	Jozini area	ZAB
1939	February	01 February 1939	St Lucia Area	ZAB
1939	February	02 February 1939	Pongola area	ZAB
1939	February	12 February 1939	Nongoma & Berg area	ZAB
1939	February	13 February 1939	Port Edward & Vryheid area	ZAB
1939	February	23 February 1939	Underberg area	ZAB
1939	February	25 February 1939	Paulpietersburg area	ZAB
1939	March	29 March 1939	Dundee area	ZAB

Year	Month	Date	Geographic Area	Source
1939	May	18 May 1939	Jozini area	ZAB
1939	May	20 May 1939	Mtunzini area	ZAB
1939	May	21 May 1939	Mtunzini area	ZAB
1939	September	12 September 1939	Mtunzini area	ZAB
1939	September	13 September 1939	Amatikulu area	ZAB
1939	September	25 September 1939	Port Edward area	ZAB
1939	October	23 October 1939	Hlabisa area	ZAB
1939	November	26 November 1939	Cato Ridge area	ZAB
1939	December	12 December 1939	Ladysmith area	ZAB
1940	March	01 March 1940	Berg area	ZAB
1940	March	15 March 1940	Rbay area	ZAB
1940	March	23 March 1940	St Lucia Area	ZAB
1940	April	16 April 1940	Hluhluwe area	ZAB
1940	June	19 June 1940	Rbay area	ZAB
1940	June	20 June 1940	Hluhluwe area	ZAB
1940	October	29 October 1940	Dundee area	ZAB
1940	November	08 November 1940	Newcastle & Hluhluwe area	ZAB
1940	November	09 November 1940	Berg area	ZAB
1940	November	11 November 1940	Rbay area	ZAB
1940	November	21 December 1940	Nkandla area	ZAB
1941	January	20 January 1941	Berg & Ladysmith area	ZAB
1941	January	21 January 1941	Berg & Ladysmith area	ZAB
1941	January	22 January 1941	Berg & Ladysmith area	ZAB
1941	January	31 January 1941	Kokstad area	ZAB
1941	February	03 February 1941	Jozini area	ZAB
1941	February	04 February 1941	Newcastle area	ZAB
1941	February	05 February 1941	Berg area	ZAB
1941	February	21 February 1941	Utrecht & Jozini area	ZAB
1941	February	22 February 1941	Jozini area	ZAB
1941	March	12 March 1941	Nqutu area	ZAB
1941	April	02 April 1941	Jozini area	ZAB
1941	August	03 August 1941	Jozini area	ZAB
1941	December	05 December 1941	Newcastle - Ladysmith area	ZAB
1941	December	20 December 1941	Dundee & Kosi Bay area	ZAB
1941	December	22 December 1941	Pongola area	ZAB
1942	January	01 January 1942	Vryheid area	ZAB
1942	January	10 January 1942	Nqutu area	ZAB
1942	January	22 January 1942	Jozini area	ZAB
1942	February	12 February 1942	Vryheid area	ZAB
1942	February	19 February 1942	Underberg area	ZAB
1942	February	25 February 1942	Nkandla area	ZAB
1942	March	01 March 1942	Makhathini area	ZAB
1942	March	02 March 1942	St Lucia Area	ZAB
1942	March	03 March 1942	St Lucia Area	ZAB
1942	March	14 March 1942	Rbay area	ZAB
1942	March	18 March 1942	Ladysmith area	ZAB
1942	March	19 March 1942	Ladysmith area	ZAB
1942	March	31 March 1942	Jozini area	ZAB
1942	April	06 April 1942	Van Reenens area	ZAB
1942	May	16 May 1942	Port Edward area	ZAB
1942	May	30 May 1942	Jozini area	ZAB
1942	July	02 July 1942	Jozini area	ZAB
1942	July	16 July 1942	Jozini area	ZAB
1942	October	24 October 1942	St Faiths area	ZAB

Year	Month	Date	Geographic Area	Source
1942	October	28 October 1942	Nkandla area	ZAB
1942	November	27 November 1942	Dundee area	ZAB
1942	November	28 November 1942	Dundee area	ZAB
1942	December	01 December 1942	Nqutu area	ZAB
1942	December	02 December 1942	Paulpietersburg area	ZAB
1942	December	10 December 1942	Newcastle area	ZAB
1942	December	28 December 1942	Ulundi area	ZAB
1942	December	31 December 1942	Kokstad area	ZAB
1943	January	03 January 1943	Newcastle area	ZAB
1943	January	08 January 1943	Dundee area	ZAB
1943	February	25 February 1943	Durban area	ZAB
1943	March	01 March 1943	Nqutu area	ZAB
1943	March	26 March 1943	Makhathini area	ZAB
1943	March	30 March 1943	Jozini area	ZAB
1943	April	01 April 1943	Nqutu area	ZAB
1943	April	05 April 1943	Hluhluwe area	ZAB
1943	April	07 April 1943	Hluhluwe area	ZAB
1943	April	13 April 1943	Jozini area	ZAB
1943	April	17 April 1943	Rbay area	ZAB
1943	April	30 April 1943	Kosi Bay, Rbay, Newcastle	ZAB
1943	May	20 May 1943	Durban area	ZAB
1943	May	23 May 1943	Hluhluwe area	ZAB
1943	May	24 May 1943	Hluhluwe area	ZAB
1943	May	31 May 1943	Makhathini area	ZAB
1943	July	03 July 1943	Rbay area	ZAB
1943	July	04 July 1943	Makhathini area	ZAB
1943	July	05 July 1943	Makhathini area	ZAB
1943	August	01 August 1943	Nqutu area	ZAB
1943	August	23 August 1943	Ladysmith - Greytown area	ZAB
1943	October	01 October 1943	Nqutu area	ZAB
1943	October	12 October 1943	Scattered W KZN	ZAB
1943	October	13 October 1943	Moorriver area	ZAB
1943	November	07 November 1943	Dundee area	ZAB
1943	November	14 November 1943	Empangeni area	ZAB
1943	November	30 November 1943	Durban area	vB
1943	December	19 December 1943	Ulundi area	ZAB
1943	December	31 December 1943	Kokstad area	ZAB
1944	January	23 January 1944	Kosi Bay area	ZAB
1944	January	31 January 1944	Pongola area	ZAB
1944	February	01 February 1944	Northern KZN	vB
1944	February	03 February 1944	Van Reenens area	ZAB
1944	February	04 February 1944	Estcourt area	ZAB
1944	February	05 February 1944	Ladysmith area	ZAB
1944	February	10 February 1944	Makhathini area	ZAB
1944	February	17 February 1944	Jozini area	ZAB
1944	February	18 February 1944	Makhathini area	ZAB
1944	March	04 March 1944	Coastal KZN	ZAB
1944	March	05 March 1944	Mtubatuba Area	ZAB
1944	March	09 March 1944	Berg area	ZAB
1944	March	31 March 1944	Kokstad area	ZAB
1944	May	06 May 1944	Jozini area	ZAB
1944	June	15 June 1944	Rbay area	ZAB
1944	June	16 June 1944	Kosi Bay area	ZAB
1944	July	16 July 1944	Mtubatuba Area	ZAB

Year	Month	Date	Geographic Area	Source
1944	September	17 September 1944	Rbay area, Port Edward area	ZAB
1944	September	18 September 1944	Port Edward area, Mtunzini area	ZAB
1944	September	20 September 1944	Kokstad area	ZAB
1944	November	08 November 1944	Rbay area	ZAB
1944	November	28 November 1944	St Lucia Area	ZAB
1944	December	31 December 1944	Vryheid area	ZAB
1945	January	19 January 1945	Pongola area	ZAB
1945	February	01 February 1945	Nkandla area	ZAB
1945	February	02 February 1945	St Lucia Area	ZAB
1945	February	05 February 1945	Mtunzini area	ZAB
1945	February	20 February 1945	Mtubatuba Area	ZAB
1945	February	22 February 1945	Berg area	ZAB
1945	March	02 March 1945	Nkandla area	ZAB
1945	March	03 March 1945	Mtunzini area	ZAB
1945	March	05 March 1945	Hluhluwe area	ZAB
1945	March	07 March 1945	Melmoth area	ZAB
1945	March	16 March 1945	Mzimkhulu area	ZAB
1945	March	29 March 1945	Jozini area	ZAB
1945	April	23 April 1945	Hluhluwe area	ZAB
1945	October	03 October 1945	South Coast	ZAB
1946	January	09 January 1946	Jozini area	ZAB
1946	February	03 February 1946	Ladysmith. Nongoma area	ZAB
1946	February	06 February 1946	Newcastle area	ZAB
1946	March	14 March 1946	Vryheid area	ZAB
1946	April	01 April 1946	Rbay area	ZAB
1947	January	14 January 1947	Scattered Central KZN	ZAB
1947	February	01 February 1947	Dundee area	ZAB
1947	February	03 February 1947	Jozini area	ZAB
1947	February	25 February 1947	Durban	ZAB
1947	February	28 February 1947	Rbay, Ulundi, Vryheid, Weenen, Underberg Area	ZAB
1947	March	01 March 1947	Vryheid to Ulundi	ZAB
1947	March	14 March 1947	Richmond area	ZAB
1947	March	15 March 1947	Ixopo, Rbay area	ZAB
1947	March	31 March 1947	South Coast, Hluhluwe area	ZAB
1947	April	01 April 1947	Durban area	ZAB
1947	May	23 May 1947	Port Edward area	ZAB
1947	May	24 May 1947	Port Edward area	ZAB
1947	June	02 June 1947	South Coast	ZAB
1947	June	03 June 1947	Port Shepstone area	ZAB
1947	November	25 November 1947	Port Edward, Greytown area	ZAB
1947	November	30 November 1947	Nqutu area	ZAB
1947	December	25 December 1947	Babanango area	ZAB
1948	February	06 February 1948	Dundee area	ZAB
1948	February	15 February 1948	Underberg, Vryheid area	ZAB
1948	February	16 February 1948	Durban, Mkuze area	ZAB
1948	February	22 February 1948	Rbay area	ZAB
1948	March	02 March 1948	Berg area	ZAB
1948	March	04 March 1948	Berg area	ZAB
1948	March	08 March 1948	Berg area	ZAB
1948	March	10 March 1948	Berg area	ZAB
1948	March	16 March 1948	West of Ladysmith	ZAB
1948	March	20 March 1948	South Coast, Maputoland, Durban - Newcastle Axis	ZAB
1948	March	24 March 1948	Vryheid	ZAB
1948	October	09 October 1948	Durban area	ZAB

Year	Month	Date	Geographic Area	Source
1949	January	11 January 1949	Kokstad area	ZAB
1949	January	12 January 1949	Bulwer, Nkandla area	ZAB
1949	January	13 January 1949	Nqutu area	ZAB
1949	January	18 January 1949	Mbazwana area	ZAB
1949	January	22 January 1949	Mbazwana area	ZAB
1949	January	30 January 1949	Nongoma, St Lucia area	ZAB
1949	January	31 January 1949	Nkandla area	ZAB
1949	February	01 February 1949	Vryheid area	ZAB
1949	February	24 February 1949	Van Reenens area	ZAB
1949	March	02 March 1949	Hluhluwe area	ZAB
1949	March	26 March 1949	Port Edward area	ZAB
1949	March	27 March 1949	Port Edward area	ZAB
1949	November	16 November 1949	Port Edward area	ZAB
1949	November	26 November 1949	Dundee area	ZAB
1949	December	01 December 1949	Durban	ZAB
1949	December	11 December 1949	Pongola area	ZAB
1949	December	27 December 1949	Scattered Central KZN	ZAB
1949	December	28 December 1949	Eshowe area	ZAB
1950	January	09 January 1950	Rbay area	ZAB
1950	January	11 January 1950	Jozini area	ZAB
1950	January	24 January 1950	Port Edward area	ZAB
1950	January	27 January 1950	Hluhluwe area	ZAB
1950	January	31 January 1950	Kokstad area	ZAB
1950	February	11 February 1950	Kosi Bay area	ZAB
1950	February	19 February 1950	Rbay area	ZAB
1950	February	25 February 1950	Van Reenens area	ZAB
1950	March	02 March 1950	Mtunzini area	ZAB
1950	March	16 March 1950	Ladysmith area	ZAB
1950	March	23 March 1950	Makhathini area	ZAB
1950	March	31 March 1950	Rbay area	ZAB
1950	April	14 April 1950	Port Edward area	ZAB
1950	April	15 April 1950	Port Edward area	ZAB
1950	April	23 April 1950	Makhathini area	ZAB
1950	November	23 November 1950	Estcourt area	ZAB
1950	December	08 December 1950	Durban area	ZAB
1950	December	31 December 1950	Kokstad area, Vryheid area	ZAB
1951	January	13 January 1951	Port Edward area	ZAB
1951	March	05 March 1951	Durban area	ZAB
1951	March	06 March 1951	Nqutu area	ZAB
1951	March	15 March 1951	St Lucia Area	ZAB
1951	March	20 March 1951	Berg aea	ZAB
1951	April	15 April 1951	Mtubatuba Area	ZAB
1951	December	10 December 1951	Nqutu area	ZAB
1951	December	11 December 1951	KZN Coast	ZAB
1952	January	02 January 1952	Vryheid area	ZAB
1952	January	11 January 1952	Mbazwana area	ZAB
1952	January	19 January 1952	Newcastle area	ZAB
1952	January	24 January 1952	Dundee area	ZAB
1952	February	07 February 1952	Nkandla area	ZAB
1952	February	08 February 1952	Vryheid area	ZAB
1952	February	21 February 1952	Berg area	ZAB
1952	April	08 April 1952	Durban area	ZAB
1952	April	09 April 1952	Kelso area	ZAB
1952	July	14 July 1952	Kosi Bay area	ZAB

Year	Month	Date	Geographic Area	Source
1952	October	17 October 1952	Nqutu area	ZAB
1952	November	01 November 1952	Ulundi , Greytown area	vB
1952	December	31 December 1952	Kokstad area	ZAB
1953	January	07 January 1953	Mbazwana	ZAB
1953	February	01 February 1953	Nkandla area	ZAB
1953	February	08 February 1953	Kokstad, Nkandla area	ZAB
1953	February	09 February 1953	Ladysmith, coastal area	ZAB
1953	February	11 February 1953	Vryheid area	ZAB
1953	February	27 February 1953	Mkuze area	ZAB
1953	March	12 March 1953	St Lucia Area	ZAB
1953	April	02 April 1953	Ladysmith - Dundee	ZAB
1953	May	12 May 1953	Melmoth area	ZAB
1953	July	22 July 1953	Jozini area	ZAB
1953	August	26 August 1953	Scattered KZN	ZAB
1953	September	15 September 1953	Mtunzini area	ZAB
1953	October	07 October 1953	Kokstad area	ZAB
1953	October	17 October 1953	Hluhluwe area	ZAB
1953	November	04 November 1953	Nqutu area	ZAB
1953	November	17 November 1953	Vryheid area	ZAB
1953	November	18 November 1953	Ladysmith area	ZAB
1953	November	27 November 1953	Rbay area	ZAB
1953	November	28 November 1953	Rbay area	ZAB
1953	November	30 November 1953	St Lucia Area	ZAB
1953	December	01 December 1953	St Lucia Area	ZAB
1953	December	04 December 1953	Nqutu area	ZAB
1953	December	29 December 1953	Kosi Bay area	ZAB
1953	December	31 December 1953	St Lucia Area	ZAB
1954	February	11 February 1954	Pmb area	ZAB
1954	February	14 February 1954	Mtunzini area	ZAB
1954	February	24 February 1954	Durban - Rbay	ZAB
1954	March	17 March 1954	Port Edward area	ZAB
1954	March	19 March 1954	South Coast	ZAB
1954	March	31 March 1954	Kokstad area	ZAB
1954	June	21 June 1954	Hluhluwe area	ZAB
1954	September	18 September 1954	Jozini area	ZAB
1954	September	19 September 1954	Jozini area	ZAB
1954	October	10 October 1954	Kosi Bay area	ZAB
1954	October	27 October 1954	Port Edward area	ZAB
1954	October	28 October 1954	South Coast	ZAB
1954	October	29 October 1954	Port Edward area	ZAB
1954	October	31 October 1954	Kokstad area	ZAB
1954	November	09 November 1954	Hluhluwe area	ZAB
1954	November	13 November 1954	Kokstad area	ZAB
1954	November	21 November 1954	Kosi Bay area	ZAB
1954	December	29 December 1954	Kosi Bay area	ZAB
1954	December	31 December 1954	Kokstad area	ZAB
1955	January	02 January 1955	Kosi Bay area	ZAB
1955	January	19 January 1955	Kokstad area	ZAB
1955	January	22 January 1955	Kosi Bay area	ZAB
1955	January	26 January 1955	Kokstad area	ZAB
1955	January	27 January 1955	Newcastle area	ZAB
1955	January	28 January 1955	St Lucia Area	ZAB
1955	January	29 January 1955	Ladysmith area	ZAB
1955	January	30 January 1955	Kosi Bay area	ZAB

Year	Month	Date	Geographic Area	Source
1955	January	31 January 1955	Dundee area	ZAB
1955	February	02 February 1955	Richmond area	ZAB
1955	February	09 February 1955	Newcastle area	ZAB
1955	February	18 February 1955	Kokstad area	ZAB
1955	February	20 February 1955	Pmb area	ZAB
1955	March	01 March 1955	St Lucia Area	ZAB
1955	March	02 March 1955	Hluhluwe area	ZAB
1955	September	29 September 1955	Durban area	ZAB
1955	September	30 September 1955	Port Edward area	ZAB
1956	January	30 January 1956	Berg area	ZAB
1956	February	04 February 1956	Vryheid area	ZAB
1956	February	07 February 1956	Ladysmith - Dundee area	ZAB
1956	February	16 February 1956	Babanango area	ZAB
1956	March	16 March 1956	Kosi Bay area	ZAB
1956	March	26 March 1956	Newcastle area	ZAB
1956	April	20 April 1956	Mtubatuba Area	ZAB
1956	June	04 June 1956	South Coast	ZAB
1956	October	31 October 1956	Port Edward area	ZAB
1956	November	03 November 1956	Port Edward area	ZAB
1956	December	02 December 1956	Durban area	ZAB
1956	December	03 December 1956	Mkhathini area	ZAB
1956	December	17 December 1956	Heatonville area	ZAB
1957	January	19 January 1957	Rbay area	ZAB
1957	February	01 February 1957	Stanger Area	ZAB
1957	February	24 February 1957	Empangeni area	ZAB
1957	February	25 February 1957	Mbazwana, St Lucia, Pongola area	ZAB
1957	February	26 February 1957	Kosi Bay area	ZAB
1957	March	01 March 1957	Stanger, Ladysmith area	ZAB
1957	March	11 March 1957	Rbay area	ZAB
1957	March	15 March 1957	Kokstad area	ZAB
1957	March	23 March 1957	Kosi Bay area	ZAB
1957	March	28 March 1957	Mtubatuba Area	ZAB
1957	April	02 April 1957	Port Edward area	ZAB
1957	May	28 May 1957	St Lucia Area	ZAB
1957	May	29 May 1957	Hluhluwe area	ZAB
1957	July	04 July 1957	Kosi Bay area	ZAB
1957	September	27 September 1957	Nkandla area	ZAB
1957	October	13 October 1957	Hluhluwe area	ZAB
1957	November	02 November 1957	Hluhluwe area	ZAB
1957	November	03 November 1957	St Lucia Area	ZAB
1957	December	10 December 1957	Rbay area	ZAB
1957	December	12 December 1957	Durban area	ZAB
1957	December	13 December 1957	Mtunzini area	ZAB
1958	January	04 January 1958	Newcastle area	ZAB
1958	January	10 January 1958	Mbazwana, Newcastle area	ZAB
1958	January	11 January 1958	Kosi Bay area	ZAB
1958	January	20 January 1958	Makhathini area	ZAB
1958	January	21 January 1958	Jozini area	ZAB
1958	January	22 January 1958	Rbay	ZAB
1958	February	05 February 1958	Mtunzini area	ZAB
1958	February	06 February 1958	Nkandla area	ZAB
1958	February	20 February 1958	Hluhluwe area	ZAB
1958	March	02 March 1958	Mtubatuba Area	ZAB
1958	March	18 March 1958	St Lucia Area	ZAB

Year	Month	Date	Geographic Area	Source
1958	March	31 March 1958	Kokstad area	ZAB
1958	April	30 April 1958	Kokstad area	ZAB
1958	September	11 September 1958	Cato Ridge area	ZAB
1958	October	20 October 1958	South Coast	ZAB
1958	November	03 November 1958	Pmb area	ZAB
1958	November	10 November 1958	Port Edward area	ZAB
1958	November	29 November 1958	Babanango area	ZAB
1958	November	30 November 1958	Kokstad area	ZAB
1958	December	04 December 1958	Pmb area	ZAB
1958	December	08 December 1958	Kokstad area	ZAB
1958	December	10 December 1958	Nongoma area	ZAB
1958	December	23 December 1958	Dundee area	ZAB
1958	December	28 December 1958	Kosi Bay area	ZAB
1958	December	31 December 1958	Kokstad area	ZAB
1959	January	06 January 1959	Mbazwana area	ZAB
1959	January	10 January 1959	Hluhluwe area	ZAB
1959	January	16 January 1959	Makhathini area	ZAB
1959	January	27 January 1959	Berg area	ZAB
1959	January	31 January 1959	Kokstad area	ZAB
1959	February	15 February 1959	Central KZN	ZAB
1959	February	16 February 1959	Dalton area	ZAB
1959	May	20 May 1959	Sani Pass	ZAB
1959	May	31 May 1959	Kokstad area	ZAB
1959	June	10 June 1959	Pmb area	ZAB
1959	July	08 July 1959	Durban area	ZAB
1959	August	31 August 1959	Mtunzini area	ZAB
1959	September	01 September 1959	Rbay area	ZAB
1959	September	12 September 1959	Dundee area	ZAB
1959	September	13 September 1959	Dundee area	ZAB
1959	November	14 November 1959	Umzimkhulu area	ZAB
1959	November	30 November 1959	Kokstad area	ZAB
1959	December	16 December 1959	Nqutu area	ZAB
1959	December	17 December 1959	Nkandla area	ZAB
1959	December	18 December 1959	Vryheid area	ZAB
1959	December	31 December 1959	Kokstad area	ZAB
1960	February	08 February 1960	Rbay area	ZAB
1960	March	13 March 1960	Jozini area	ZAB
1960	March	18 March 1960	Sani Pass	ZAB
1960	March	20 March 1960	Sani Pass	ZAB
1960	March	31 March 1960	Kokstad area	ZAB
1960	April	14 April 1960	Rbay area	ZAB
1960	April	25 April 1960	Mtunzini area	ZAB
1960	April	30 April 1960	Kokstad area	ZAB
1960	May	14 May 1960	Rbay area	ZAB
1960	November	20 November 1960	Kosi Bay area	ZAB
1960	December	05 December 1960	Mtunzini area	ZAB
1960	December	18 December 1960	Van Reenens - Newcastle	ZAB
1960	December	19 December 1960	Mtunzini area	ZAB
1960	December	20 December 1960	Vryheid area	ZAB
1960	December	25 December 1960	Rbay area	ZAB
1961	January	05 January 1961	St Lucia Area	ZAB
1961	January	18 January 1961	Ulundi area	ZAB
1961	February	05 February 1961	Mtunzini area	ZAB
1961	February	06 February 1961	Mtunzini area	ZAB

Year	Month	Date	Geographic Area	Source
1961	February	12 February 1961	St Lucia Area	ZAB
1961	February	14 February 1961	Hluhluwe area	ZAB
1961	February	15 February 1961	Hluhluwe area	ZAB
1961	March	12 March 1961	South Coast	ZAB
1961	April	06 April 1961	Durban, Mtunzini area	ZAB
1961	April	07 April 1961	Mtunzini area	ZAB
1961	April	08 April 1961	Rbay area	ZAB
1961	April	22 April 1961	Mkuze area	ZAB
1961	June	18 June 1961	St Lucia Area	ZAB
1961	June	20 June 1961	Durban area	ZAB
1961	July	22 July 1961	Port Edwards area	ZAB
1961	August	07 August 1961	Kosi Bay area	ZAB
1961	September	24 September 1961	Makhathini area	ZAB
1961	September	25 September 1961	Kosi Bay area	ZAB
1961	October	29 October 1961	Scattered Northern KZN	ZAB
1962	January	05 January 1962	West of Ladysmith	ZAB
1962	January	20 January 1962	Newcastle Area	ZAB
1962	February	06 February 1962	Ladysmith area	ZAB
1962	February	13 February 1962	Ixopo area	ZAB
1962	February	19 February 1962	Sani Pass area	ZAB
1962	April	04 April 1962	Makhathini area	ZAB
1962	April	26 April 1962	St Lucia Area	ZAB
1962	November	03 November 1962	Durban area	ZAB
1962	November	15 November 1962	Rbay area	ZAB
1962	November	19 November 1962	Berg, Durban area	ZAB
1962	December	15 December 1962	Ulundi area	ZAB
1963	January	10 January 1963	Durban area	ZAB
1963	January	31 January 1963	Pongola area	ZAB
1963	February	23 February 1963	St Lucia Area	ZAB
1963	March	05 March 1963	Port Edward area	ZAB
1963	March	13 March 1963	Makhathini Flats	ZAB
1963	March	14 March 1963	Mkuze area	ZAB
1963	March	15 March 1963	Heatonville	ZAB
1963	March	17 March 1963	Rbay Area	ZAB
1963	March	18 March 1963	Stanger area	ZAB
1963	October	10 October 1963	Kosi Bay area	ZAB
1963	October	11 October 1963	Kosi Bay area	ZAB
1963	November	10 November 1963	Hluhluwe area	ZAB
1963	November	11 November 1963	Sani Pass area	ZAB
1963	December	16 December 1963	Durban area	ZAB
1964	January	01 January 1964	Greytown, Nkandla area	ZAB
1964	January	12 January 1964	Sani Pass area	ZAB
1964	January	13 January 1964	St Lucia Area	ZAB
1964	January	15 January 1964	Ixopo area	ZAB
1964	January	16 January 1964	St Lucia Area	ZAB
1964	February	01 February 1964	Hluhluwe area	ZAB
1964	April	10 April 1964	St Lucia Area	ZAB
1964	April	27 April 1964	Rbay area	ZAB
1964	October	31 October 1964	Sani Pass area	ZAB
1964	November	04 November 1964	Berg area	vB
1964	November	27 November 1964	St Lucia Area	ZAB
1964	December	27 December 1964	Sani Pass, Vryheid area	ZAB
1965	January	05 January 1965	Hluhluwe area	ZAB
1965	January	07 January 1965	Pmb area	ZAB

Year	Month	Date	Geographic Area	Source
1965	January	19 January 1965	Sani pass area	ZAB
1965	February	12 February 1965	Ulundi, Nkandla area	ZAB
1965	March	25 March 1965	Mkhathini area	ZAB
1965	May	31 May 1965	KZN Coast	ZAB
1965	September	30 September 1965	South Coast	ZAB
1965	October	01 October 1965	Hluhluwe area	ZAB
1965	November	19 November 1965	St Lucia Area	ZAB
1966	January	08 January 1966	Rbay area	ZAB
1966	January	09 January 1966	St Lucia Area	ZAB
1966	January	22 January 1966	Sani Pass area	ZAB
1966	January	23 January 1966	Ladysmith area	ZAB
1966	January	28 January 1966	Newcastle Area	ZAB
1966	January	31 January 1966	Sani Pass area	ZAB
1966	February	01 February 1966	Vryheid area	ZAB
1966	February	06 February 1966	St Lucia Area	ZAB
1966	February	10 February 1966	Sani Pass area	ZAB
1966	February	16 February 1966	Sani Pass area	ZAB
1966	February	20 February 1966	St Lucia Area	ZAB
1966	February	21 February 1966	Ladysmith area	ZAB
1966	March	06 March 1966	Hluhluwe area	ZAB
1966	April	08 April 1966	Hluhluwe area	ZAB
1966	April	28 April 1966	Jozini area	ZAB
1966	November	04 November 1966	Bulwer area	ZAB
1966	December	18 December 1966	Ladysmith area	ZAB
1966	December	21 December 1966	Ulundi area	ZAB
1967	January	18 January 1967	Mkhathini area	ZAB
1967	January	19 January 1967	Sani Pass	ZAB
1967	January	23 January 1967	Ladysmith	ZAB
1967	February	06 February 1967	Sani Pass	ZAB
1967	February	07 February 1967	Durban	ZAB
1967	February	14 February 1967	Jozini, St Lucia	ZAB
1967	February	28 February 1967	Berg area	ZAB
1967	March	11 March 1967	Rbay area	ZAB
1967	March	12 March 1967	Mtunzini area	ZAB
1967	March	17 March 1967	St Lucia Area	ZAB
1967	March	18 March 1967	Berg area	ZAB
1967	March	25 March 1967	Dundee area	ZAB
1967	April	05 April 1967	Port Edward area	ZAB
1967	April	13 April 1967	Hluhluwe area	ZAB
1967	May	02 May 1967	St Lucia Area	ZAB
1967	December	21 December 1967	Underberg area	ZAB
1967	December	27 December 1967	Ixopo area	ZAB
1968	January	22 January 1968	Sani Pass area	ZAB
1968	February	12 February 1968	Rbay Area	ZAB
1968	February	16 February 1968	Rbay Area	ZAB
1968	March	03 March 1968	Durban area	vB
1968	March	06 March 1968	Mtunzini area	ZAB
1968	March	07 March 1968	Mkhathini area	ZAB
1968	March	09 March 1968	Mkhathini area	ZAB
1968	March	17 March 1968	Sani Pass area	ZAB
1968	August	09 August 1968	Durban Coastal area	ZAB
1968	August	10 August 1968	Hibberdene area	ZAB
1968	November	20 November 1968	Rbay Area	ZAB
1968	December	23 December 1968	Tongaat area	ZAB

Year	Month	Date	Geographic Area	Source
1969	January	01 January 1969	Greytown area	ZAB
1969	January	06 January 1969	Berg area	ZAB
1969	February	07 February 1969	Hluhluwe area	ZAB
1969	February	25 February 1969	Berg area	ZAB
1969	September	29 September 1969	St Lucia area	ZAB
1969	November	18 November 1969	St Lucia Area	ZAB
1969	November	28 November 1969	Mooirivver area	ZAB
1969	December	07 December 1969	Umzinto area	ZAB
1970	January	02 January 1970	Hluhluwe area	ZAB
1970	January	16 January 1970	Stanger area	ZAB
1970	January	17 January 1970	Paulpietersburg area	ZAB
1970	January	19 January 1970	Dundee area	ZAB
1970	January	29 January 1970	Balgowan area	ZAB
1970	February	01 February 1970	Kokstad area	ZAB
1970	March	01 March 1970	Kokstad area	ZAB
1970	March	06 March 1970	Rbay area	ZAB
1970	June	12 June 1970	St Lucia Area	ZAB
1970	June	26 June 1970	Port Edward area	ZAB
1970	November	30 November 1970	Kosi Bay area	ZAB
1970	December	05 December 1970	Port Edward area	ZAB
1970	December	15 December 1970	Hluhluwe area	ZAB
1971	January	11 January 1971	Vryheid area	ZAB
1971	January	13 January 1971	Ladysmith area	ZAB
1971	January	15 January 1971	Mfolizi GR	ZAB
1971	February	01 February 1971	Nqutu area	ZAB
1971	February	14 February 1971	St Lucia Area	ZAB
1971	February	15 February 1971	Hibberdene area	ZAB
1971	March	22 March 1971	Newcastle Area	ZAB
1971	March	27 March 1971	Durban area	ZAB
1971	March	28 March 1971	Durban area	ZAB
1971	March	29 March 1971	Rbay area	ZAB
1971	April	03 April 1971	South Coast	ZAB
1971	April	11 April 1971	St Lucia Area	ZAB
1971	May	02 May 1971	Rbay area	ZAB
1971	May	30 May 1971	Mtunzini area	ZAB
1971	May	31 May 1971	Rbay area	ZAB
1971	July	04 July 1971	Coastal belt	ZAB
1971	October	08 October 1971	Port Edward area	ZAB
1971	October	09 October 1971	Port Edward area	ZAB
1972	January	10 January 1972	Scattered KZN	ZAB
1972	January	11 January 1972	Bulwer area	ZAB
1972	January	14 January 1972	Mtunzini area	ZAB
1972	January	19 January 1972	Jozini area	ZAB
1972	January	21 January 1972	Port Shepstone, Rnay area	ZAB
1972	January	22 January 1972	Bulwer area	ZAB
1972	March	01 March 1972	Berg area	ZAB
1972	March	26 March 1972	Hluhluwe area	ZAB
1972	March	08 March 1972	Mtunzini area	ZAB
1972	March	16 March 1972	Balgowan area	ZAB
1972	March	23 March 1972	Hluhluwe area	ZAB
1972	April	10 April 1972	Jozini area	ZAB
1972	April	14 April 1972	Tongaat area	ZAB
1972	April	20 April 1972	Jozini area	ZAB
1972	May	15 May 1972	Tongaat area	ZAB

Year	Month	Date	Geographic Area	Source
1972	November	22 November 1972	Umzimkhulu area	ZAB
1972	November	30 November 1972	Jozini area	ZAB
1972	December	25 December 1972	St Lucia Area	ZAB
1973	January	02 January 1973	Vryheid area	ZAB
1973	January	05 January 1973	Greytown area	ZAB
1973	January	12 January 1973	St Lucia Area	ZAB
1973	January	21 January 1973	Jozini area	ZAB
1973	January	22 January 1973	Mkuze area	ZAB
1973	February	06 February 1973	Nongoma area	ZAB
1973	February	08 February 1973	Melmoth area	ZAB
1973	February	19 February 1973	Greytown area	ZAB
1973	February	24 February 1973	Scattered KZN	ZAB
1973	March	09 March 1973	Mkhathini area	ZAB
1973	March	19 March 1973	Bulwer area	ZAB
1973	March	27 March 1973	Mkhathini area	ZAB
1973	April	08 April 1973	Mtunzini area	ZAB
1973	April	09 April 1973	Mtunzini area	ZAB
1973	May	03 May 1973	Jozini area	ZAB
1973	May	19 May 1973	Mkhathini area	ZAB
1973	August	29 August 1973	Cato Ridge area	ZAB
1973	September	04 September 1973	St Lucia Area	ZAB
1973	September	05 September 1973	St Lucia Area	ZAB
1973	November	01 November 1973	Nqutu area	ZAB
1973	November	21 November 1973	Scattered KZN	ZAB
1973	December	20 December 1973	Jozini area	ZAB
1973	December	23 December 1973	Mkhathini area	ZAB
1973	December	24 December 1973	Mbazwana area	ZAB
1974	January	01 January 1974	Mkhathini area	ZAB
1974	January	04 January 1974	Kosi Bay area	ZAB
1974	January	10 January 1974	Bulwer area	ZAB
1974	January	11 January 1974	Ladysmith area	ZAB
1974	January	16 January 1974	Scattered Southern KZN	ZAB
1974	January	17 January 1974	Scattered Southern KZN	ZAB
1974	January	21 January 1974	Scattered KZN	ZAB
1974	January	23 January 1974	Vryheid area	ZAB
1974	January	24 January 1974	Mkhathini area	ZAB
1974	January	25 January 1974	Kosi Bay area	ZAB
1974	January	29 January 1974	Pongola area	ZAB
1974	February	01 February 1974	Mkhathini area	ZAB
1974	February	10 February 1974	Berg area	ZAB
1974	March	08 March 1974	Utrecht	ZAB
1974	March	11 March 1974	Durban area	ZAB
1974	April	26 April 1974	Mkhathini area	ZAB
1974	May	01 May 1974	Jozini area	ZAB
1974	May	16 May 1974	Underberg area	ZAB
1974	May	20 May 1974	Rbay area	ZAB
1974	July	02 July 1974	Kosi Bay area	ZAB
1974	November	07 November 1974	Mkhathini area	ZAB
1974	November	19 November 1974	Scattered Northern KZN	ZAB
1974	December	02 December 1974	Scattered KZN	ZAB
1974	December	03 December 1974	Scattered KZN	ZAB
1974	December	20 December 1974	St Lucia Area	ZAB
1974	December	25 December 1974	Port Shepstone area	ZAB
1975	January	02 January 1975	Durban area	ZAB

Year	Month	Date	Geographic Area	Source
1975	January	16 January 1975	St Lucia Area	ZAB
1975	January	24 January 1975	Mkhathini area	ZAB
1975	January	26 January 1975	Dundee area	ZAB
1975	January	29 January 1975	St Lucia Area	ZAB
1975	February	20 February 1975	St Lucia Area	ZAB
1975	February	27 February 1975	Scattered Northern KZN	ZAB
1975	February	28 February 1975	Ulundi area	ZAB
1975	March	01 March 1975	Mkhathini area	ZAB
1975	March	03 March 1975	Berg area	ZAB
1975	March	15 March 1975	Berg area	ZAB
1975	March	18 March 1975	Melmoth area	ZAB
1975	March	30 March 1975	Hluhluwe area	ZAB
1975	April	03 April 1975	Mkhathini area	ZAB
1975	April	16 April 1975	Mkhathini area	ZAB
1975	April	21 April 1975	Eshowe area	ZAB
1975	May	03 May 1975	Mtubatuba Area	ZAB
1975	June	05 June 1975	Mkhathini area	ZAB
1975	September	25 September 1975	St Lucia Area	ZAB
1975	September	26 September 1975	Scattered KZN	ZAB
1975	November	25 November 1975	Vryheid area	ZAB
1975	December	15 December 1975	Scattered KZN	ZAB
1975	December	17 December 1975	Volksrust area	ZAB
1975	December	25 December 1975	Nongoma area	ZAB
1976	January	04 January 1976	Scattered KZN	ZAB
1976	January	06 January 1976	Mtubatuba Area	ZAB
1976	January	08 January 1976	Rbay area	ZAB
1976	January	24 January 1976	Ladysmith area	ZAB
1976	January	26 January 1976	Scattered KZN	ZAB
1976	January	27 January 1976	Berg area	ZAB
1976	February	02 February 1976	Western KZN	ZAB
1976	February	07 February 1976	Wartburg	ZAB
1976	February	23 February 1976	Berg area	ZAB
1976	February	24 February 1976	St Lucia Area	ZAB
1976	March	12 March 1976	Underberg area	ZAB
1976	March	17 March 1976	Berg area	ZAB
1976	March	26 March 1976	St Lucia Area	ZAB
1976	April	01 April 1976	Coast	ZAB
1976	April	10 April 1976	Jozini area	ZAB
1976	April	11 April 1976	Tongaat area	ZAB
1976	April	14 April 1976	St Lucia Area	ZAB
1976	April	15 April 1976	Berg area	ZAB
1976	May	02 May 1976	Mtubatuba Area	ZAB
1976	May	03 May 1976	St Lucia Area	ZAB
1976	May	04 May 1976	South Coast	ZAB
1976	May	05 May 1976	Umkomaas area	ZAB
1976	July	19 July 1976	Amatikulu area	ZAB
1976	October	04 October 1976	South Coast	vB
1976	December	22 December 1976	Rbay area	ZAB
1976	December	24 December 1976	Ladysmith area	ZAB
1977	January	10 January 1977	Durban area	ZAB
1977	January	28 January 1977	Umzimkhulu area	ZAB
1977	January	29 January 1977	Paulpietersburg area	ZAB
1977	January	31 January 1977	Bergville area	ZAB
1977	February	01 February 1977	Rbay area	ZAB

Year	Month	Date	Geographic Area	Source
1977	February	04 February 1977	Port Shepstone Area	ZAB
1977	February	13 February 1977	Southern KZN	ZAB
1977	March	04 March 1977	Durban area, Hluhluwe area	ZAB
1977	March	14 March 1977	Ulundi, Mtunzini area	ZAB
1977	March	15 March 1977	Rbay area	ZAB
1977	May	07 May 1977	Jozini area	ZAB
1977	September	20 September 1977	Eshowe area	ZAB
1977	September	24 September 1977	Rbay area	ZAB
1977	October	07 October 1977	Vryheid area	ZAB
1977	November	09 November 1977	St Lucia Area	ZAB
1977	November	26 November 1977	Jozini area	ZAB
1977	November	27 November 1977	Mkhathini area	ZAB
1977	December	19 December 1977	Eshowe area	ZAB
1977	December	23 December 1977	Mbazwana	ZAB
1977	December	31 December 1977	Ixopo area	ZAB
1978	January	07 January 1978	Nongoma area	ZAB
1978	January	23 January 1978	Newcastle area	ZAB
1978	February	11 February 1978	West of Dundee	ZAB
1978	February	21 February 1978	Mtubatuba Area	ZAB
1978	February	26 February 1978	South Coast	ZAB
1978	March	05 March 1978	Kosi Bay area	ZAB
1978	March	07 March 1978	Babanango area	ZAB
1978	March	14 March 1978	South Coast, Durban area	ZAB
1978	March	30 March 1978	Albert Falls area	ZAB
1978	April	01 April 1978	Mbazwana area	ZAB
1978	April	02 April 1978	Mtunzini area	ZAB
1978	May	14 May 1978	South Coast	ZAB
1978	September	08 September 1978	Ixopo area	ZAB
1978	October	19 October 1978	Ladysmith	vB
1978	November	01 November 1978	Babanango area	ZAB
1978	November	07 November 1978	Durban area	ZAB
1978	November	12 November 1978	Hluhluwe area	ZAB
1978	November	18 November 1978	Tongaat area	ZAB
1978	December	04 December 1978	Mbazwana area	ZAB
1978	December	20 December 1978	Berg area	ZAB
1978	December	21 December 1978	Berg area	ZAB
1978	December	28 December 1978	Greytown area	ZAB
1979	January	11 January 1979	Babanango area	ZAB
1979	January	27 January 1979	Mtunzini area	ZAB
1979	January	29 January 1979	Nongoma area	ZAB
1979	February	18 February 1979	Dalton area	ZAB
1979	February	19 February 1979	Dalton area	ZAB
1979	February	22 February 1979	Dundee, Ladysmith area	ZAB
1979	April	21 April 1979	Jozini area	ZAB
1979	April	24 April 1979	Kokstad area	ZAB
1979	May	19 May 1979	Rbay area	ZAB
1979	July	20 July 1979	South Coast	ZAB
1979	July	21 July 1979	Port Edward area	ZAB
1979	July	23 July 1979	Ixopo area	ZAB
1979	August	16 August 1979	Kokstad area	ZAB
1979	August	17 August 1979	Rbay area	ZAB
1979	August	18 August 1979	Umzimkhulu area	ZAB
1979	October	20 October 1979	Berg area	ZAB
1979	October	21 October 1979	Berg area	ZAB

Year	Month	Date	Geographic Area	Source
1979	November	21 November 1979	Berg area	ZAB
1979	November	23 November 1979	Berg area	ZAB
1980	January	20 January 1980	Newcastle area	ZAB
1980	January	28 January 1980	Jozini area	ZAB
1980	January	30 January 1980	Babanango area	ZAB
1980	February	27 February 1980	Newcastle area	ZAB
1980	March	13 March 1980	Berg area	ZAB
1980	March	18 March 1980	Estcourt area	ZAB
1980	March	20 March 1980	Mbazwana area	ZAB
1980	April	06 April 1980	Estcourt area	ZAB
1980	July	18 July 1980	Jozini area	ZAB
1980	November	24 November 1980	Ladysmith area	ZAB
1980	November	27 November 1980	Ulundi area	ZAB
1980	December	12 December 1980	Babanango area	ZAB
1980	December	13 December 1980	Tongaat area	ZAB
1980	December	14 December 1980	Mooi River, Durban area	ZAB
1981	January	08 January 1981	St Lucia Area	ZAB
1981	January	17 January 1981	Kosi Bay area	ZAB
1981	January	18 January 1981	Hluhluwe area	ZAB
1981	January	21 January 1981	Ladysmith area	ZAB
1981	February	09 February 1981	Mtunzini area	ZAB
1981	February	12 February 1981	Mtunzini area	ZAB
1981	February	13 February 1981	Van Reenens area	ZAB
1981	February	16 February 1981	Babanango area	ZAB
1981	February	18 February 1981	Eshowe area	ZAB
1981	February	27 February 1981	Berg area	ZAB
1981	March	26 March 1981	Kosi Bay area	ZAB
1981	August	28 August 1981	Tongaat area	ZAB
1981	August	29 August 1981	Rbay area	ZAB
1981	August	30 August 1981	Tongaat area	ZAB
1981	September	09 September 1981	Mbazwana area	ZAB
1981	September	10 September 1981	Mkhathini area	ZAB
1981	October	26 October 1981	Mbazwana area	ZAB
1981	November	19 November 1981	Stanger area	ZAB
1981	November	27 November 1981	Berg area	ZAB
1981	December	16 December 1981	Port Shepstone Area	ZAB
1982	January	04 January 1982	Port Shepstone area	ZAB
1982	January	17 January 1982	Nongoma area	ZAB
1982	January	20 January 1982	Maputuland	ZAB
1982	January	21 January 1982	North Coast, Maputuland	ZAB
1982	February	16 February 1982	Greytown area	ZAB
1982	March	03 March 1982	Stanger area	ZAB
1982	March	14 March 1982	Port Edward area	ZAB
1982	March	21 March 1982	Rbay area	ZAB
1982	April	21 April 1982	St Lucia Area	ZAB
1982	December	30 December 1982	Pmb area	ZAB
1983	January	17 January 1983	Dalton area	ZAB
1983	February	12 February 1983	Mbazwana area	ZAB
1983	April	05 April 1983	Ixopo area	ZAB
1983	July	24 July 1983	Coastal Belt	ZAB
1983	August	07 August 1983	Jozini area	ZAB
1983	August	24 August 1983	St Lucia Area	ZAB
1983	October	06 October 1983	Hibberdene area	ZAB
1983	October	07 October 1983	Kokstad area	ZAB

Year	Month	Date	Geographic Area	Source
1983	November	28 November 1983	St Lucia Area	ZAB
1983	November	29 November 1983	Mtubatuba Area	ZAB
1983	December	09 December 1983	Mbazwana area	ZAB
1983	December	10 December 1983	Kosi Bay area	ZAB
1983	December	25 December 1983	Durban area	ZAB
1983	December	26 December 1983	Dundee area	ZAB
1983	December	30 December 1983	St Lucia Area	ZAB
1984	January	06 January 1984	St Lucia Area	ZAB
1984	January	07 January 1984	Kokstad area	ZAB
1984	January	09 January 1984	Mbazwana area	ZAB
1984	January	13 January 1984	Port Edward area	ZAB
1984	January	17 January 1984	Nqutu area	ZAB
1984	January	18 January 1984	Paddock area	ZAB
1984	January	27 January 1984	Jozini area	ZAB
1984	February	02 February 1984	Newcastle Rbay, Maputoland	ZAB
1984	February	10 February 1984	Wartburg	ZAB
1985	February	12 February 1984	Rbay, Berg area	ZAB
1984	February	15 February 1984	Mission Rocks	ZAB
1984	February	16 February 1984	Mission Rocks, Rbay area	ZAB
1984	February	22 February 1984	Cape Vidal area	ZAB
1984	March	21 March 1984	Paulpietersburg area	ZAB
1984	March	24 March 1984	Mkhathini area	ZAB
1984	May	21 May 1984	Durban area	ZAB
1984	June	23 June 1984	Mbazwana area	ZAB
1984	June	24 June 1984	Mkhathini area	ZAB
1984	July	23 July 1984	Mbazwana area	ZAB
1984	August	29 August 1984	Jozini area	ZAB
1984	October	23 October 1984	Amatikulu area	ZAB
1984	October	24 October 1984	Mtunzini area	ZAB
1984	December	14 December 1984	Berg area	ZAB
1984	December	17 December 1984	Mbazwana area	ZAB
1984	December	23 December 1984	Ladysmith	vB
1984	December	23 December 1984	Nqutu area	ZAB
1985	January	13 January 1985	Estcourt area	ZAB
1985	January	14 January 1985	Ixopo area	ZAB
1985	January	24 January 1985	Amatikulu area	ZAB
1985	February	12 February 1985	Rbay area	ZAB
1985	February	18 February 1985	Rbay area	ZAB
1985	March	03 March 1985	Mbazwana area	ZAB
1985	May	09 May 1985	Jozini area	ZAB
1985	June	01 June 1985	Mtunzini area	ZAB
1985	June	02 June 1985	Amatikulu area	ZAB
1985	June	23 June 1985	Rbay area	ZAB
1985	July	13 July 1985	Rbay area	ZAB
1985	July	26 July 1985	St Lucia Area	ZAB
1985	August	13 August 1985	St Lucia Area	ZAB
1985	September	15 September 1985	Hlibaisa area	ZAB
1985	December	03 December 1985	Underberg area	ZAB
1985	December	29 December 1985	Mkhathini area	ZAB
1986	January	01 January 1986	Weenen area	ZAB
1986	January	10 January 1986	Weenen area	ZAB
1986	January	21 January 1986	Weenen area	ZAB
1986	February	09 February 1986	Dundee area	ZAB
1986	February	12 February 1986	Babanango area	ZAB

Year	Month	Date	Geographic Area	Source
1986	February	22 February 1986	Babanango area	ZAB
1986	March	08 March 1986	Underberg area	ZAB
1986	March	10 March 1986	Weenen area	ZAB
1986	March	11 March 1986	Coastline	ZAB
1986	March	16 March 1986	Kosi Bay area	ZAB
1986	March	17 March 1986	Jozini area	ZAB
1986	April	11 April 1986	Rbay area	ZAB
1986	April	12 April 1986	St Lucia Area	ZAB
1986	April	13 April 1986	Rbay area	ZAB
1986	May	19 May 1986	Jozini area	ZAB
1986	June	04 June 1986	Rbay area	ZAB
1986	August	28 August 1986	South Coast	ZAB
1986	October	01 October 1986	Port Edward area	ZAB
1986	November	29 November 1986	Jozini area	ZAB
1986	December	07 December 1986	Stanger area	ZAB
1986	December	27 December 1986	Volksrust area	ZAB
1986	December	29 December 1986	Rbay area	ZAB
1987	January	09 January 1987	St Lucia Area	ZAB
1987	January	10 January 1987	Newcastle area	ZAB
1987	January	14 January 1987	Cape Vidal area	ZAB
1987	February	03 February 1987	Kokstad area	ZAB
1987	February	10 February 1987	Pongola, Ladysmith, Berg area	ZAB
1987	March	05 March 1987	Port Edward	ZAB
1987	March	06 March 1987	Maputoland, Mtubatuba	ZAB
1987	March	17 March 1987	Berg area	ZAB
1987	March	20 March 1987	Rbay area	ZAB
1987	March	21 March 1987	Port Edward area	ZAB
1987	March	22 March 1987	Umzimkhulu area, PMB area, Kosi bay	ZAB
1987	April	06 April 1987	Hluhluwe Area	ZAB
1987	May	21 May 1987	Coastal Belt	ZAB
1987	May	20 May 1987	Durban area	ZAB
1987	June	26 June 1987	Rbay area	ZAB
1987	June	28 June 1987	Rbay area	ZAB
1987	August	23 August 1987	Kosi Bay area	ZAB
1987	August	25 August 1987	Kosi Bay area	ZAB
1987	August	26 August 1987	St Lucia Area	ZAB
1987	September	21 September 1987	South Coast	ZAB
1987	November	06 November 1987	Port Edward area	ZAB
1987	December	03 December 1987	Rbay to Ulundi	ZAB
1987	December	14 December 1987	Vryheid area	ZAB
1988	January	06 January 1988	Dundee area	ZAB
1988	January	14 January 1988	Hibberdene area	ZAB
1988	January	18 January 1988	Greytown area	ZAB
1988	January	19 January 1988	Dalton area	ZAB
1988	February	14 February 1988	Kokstad area	ZAB
1988	February	16 February 1988	Estcourt, Stanger, Port Edward area	ZAB
1988	February	28 February 1988	Kokstad area	ZAB
1988	March	26 March 1988	St Lucia Area	ZAB
1988	March	28 March 1988	Hluhluwe Area	ZAB
1988	April	07 April 1988	Babanango area	ZAB
1988	April	17 April 1988	Mbazwana area	ZAB
1988	May	15 May 1988	Jozini area	ZAB
1988	September	01 September 1988	Port Edward area	ZAB
1988	September	15 September 1988	Port Edward area	ZAB

Year	Month	Date	Geographic Area	Source
1988	September	27 September 1988	Greytown area	ZAB
1988	September	28 September 1988	Greytown area	ZAB
1988	November	19 November 1988	Cape Vidal area	ZAB
1988	November	28 November 1988	Vryheid area	ZAB
1988	December	05 December 1988	Port Shepstone area	ZAB
1988	December	15 December 1988	Kosi Bay area	ZAB
1988	December	16 December 1988	Rbay area	ZAB
1988	December	17 December 1988	Ulundi area	ZAB
1988	December	18 December 1988	Rbay area	ZAB
1988	December	24 December 1988	Durban area	ZAB
1988	December	29 December 1988	Richmond area	ZAB
1988	December	30 December 1988	Rbay area	ZAB
1989	January	08 January 1989	Kokstad area	ZAB
1989	January	15 January 1989	Cape Vidal area	ZAB
1989	January	31 January 1989	Mkhathini area	ZAB
1989	February	19 February 1989	Kokstad area	ZAB
1989	February	21 February 1989	Sani Pass area	ZAB
1989	February	22 February 1989	Nongoma area	ZAB
1989	February	25 February 1989	Stanger area	ZAB
1989	March	14 March 1989	Mbazwana area	ZAB
1989	September	23 September 1989	South Coast	ZAB
1989	November	03 November 1989	Port Shepstone area	ZAB
1989	November	05 November 1989	Kokstad area	ZAB
1989	December	03 December 1989	Paulpietersburg, Eshowe	ZAB
1989	December	04 December 1989	Hluhluwe Area	ZAB
1989	December	06 December 1989	Keats Drift	ZAB
1989	December	07 December 1989	Nqutu, Stanger, Paulpietersburg, Ulundi, Kosi Bay	ZAB
1989	December	08 December 1989	Jozini area	ZAB
1989	December	09 December 1989	Ulundi	ZAB
1989	December	13 December 1989	Mtubatuba Area	ZAB
1989	December	14 December 1989	Scattered KZN	ZAB
1989	December	15 December 1989	Berg area	ZAB
1990	February	24 February 1990	Hluhluwe Area	ZAB
1990	March	14 March 1990	Rbay area	ZAB
1990	March	15 March 1990	Durban area	ZAB
1990	March	19 March 1990	Jozini area	ZAB
1990	April	24 April 1990	Mtubatuba Area	ZAB
1990	July	13 July 1990	Mkuze area	ZAB
1990	August	29 August 1990	Nongoma area	ZAB
1990	October	18 October 1990	Rbay area	ZAB
1990	October	19 October 1990	Stanger area	ZAB
1990	December	05 December 1990	Sani Pass area	ZAB
1990	December	06 December 1990	Mtunzini area	ZAB
1991	January	08 January 1991	Kosi Bay area	ZAB
1991	January	16 January 1991	Pongola area	ZAB
1991	January	23 January 1991	Nottingham Road	ZAB
1991	January	24 January 1991	Nongoma area	ZAB
1991	January	25 January 1991	Rbay area	ZAB
1991	January	29 January 1991	Stanger area	ZAB
1991	February	07 February 1991	Dundee area	ZAB
1991	February	15 February 1991	Scattered KZN	ZAB
1991	February	17 February 1991	Tongaat area	ZAB
1991	February	18 February 1991	Rbay area	ZAB
1991	March	10 March 1991	Umzimkhulu area	ZAB

Year	Month	Date	Geographic Area	Source
1991	March	16 March 1991	Mbazwana area	ZAB
1991	March	23 March 1991	Kosi Bay area	ZAB
1991	March	24 March 1991	Coastla Belt	ZAB
1991	April	16 April 1991	Mbazwana area	ZAB
1991	November	14 November 1991	South Coast	ZAB
1991	December	11 December 1991	Berg area	ZAB
1992	January	23 January 1992	Kokstad area	ZAB
1992	February	17 February 1992	Ulundi area	ZAB
1992	March	17 March 1992	Berg area	ZAB
1992	April	21 April 1992	Mkuze area	ZAB
1992	November	01 November 1992	Babanango area	ZAB
1992	November	11 November 1992	Stanger area	ZAB
1992	November	15 November 1992	Pomeroy area	ZAB
1992	December	08 December 1992	Greytown area	ZAB
1992	December	12 December 1992	Kosi Bay area	ZAB
1993	January	09 January 1993	Mbazwana area	ZAB
1993	February	14 February 1993	Ladysmith, Kokstad area	ZAB
1993	February	18 February 1993	Mbazwana area	ZAB
1993	February	22 February 1993	Newcastle area	ZAB
1993	March	03 March 1993	Sani Pass area	ZAB
1993	March	21 March 1993	Hluhluwe Area	ZAB
1993	April	29 April 1993	St Lucia Area	ZAB
1993	September	22 September 1993	South Coast	ZAB
1993	September	26 September 1993	Pomeroy area	ZAB
1993	October	03 October 1993	Dundee	ZAB
1993	October	30 October 1993	Hlabisa area	ZAB
1993	November	29 November 1993	Hlabisa area	ZAB
1994	January	03 January 1994	Dundee area, Kokstad area	ZAB
1994	January	21 January 1994	Eshowe area	ZAB
1994	January	23 January 1994	Rbay area	ZAB
1994	January	28 January 1994	Hluhluwe Area	ZAB
1994	February	04 February 1994	Vryheid area	ZAB
1994	February	06 February 1994	Dundee area	ZAB
1994	February	11 February 1994	Port Edward area	ZAB
1994	February	12 February 1994	South Coast	ZAB
1994	March	02 March 1994	Greytown area	ZAB
1994	March	03 March 1994	Tongaat area	ZAB
1994	March	29 March 1994	Jozini area	ZAB
1994	July	25 July 1994	South Coast	ZAB
1994	July	26 July 1994	Cato Ridge area	ZAB
1994	October	28 October 1994	Newcastle area	ZAB
1994	October	30 October 1994	Vryheid, Keats Drift	ZAB
1994	December	08 December 1994	Ladysmit area	ZAB
1994	December	09 December 1994	Dundee area	ZAB
1994	December	26 December 1994	South Coast	ZAB
1995	January	18 January 1995	Newcastle area	ZAB
1995	January	29 January 1995	Pomeroy area	ZAB
1995	March	23 March 1995	Tongaat area	ZAB
1995	March	22 March 1995	Durban area	ZAB
1995	May	02 May 1995	Tongaat area	ZAB
1995	May	10 May 1995	St Lucia Area	ZAB
1995	July	16 June 1995	St Lucia Area	ZAB
1995	July	17 June 1995	Coastal Belt	ZAB
1995	September	13 September 1995	Vryheid area	ZAB

Year	Month	Date	Geographic Area	Source
1995	November	19 November 1995	St Lucia Area	ZAB
1995	December	27 December 1995	Matatiele area	ZAB
1996	January	04 January 1995	Newcastle area	ZAB
1996	January	19 January 1995	Kosi Bay area	ZAB
1996	February	22 February 1995	Babanango area	ZAB
1996	February	23 February 1995	Vryheid area	ZAB
1996	February	25 February 1995	Newcastle area	ZAB
1996	February	26 February 1995	Hluhluwe Area	ZAB
1996	March	02 March 1995	Newcastle area	ZAB
1996	March	03 March 1995	Scattered KZN	ZAB
1996	March	12 March 1995	Dalton area	ZAB
1996	March	13 March 1995	Hluhluwe Area	ZAB
1996	March	14 March 1995	Umzimkhulu area	ZAB
1996	July	02 July 1995	Cato Ridge area	ZAB
1996	July	21 July 1995	Durban area	ZAB
1996	October	22 October 1995	Northern KZN	ZAB
1996	November	17 November 1995	Port Shepstone area	ZAB
1996	November	22 November 1995	St Lucia Area	ZAB
1996	December	04 December 1995	Newcastle area	ZAB
1996	December	22 December 1995	Port Shepstone area	ZAB
1997	January	16 January 1997	Estcourt area	ZAB
1997	January	22 January 1997	Cape Vidal area	ZAB
1997	January	23 January 1997	Hluhluwe Area	ZAB
1997	January	26 January 1997	Berg, Tongaat area	ZAB
1997	January	27 January 1997	Rbay area	ZAB
1997	January	28 January 1997	Mtunzini area	ZAB
1997	March	04 March 1997	Scattered KZN	ZAB
1997	March	10 March 1997	Jozini area	ZAB
1997	March	20 March 1997	Pongola area	ZAB
1997	March	21 March 1997	Pongola area	ZAB
1997	April	01 April 1997	Coastal Belt	ZAB
1997	May	02 May 1997	St Lucia Area	ZAB
1997	July	01 July 1997	Durban area	ZAB
1997	August	30 August 1997	Berg area	ZAB
1997	September	09 September 1997	Cape Vidal area	ZAB
1997	October	10 October 1997	Hluhluwe Area	ZAB
1997	November	13 November 1997	Sani Pass area	ZAB
1997	November	27 November 1997	Coastal Belt	ZAB
1997	November	28 November 1997	Mooi River Area	ZAB
1997	November	29 November 1997	Vryheid area	ZAB
1997	November	30 November 1997	Vryheid area	ZAB
1997	December	10 December 1997	Sani Pass area	ZAB
1997	December	31 December 1997	Volksrust area	ZAB
1998	January	01 January 1998	Volksrust area	ZAB
1998	January	07 January 1998	Mkhathini area	ZAB
1998	January	17 January 1998	Volksrust area	ZAB
1998	February	02 February 1998	Kokstad area	ZAB
1998	February	14 February 1998	Kokstad area	ZAB
1998	February	15 February 1998	Richmond area	ZAB
1998	February	16 February 1998	Coastal Belt	ZAB
1998	February	17 February 1998	Mkhathini area	ZAB
1998	February	18 February 1998	Kosi Bay area	ZAB
1998	February	21 February 1998	Rbay area	ZAB
1998	February	28 February 1998	Mkuze area	ZAB

Year	Month	Date	Geographic Area	Source
1998	March	01 March 1998	Port Shepstone, Vryheid area	ZAB
1998	March	19 March 1998	St Lucia Area	ZAB
1998	April	14 April 1998	Durban area	ZAB
1998	April	15 April 1998	Hibberdene area	ZAB
1998	April	16 April 1998	Port Shepstone area	ZAB
1998	August	10 August 1998	St Lucia Area	ZAB
1998	November	25 November 1998	Rbay area	ZAB
1998	December	01 December 1998	Port Shepstone area	ZAB
1999	January	10 January 1999	Kokstad area	ZAB
1999	January	11 January 1999	PMB	ZAB
1999	January	12 January 1999	Kosi Bay area	ZAB
1999	January	18 January 1999	St Lucia Area	ZAB
1999	January	27 January 1999	Babanango area	ZAB
1999	January	28 January 1999	Kokstad area	ZAB
1999	January	29 January 1999	Kokstad area	ZAB
1999	January	31 January 1999	Vryheid area	ZAB
1999	February	02 February 1999	Kokstad area	ZAB
1999	February	11 February 1999	Newcastle area	ZAB
1999	February	12 February 1999	Tongaat area	ZAB
1999	March	06 March 1999	Hluhluwe Area	ZAB
1999	March	07 March 1999	Cape Vidal area	ZAB
1999	April	21 April 1999	Hluhluwe Area	ZAB
1999	April	26 April 1999	St Lucia Area	ZAB
1999	May	18 May 1999	Kokstad area	ZAB
1999	May	19 May 1999	Jozini area	ZAB
1999	May	27 May 1999	Cape Vidal area	ZAB
1999	September	11 September 1999	Kosi Bay area	ZAB
1999	September	26 September 1999	Kokstad area	ZAB
1999	November	26 November 1999	Mkhathini area	ZAB
1999	November	27 November 1999	Mtubatuba Area	ZAB
1999	November	28 November 1999	Mbazwana area	ZAB
1999	December	09 December 1999	Dalton area	ZAB
1999	December	10 December 1999	Ulundi area	ZAB
1999	December	26 December 1999	Estcourt, Hluhluwe area	ZAB
1999	December	27 December 1999	Hibberdene area	ZAB
1999	December	29 December 1999	Ulundi area	ZAB
2000	January	02 January 2000	Newcastle area	ZAB
2000	January	03 January 2000	Pongola area	ZAB
2000	January	07 January 2000	Newcastle area	ZAB
2000	January	13 January 2000	Stanger area	ZAB
2000	January	23 January 2000	Port Shepstone area	ZAB
2000	January	26 January 2000	Umzimkhulu area	ZAB
2000	January	27 January 2000	Umzimkhulu area	ZAB
2000	January	28 January 2000	Dalton area	ZAB
2000	January	29 January 2000	Hluhluwe Area	ZAB
2000	February	06 February 2000	Mkhathini area	ZAB
2000	February	08 February 2000	Ulundi area	ZAB
2000	February	11 February 2000	Kokstad area	ZAB
2000	February	12 February 2000	Coastal Belt	ZAB
2000	February	13 February 2000	Coastal Belt	ZAB
2000	February	14 February 2000	Durban area	ZAB
2000	February	24 February 2000	Tongaat area	ZAB
2000	March	01 March 2000	Sani Pass area	ZAB
2000	March	05 March 2000	Ixopo, Mbazwana area	ZAB

Year	Month	Date	Geographic Area	Source
2000	March	06 March 2000	Port Edward, Kokstad area	ZAB
2000	March	07 March 2000	Port Shepstone area	ZAB
2000	March	16 March 2000	Port Shepstone, Kosi Bay area	ZAB
2000	March	17 March 2000	Rbay, Mbazwana area	ZAB
2000	March	19 March 2000	Scattered KZN	ZAB
2000	April	17 April 2000	Hluhluwe Area	ZAB
2000	May	22 May 2000	Mbazwana area	ZAB
2000	May	23 May 2000	Tongaat area	ZAB
2000	November	07 November 2000	Port Edward area	ZAB
2000	December	11 December 2000	Stanger area	ZAB
2000	December	20 December 2000	St Lucia Area	ZAB

APPENDIX VI – CLIMATE DATA SOURCES

Climate Data	Description	Timeframe	Units
Mean Annual Precipitation (MAP)	Extracted from the Daily Rainfall Extractor program database produced by Lynch (2003). Rainfall station data for the study area was averaged per annum to produce the MAP	1890 - 2000	mm per annum
Wet/Dry Cycles	data was taken from Tyson (1986). These are divided into blocks representing wet and dry years	1848 - 2000	Yearly groupings
ENSO	The Multivariate ENSO Index (MEI) Extension data (Wolter & Timlin 2011) is obtained from the NOAA website (NOAA 2013). The MEI is a computation of observed variables over the Pacific Ocean and is processed in bi-monthly units	1871 - present	Multivariate rank from 1 – 63 where 1 – 12 denote La Niña and 52 – 63 denote El Niño events. Rank 13 – 51 is ENSO neutral
Southern Oscillation Index (SOI)	Obtained from the University of East Anglia Climate Research Unit website (CRU 2010)	1866 - present	Normalised pressure difference between Tahiti and Darwin (Können et al. 1998)
Indian Ocean Dipole (IOD)	from the Japan Agency for Marine-Earth-Science and Technology website (JAMSTEC 2012).	1871 - present	Normalised anomaly in SST between the western and eastern equatorial Indian Ocean (Saji et al. 1999)
Antarctic Oscillation (AAO)	Obtained from the University of Washington Joint Institute for the Study of the Atmosphere and Ocean (JISAO 2012).	1948 - 2002	Geo-potential height in hPa.
Pacific Decadal Oscillation (PDO)	Obtained from the University of Washington Joint Institute for the Study of the Atmosphere and Ocean (JISAO 2013).	1900 - present	Standardised SST anomalies in the North Pacific Ocean (Zhang et al. 1997; Mantua et al. 1997)
Sea surface temperatures (SST)	Obtained from NOAA Climatic Data Center (NOAA_ERSST_V3 2012).	1880 - 2010	Standardised anomalies relative to a 30 year climatological mean (Xue et al. 2003)
Global temperatures	Obtained from NASA Goddard Space Flight Center (NASA 2012)	1880 - 2011	Temperature anomalies relative to a 1951 – 1980 mean global temperature (Hansen et al. 1999)

Climate Data	Description	Timeframe	Units
Lunar Nodal Cycle	Self generated	1900 - present	
Atmospheric CO ₂ (Keeling Curve)	Obtained from NOAA Earth System Research Laboratory (NOAA/ESRLa 2012).	1959 - present	ppm expressed as the mole fraction in dry air (micromol/mol)
Interdecadal Pacific Oscillation	Metereological Office, Hadley Centre for Climate Change, Exceter, UK (Folland 2008)	1850 - 2008	SST anomalies based on an 11 year low pass filter
Atlantic Multidecadal Oscillation	Obtained from NOAA Earth System Research Laboratory (NOAA/ESRLb 2012)	1856 - present	SST anomalies based on the 1951 - 1980 period for the North Atlantic Ocean